



저작자표시-비영리-변경금지 2.0 대한민국

이용자는 아래의 조건을 따르는 경우에 한하여 자유롭게

- 이 저작물을 복제, 배포, 전송, 전시, 공연 및 방송할 수 있습니다.

다음과 같은 조건을 따라야 합니다:



저작자표시. 귀하는 원저작자를 표시하여야 합니다.



비영리. 귀하는 이 저작물을 영리 목적으로 이용할 수 없습니다.



변경금지. 귀하는 이 저작물을 개작, 변형 또는 가공할 수 없습니다.

- 귀하는, 이 저작물의 재이용이나 배포의 경우, 이 저작물에 적용된 이용허락조건을 명확하게 나타내어야 합니다.
- 저작권자로부터 별도의 허가를 받으면 이러한 조건들은 적용되지 않습니다.

저작권법에 따른 이용자의 권리는 위의 내용에 의하여 영향을 받지 않습니다.

이것은 [이용허락규약\(Legal Code\)](#)을 이해하기 쉽게 요약한 것입니다.

[Disclaimer](#)

A THESIS
FOR THE DEGREE OF DOCTOR OF PHILOSOPHY

3-Hydroxy-5,6-epoxy- β -ionone isolated from *Sargassum horneri*, inhibits fine dust induced inflammation through TLR/MyD88 mediated anti-inflammatory pathway and Nrf2/HO-1 mediated antioxidant pathways

KALU KAPUGE ASANKA SANJEEWA

Department of Marine Life Sciences

SCHOOL OF BIOMEDICAL SCIENCE

JEJU NATIONAL UNIVERSITY

REPUBLIC OF KOREA

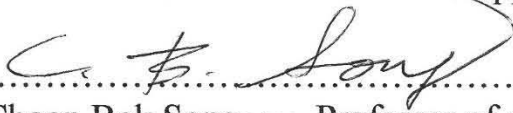
February, 2019

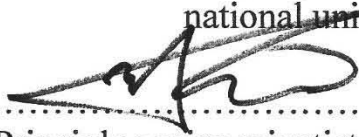
3-Hydroxy-5,6-epoxy- β -ionone isolated from *Sargassum horneri*,
inhibits fine-dust induced inflammation through TLR/MyD88 mediated
anti-Inflammatory pathway and Nrf2/HO-1 mediated antioxidant
pathways


Kalu Kapuge Asanka Sanjeewa
(Supervised by Professor You-Jin Jeon)


A thesis submitted in partial fulfilment of the requirement for the degree of
DOCTOR OF PHILOSOPHY
February 2019

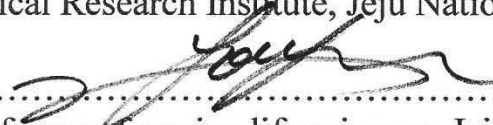
The thesis has been examined and approved by


.....
Thesis director, Choon Bok Song_(PhD), Professor of marine life sciences, Jeju
national university


.....
Soo-Jin Heo_(PhD), Principle senior scientist, Korea institute of ocean science and
technology


.....
Gi-Young Kim_(PhD), Professor of marine life sciences, Jeju national university


.....
Youngheun Jee_(PhD), Professor of Department of Veterinary Medicine and
Veterinary Medical Research Institute, Jeju National University


.....
You-Jin Jeon_(PhD), Professor of marine life sciences, Jeju national university

2019/2
Date

Department of marine Life Sciences

Graduate School
Jeju National University
Republic of Korea

Contents

Contents	i
Summary	IX
List of figures	XII
List of tables.....	XXII
Background.....	1
Fine dust.....	1
What is inflammation?	2
What is Oxidative stress?.....	3
Importance of seaweeds as a food source to avoid FD-induced inflammation and oxidative stress.....	4
<i>Sargassum horneri</i> , the brown seaweed used to isolate pure compounds	5
Selection of suitable extraction method.....	6
Water extraction methods	6
Enzyme-assisted extraction methods	7
Organic solvent assisted extraction methods	7
Part- 1	8
Initial screening of seaweeds to identify potential candidates for separate anti- inflammatory compounds	8
Abstract.....	9
Graphical abstract	11
1.1. introduction.....	12
1.2. Materials and Methods.....	14
1.2.1. Sample collection.....	14

1.2.2. Chemicals and reagents	14
1.2.3. preparation of crude 80% methanolic extracts from seaweeds.....	14
1.2.4. Preparation of enzymatic digests from seaweeds	15
1.2.5. Analysis of chemical composition	15
1.2.6. purification of bioactive compounds from <i>S. horneri</i>	17
1.2.7 Apparatus used for the isolation of active compounds	17
1.2.8. HPCPC separation of <i>S. horneri</i> compounds.....	18
1.2.9. HPCPC separation procedure	18
1.2.10. HPLC analysis	18
1.2.11. Cell culture.....	19
1.2.12. Cell viability assay	19
1.2.13. Determination of NO production.....	19
1.2.14. Determination of PGE ₂ , TNF- α , IL-6, and IL-1 β production.....	20
1.2.15. Total RNA extraction and cDNA synthesis.....	20
1.2.16. Quantitative real-time PCR (qPCR) analysis.....	20
1.2.17. Western blot analysis	21
1.2.18. Statistical analysis.....	24
1.3. Results and discussion	25
1.3.1 Extraction efficiency of seaweed samples	25
1.3.3 Anti-inflammatory effects of seaweed extracts against LPS-induced NO production in RAW 264.7 cells	30
1.3.4 PGE ₂ and Pro-inflammatory cytokine inhibitory effect of 80 % methanolic extracts of <i>E. cava</i> and <i>S. horneri</i>	34
1.3.5 Effects of the seaweed extracts on LPS-induced iNOS and COX2 expression in RAW 264.7 cells.....	36

1.3.6. Effect of <i>S. horneri</i> extracts on LPS-induced NF- κ B protein expressions	38
1.3.7. The effects of <i>S. horneri</i> 80% methanol extract against pro-inflammatory gene expression in LPS-exposed RAW 264.7 cells.	39
1.3.8. fractionation of <i>S. horneri</i> 80% methanol extract for isolate bioactive compounds	42
1.3.9 NO inhibitory effect of three solvent fractions separated from <i>S. horneri</i> against LPS-induced RAW 264.7 cells	42
1.3.10. HPCPC and HPLC spectrums of SHMC after HPCPC chromatography	46
1.3.11. Anti-inflammatory properties and cytoprotective effect of four pure compounds isolated from <i>S. horneri</i>	50
1.4. Conclusions.....	52
1.5. References.....	53
 Part- 2	 60
3-Hydroxy-5,6-epoxy- β -ionone isolated from <i>Sargassum horneri</i> protect MH-S mouse lung cells against fine dust induced inflammation and oxidative stress	60
Abstract	61
Graphical abstract	63
2.1. Introduction.....	64
2.2. Materials and methods	66
2.2.1. Chemicals and reagents	66
2.2.2. Purification and isolation of HEBI from <i>S. horneri</i>	66
2.2.3. Estimation of fine dust particle size by scanning electron microscopy	69
2.2.4. Cell culture.....	69
2.2.5. Determination of cell viability	69

2.2.6. Evaluation of cell death rates by analysis of lactate dehydrogenase (LDH) levels	70
2.2.7. Determination of NO inhibition effect.....	70
2.2.8. Determination of PGE ₂ and pro-inflammatory cytokine production.....	70
2.2.9. Western blot assay	71
2.2.10. Level of ROS in fine-dust exposed MH-S cells.....	71
2.2.11. Analysis of SOD Activities.....	72
2.2.12. Effect of HEBI on MAPK pathway related proteins	72
2.2.13. Total RNA extraction and cDNA synthesis.....	73
2.2.14. Quantitative real-time PCR (qPCR) analysis.....	73
2.2.15. Statistical analysis.....	77
2.3. Results and discussion	78
2.3.1-Anti-inflammatory properties of HEBI against fine dust induced inflammation in MH-S cells	78
2.3.1.1. Composition of fine dust.....	78
2.3.1.2. cell viability and NO production in fine dust exposed MH-S cells	80
2.3.1.3. Cyto-toxic effect of HEBI on MH-S cells	80
2.3.1.4. Protective effect of HEBI against fine dust-induced cell death and NO production in MH-S cells.....	82
2.3.1.5. Effects of HEBI on fine dust induced PGE ₂ and pro-inflammatory cytokine secretion (ELISA).....	84
2.3.1.6. Effects of HEBI on FD-induced iNOS and COX2 protein production	84
2.3.1.7. Suppressive effect of HEBI in fine dust induced NF- κ B phosphorylation and translocation to the nucleus in MH-S macrophages	88
2.3.1.8. HEBI inhibits MAPK protein expression in fine dust exposed MH-S sells.....	92

2.3.1.9. Effect of HEBI against fine dust induced inflammatory gene expression in MH-S cells	95
2.3.1.10 inhibitory effect of HEBI against fine dust induced TLR activations (RT-qPCR).....	97
2.3.2-Anti-oxidant properties of HEBI against FD-induced inflammation in MH-S cells	100
2.3.2.1 HEBI inhibits fine dust induced ROS levels in MH-S cells	101
2.3.2.2. Effect of HEBI in fine dust induced SOD and catalase levels in MH-S cells	101
2.3.2.3. HEBI increased the cytosolic antioxidant protein levels in fine dust exposed MH-S cells	104
2.2.2.4 HEBI induced antioxidant mechanism in fine dust exposed MH-S cells through Nrf2/Keap1 mediated antioxidant pathway.	106
2.2.2.5. Fine dust induced NO production and Effect of MAPK inhibitors	109
2.4. Conclusions.....	111
2.5. References.....	112
 Part- 3.....	 119
Anti-inflammatory and antioxidant mechanisms of 3-Hydroxy-5,6-epoxy- β -ionone isolated from <i>Sargassum horneri</i> on fine dust-exposed CMT-93 mouse epithelial cells (digestive tract)	119
Abstract.....	120
3.1. Introduction.....	122
3.2. Materials and methods	125
3.2.1. Chemicals and regents	125
3.2.2. Estimation of fine dust particle size by scanning electron microscopy	125

3.2.3. Culture conditions of CMT-93 cell line.....	125
3.2.4. Cell viability assay (MTT) and measurement of nitrite by Griess reaction.....	126
3.2.5. Determination of PGE ₂ and pro-inflammatory cytokine secretion levels	127
3.2.6. Total RNA extraction and cDNA synthesis.....	127
3.2.7. Quantitative real-time PCR (qPCR) analysis.....	127
3.2.8. Western blot analysis	128
3.2.9. Statistical analysis	131
3.3. Results and discussion	132
3.3.1. Composition of fine dust and size distribution	132
3.3.2. cell viability and NO production in fine dust exposed MH-S cells	136
3.3.3 HEBI inhibits fine dust-induced PGE ₂ and pro-inflammatory cytokine production from CMT-93 cells (ELISA)	136
3.3.4 HEBI inhibits fine dust-induced inflammatory cytokine related gene production from CMT-93 cells (ELISA)	140
3.3.5 Inhibitory effect of HEBI against iNOS and COX2 production from fine dust stimulated CMT-93 cells.....	142
3.3.6 inhibitory effect of HEBI against fine dust induced TLR activations in CMT-93 cells (RT-qPCR).....	144
3.3.7. Effect of HEBI against MyD88 protein expression in fine dust exposed CMT-93 cells	149
3.3.8. Effect of HEBI against fine dust induced NF-κB protein expression in CMT-93 cells	151
3.3.9. Effect of HEBI against fine dust induced MAPK expression in CMT-93 cells	155
3.3.10 HEBI up-regulates anti-oxidant proteins expression in fine dust exposed CMT- 93 cells	157

3.3.11 HEBI upregulates anti-oxidant gene expressions in fine dust exposed CMT-93 cells	160
3.4. Conclusions.....	164
3.5 References.....	165
Part- 4	173
Abstract.....	174
Graphical abstract	176
4.1 Introduction.....	177
4.2. Materials and methods	180
4.2.1. Sample collection and purification	180
4.2.2. Chemicals and reagents	182
4.2.3. Estimation of fine dust particle size by scanning electron microscopy	182
4.2.4. In vivo zebrafish experiments.....	183
4.2.4.1. Origin and maintenance of parental zebrafish	183
4.2.4.2. Measurement of the toxicity of fine dust and HEBI on zebrafish embryo	183
4.2.4.3. Measurement of heart-beating rate of zebrafish	183
4.2.4.4. The toxicity of HEBI on zebrafish embryo by means of the cell death.....	184
4.2.4.5. Estimation of fine dust induced ROS generation.....	184
4.2.4.6. Measurement of in vivo NO production	184
4.2.5. Western blot analysis	185
4.2.6 RNA extraction, cDNA synthesis and RT-qPCR analysis	185
4.2.7 Statistical analysis.....	188
4.3. Results and discussion	189
4.3.1. Composition of fine dust and size distribution analysis of fine dust	189

4.3.2. Fine dust induced toxicity rates in zebrafish embryo	193
4.3.3. Effects of HEBI on fine dust-exposed heart-beating rate of zebrafish model .	196
4.3.4. Protective effect of HEBI against fine dust induced cell deaths in zebrafish embryos.....	198
4.3.5. protective effect of HEBI on fine dust –induced ROS production in zebrafish embryo	198
4.3.6. Protective effect of HEBI against fine dust induced NO production in zebrafish embryos.....	199
4.3.7. HEBI down-regulate fine dust-induced iNOS and COX2 expression in zebrafish embryos.....	203
4.3.8 HEBI protects zebrafish embryo against fine dust induced pro-inflammatory cytokine production	205
4.4. Conclusions.....	207
4.5. References.....	208
Acknowledgements.....	214

Summary

In East-Asia region (China, Korea, and Japan) fine dust (FD) have become a major threat of air pollutions and causing negative health effects on human skin, respiratory system, and digestive system. Specifically, the extensive arid or semiarid highlands of northern China and Mongolia (Gobi Desert, Hunshdak Sandy Lands, Loess Plateau, and Taklimakan desert) are considering as the major sources of dust in Asia region. However, coal-burning power plants, rapid developments in industrialization, numerous petroleum vehicles, and large-scale mining operations have contributed to increase the FD concentration in the urban areas located in East-Asia region. Continuous exposure to air pollution such as FD can induce oxidative stress, inflammation, and poses a serious risk to human health.

Alveolar macrophages, who lives in lower respiratory tract are capable to phagocyte FD particles reach the lower respiratory. However, depending on the size and particle composition, exposed macrophages may produce inflammatory responses. Recently, several studies reported that, the exposure of FD to macrophages led to inflammatory responses in macrophages including RAW 264.7 cells. According to the recent studies, the exposure of macrophages to FD triggers inflammatory responses in macrophages via altering multiple cell signaling pathways. The endotoxins presented in FD particles found to induce the toll-like receptor-4 mediated inflammation, and reactive oxygen species induce pro-inflammatory cytokine production in macrophages. The continuous/uncontrolled inflammatory activities leading to develop chronic inflammatory responses and end up with the pathogenesis of catastrophic disease conditions like cancer and immunomodulatory diseases. In addition, dust particles inside of the lungs attacked/consumed by alveolar macrophages, and then activated cells removed by lysosomes. Thus, number of healthy macrophages decrease and which might

affect to the immune system that further results in less immunity in our body. Therefore, it is very important to down-regulate inflammation induced by FD particles to reduce health concerns associated with FD. Besides the respiratory system, FD also has a possibility to damage digestive system as some part of inhaled dust moved to the digestive system and directly going to the digestive tract with FD contaminated foods. Thus, effect of FD to digestive system cannot neglect and require in-depth studies to expose it effects on a digestive system like inflammation and oxidative stress.

According to the statistics cancer incidents reported from colon and rectum were nearly doubled from 1999 to 2012 period, where lung cancer levels were remaining constant in that period. Other than the bad food habits FD also might responsible for this increased levels of colon and rectum cancers. Therefore, author also attempted to evaluate effect of fine dust using digestive tract epithelial cells. CMT-93 is an epithelial cell line separated from a 19 months old male mouse rectum. Recent studies carried out with CMT-93 reported the exposure of CMT-93 to LPS, triggers the inflammatory responses in CMT-93 cells. Therefore, CMT-93 cell model is a promising model to evaluate complication associated with the inflammation in digestive system.

However, use of *in vitro* results for the development of functional materials have limited possibility as the culture cells were maintained in artificial conditions. Therefore, to validate *in vitro* results it is compulsory to use *in vivo* research models. Recently, zebrafish (*Danio rerio*) has been recognized as a promising *in vivo* model to use in research areas such as cancer, stem cell research and immunology and infectious diseases research due to its morphological and physiological similarity to the mammals, transparency, easy to handle, and less maintenance cost. Other than that, the optical transparency of zebrafish embryos allows for non-destructive and live imaging of the

inflammatory responses developed in embryos. Due to these specific morphological and physiological features of zebrafish models provide great opportunities to accelerate the process of drug discovery including target identification, disease modelling, lead discovery, and toxicology.

Taken together, during this study author attempted to screen seaweeds with potential anti-inflammatory compounds to develop as a functional ingredient to act against FD induced inflammatory complications. For preliminary screening author used 4 seaweeds (*Ecklonia cava*, *Ishige okamurae*, *Sargassum horneri*, and *Porphyra yezoensis*). According to the results, *Sargassum horneri* and *Ecklonia cava* had strong anti-inflammatory properties against FD-induced inflammation in macrophage cells. Moreover, our results revealed that the treatment of 3-Hydroxy-5,6-epoxy- β -ionone, the active compound isolated from *S. horneri* blocked the FD-induced inflammation via inhibiting NF- κ B, MAPK, and NRF2/HO-1 signal pathways. The evidence in this study providing solid information's to develop functional materials from *S. horneri* against dust induced inflammation.

List of figures

Part 1

Figure 1-1. Cyto-protective effects of seaweed extracts in RAW 264.7 macrophages. RAW cells were pretreated with different concentrations of seaweed extracts and incubated 24 h. Colorimetric MTT assay was used to determined cell viability. Experiments were carried out in triplicate and the results are represented as means \pm SD. *P < 0.05 and **P < 0.01.....32

Figure 1-2. Effect of seaweed extracts on NO production in LPS-stimulated RAW 264.7 cells. The cells were incubated with the 50 and 100 μ g/ml concentrations of seaweed extracts for 24 h with or without LPS. NO levels in the culture mediums were quantified using Griess assay. Data are expressed as mean \pm SD from three independent experiments and analyzed using one-way ANOVA. #p < 0.01 vs. control, *p < 0.05 and **p < 0.01 vs. LPS alone treatment.33

Figure 1-3. PGE₂ and pro-inflammatory cytokine expression inhibitory effect of Ecklonia cava and Sargassum horneri in LPS-activated RAW 264.7 macrophages. RAW 264.7 macrophages were incubated with 31.3 -125 μ g/ml of seaweed extracts for 24 h, and subsequently, they were stimulated with 1 μ g/ml of LPS for 24 h. Elisa kits were used to measure PGE₂ (a), TNF- α (b), IL-1 β (c), and IL-6 (d) secretion into cell culture medium. Data are expressed as mean \pm SD from three independent experiments and analyzed using one-way ANOVA. *P < 0.05, **P < 0.01.35

Figure 1-4. Effect of 80% methanolic extracts of Ecklonia cava (a) and Sargassum horneri (b) on iNOS and COX2 protein expressions in LPS-stimulated RAW 264.7 cells. The cells were incubated with the indicated concentrations of seaweed extracts for 24 h with or without LPS. The protein levels of iNOS and COX2 were determined using Western blot analysis. The bar chart shows the quantitative evaluation of iNOS and COX2 bands by densitometry. Data are expressed as mean \pm SD from three independent experiments and analyzed using one-way ANOVA. *P < 0.05, **P < 0.01.37

Figure 1-5. Inhibitory effect of 80% methanol extract of Sargassum horneri against LPS-induced NF- κ B phosphorylation and translocation in RAW 264.7 cells. Macrophages were stimulated with LPS (1 μ g/ml) and S. horneri extract (31.3 - 125 μ g/ml) for 30 min,

and the cell lysates were analyzed for the expression of both P50 and P65 in the cytosol (a) and nucleus (b). Results are expressed as mean \pm SD from three independent experiments and analyzed using one-way ANOVA. *P < 0.05, **P < 0.01.40

Figure 1-6. Inhibition of LPS- induced iNOS (a), COX2 (b), IL-1 β (c), IL-6 (d), and TNF- α (e) mRNA expression by *Sargassum horneri* extracts in RAW 264.7 macrophages. The results were analyzed by the Delta-Ct method and expression of target genes was normalized to GAPDH expression. Control was obtained in the absence of LPS and *S. horneri*. The values shown are the means \pm SEs of three independent experiments; *p < 0.05, **p < 0.01 vs. the fine dust treated group.41

Figure 1-7. Extraction and fractionation of *Sargassum horneri*. First the freeze dried seaweed powder was extracted with 80% methanol, concentrated using rotary evaporator and freeze dried. Then the freeze dried samples were further purified using solvent-solvent partition chromatography and High performance centrifugal partition chromatography.....44

Figure 1-8. Protective effect of *Sargassum horneri* 80% methanol extract and its fractions against LPS-exposed macrophages. The cells were incubated with the 31.3 -125 μ g/ml concentrations of SHM, SHMH, SHMC, and SHME for 24 h with or without LPS. The level of NO in the culture media was quantified using Griess assay. Data are expressed as mean \pm SD from three independent experiments and analyzed using one-way ANOVA. Means with same letters are not significantly different at 0.05 sigma level.....45

Figure 1-9. HPCPC chromatography (a) & HPLC spectrums (b) of each fraction obtained from *Sargassum horneri* chloroform fraction.47

Figure 1-10. proton and ¹³C NMR spectrums of 2 novel compounds isolated from *Sargassum horneri* and their structures with IUPAC nominations48

Figure 1-11. proton and ¹³C NMR spectrums of Apo-9'-fucoxanthinon and its structure (a). The LC-MS spectrum and the structure of Sargacromnol B (b) isolated from *Sargassum horneri*.....49

Figure 1-12. Cyto-protective effect and NO inhibitory properties of 4 compounds isolated from *Sargassum horneri* in LPS-activated macrophages. Data are expressed as

mean \pm SD from three independent experiments. The values shown are the means \pm SEs of three independent experiments; * p < 0.05, ** p < 0.01 vs. the LPS-stimulated group.51

Part 2

Figure 2-1. The molecular structure of 3-Hydroxy-5,6-epoxy- β -ionone isolated from *Sargassum horneri*. (MW: 224.2), PubChem CID: 5371267, Abbreviation : HEBI68

Figure 2-2. Scanning electron microscope image of fine dust particles purchased from the national institute for environmental studies, Ibaraki, Japan (certified reference material no. 28). Scale bar represent 10 μ m lengthy.79

Figure 2-3. Cytotoxicity (a) and NO production levels (b) in fine dust-exposed MH-S cells. Results represent the pooled mean \pm SE of three independent experiments, performed in triplicate. * p < 0.05, ** p < 0.01, face to the respective control.81

Figure 2-4. Viability of MH-S cells exposed to 3-Hydroxy-5,6-epoxy- β -ionone (HEBI) and fine dust (FD). Cells were exposed to HEBI with or without FD (31.3 μ g/ml) at the doses of 15.6 - 62.5 μ g/ml. After 24 h, cell viability was measured by the MTT (a, b) and LDH assays (c). Secreted NO in the culture media was quantified using Griess assay (d). Statistical significance was tested using a Student's t-test. HEBI group vs FD group * p < 0.05, ** p < 0.01; FD vs control group (positive control) # p < 0.01.83

Figure 2-5. Effects of HEBI on production of PGE₂ and pro-inflammatory cytokines in fine dust (FD)-activated MH-S cells. Percentage of PGE₂ (a), IL-6 (b), IL-1 β (c), and TNF- α (d) in cell cultures. Results represent the pooled mean \pm SE of three independent experiments, performed in triplicate. * p < 0.05, ** p < 0.01, face to the respective control (ANOVA, Duncan's multiple range test).86

Figure 2-6. Effects of HEBI on the fine dust (FD)-induced expression of MyD-88, iNOS, and COX2 in MH-S macrophages (a). Lysates were prepared from cells that were not treated or pre-treated with HEBI (15.6 - 62.5 μ g/ml) for 1 h and then stimulated FD (31.3 μ g/ml) for 24 h. Density ratios of COX2 (b), iNOS (c), and MyD88 (d) were measured

using densitometry. The values shown are the means \pm SD of three independent experiments. * $p < 0.05$, ** $p < 0.01$87

Figure 2-7. The graphical illustration of activation and translocation of NF- κ B from cytosol to nucleus (a). The inhibitory effects of HEBI on fine dust (FD)-stimulated NF κ B related (I κ B- α , and p-I κ B- α) protein expression (b). The gel shown is a representative of the results from three separate experiments. * $p < 0.05$, ** $p < 0.01$, face to the respective control (ANOVA, Duncan's multiple range test).90

Figure 2-8. The effects of HEBI on NF- κ B expression in fine dust (FD)-exposed MH-S cells. Western blotting was performed to analyze the protein phosphorylation of NF- κ B p50 and p65 in the cytosol (a) and the nucleus (b). The values presented are the mean \pm SD of three independent experiments. * $p < 0.05$, ** $p < 0.01$, face to the respective control (ANOVA, Duncan's multiple range test).91

Figure 2-9. Effect of HEBI MAP kinases in fine dust (FD)-stimulated MH-S macrophages. Data represent the mean \pm SEM of three independent experiments (N = 3). One of the similar results from three separate experiments is represented, and the relative ratio (%) is also shown, where the p-p38, p-JNK and p-ERK signals were normalized to the p38, JNK and ERK signals. * $p < 0.05$, ** $p < 0.01$, face to the respective control (ANOVA, Duncan's multiple range test).94

Figure 2-10. Inhibition of fine dust induced iNOS (a), COX2 (b), IL-1 β (c), IL-6 (d), and TNF- α (e) mRNA expression by HEBI in MH-S macrophages. The results were analyzed by the Delta-Ct method and expression of target genes was normalized to GAPDH expression. Control was obtained in the absence of fine dust and HEBI. The values shown are the means \pm SEs of three independent experiments; * $p < 0.05$, ** $p < 0.01$ vs. the fine dust treated group or # $p < 0.05$, ## $p < 0.01$ vs. the un-stimulated group.96

Figure 2-11. Effect of HEBI against mRNA expression of fine dust (FD)-induced toll like receptors (TLR) (1-9; a-h) in MH-S macrophages. After FD exposure for 6 h, total RNA was extracted from MH-S macrophages and RT-qPCR was performed for the TLR genes using TaqMan reagents. The results were analyzed by the Delta-Ct method and expression of target genes was normalized to GAPDH expression. Control was obtained in the absence of FD and HEBI. The values shown are the means \pm SEs of three

independent experiments; *p < 0.05, **p < 0.01 vs. the FD treated group or #p < 0.05, ##p < 0.01 vs. the un-stimulated group.99

Figure 2-12. Effect of HEBI against fine dust (FD)-induced ROS production (a), cell viability (b), and SOD levels (c) in MH-S cells. The experiments were performed as described in the materials and methods sections. The values shown are the means ± SEs of three independent experiments; *p < 0.05, **p < 0.01 vs. the fine dust treated group or ##p < 0.01 vs control. 103

Figure 2-13. HEBI is involved in the regulation of antioxidant enzymes function. The relative protein levels of catalase Cu/Zn-SOD in fine dust (FD)-exposed MH-S cells prior to HEBI treatment. Western blotting analysis showing the expression of catalase and Cu/Zn-SOD in cells treated as in the figure. Western blotting signal of individual enzyme was normalized by β-actin and FD induced group was defined as 1 of relative expression. *p < 0.05, **p < 0.01 vs. the FD treated group or ##p < 0.01 vs control. . 105

Figure 2-14. Effect of HEBI against fine dust (FD)-induced cytosolic HO-1, Nrf-2, and Keap-1 expressions. β- actin was used as internal control. Quantitative data was analyzed using ImageJ software (1.43V). Results are expressed as the mean ± SD of three separate experiments. *p < 0.05 and **p < 0.01..... 107

Figure 2-15. Protective effect of HEBI against fine dust (FD)-induced HO-1 and Nrf2 suppression. The expression levels of proteins were measured by western blot (a) and relevant quantitative data(d). Nucleolin was used as internal control. Quantitative data was analyzed using ImageJ software (1.43V). Results are expressed as the mean ± SD of three separate experiments. *p < 0.05 and **p < 0.01..... 108

Figure 2-16. The antioxidant effect of HEBI against the fine dust (FD)-induced oxidative damage in MH-S cells. (a) Cell viability and (b) NO inhibitory effect in the presence of specific MAPK inhibitors. The cells were treated with indicated concentrations of HEBI (31.3 μg ml⁻¹) for 24 h in the presence or absence of each selective inhibitor. SB 202190 (p38 inhibitor) SP 600125 (JNK inhibitor), and PD98059 (ERK inhibitor). (c) Effects of HEBI on FD-induced NFR2/Keap-1 pathway related p38 expression in MH-S cells. P38 and p-P38 levels were determined using western blotting. Quantitative data was analyzed

using ImageJ software. Results are expressed as the mean \pm SD of three separate experiments. * $p < 0.05$ and ** $p < 0.01$ 110

Part 3

Figure 3-1. 3-Hydroxy-5,6-epoxy- β -ionone isolated from *Sargassum horneri*. PubChem CID: 5371267, Abbreviation : HEBI..... 124

Figure 3-2. Scanning electron microscope image (a) and particle size distribution of fine dust particles (b) obtained from the national institute for environmental studies, Ibaraki, Japan (certified reference material no. 28). Scale bar represent 10 μ m lengthly. Source - <https://www.nies.go.jp/labo/crm-e/aerosol.html>..... 133

Figure 3-3. Cytotoxicity (a) and NO production levels (b) in fine dust(FD)-exposed CMT-93 cells. CMT-93 cells exposed to the FD (62.5 -500 μ g/ml) for 24. Then MTT and Griess assays were used to evaluate cell viability and NO production, respectively. Protective effect of HEBI against FD exposed MH-S cells. Cells were exposed to HEBI with or without FD (250 μ g/ml) at the doses of 31.3 - 125 μ g/ml. After 24 h cell viability was measured by the MTT (c) and NO secreted in the culture media was quantified using Griess assay (d). Statistical significance was tested using a Student's t-test. HEBI group vs FD group * $p < 0.05$, ** $p < 0.01$ 138

Figure 3-4. Effects of HEBI isolated from *Sargassum horneri* against fine dust (FD)-induced PGE₂ and pro-inflammatory cytokines secretion in CMT-93 cells. Percentage of PGE₂ (a), IL-6 (b), IL-1 β (c), and TNF- α (d) in cell cultures. Results represent the pooled mean \pm SE of three independent experiments, performed in triplicate. * $p < 0.05$, ** $p < 0.01$, face to the respective control (ANOVA, Duncan's multiple range test). 139

Figure 3-5. Effect of HEBI against fine dust (FD)-induced IL-1 β (a), IL-6 (b), and TNF- α (c), IFN- γ (d), and IL-4 (e) mRNA expression in CMT-93 cells. Cells exposed to FD for 6 h and total RNA was extracted from CMT-93 cells. RT-qPCR was performed using TaqMan reagents. The results were analyzed by the Delta-Ct method and expression of target genes was normalized to GAPDH expression. Control was obtained in the absence

of FD and HEBI. The values shown are the means \pm SEs of three independent experiments; *p < 0.05, **p < 0.01 vs. the FD treated group..... 141

Figure 3-6. Effect of HEBI against fine dust (FD)-induced iNOS and COX2 expression in CMT-93 cells. The protein expression levels (a, b) and mRNA expression levels (c, d) of iNOS and COX2. Western blots and RT-qPCR used evaluate proteins and gene expression levels, respectively. Control was obtained in the absence of FD and HEBI. The values shown are the means \pm SEs of three independent experiments; *p < 0.05, **p < 0.01 vs. the FD treated group; #p < 0.05, ##p < 0.01 vs. the un-stimulated group. ... 143

Figure 3-7. Effect of HEBI against mRNA expression of fine dust (FD)-induced toll like receptors (TLR) (1-9; a-h) in CMT-93 cells. After FD exposure for 6 h, total RNA was extracted from CMT-93 cells and RT-qPCR was performed for the TLR genes using TaqMan reagents. The results were analyzed by the Delta-Ct method and expression of target genes was normalized to GAPDH expression. Control was obtained in the absence of FD and HEBI. The values shown are the means \pm SEs of three independent experiments; *p < 0.05, **p < 0.01 vs. the FD treated group; #p < 0.05, ##p < 0.01 vs. the un-stimulated group. 147

Figure 3-8. Graphical illustration of toll like receptor expression and their down-stream signal transduction mechanisms. Source: <https://resources.rndsystems.com/images/Pathways/full-pathway-image/toll-like-recept-signaling-pathways-rnd-systems.png>..... 148

Figure 3-9. Effects of HEBI on the fine dust (FD)-induced expression of MyD88 in CMT-93 cells (a). Density ratios of MyD88 versus β -actin (b) were measured using densitometry. The values shown are the means \pm SEs of three independent experiments; *p < 0.05, **p < 0.01 vs. the fine dust treated group; #p < 0.05, ##p < 0.01 vs. the un-stimulated group..... 150

Figure 3-10. Effects of HEBI on the fine dust (FD)-induced expression of cytosolic NF- κ B activation in CMT-93 cells (a). Density ratios of each protein was measured using densitometry (b). The values shown are the means \pm SD of three independent experiments. *p < 0.05, **p < 0.01. 153

Figure 3-11. HEBI inhibits fine dust (FD)-induced NF- κ B translocation to the nucleus. Density ratios of each protein was measured using densitometry (b). The values shown are the means \pm SD of three independent experiments. * p < 0.05, ** p < 0.01. 154

Figure 3-12. Effects of HEBI on the phosphorylation of MAPK cascade (pERK1/2, pJNK, and pP38) (a). The relative band intensity was measured as compared with β -actin (b). The values shown are the means \pm SD of three independent experiments. * p < 0.05, ** p < 0.01. 156

Figure 3-13. Effect of HEBI against fine dust (FD)-induced ROS production (a), and SOD suppression (b) in CMT-93 cells. The relative protein levels of catalase and Cu/Zn-SOD in FD induced CMT-93 cells with or without HEBI (c). The values shown are the means \pm SEs of three independent experiments; * p < 0.05, ** p < 0.01 vs. the FD treated group; # p < 0.05, ## p < 0.01 vs. the un-stimulated group. 159

Figure 3- 14. Effect of HEBI against fine dust (FD)-induced cytosolic HO-1, Nrf-2, and Keap-1 expressions in CMT-93 cells. β - actin was used as internal control. Quantitative data was analyzed using ImageJ software (1.43V). Results are expressed as the mean \pm SD of three separate experiments. * p < 0.05 and ** p < 0.01. 162

Figure 3- 15. Effect of HEBI against fine dust (FD)-induced HO-1 and Nrf2 protein (a, b) and mRNA expression (c,d). Western blots and RT-qPCR used evaluate proteins and gene expression levels, respectively. Control was obtained in the absence of FD and HEBI. The values shown are the means \pm SEs of three independent experiments; * p < 0.05, ** p < 0.01 vs. the FD treated group; # p < 0.05, ## p < 0.01 vs. the un-stimulated group. 163

Part 4

Figure 4-1. The molecular structure of 3-Hydroxy-5,6-epoxy- β -ionone isolated from *Sargassum horneri*. (MW: 224.2), PubChem CID: 5371267, Abbreviation: HEBI ... 181

Figure 4-2. Particle size distribution (a) and scanning electron microscope image (b) of fine dust particles. The particle size distribution graph was obtained from the national

institute for environmental studies, Ibaraki, Japan (certified reference material no. 28).
Scale bar represent 10 μm lengthy..... 190

Figure 4-3. Evaluation of fine dust (a) and HEBI (b) induced zebrafish embryo death rates. Experiments were performed in triplicate, and the data are expressed as mean \pm SD, * $p < 0.01$ (n=15) 195

Figure 4-4. Protective effect of HEBI against fine dust induced toxicity (death rates) (a) heart beating rates (b). Experiments were performed in triplicate, and the data are expressed as mean \pm SD, * $p < 0.01$ (n=15) 197

Figure 4-5. HEBI protects zebrafish embryos against fine dust-induced cell death. The cell death levels were measured after acridine orange staining by image analysis and fluorescence microscope. The cell death rates in embryos were quantified using an image J program. Experiments were performed in triplicate, and the data are expressed as mean \pm SD, * $p < 0.01$ (n=15) 200

Figure 4-6. Protective effect of HEBI against fine dust-induced ROS generation in zebrafish embryo. ROS levels were measured after DCF-DA staining by image analysis and fluorescence microscope. The cell death rates were quantified using image J program. Experiments were performed in triplicate, and the data are expressed as mean \pm SD, * $p < 0.01$ (n=15) 201

Figure 4-7. HEBI reduced fine dust-induced NO production in zebrafish larvae. The NO levels were measured by image analysis and fluorescence microscope. Individual zebrafish fluorescence intensity was quantified using image J program. Experiments were performed in triplicate, and the data are expressed as mean \pm SD, * $p < 0.01$ (n=15) 202

Figure 4-8. Effect of HEBI against fine dust (FD)-induced iNOS and COX2 expression in zebrafish embryos. The mRNA expression levels (a, b) and protein expression levels (c, d) of iNOS and COX2. Western blots and RT-qPCR used evaluate proteins and gene expression levels, respectively. Control was obtained in the absence of FD and HEBI. The values shown are the means \pm SEs of three independent experiments; * $p < 0.05$, ** $p < 0.01$ vs. the FD treated group..... 204

Figure 4-9. Inhibitory effect of HEBI on pro-inflammatory mRNA expression in fine dust exposed zebrafish embryos. Zebrafish embryos were stimulated with fine dust in the presence of HEBI for 3 dpf. The mRNA expression of IL-1 β (a), IL-6 (b), and TNF- α (c), were evaluated through RT-qPCR. The values are expressed as the mean \pm SE. Significant differences from the untreated group were identified at * $p < 0.05$ and ** $p < 0.01$206

List of tables

Part 1

Table 1-1. Extraction conditions used for the collect seaweed extracts	16
Table 1-2. Sequence of the primers used to evaluate inflammation related gene expression levels	23
Table 1-3. Extraction efficiency of seaweeds with water, enzymes, and 80% methanol	27
Table 1-4. Polysaccharide composition of seaweed extracts.....	28
Table 1-5. Polyphenol composition of seaweed extracts.....	29

Part 2

Table 2-1. Sequence of the primers used to evaluate inflammation related RNA expression levels.	75
Table 2-2. Primer sequences of mouse TLRs used for the Real-time RT-qPCR	76

Part 3

Table 3-1. Sequence of the primers used to evaluate RNA expression levels.....	129
Table 3-2. Primer sequences of mouse TLRs for Real-time RT-PCR.....	130
Table 3- 3. Certified values of NIES CRM No. 28 Urban Aerosols	134
Table 3-4. Mass fraction of PAHs in NIES CRM No. 28 Urban Aerosols	135
Table 3-5. Toll like receptors and their stimulators.....	145

Part 4

Table 4-1. Sequence of the primers used to evaluate RNA expression levels in zebrafish embryo.	187
Table 4-2. Certified elements values of NIES CRM No. 28 Urban Aerosols	191
Table 4-3. Mass fraction of PAHs in NIES CRM No. 28 Urban Aerosols	192

Background

Fine dust

Air pollution is a process that mixing of pollutants into the atmosphere, which are potentially harm to humans, and cause negative impacts to the surrounding environment (biotic and abiotic). The negative health effects associated with air pollution, have been reported from both indoor and outdoor environments. Due to the high exposure risk even at the low concentrations of fine dust (FD), which become a major health threat to human society. According to the WHO 2017 report 4.2 million deaths report in each year as a direct consequence of air pollution through damage to the respiratory system and lungs (<http://www.who.int/airpollution/en/>). In the East-Asia region (China, Korea, and Japan) fine dust have become a major threat of air pollutions and causing negative health effects on human skin and respiratory system. Specifically, the extensive arid or semiarid highlands of northern China and Mongolia (Gobi Desert, Hunshdak sandy lands, Loess plateau, and Taklimakan desert) are considering as the major sources of dust in Asia region. In addition to the natural phenomenon, coal-burning power plants, rapid developments in industrialization, numerous petroleum vehicles, and large-scale mining operations have contributed to increase the FD concentration in the urban areas located in East-Asia region. Continuous exposure to air pollution such as FD can induce oxidative stress, inflammation, and poses a serious risk to human health. Specifically, it has been reported that the continues exposure to FD contributes to increase the increased use of asthma medication, asthma attacks in patients having asthma, chronic obstructive pulmonary disease (COPD) attacks, hospital admissions for cardiovascular diseases, deaths from heart attacks, strokes and respiratory problems.

According to the Incen AG – Staad, Switzerland, concentrations of FD higher than the $35 \mu\text{g}/\text{m}^3$ to $49.9 \mu\text{g}/\text{m}^3$ in the atmosphere could be contributed to development of pulmonary diseases, cancers, and cardiovascular diseases. Unfortunately, in Korea during 2017 most major cities (Seoul, Suwon, Daegu, Gwangju, and Jeju) had over $90 \mu\text{g}/\text{m}^3$ FD in their atmospheres. Specifically, in Jeju highest FD level was recorded as $250 \mu\text{g}/\text{m}^3$. Therefore, immediate and long-term actions required to reduce negative health effects associated with the FD.

What is inflammation?

Inflammation is a physical response that defends against injury, infection, and irritants through multiple mechanisms. Macrophages play critical role during the inflammatory responses and which are considered as the first line of host-defence against inflammation. Macrophages release a variety of inflammatory mediators including nitric oxide (NO), prostaglandin E2 (PGE₂), and a number of pro-inflammatory cytokines during the inflammatory process. Pro-inflammatory cytokines released by macrophages during the inflammation (interleukin (IL)-1 β , IL-6, and tumour necrosis factor- α ; TNF- α) consequently induce the amount of neutrophils, monocytes, and lymphocytes in the blood stream. As well as those are concentrated at the damaged or infected areas to facilitate tissue recovery and immunostimulant removal from the host. Inflammation is usually fallen into two categories as acute inflammation and chronic inflammation. Acute inflammation is an initial response to the inflammatory agents which initiate rapid and short-term immune responses. Long-term and inappropriate acute inflammatory responses are known as chronic inflammation. The up-regulated pro-inflammatory cytokines production, dysregulation of lipid metabolism, cancer progression, and insulin

resistance are some characteristics features of chronic inflammation. To the date, an infinite number of synthetic anti-inflammatory drugs (SAD) have been developed to treat the diseases associated with chronic inflammation. However, most of the SAD demonstrated adverse side effects such as ulcers, stroke, renal failure irritations, and skin eruptions. In addition to the side effects associated with the SAD, cause to alters genetic and metabolic pathways. In this point of view, natural products are considered as a good alternative for replace SAD as natural compounds are effective and have no or fewer side effects. With the growing body of scientific evidences, seaweeds are promising candidate to develop functional products to reduce inflammation related complications. Therefore, in this Ph.D. dissertation I mainly focused to identify possible anti-inflammatory compound from seaweeds and evaluate their anti-inflammatory mechanisms using LPS and fine dust as inflammatory stimuli using RAW 264.7, MH-S lung macrophages, and zebrafish model. In addition, fine dust exposed CMT-93; digestive tract epithelial cells used to demonstrate effect of FD accumulation in digestive tract and protective effect of compounds isolated from seaweeds against inflammation in digestive system.

What is Oxidative stress?

Free radicals are generally categorized into two groups as reactive oxygen species (ROS) and reactive nitrogen species (RNS). ROS and RNS are molecules/molecular fragments containing unpaired electrons (one or several). The presence of unpaired electrons usually makes them highly reactive in biological systems. The hydroxyl radical (OH), nitric oxide (NO), the superoxide radical anion (O_2^-), and peroxy radicals (ROO) are few well-known free radical species identified in biological systems. Oxidative stress can define as an imbalance between the production of free radicals and the ability of the

cells or organs to defeat or detoxify their harmful effects through neutralization by antioxidants. Internal antioxidant defence mechanisms such as antioxidants (ascorbic acid, tocopherols, and glutathione) and enzymes (superoxide dismutase; SOD, peroxidase, and catalase) are capable to maintain safe levels of ROS inside the cellular environments. However, failures of antioxidant defence mechanisms lead to modifies proteins, making them resistant to ubiquitination. In addition, oxidative stress also damaged to the lipids, and DNA, which could contribute to cytotoxicity, geno-toxicity, aging, and carcinogenesis (breast, bladder, colon, liver, pancreatic, prostate, and skin cancer).

Moreover, oxidative stress is important aspect in inflammation as well pulmonary diseases linked with fine dust such as severe asthma and chronic obstructive pulmonary disease (COPD). Oxidative stress activates the pro-inflammatory cytokines production through transcription factors such as nuclear factor Kappa-B (NF- κ B) and mitogen activated protein kinases (MAPKs) resulting in enhanced inflammation. Oxidative stress is increased in patients with COPD, particularly during exacerbations, and reactive oxygen species contribute to its pathophysiology.

Importance of seaweeds as a food source to avoid FD-induced inflammation and oxidative stress

Seaweeds are a heterogeneous group of plants with the low content of lipids, high amount of polysaccharides, polyunsaturated fatty acids, vitamins, and bioactive molecules. In contrast to the terrestrial plants, algae require flexible structure to withstand the constant stress coming from the ocean currents and motion. According to the botanical definitions, leaves, roots, or vascular systems are absent in typical seaweed. Thus, seaweeds use osmosis to transport nutrients and minerals for growth and development. In addition to

the food value, seaweeds contain diverse secondary metabolites with great pharmaceutical, cosmeceutical, and nutraceutical values. South Korea is one of the top consumer and producer of seaweeds in global market. Traditionally, Korean people consume seaweeds as a vegetable or used as a medicine. Compared to Europe, the food applications and the medicinal applications of seaweeds have strong history in East-Asia including Korea, China, and Japan. Koreans consume seaweeds in fresh forms as well as eat as a dry product after drying under sun. Within Korean traditional diet, seaweeds use to prepare soups (Mi-yeok-guk and Mom-guk,), snacks (Kimbugak), vegetables, pickles, and salads or to prepare gim-bap.

Sargassum horneri the brown seaweed used to isolate pure compounds

Sargassum horneri (Sargassaceae, Fucales, Phaeophyta) is an edible brown seaweed, abundant worldwide in shallow sea-water ecosystems. Thallus of *S. horneri* is a large, macroscopic, and brown-coloured, attached by a solid holdfast, but can also form free-floating mats. Plant body is sporophytic and looks like an angiospermic herb. Main axis or “stem” is cylindrical, erect and flat. Holdfast is irregular, thick and solid structure (up to 3 cm), and helps in the attachment of plant to some substratum. Young plants resemble ferns, with opposite leaf-like blades, extending from a central axis. The blades have broad, deeply incised, ragged tips. As the plant grows, it becomes a single frond, loosely branched, in a zig-zag pattern. Once it matures, the blades become narrower and the branches develop small, ellipsoidal air bladders and larger spindle-shaped reproductive receptacles, both on stalks. The leaves of the young plant and the lateral branches of the primary lateral were produced spirally with a divergence of $2/5$, and this pattern did not change for the entire length of the primary lateral. The airbladders keep the seaweeds upright in the water column. In some locations like Japan, plants can reach 2.5 - 5 m in

height. Other than the ecological importance of this seaweed, which also popular as a nutrient rich edible seaweed specifically in the East-Asian countries. Usually Korean people consume this seaweed as a soup which is a mixture of boiling meat or fish. In Japan, *S. horneri* is known as “akamoku” and is harvested at the maturation stage for eating in regions along the Sea of Japan.

Selection of suitable extraction method

Selection of extraction method for extract target bioactive compounds from seaweeds is one of the important step which has a great impact on the research outcomes. The extraction efficiency depends on the several factors including type of solvent, temperature, particle size, and growth phase of seaweed. However, the selection of suitable extraction method depends on the target compounds.

Water extraction methods

Use of water as an extraction medium is a well-known green extraction technique use to isolate bioactive compounds from seaweeds. Low-cost, non-toxic nature, and the less environmental pollution are some advantages of water extraction. Both hot and cold forms of water use as the extraction medium to isolate water-soluble metabolites from seaweeds. During the last few years, a number of studies reported, the crude and pure compounds separated from seaweeds via water-assisted extraction techniques had the potential to developed as the anti-inflammatory agents. However, low extraction efficiency, high time consumptions are the major dis-advantages of hot water and cold water extractions methods. Thus, the adaptation of water extraction methods for industrial level applications are limited.

Enzyme-assisted extraction methods

Enzyme-assisted extraction is a common extraction method applying to isolate bioactive metabolites from seaweeds. For seaweed extractions carbohydrate degradation enzymes or protease enzymes are mainly use to extract bioactive metabolites from seaweeds. The large amount of cell wall polysaccharides reduce the extraction efficiency and reduce the release of active compounds to the extraction medium. Therefore, enzyme-assisted extraction methods are considering as useful approach to increase the digestion of cell wall materials. In general, extracts separated from food-grade enzyme-assisted extraction methods consider as non-toxic materials. Thus, crude and pure compounds isolated from enzyme-assisted extraction have high demand to use as an active ingredient in products like nutraceuticals, cosmeceuticals, and functional foods.

Organic solvent assisted extraction methods

Organic solvent assisted extraction (OSE) methods are also apply to isolate bioactive compounds from seaweeds. Incubation of seaweed with organic solvents in the room temperature and sonicate seaweed with organic solvents are popular OSE methods. Organic solvents like chloroform, di-chloromethanol, ether, and acetone mainly used isolate compounds like polyphenols, tannins, flavonoids, and terpenoids. Most of the time, OSE methods use to isolate phlorotannins from seaweeds. Specifically, phlorotannins dissolve in the extractants having less polarity than water. Therefore, different combinations of water with methanol, ethanol, or acetone use to extract phlorotannins from brown seaweeds. OSE methods are popular in the industrial level extractions due to the high extraction efficiency and less time consumption.

Part- 1

**Initial screening of seaweeds to identify potential candidates for
separate anti-inflammatory compounds**

Abstract

Background

Recently, seaweeds have gained considerable research attention due to their strong bioactive properties. Generally, seaweeds produce substantial amounts of phytochemicals to avoid the herbivorous and protect them from abiotic stress conditions such as UV radiation. A number of studies have confirmed, compounds produced by seaweeds to protect themselves possess strong bioactive properties under *in vivo* and *in vitro* conditions. However, until now limited number of compounds commercialized for public use and large number of compounds remains under study for bioactivities or not yet consider for biological studies. Specially, compounds produced by seaweeds with anti-inflammatory properties have the potential to develop as functional foods and nutraceuticals. Which will be a solution in the future to reduce chronic inflammatory complications such as autoimmune diseases and some cancers.

Methodology

Four seaweeds *Ecklonia cava*, *Sargassum horneri*, *Ishige okamurae*, and *Porphyra yezoensis* extracted using enzyme assisted extraction methods and 80% methanol. Then the anti-inflammatory effects of each extract evaluated using LPS-activated RAW 264.7 cells. The anti-inflammatory properties of each target evaluated using western blots, ELISA, and RT-qPCR. The identities of purified compounds were confirmed using ¹³C-NMR and mass spectra (FAB-MS and EIMS).

Results

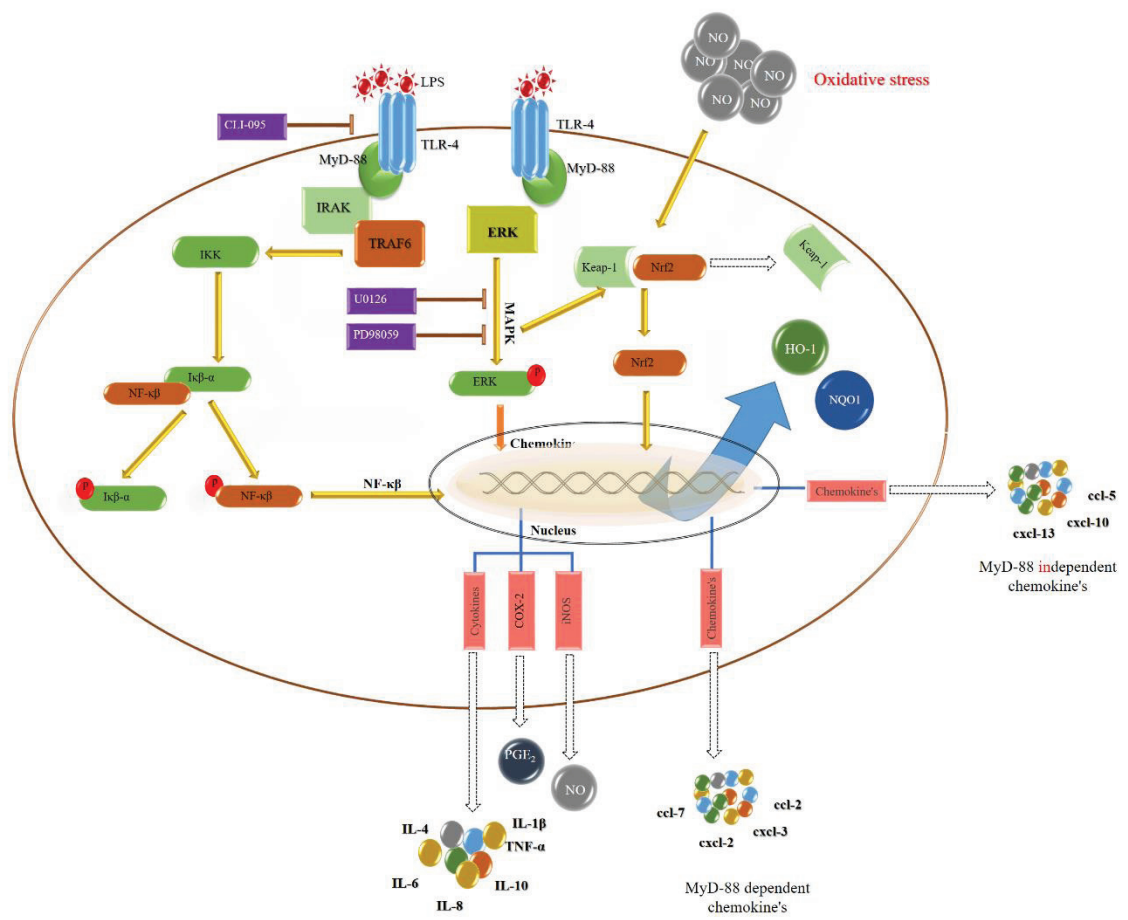
Bioactive guided fractionation led to isolate four bioactive compounds from *S. horneri*. Out of four isolated compounds 2 were first reported from *S. horneri*. The two novel

compounds identified from *S. horneri* were identified as 6-6-hydroxy-4,4,7a-trimethyl-5,6,7,7a-tetrahydrobenzofuran-2(4H)-one (MW: 196.2 Da; Abbreviation: HTT) and 3-Hydroxy-5,6-epoxy- β -ionone (MW: 224.2; Abbreviation: HEBI). The other two were identified as Sargachromanol B and Apo-9'-fucoxanthinone. Specifically, 80% methanol extract of *S. horneri* suppress the LPS-induced inflammation in macrophages via down-regulating NF- κ B and MAPK signal transduction pathways. In addition, gene expression of pro-inflammatory cytokines also reduced with *S. horneri* treatment in LPS-activated macrophages.

Conclusions

According to the results, *S. horneri* strongly reduced fine dust induced inflammation in RAW 264.7 macrophages. Specifically, HEBI isolated from *S. horneri* might have the potential to develop as functional products due to the promising anti-inflammatory properties.

Graphical abstract



Graphical abstract: Responses of macrophages to LPS

1.1. introduction

Within recent recedes, natural ingredients had gained more interest in the industries like functional food, nutraceuticals, and cosmeceuticals. Seaweeds are considering as an interesting marine organism, with great ecological importance and which are contributed to increase the biodiversity of eco-systems where they were originated and habitat (Sanjeewa and Jeon 2018). With the developing interest on seaweed metabolites, the discovery of bioactive secondary metabolites from seaweeds have significantly been increased. Specifically, bioactive secondary metabolites such as, sulphated polysaccharides, carotenoids, and phlorotannins isolated from different seaweed species found to possess the range of bioactive properties including anticancer, anti-inflammation, anti-obesity, antioxidant, anti-allergic, anti-wrinkling, and anti-diabetic. With the aforementioned bioactive properties seaweeds have been considering as an ideal raw material for many industries (Ferreira et al. 2018; Sanjeewa et al. 2017; Sun et al. 2018).

Enzyme-assisted and organic solvent-assisted extractions are two common extraction methods use in different seaweed related industrial applications. Carbohydrate degradation enzymes (Celluclast, viscozyme, and AMG) or protease enzymes (Alcalase and Neutrase) commonly used to extract polysaccharides from seaweeds. The extracts separated using food-grade enzymes consider as non-toxic raw materials for many consumer products such as cosmeceuticals and functional foods (Charoensiddhi et al. 2016). Thus, crude and pure compounds isolated from enzyme-assisted extraction have a high demand to use as an active ingredient in products like nutraceuticals, cosmeceuticals, and functional foods (Wijesinghe and Jeon 2012). In contrast to enzymes, organic solvent assisted extraction (OSE) is a one of the easiest and popular

extraction method applying to separate phlorotannins from brown seaweeds (Sathya et al. 2017). Phlorotannins are easily dissolved in extractants having less polarity than water. Therefore, a mixture of water and methanol, ethanol, or acetone can be used to extract phlorotannins from brown seaweeds. Recently, a number of studies suggested, OSEs are more suitable to isolate phlorotannins from brown seaweed than the EAE (Tierney et al. 2013).

The word inflammation is used to define the complex biological responses of infected or damaged cells to protect host cells from offending agents such as bacteria, virus, and other pathogens (Ptaschinski and Lukacs 2018). However, studies have been revealed that prolong and uncontrolled inflammatory responses have a potential to induce disease conditions such as Alzheimer's disease, rheumatoid arthritis, inflammatory bowel disease, and cancer. Term anti-inflammation refers a property of a treatment or substance which has the ability to modulate inflammatory responses in a host (Annunziato et al. 2015; Grivennikov et al. 2010). Interestingly a large number of studies reported that secondary metabolites presents in seaweed have potential anti-inflammatory activities in *in vitro* and *in vivo* models (Barbosa et al. 2017; de Araújo et al. 2011). In the present study, author attempted to identify suitable extraction method and candidate seaweed to developed anti-inflammatory drugs from brown seaweeds collected along the shores of Jeju Island.

1.2. Materials and Methods

1.2.1. Sample collection

All seaweed species (*Ecklonia cava*, *Sargassum horneri*, *Ishige okamurae*, and *Porphyra yezoensis*) were collected in May and June in 2016 along the shallow costs of Jeju Island in South Korea.

1.2.2. Chemicals and reagents

The murine macrophage cell line RAW 264.7 was purchased from the Korean Cell Line Bank Seoul, Korea. Dulbecco's modified Eagle's medium (DMEM), penicillin-streptomycin, and fetal bovine serum (FBS) were purchased from Gibco BRL (Burlington, ON, Canada). Pierce™ BCA Protein Assay Kit was purchased from Thermo Scientific, Rockford, IL, USA. 3-(4, 5- dimethyl sulfoxide (DMSO), Dimethylthiazol-2-yl)-2, 5-diphenyltetrazolium bromide (MTT), were purchased from Sigma-Aldrich (St. Louis, MO, USA). AMG, Celluclast, Viscozyme, and Alcalase were purchased from Novo Nordisk (Bagsvaerd, Denmark). NE-PER® nuclear and cytoplasmic extraction kit was purchased from Thermo scientific, Rockford, USA. Watman No.4 filter papers were purchased from GE Healthcare, Buckinghamshire, UK. Enzyme-linked immunosorbent assay (ELISA) kits for TNF- α , IL-1 β and PGE₂ were purchased from R&D Systems Inc. (Minneapolis, MN, USA). HPLC grade solvents were purchased from Burdick & Jackson (MI, USA). All other chemicals and reagents used in these experiments were of analytical grade.

1.2.3. preparation of crude 80% methanolic extracts from seaweeds

The freeze-dried seaweed samples were homogenized with a grinder and then, 2 g of seaweed powder was mixed with 100 ml of 80% methanol solution and incubated 24 h

in a shaking incubator. Reaction mixtures were then centrifuged at 5000 x g for 5 min and the supernatants were filtered with Watman No.4 (GE Healthcare, Buckinghamshire, UK) filter papers. The filtrates were concentrated using a rotary evaporator followed by freeze dryer. The freeze-dried powder of seaweed considered as the crude methanolic extract.

1.2.4. Preparation of enzymatic digests from seaweeds

2 g of freeze-dried and homogenized powdered seaweed particles were incubated in 100 ml of distilled water (DW) with 20 µl or 20 mg of each enzyme separately at the optimum temperature and pH (Table 1). After 24 h, the samples were centrifuged at 2,500 x g for 10 min and the supernatants were filtered with Watman No.4 filter papers. Then, the supernatants were freeze-dried and used as enzymatic digests.

1.2.5. Analysis of chemical composition

Total polysaccharide content was measured by the phenol-sulfuric acid method as described by DuBois et al. (1956). Total phenol content was quantified by using a protocol similar to that described by Chandler and Dodds in 1983 (Chandler and Dodds 1983). The protein content of all samples was quantified using the Pierce™ BCA Protein Assay Kit.

Table 1-1. Extraction conditions used for the collect seaweed extracts

Medium	PH	Temperature (°C)	Time
DW	7	RT	24 X 3 h
80 % methanol	7	RT	24 X 3 h
Viscozyme	4.5	50	24 h
Cellucalst	4.5	50	24 h
AMG	4.5	60	24 h
Pepsin	2	37	24 h
Trypsin	8	37	24 h
Protamax	6	40	24 h
Alcalse	8	50	24 h

1.2.6. purification of bioactive compounds from *S. horneri*

The freeze dried *S. horneri* sample (50 g) was extracted three times (less than 40 °C) in 80% methanol solution (1000 ml) using a shaking incubator. The liquid layer was obtained via vacuum filtration, and the filtrates were concentrated using rotary evaporator followed by freeze dryer. The freeze dried powder was considered as the crude methanolic extract of *S. horneri* (CMS). Then the CMS powder was dissolved in distilled water and partitioned according to the polarity using n-hexane (CMSH), chloroform (CMSC), and ethyl acetate (CMSE), respectively. The resulting solvent fractions were concentrated using rotary evaporator and freeze-dried.

1.2.7 Apparatus used for the isolation of active compounds

High performance centrifugal partition chromatography (HPCPC) (Sanki Engineering, Kyoto, Japan) was used in separation procedure. The total cell volume was 240 ml. A four-way switching valve incorporated in the HPCPC, which facilitate the operation of HPCPC in either ascending or descending mode. This HPCPC system was equipped with L-4000 UV detector (Hitachi, Japan) Gilson FC 203B fraction collector (Gilson, France), and Hitachi 6000 pump The chloroform fraction of *S. horneri* was manually injected through a Rheodyne valve (Rheodyne, CA, USA) with a 2 ml sample loop.

The recycle HPLC system was equipped with a liquid feed pump type L-7100 (JAI, Japan), and JAI UV detector 3702 (JAI). The HPLC system contained binary Gilson 321 pump, Gilson 234 auto-injector, 506C interface module (Gilson), and Gilson UV-Vis 151 detector. The ¹H-NMR spectra were measured with a JEOL JNM-LA 300 spectrometer (JEOL Ltd., Tokyo, Japan) and ¹³C-NMR spectra with a Bruker AVANCE

400 spectrometer (BRUKER, Germany). The mass spectra (FAB-MS and EIMS) were recorded on a JEOL JMS 700 spectrometer.

1.2.8. HPCPC separation of *S. horneri* compounds

The HPCPC was performed using a two-phase solvent system composed of water: ethyl acetate: n-Hexane: methanol (1:1:1:1, v/v). The two phase of organic solvents and water mixture was separated using a separation funnel at room temperature after. The top organic phase was used as the stationary phase, whereas the bottom aqueous phase was used as the mobile phase.

1.2.9. HPCPC separation procedure

The HPCPC column was filled with the organic stationary phase and then operated at 1,000 rpm while the mobile phase was pumped into the column in the descending mode at the flow rate used for the separation (2 ml/min). When the mobile phase emerged from the column, indicating that hydrostatic equilibrium had been reached (back pressure: 3.8 MPa). CMSC (0.5 g) dissolved in 6 ml of a 1:1 (v/v) mixture of the two HPCPC solvent system phases was injected through the Rheodyne injection valve. The effluent from the HPCPC was monitored in UV at 254 nm and fractions were collected with 6ml by a Gilson FC 203 B fraction collector.

1.2.10. HPLC analysis

The HPLC system used in this study was equipped with a Waters Reagent Pump, a Waters PDA detector, a Waters auto sampler (Waters Corporation, USA). A 10 ul of 5mg/ml sample solution was injected on C18 column (4.6 × 150 mm, sunfire C18 ODS) using a gradient acetonitrile - water solvent system. The mobile phase was acetonitrile –

water in gradient mode as follows: acetonitrile – water (0 min - 60 min: 5:95 v/v - 100:0 v/v, - 70 min - 100:0 v/v). The flow rate was 1.0 ml/min with various wavelengths by PDA detector.

1.2.11. Cell culture

RAW 264.7 cells were grown in DMEM supplemented with 10% heat-inactivated FBS (30 min in 55 °C), 1% streptomycin (100 µg/ml), and penicillin (100 unit/ml). RAW 264.7 cells were incubated with 5% CO₂ at 37 °C (Sanyo MCO-18AIC CO₂ Incubator; Moriguchi, Japan). Cultured cells from passage 4-6 were used for the experiments.

1.2.12. Cell viability assay

Macrophages (1×10^5 cells/ml) were seeded in a 24-well plate and incubated for 24 h. Then, the cells were incubated with seaweed extracts for 24 h. Then the cells incubated with 50 µl of MTT (200 50 µg/ml). After 3 h of incubation, formosan crystals were dissolved in DMSO, and the color development of blue-black formazan was determined using plate reader machine (BioTek Instruments, Inc., Winooski, USA) at 540 nm.

1.2.13. Determination of NO production

To determine the effect of seaweed extracts on NO production in LPS-stimulated RAW 264.7 cells, author performed Griess assay following a method described by Leiro et al. (2002) with slight modifications. Briefly, the cells (1×10^5 cells/ml) were seeded in 24-well plates and incubated for 24 h. Then, the cells were treated with seaweed extracts (50 µg/ml and 100 µg/ml) for 1 h and stimulated with LPS (1 µg/ml) for 24 h. Finally, equal amounts of culture medium and Griess reagent were reacted in a 96-well plate for

10 min. Then the absorbance was measured at 540 nm using an ELISA plate reader. The results expressed as mean percentages of the NO production versus the NO production of only LPS-treated cells.

1.2.14. Determination of PGE₂, TNF- α , IL-6, and IL-1 β production

RAW 264.7 macrophages (1×10^5 cells/ml) were treated with measured concentrations of seaweed extracts. 1 h later, the macrophages were stimulated with LPS (1 μ g/ml). After 24 h of incubation, the PGE₂, TNF- α , IL-6, and IL-1 β concentration in the supernatant was quantified by using a competitive enzyme immunoassay kits by following the vender's instruction.

1.2.15. Total RNA extraction and cDNA synthesis

Total RNA from RAW 264.7 cells was extracted using Tri-Reagent™ (Sigma-Aldrich, St. Louis, MO, USA) by following the manufactures instructions. Absorbance was measured at 260 nm and 280 nm using a μ Drop Plate (Thermo Scientific) to determine the concentration and purity of the extracted RNA. Then, RNA samples were diluted (1 μ g/ μ l) and first strand cDNA was synthesized using prime Script™ first-strand cDNA synthesis kit (TaKaRa BIO INC, Japan) according to the manufactures instructions. Finale products were stored in a medical refrigerator at -80 °C until use.

1.2.16. Quantitative real-time PCR (RT-qPCR) analysis

Expression levels of pro-inflammatory cytokines were analyzed using SYBR Green quantitative real-time PCR (qPCR) technique with the thermal cycler dice-real time system (TaKaRa, Japan). GAPDH was used as an internal reference gene in amplification. Reactions were carried out in a 10 μ l volume containing 3 μ l diluted cDNA

(20 times diluted in PCR grade water), 0.4 μ l each of the forward and reverse gene specific primers (10 pM), 1.2 μ l of PCR grade water, and 5 μ l of 2 \times TaKaRa ExTaqTM SYBR premix. The reaction was performed using the following thermal profile: one cycle at 95 °C for 10 s, followed by 40 cycles at 95 °C for 5 s, 55 °C for 10 s, and 72 °C for 20 s, and a final single cycle at 95 °C for 15 s, 55 °C for 30 s, and 95 °C for 15 s. The relative expression levels were analyzed according to the method [(2^{- $\Delta\Delta$ CT})] method] describe by Livak and Schmittgen (2001). The base line was automatically set by DiceTM Real Time System software (version 2.00) to keep reliability. The sequence of primers used in this study were shown in Table 1-2 (Bioneer, Seoul, Korea). The data are presented as the mean \pm standard error (SE) of the relative mRNA expression from three consecutive experiments. The two-tailed unpaired Students t-test was used to determine statistical significance (* = $p < 0.05$ and ** = $p < 0.01$).

1.2.17. Western blot analysis

RAW 264.7 macrophages (1×10^5 cells/ml) were seeded in 6-well plates and incubated for 24 h. The cells were treated with the seaweed samples for 1 h and then stimulated with LPS (1 μ g/ml) for 24 h. To determine the NF- κ B and MAPK protein expression levels, first macrophages (1×10^5 cells/ml) were cultured in 6-well plates and incubated for 24 h. Then, the cells were incubated with or without samples (100 μ g/ml) for 1 h and then stimulated with LPS (1 μ g/ml) for 30 min. Cytosolic and nucleus proteins were extracted from macrophages using a NE-PER[®] nuclear and cytoplasmic extraction kit. After separation on a 10% SDS–polyacrylamide gel under denaturing conditions, the cytoplasmic proteins (40 μ g) were electrotransferred onto a nitrocellulose membrane. After blocking with 5% non-fat milk for 1 h, the blots were separately incubated with the following primary antibodies: rabbit polyclonal antibodies (iNOS, p65, pp65, p50,

pp50, and nucleolin), and mouse monoclonal antibodies (COX2, and β -actin) (Cell Signalling Technology, Beverly, MA, USA) for 1 h. The blots were washed twice with Tween 20/Tris-buffered saline (TTBS) and then incubated with HRP-conjugated anti-mouse or anti-rabbit IgG for 60 min. Antibody binding was visualized by using enhanced chemiluminescence (ECL) reagents (Amersham, Arlington Heights, IL, USA). The basal levels of each protein were normalized by analysing the level of β -actin or nucleolin protein by using ImageJ program (V 1.4).

Table 1-2. Sequence of the primers used to evaluate inflammation related gene expression levels

Gene	Primer	Sequence
GAPDH	Sense	5'- AAGGGTCATCATCTCTGCCC-3'
	Antisense	5'-GTGATGGCATGGACTGTGGT-3'
iNOS	Sense	5'-ATGTCCGAAGCAAACATCAC-3'
	Antisense	5'-TAATGTCCAGGAAGTAGGTG-3'
COX2	Sense	5'-CAGCAAATCCTTGCTGTTCC-3'
	Antisense	5'-TGGGCAAAGAATGCAAACATC-3'
IL-1 β	Sense	5'-CAGGATGAGGACATGAGCACC-3'
	Antisense	5'-CTCTGCAGACTCAAACCTCCAC-3'
IL-6	Sense	5'-GTACTCCAGAAGACCAGAGG-3'
	Antisense	5'-TGCTGGTGACAACCACGGCC-3'
TNF- α	Sense	5'-TTGACCTCAGCGCTGAGTTG-3'
	Antisense	5'-CCTGTAGCCCACGTCGTAGC-3'

1.2.18. Statistical analysis

All the data were expressed as the mean \pm standard of three determinations ($n = 3$). The collected data were analyzed by analysis of variance using the SPSS V20 statistical analysis package. The mean values of each experiment were compared using one-way analysis of variance. Duncan's multiple range test (DMRT) was used to determine mean separation. A p -value < 0.05 and 0.01 were considered to be statistically significant.

1.3. Results and discussion

1.3.1. Extraction efficiency of seaweed samples

A number of studies reported the extraction efficiency and bioactive properties of extractants depend on the extraction method (Heffernan et al. 2016). Specifically, organic solvent assisted extraction methods have been used to extract phlorotannins from seaweeds and EAEs are used to extract polysaccharide from seaweeds (Wijesinghe and Jeon 2012). According to the results, 80% methanol extraction had the lowest extraction efficiency compared to the other two methods. Moreover, comparatively extraction efficiency of enzyme assisted extraction had highest efficiency than the water extraction method. The extraction yields of each seaweed shown in the Table 1-3. The extraction efficiency of *Porphyra yezoensis* (red seaweed) overall high compared to the other three brown seaweed species. In addition, extraction efficiency of Celluclast was high compared to the other enzymes. Extraction efficiency of each tested seaweed are shown in Table 1-3.

As the next study author attempted to compare general components of seaweed extracts. As shown in Table 1-4 the lowest polysaccharide composition was recorded from 80% methanolic extract and ranged between 8.61 - 12.14%. The polysaccharides composition of enzyme-assisted extracts were higher than the DW extracts. This results suggesting that the EAEs have the potential to increase polysaccharide extraction efficiency from seaweeds. Moreover, polysaccharide contents of tested enzymes were ranged between 12 - 53%. However, in water extracts the polysaccharide composition was around 13 - 27%. In contrast to polysaccharides, polyphenol composition was high

in the 80% methanolic extracts compared to the EAEs and water extracts (Table 1-5). Specifically, 80% methanol extract of *E. cava* had large amounts of polyphenols (~ 18%).

Table 1-3. Extraction efficiency of seaweeds with water, enzymes, and 80% methanol

Extraction method	<i>Ecklonia cava</i>	<i>Porphyra yezoensis</i>	<i>Sargassum horneri</i>	<i>Ishige okamurae</i>
DW	23.00 ± 2.29	24.50 ± 1.73	16.90 ± 0.87	12.00 ± 1.50
80% MeOH	11.00 ± 0.50	12.33 ± 1.89	12.50 ± 1.80	14.33 ± 1.50
AMG	36.67 ± 1.44	44.33 ± 1.04	24.17 ± 1.53	30.17 ± 0.58
Celluclast	44.83 ± 0.76	57.50 ± 1.32	26.83 ± 1.26	32.33 ± 1.61
Viscozyme	39.17 ± 1.15	56.17 ± 2.84	25.00 ± 2.18	28.66 ± 0.57
Alcalase	37.83 ± 0.76	62.17 ± 0.79	25.50 ± 0.87	30.25 ± 1.84
Pepsin	36.33 ± 0.76	51.83 ± 1.26	17.17 ± 0.76	35.83 ± 1.04
Protamex	26.50 ± 0.51	45.50 ± 1.01	19.50 ± 0.52	23.00 ± 0.52
Trypsin	33.50 ± 0.87	42.33 ± 1.15	21.17 ± 1.53	28.00 ± 1.03

Data are expressed as mean ± SD from three independent experiments (n = 3).

Table 1-4. Polysaccharide composition of seaweed extracts

Extraction method	<i>Ecklonia cava</i>	<i>Porphyra yezoensis</i>	<i>Sargassum horneri</i>	<i>Ishige okamurae</i>
DW	27.46 ± 0.28	26.18 ± 0.14	34.28 ± 0.35	13.91 ± 0.42
80% MeOH	12.14 ± 0.29	10.75 ± 0.71	32.22 ± 0.19	8.61 ± 0.56
AMG	25.06 ± 1.83	31.43 ± 0.67	34.49 ± 0.67	29.35 ± 0.67
Celluclast	41.00 ± 0.51	31.96 ± 0.25	53.29 ± 0.17	21.15 ± 0.12
Viscozyme	35.56 ± 0.01	37.93 ± 0.67	38.52 ± 1.17	33.98 ± 0.15
Alcalase	31.31 ± 2.84	23.76 ± 0.17	32.66 ± 1.58	13.65 ± 0.99
Pepsin	20.67 ± 0.06	25.81 ± 0.08	26.87 ± 0.25	15.93 ± 0.16
Protamex	28.06 ± 0.30	29.22 ± 0.45	34.93 ± 1.79	16.69 ± 0.67
Trypsin	31.31 ± 0.84	36.39 ± 0.51	41.12 ± 0.33	12.82 ± 0.74

Total polysaccharide content was measured by the phenol sulfuric acid method. Glucose used as the standard. Values are mean ± standard deviation (n = 3)

Table 1-5. Polyphenol composition of seaweed extracts

Extraction method	<i>Ecklonia cava</i>	<i>Porphyra yezoensis</i>	<i>Sargassum horneri</i>	<i>Ishige okamurae</i>
DW	7.90 ± 0.14	1.67 ± 0.30	2.46 ± 0.10	2.84 ± 0.33
80% MeOH	18.09 ± 0.62	2.35 ± 0.15	8.72 ± 0.12	6.67 ± 0.25
AMG	7.30 ± 0.33	2.05 ± 0.25	2.20 ± 0.14	2.98 ± 0.00
Celluclast	7.88 ± 0.07	1.64 ± 0.01	2.47 ± 0.01	2.18 ± 0.03
Viscozyme	8.59 ± 0.03	1.73 ± 0.01	2.38 ± 0.05	2.72 ± 0.07
Alcalase	7.16 ± 0.38	0.85 ± 0.03	1.77 ± 0.08	2.26 ± 0.03
Pepsin	4.66 ± 0.03	1.50 ± 0.05	1.11 ± 0.02	2.46 ± 0.12
Protamex	9.29 ± 0.18	2.13 ± 0.15	2.48 ± 0.22	3.35 ± 0.03
Trypsin	8.65 ± 0.51	2.18 ± 0.02	2.66 ± 0.06	3.07 ± 0.12

Total phenol content was quantified by using a protocol described by Chandler and Dodds (1983) using gallic acid as the standard. Values are mean ± standard deviation (n = 3).

1.3.2 Cytotoxicity of seaweed extracts on RAW 264.7 cells

Before evaluate the bioactive properties, author attempted to evaluate cytotoxicity of each seaweed extract using RAW 264.7 cells. Initially two concentrations (50 and 100 µg/ml) used to determine cytotoxicity of extracts. According to the results, 50 and 100 µg/ml concentrations were not affected to the viability of RAW 264.7 cells. However, some extracts of *P. yezoensis* (AMG and Pepsin) showed considerable cytotoxic effect on RAW 264.7 cells. With this results, author decided to discontinue the study with *P. yezoensis* as it having some cytotoxic effect on RAW 264.7 cells under the tested conditions. However, *P. yezoensis* is a popular edible red seaweed in Korea (Herath et al. 2017).

1.3.3 Anti-inflammatory effects of seaweed extracts against LPS-induced NO production in RAW 264.7 cells

Inflammation is a physiological response of the organisms against the damages to the tissues or cells. The inflammatory response leads to activate defence mechanisms such as activation and recruitment of leukocytes to the damage area, triggers the production of NO and stimulate the production of pro-inflammatory mediators such as TNF- α , IL-6, and IL-1 β (Alvarez-Suarez et al. 2017; Ham et al. 2015). According to the previous studies, un-controlled and excessive production of pro-inflammatory mediators has been closely related with the activation of macrophages and the pathogenesis of several chronic diseases (cancer, rheumatoid arthritis, atherosclerosis, and diabetes) (Alvarez-Suarez et al. 2017). LPS is one of the leading activator of macrophages, and the LPS-exposed macrophages produce inflammatory responses through the various inflammatory pathways. The activated macrophages play important roles during the

inflammation through the up-regulated production of NO (Bezerra et al. 2018). The production of NO from macrophages plays a key role in the pathogenesis of inflammation associated diseases and it also cause to induce oxidative stress in the cells (Pacher et al. 2007). Therefore, as the first screening study author compared the NO inhibitory effects of seaweed extracts against LPS-activated macrophages (fig. 1-2). According to the results, 80% methanol extract had highest cyto-protective effect against LPS-induced toxicity in macrophages. Overall, all seaweed extracts significantly increased the viability rates of macrophages against LPS-induced toxicity. However, AMG extract of *E. cava* and DW extract of *I. okamurae* not showed any cyto-protection against LPS-induced toxicity in macrophages. Similar to the cytoprotective data ethanol extracts of 3 tested seaweeds showed strong NO suppressive effect against LPS-stimulated NO production in macrophages. In addition, enzymatic extracts of *I. okamurae* found to possess weaker NO inhibition compared to the other two seaweeds. Previously, it has been reported that the OSE extracts of brown seaweeds are rich in phlorotannins and are more active than the polysaccharides against LPS-induced inflammation in macrophages. In addition, a number of studies demonstrated the methanol extracts were rich in phlorotannins as well as they inhibit LPS-induced NO production from macrophages than the enzyme assisted extracts. (Islam et al. 2013; Lee et al. 2012). Similar to the previous observations, the 80% methanolic extracts showed better cyto-protection as well as NO inhibition levels in LPS-exposed macrophages. With these results author decided to use only 80% methanolic extracts of *E. cava* and *S. horneri* for further studies.

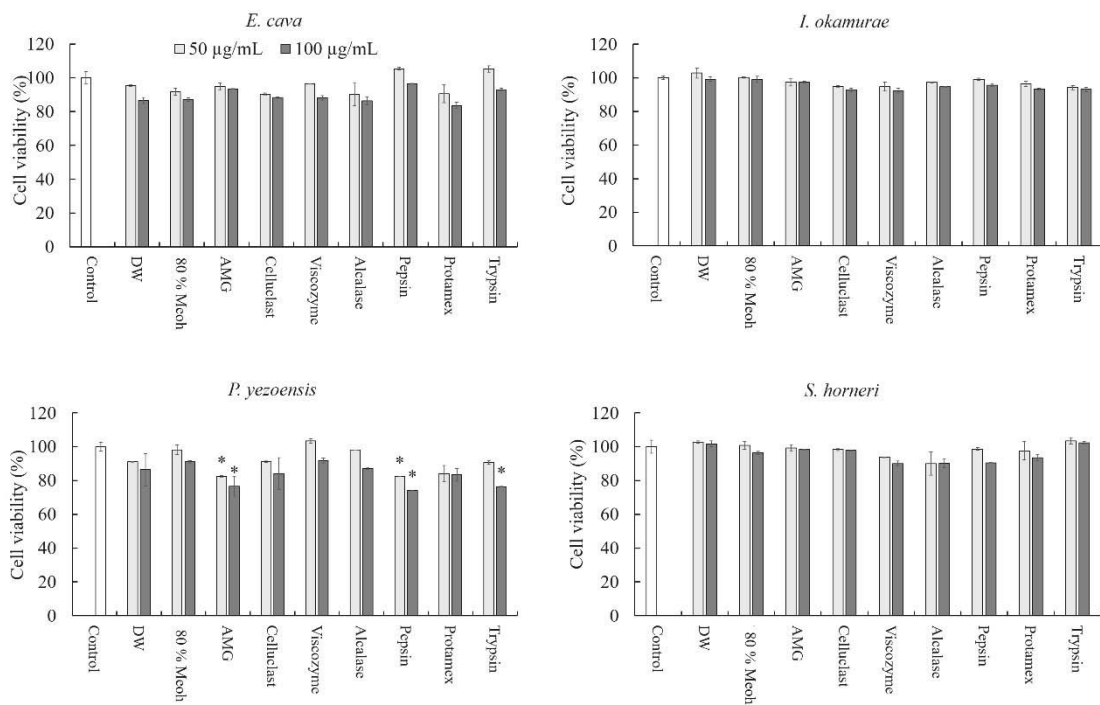


Figure 1-1. Cyto-protective effects of seaweed extracts in RAW 264.7 macrophages. RAW cells were pretreated with different concentrations of seaweed extracts and incubated 24 h. Colorimetric MTT assay was used to determined cell viability. Experiments were carried out in triplicate and the results are represented as means \pm SD. * $P < 0.05$ and ** $P < 0.01$.

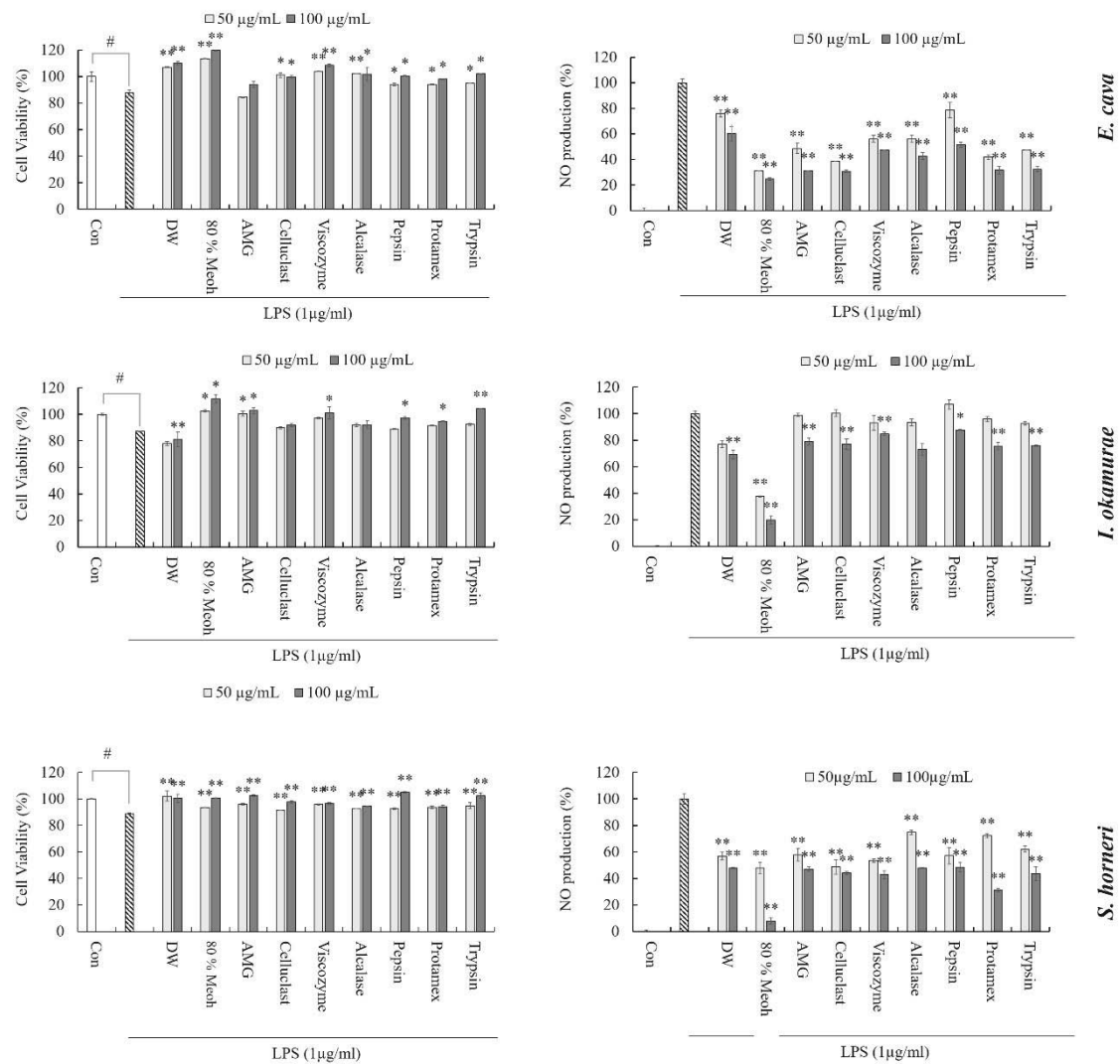


Figure 1-2. Effect of seaweed extracts on NO production in LPS-stimulated RAW 264.7 cells. The cells were incubated with the 50 and 100 µg/ml concentrations of seaweed extracts for 24 h with or without LPS. NO levels in the culture mediums were quantified using Griess assay. Data are expressed as mean \pm SD from three independent experiments and analyzed using one-way ANOVA. # p < 0.01 vs. control, * p < 0.05 and ** p < 0.01 vs. LPS alone treatment.

1.3.4 PGE₂ and Pro-inflammatory cytokine inhibitory effect of 80 % methanolic extracts of *E. cava* and *S. horneri*

PGE₂ is an important inflammatory mediator, which produced during inflammatory responses (Cha et al. 2016). Cytokines also play an important role during the inflammation, which are a group of large proteins (15 - 25 kDa) mainly secreted from immune cells. The production of cytokines useful to inhibit inflammatory responses and active removal of immune stimulants from the site of infection. However, excessive production of pro-inflammatory cytokines (IL-1 β , IL-6, and TNF- α) lead to chronic inflammatory complications in the host tissues and organs (Charrad et al. 2016; Kim et al. 2016).

Therefore, in the present study, author compared PGE₂ and pro-inflammatory cytokine levels in LPS-induced RAW 264.7 cells after the treatment of *S. horneri* and *E. cava* extracts. The exposure of LPS triggers the production of PGE₂ (fig. 1-3a) and pro-inflammatory cytokines from macrophages (fig. 4). However, pre-incubation of seaweed extracts decreased the elevated PGE₂ levels in LPS-exposed RAW 264.7 cells. Moreover, pro-inflammatory cytokines including TNF- α (fig. 1-3b), IL-1 β (fig. 3c), and IL-6 (fig. 1-3d) levels in the culture media was quantified using ELISA method. The results revealed that, pre-treatment of both seaweed extracts suppressed the elevated pro-inflammatory cytokine release from activated macrophages. Specifically, *S. horneri* extract effectively inhibited the TNF- α and IL-6 production from LPS-induced macrophages compared to *E. cava* extract. However, IL-1 β inhibition was high in *E. cava* extract compared to *S. horneri* extract.

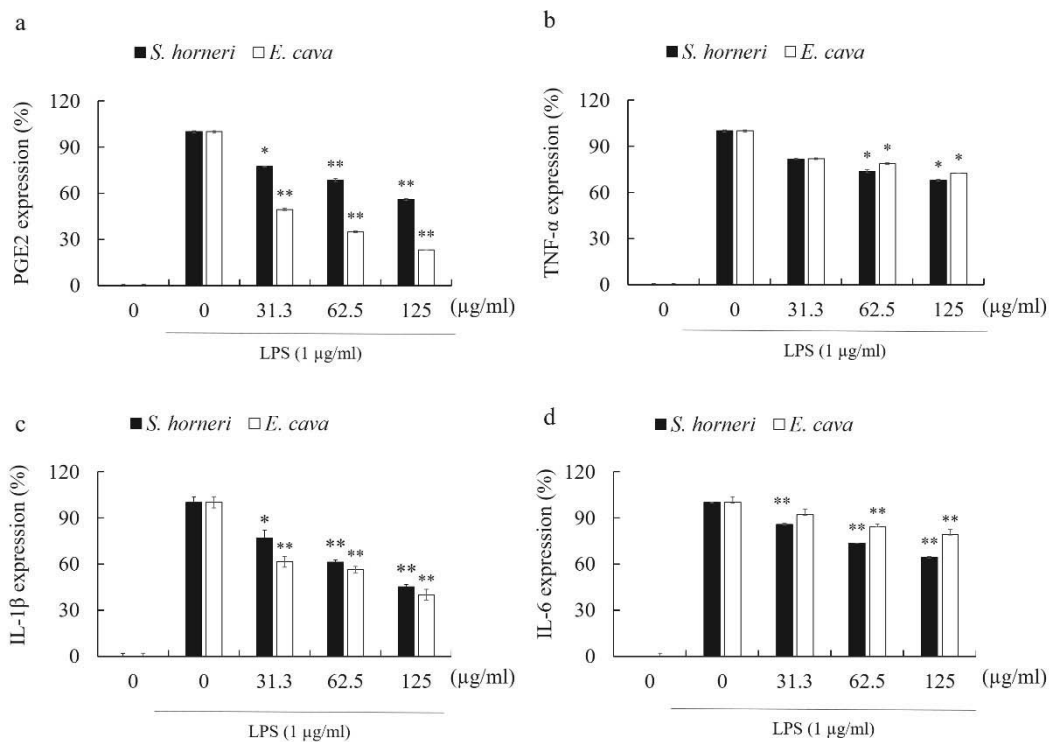


Figure 1-3. PGE₂ and pro-inflammatory cytokine expression inhibitory effect of *Ecklonia cava* and *Sargassum horneri* in LPS-activated RAW 264.7 macrophages. RAW 264.7 macrophages were incubated with 31.3 -125 μg/ml of seaweed extracts for 24 h, and subsequently, they were stimulated with 1 μg/ml of LPS for 24 h. ELISA kits were used to measure PGE₂ (a), TNF-α (b), IL-1β (c), and IL-6 (d) secretion into cell culture medium. Data are expressed as mean ± SD from three independent experiments and analyzed using one-way ANOVA. **P* < 0.05, ***P* < 0.01.

1.3.5 Effects of the seaweed extracts on LPS-induced iNOS and COX2 expression in RAW 264.7 cells

The iNOS and COX2 responsible for the production of NO and PGE₂, respectively in activated macrophages. NO production reflects the degree of inflammation and provides a measure to assess the effect of anti-inflammatory drugs. The activated macrophages produce iNOS in response to LPS, which induce the mass production of NO (Cha et al. 2016; Song et al. 2016). In addition to the NO; PGE₂ is another pro-inflammatory PGs and which has important roles during the inflammation, such as the regulation of immune response, fertility, blood pressure, and gastrointestinal integrity; it is produced by COX2 (Choi et al. 2018).

The expression levels of iNOS and COX2 proteins were evaluated using western blot assay (fig. 1-4). According to the results, expression of iNOS and COX2 protein was markedly increased with the LPS stimulation. However, both seaweed extracts significantly inhibited the up-regulated iNOS and COX2 levels in LPS-induced macrophages. Similar to PGE₂ inhibition *S. horneri* strongly suppressed the COX2 than *E. cava* extract. These results indicating that *S. horneri* and *E. cava* extract decreases NO and PGE₂ production in LPS-induced macrophages via inhibiting iNOS and COX2, respectively. According to the results, 80% methanolic extract of *S. horneri* had comparatively high suppressive effect on inflammatory mediators such as NO, PGE₂, TNF- α , IL-1 β , IL-6, iNOS, and COX2 expressions. Therefore, further studies carried out with *S. horneri* extracts.

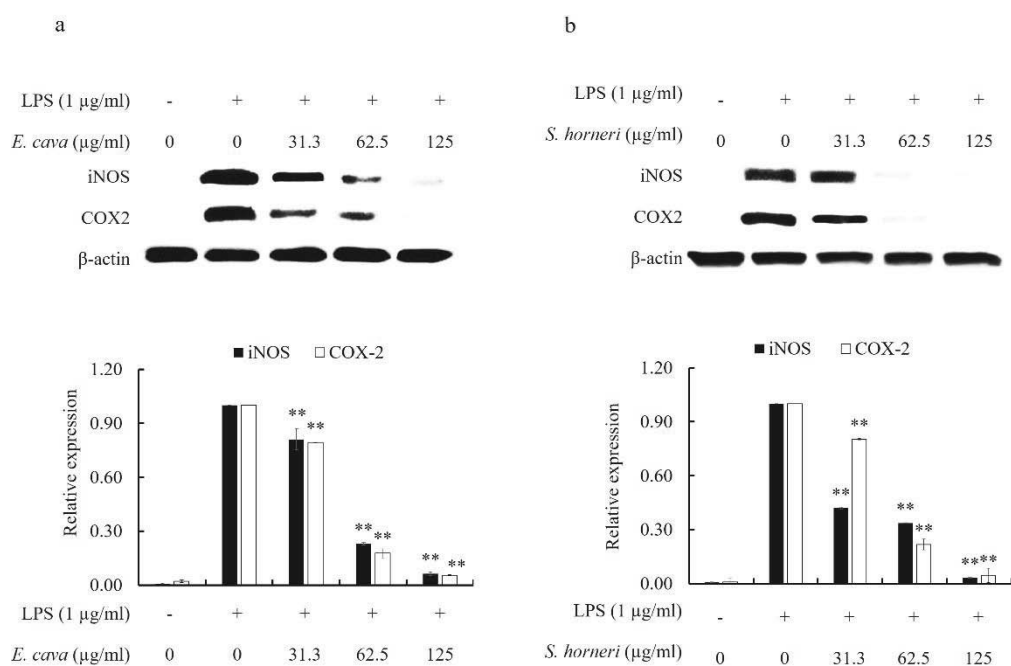


Figure 1-4. Effect of 80% methanolic extracts of *Ecklonia cava* (a) and *Sargassum horneri* (b) on iNOS and COX2 protein expressions in LPS-stimulated RAW 264.7 cells. The cells were incubated with the indicated concentrations of seaweed extracts for 24 h with or without LPS. The protein levels of iNOS and COX2 were determined using Western blot analysis. The bar chart shows the quantitative evaluation of iNOS and COX2 bands by densitometry. Data are expressed as mean \pm SD from three independent experiments and analyzed using one-way ANOVA. * $P < 0.05$, ** $P < 0.01$.

1.3.6. Effect of S. horneri extracts on LPS-induced NF-κB protein expressions

In response to inflammatory stimuli (LPS), macrophages response via activating Toll-like receptors (TLRs) mediated inflammation pathway. In general, TLR-2 and TLR-4 binds to LPS and triggers the subsequent phosphorylation of cytoplasmic proteins, such as MAPK transcription factors related proteins including p38, ERK, and JNK. The activation of TLR-2/4 cause to activate NF-κB and its down-stream transcriptional mediators that induce and increase the inflammation related complications (de Oliveira et al. 2017). In normal cells or at un-stimulated conditions, NF-κB forms a complex with I-κB and is concentrated in the cytosol as an inactivated complex. After the phosphorylation, IκB is ubiquitinated and degraded by 26S proteasome, which resulting the translocation of NF-κB to the nucleus where it activates the transcription of a variety of target genes (Hatada et al. 2000). The activation of NF-κB increase the production of pro-inflammatory mediators such as TNF-α, IL-1β, IL-6, PGE₂, and the activation of inducible enzymes like iNOS and COX2 (Kim et al. 2018). Therefore, inhibition of NF-κB associated protein expression is an important target in anti-inflammatory drugs (Sanjeeva et al. 2017).

Recently a number of studies reported, the extracts separated from seaweeds have the potential to inhibit and translocation of NF-κB proteins to nucleus (Lin et al. 2016; Pádua et al. 2015). Specifically, species belong to family Sargassaceae found to possess strong anti-inflammatory properties under *in vitro* and *in vivo* conditions (Wu et al. 2016) (Chen et al. 2014). Thus, in the current study, author attempted to evaluate effect of *S. horneri* extracts on NF-κB proteins expressions in LPS-exposed macrophages. Similar to previous observations, 80% methanol extract of *S. horneri* has inhibitory effect on LPS-induced phosphorylation of NF-κB P50/65 (fig. 1-5a) and translocation of those

proteins in to the nucleus (fig. 1-5b). These results suggesting, *S. horneri* extract effectively reduced the LPS-induced inflammation responses via blocking the NF- κ B mediated inflammation pathway. Specifically, the inhibition of NF- κ B signal transduction pathway might be the possible reason for the down-regulated expression of iNOS, COX2, and other inflammatory mediators.

1.3.7. The effects of S. horneri 80% methanol extract against pro-inflammatory gene expression in LPS-exposed RAW 264.7 cells.

Gene expression analysis is a key tool which widely used to elucidate the complex regulatory networks of the genetic, signalling, and metabolic pathways. Reverse transcription quantitative real-time polymerase chain reaction (RT-qPCR) is used to determine the fold change of the expression of genes of interest or as a technique to confirm the results of differential protein studies obtained by proteomic analyses (Meng et al. 2017; Murase et al. 2018; Petriccione et al. 2015). Previously, it has been reported that, exposure of macrophages to LPS cause to induce the expression of inflammation related genes such as IL-1 β , IL-4, IL-6, and TNF- α (Kats et al. 2016; Lee et al. 2017). The mRNA expression levels of iNOS (fig. 6a), COX2 (fig.6b), and pro-inflammatory cytokines (IL-1 β , IL-4, IL-6, and TNF- α) in LPS-induced RAW 264.7 cells were quantified using qPCR. Compared to the un-treated control mRNA levels were dramatically increased in LPS-stimulated macrophages (fig. 6). However, treatment of *S. horneri* extract, reduced the elevated mRNA levels in LPS-exposed macrophages in a dose-dependent manner.

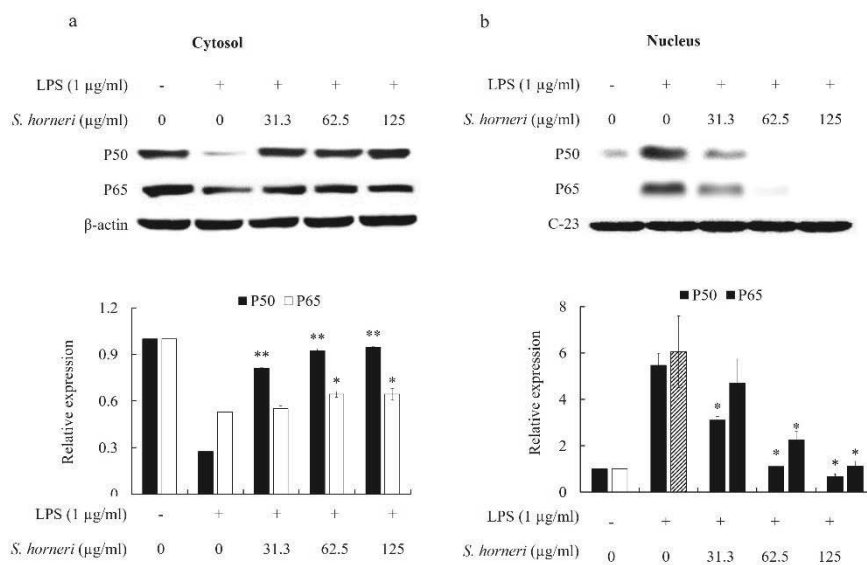


Figure 1-5. Inhibitory effect of 80% methanol extract of *Sargassum horneri* against LPS-induced NF-κB phosphorylation and translocation in RAW 264.7 cells. Macrophages were stimulated with LPS (1 μg/ml) and *S. horneri* extract (31.3 - 125 μg/ml) for 30 min, and the cell lysates were analyzed for the expression of both P50 and P65 in the cytosol (a) and nucleus (b). Results are expressed as mean ± SD from three independent experiments and analyzed using one-way ANOVA. * $P < 0.05$, ** $P < 0.01$.

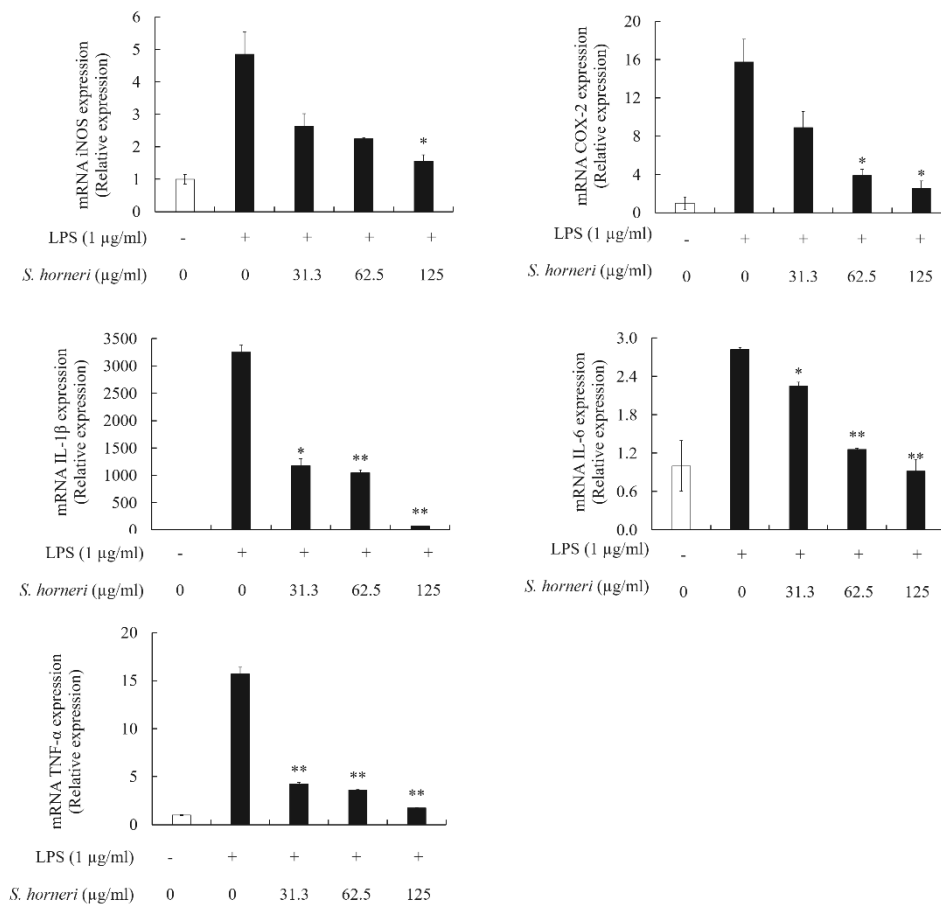


Figure 1-6. Inhibition of LPS- induced iNOS (a), COX2 (b), IL-1β (c), IL-6 (d), and TNF-α (e) mRNA expression by *Sargassum horneri* extracts in RAW 264.7 macrophages. The results were analyzed by the Delta-Ct method and expression of target genes was normalized to GAPDH expression. Control was obtained in the absence of LPS and *S. horneri*. The values shown are the means ± SEs of three independent experiments; * $p < 0.05$, ** $p < 0.01$ vs. the fine dust treated group.

1.3.8. fractionation of S. horneri 80% methanol extract for isolate bioactive compounds

The organic solvent-assisted extraction (ethanol and methanol) and fractionation of extractants with solvent-solvent partition chromatography is a popular and common technique used to identify bioactive metabolites from seaweeds (Pangestuti and Siahaan 2018; Rahelivao et al. 2015; Sanjeeva et al. 2016). Based on the previous results, 80% methanol extract of *S. horneri* (SHM) purified using solvent-solvent partition chromatography (fig. 1-7). SHM was dissolved in DW and fractionated between n-hexane, chloroform, and ethyl acetate (1:1, v/v of sample). During the biological studies, the authors noted the chloroform fraction had strong NO inhibitory effect and cytoprotective effect in LPS-induced macrophages (fig. 1-8). Thus, chloroform fraction was resolved and further purified by pre-optimized HPCPC. The bioactive fraction was analyzed and confirmed by high-performance liquid chromatography (HPLC) LC-DAD-ESI/MS for structure and purity.

1.3.9. NO inhibitory effect of three solvent fractions separated from S. horneri against LPS-induced RAW 264.7 cells

SHM was fractionated into n-hexane (SHMH), chloroform (SHMC), and ethyl acetate (SHME) to identify active fractions and to concentrate bioactive compounds. The three fractions separated from liquid-liquid chromatography were evaluated for anti-inflammatory activities using LPS-activated macrophages (fig. 1-8). The results revealed that, SHMC had significant NO inhibition compared to the other fractions. Specifically, SHMC dose-dependently increased the cell viability of LPS-exposed macrophages. In addition, 125 µg/ml of SHMC had the highest NO inhibition under the tested conditions.

Thus, SHMC further purified using HPCPC. The HPLC spectrum of SHM and SHMC are represented in the figure 1.9.

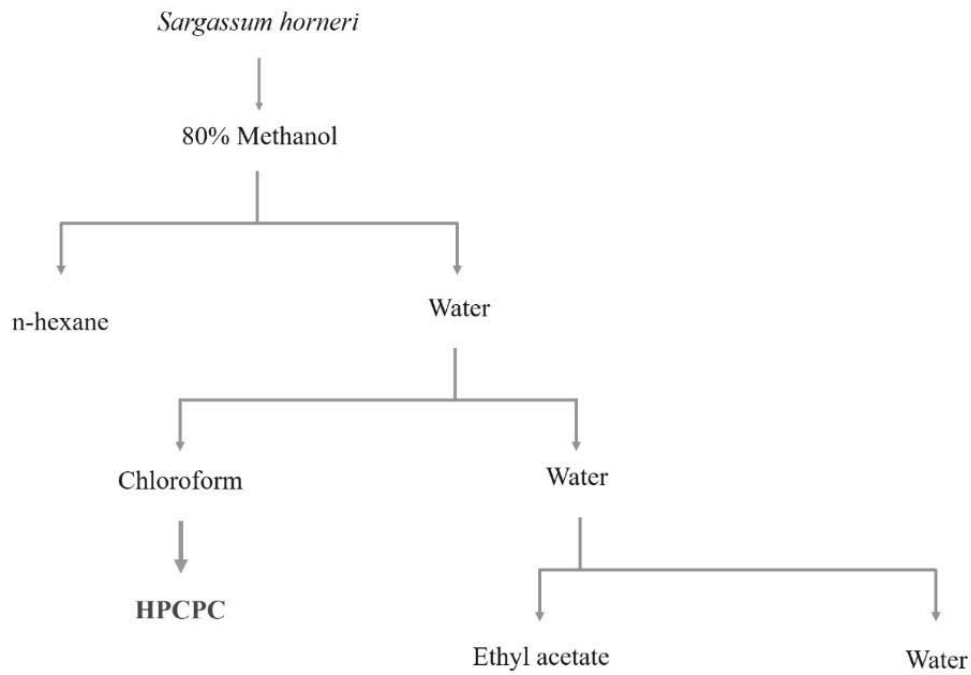


Figure 1-7. Extraction and fractionation of *Sargassum horneri*. First the freeze dried seaweed powder was extracted with 80% methanol, concentrated using rotary evaporator and freeze dried. Then the freeze dried samples were further purified using solvent-solvent partition chromatography and High performance centrifugal partition chromatography.

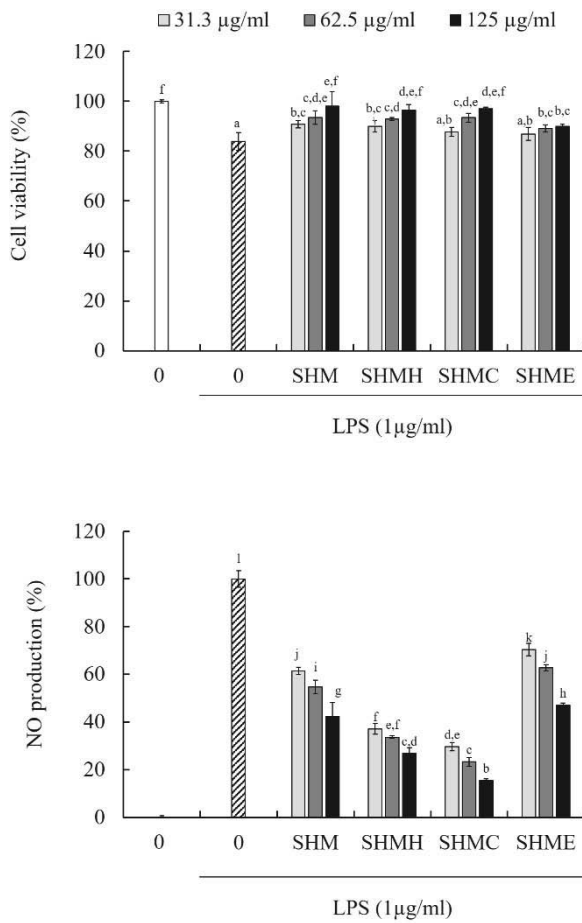


Figure 1-8. Protective effect of *Sargassum horneri* 80% methanol extract and its fractions against LPS-exposed macrophages. The cells were incubated with the 31.3 - 125 µg/ml concentrations of SHM, SHMH, SHMC, and SHME for 24 h with or without LPS. The level of NO in the culture media was quantified using Griess assay. Data are expressed as mean ± SD from three independent experiments and analyzed using one-way ANOVA. Means with same letters are not significantly different at 0.05 sigma level

*SHM- 80% methanol extract of *S. horneri*. The fourth character followed by SHM is standard for the fractions of SHM. (hexane (H), chloroform (C), and ethyl acetate (E))

1.3.10. HPCPC and HPLC spectrums of SHMC after HPCPC chromatography

Based on the anti-inflammatory properties of SHMC fraction, which was further purified using HPCPC system. After the HPCPC chromatography author obtained 5 fractions from the initial sample as shown in the figure 1-9a. Then the purity of each fraction evaluated using HPLC with different wave lengths (fig. 1-9b). Based on NO suppressive effect in LPS-activated macrophages (data not shown) SHMC-II-B, SHMC-III-C, and SHMC-III-D used to further study. Under different wave lengths 230 nm and 254 nm SHMC-II-B yielded 2 different spectrums (Data not present). Therefore, under different wavelengths the active peaks were concentrated using HPLC and purity of each compound confirmed using NMR and GC-MS techniques (fig. 1-10 and 1-11). Out of 4 isolated compounds two were newly identified from *S. horneri*. The two compounds were known as 6-hydroxy-4,4,7a-trimethyl-5,6,7,7a-tetrahydrobenzofuran-2(4H)-one (MW: 196.2 Da; Abbreviation: HTT) and 3-Hydroxy-5,6-epoxy- β -ionone (also known as- 3-Hydroxy-5,6-epoxy- β -ionone) (MW: 224.2; Abbreviation: HEBI). The other two were identified as Sargachromanol B and Apo-9'-fucoxanthinone.

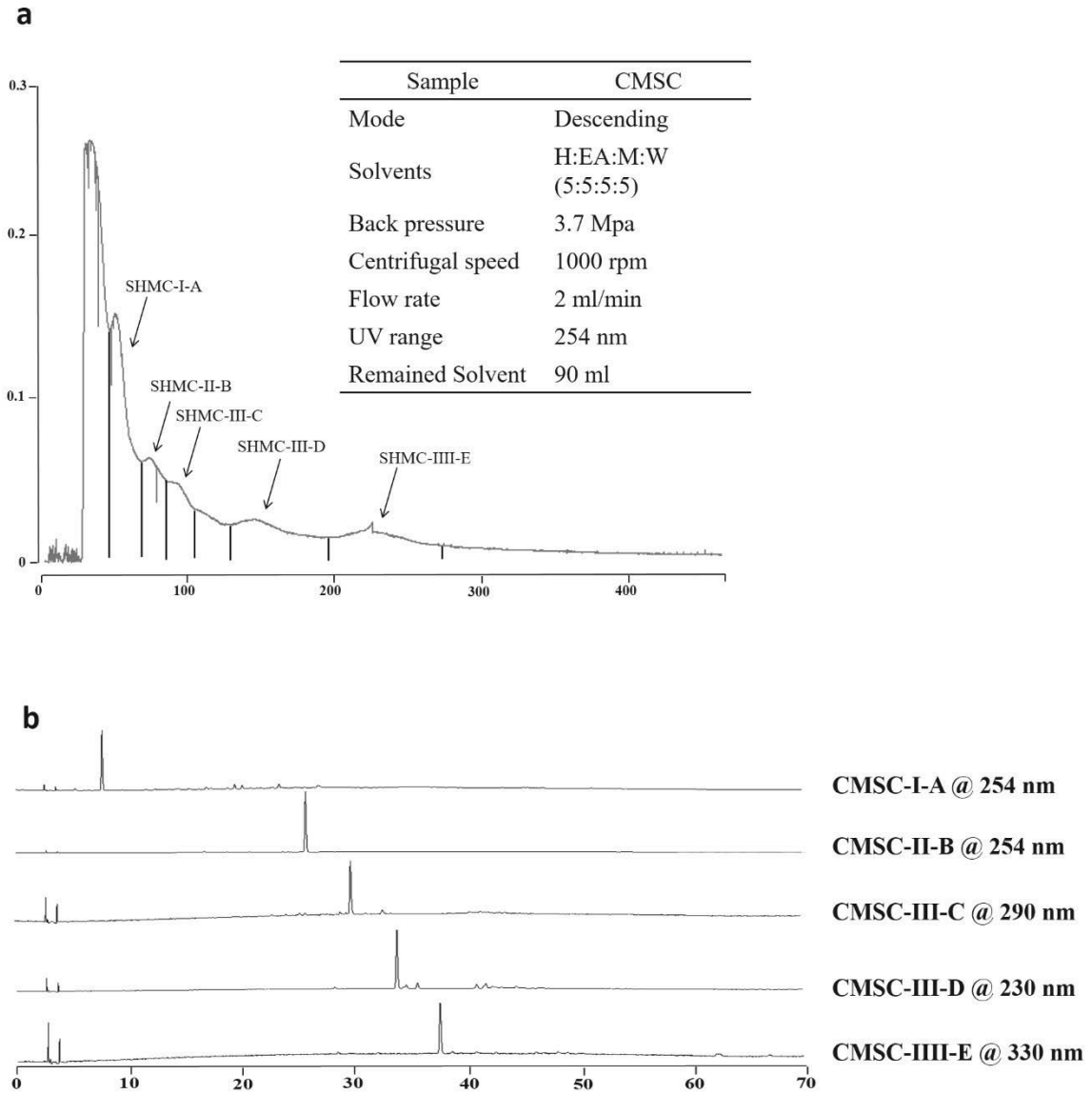
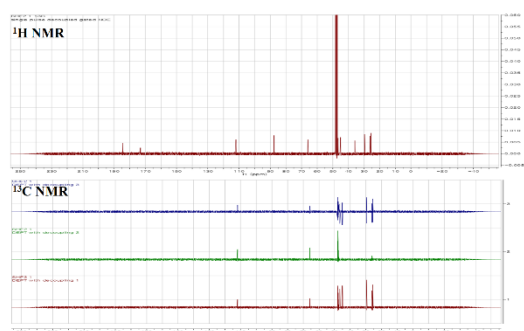
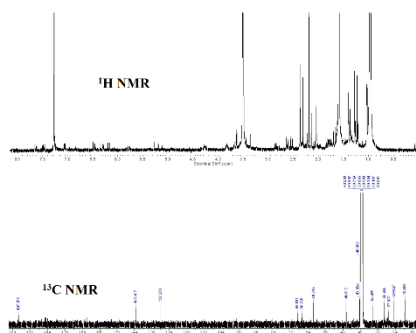


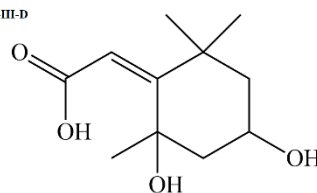
Figure 1-9. HPCPC chromatography (a) & HPLC spectrums (b) of each fraction obtained from *Sargassum horneri* chloroform fraction



CMSC-II-B-b

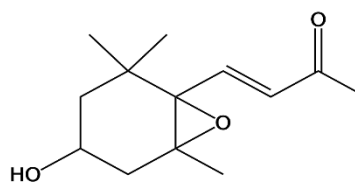


CMSC-II-D



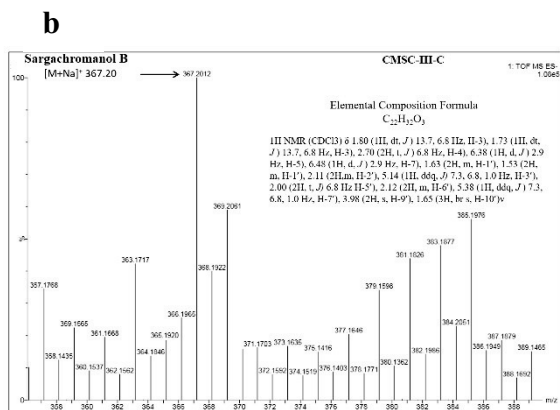
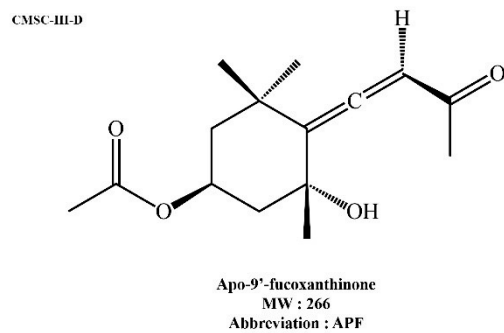
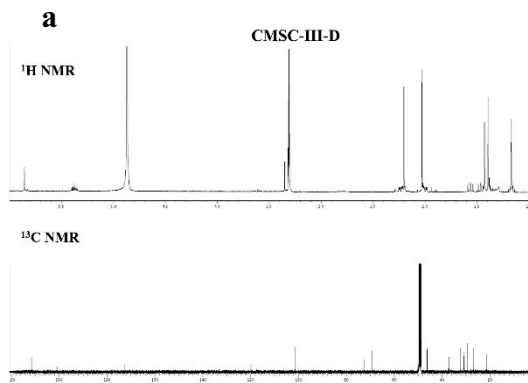
6-(6-hydroxy-4,4,7a-trimethyl-5,6,7,7a-tetrahydrobenzofuran-2(4H)-one
MW: 196.2 Da
Abbreviation : HTT

SHF2-2
DMSO



3-buten-2-one, 4-(4-hydroxy-2,2,6-trimethyl-7-oxabicyclo[4.1.0]hept-1-yl)- or
3-hydroxy-5,6-epoxy- β -ionone
MW: 224.2
Abbreviation : HEI

Figure 1-10. proton and ^{13}C NMR spectrums of 2 novel compounds isolated from *Sargassum horneri* and their structures with IUPAC nominations



LC/MS spectrum

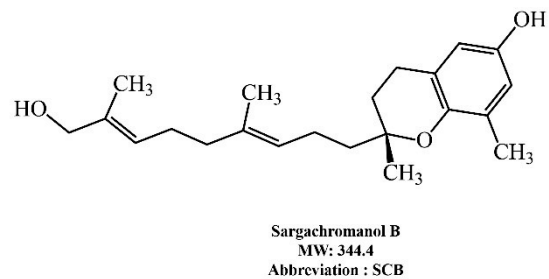


Figure 1-11. Proton and ¹³C NMR spectrums of Apo-9'-fucoxanthinon and its structure (a). The LC-MS spectrum and the structure of Sargachromanol B (b) isolated from *Sargassum horneri*

1.3.11. Anti-inflammatory properties and cytoprotective effect of four pure compounds isolated from S. horneri.

As the last study of preliminary study, author attempted to evaluate NO inhibitory effect of isolated compounds using LPS-activated RAW 264.7 macrophages. According to the results, all isolated compounds had a protective effect against LPS-induced toxicity in RAW macrophage cells (fig. 1-12a). Furthermore, the compound 2 (HEBI) strongly suppressed the LPS-induced NO production and the IC₅₀ was less than 15.6 µg/ml. In addition, the compound 3; Sargachromanol B also strongly suppressed the LPS-induced NO production from RAW 264.7 cells. However, the compound 1; HTT and the compound 4; Apo-9'-fucoxanthinone had less NO suppressive effect between 15.6 – 62.5 µg/ml. Based on these results, HEBI is a possible candidate compound to develop functional products from *S. horneri*.

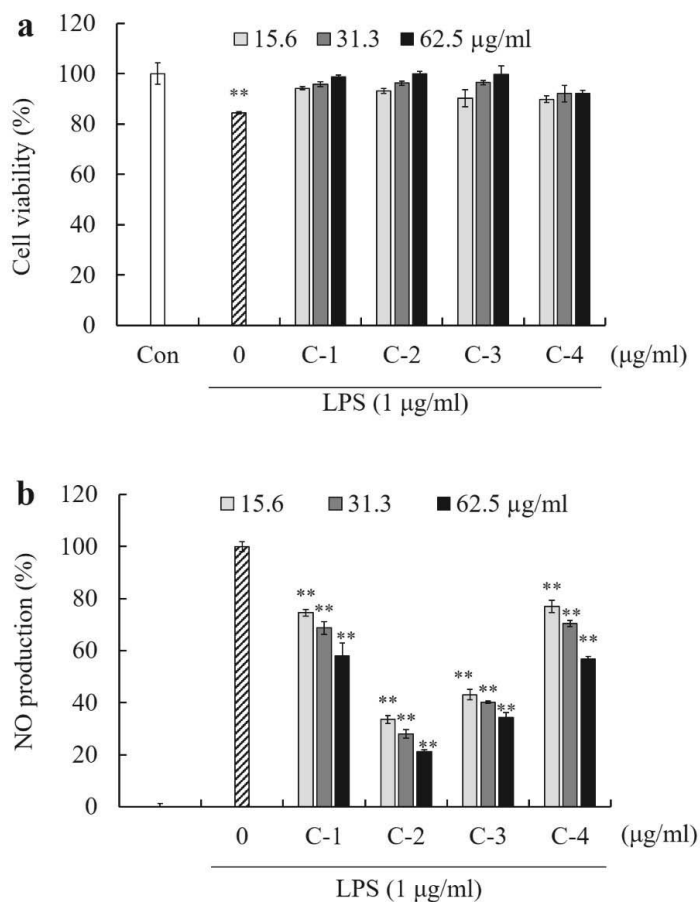


Figure 1-12. Cyto-protective effect and NO inhibitory properties of 4 compounds isolated from *Sargassum horneri* in LPS-activated macrophages. Data are expressed as mean \pm SD from three independent experiments. The values shown are the means \pm SEs of three independent experiments; * p < 0.05, ** p < 0.01 vs. the LPS-stimulated group.

C-1; 6-6-hydroxy-4,4,7a-trimethyl-5,6,7,7a-tetrahydrobenzofuran-2(4H)-one; HTT

C-2; 3-Hydroxy-5,6-epoxy- β -ionone; HEBI

C-3; Sargachromanol B

C-4; Apo-9'-fucoxanthinone

1.4. Conclusions

Based on the extraction results, the extraction efficiency of seaweeds depends on the method of extraction. Specifically, the enzyme assisted extraction methods are ideal to extract polysaccharides for industrial applications than the organic solvent assisted extraction methods. However, OSEs are ideal to isolate phenolic compounds from seaweeds.

However, according to the bio-activities of 80% methanolic extracts had better anti-inflammatory activities under tested conditions. High percentage of polyphenol in the 80% methanolic extracts of seaweeds might be the possible reason for this improved anti-inflammatory properties. During the initial screening studies, *S. horneri* showed strong anti-inflammatory properties than the other seaweeds. Therefore, only 80% methanol extract of *S. horneri* used to evaluate anti-inflammatory properties against LPS-activated RAW 264.7 macrophages. According to the ELISA and RT-qPCR data IL-6 and TNF- α levels in LPS-activated macrophages were reduced by the *S. horneri* extract; which are considering as the bio-markers of fine dust induced inflammation. According to the bioassays guided fractionations, four compounds were isolated from *S. horneri* and all isolated compounds had strong NO inhibitory properties. However, 2nd compound (HEBI) strongly suppressed the LPS-induced NO production from macrophages. Our results revealed *S. horneri* extract and its pure compounds has inhibitory effect on NF- κ B mediated inflammatory pathway and pro-inflammatory gene expression in LPS-exposed macrophages.

1.5. References

Alvarez-Suarez J. M., Carrillo-Perdomo E., Aller A., Giampieri F., Gasparrini M., Gonzalez-Perez L., Beltran-Ayala P., and Battino M. (2017). Anti-inflammatory effect of Capuli cherry against LPS-induced cytotoxic damage in RAW 264.7 macrophages. *Food Chem Toxicol*, **102**. Pp: 46-52. DOI: 10.1016/j.fct.2017.01.024

Annunziato F., Romagnani C., and Romagnani S. (2015). The 3 major types of innate and adaptive cell-mediated effector immunity. *J Allergy Clin Immunol*, **135**(3). Pp: 626-35. DOI: 10.1016/j.jaci.2014.11.001

Barbosa M., Lopes G., Ferreres F., Andrade P. B., Pereira D. M., Gil-Izquierdo Á., and Valentão P. (2017). Phlorotannin extracts from Fucales: Marine polyphenols as bioregulators engaged in inflammation-related mediators and enzymes. *Algal Research*, **28**. Pp: 1-8. DOI: <https://doi.org/10.1016/j.algal.2017.09.009>

Bezerra I. L., Caillot A. R. C., Palhares L., Santana-Filho A. P., Chavante S. F., and Sasaki G. L. (2018). Structural characterization of polysaccharides from Cabernet Franc, Cabernet Sauvignon and Sauvignon Blanc wines: Anti-inflammatory activity in LPS stimulated RAW 264.7 cells. *Carbohydr Polym*, **186**. Pp: 91-99. DOI: 10.1016/j.carbpol.2017.12.082

Cha S. M., Cha J. D., Jang E. J., Kim G. U., and Lee K. Y. (2016). Sophoraflavanone G prevents *Streptococcus mutans* surface antigen I/II-induced production of NO and PGE2 by inhibiting MAPK-mediated pathways in RAW 264.7 macrophages. *Arch Oral Biol*, **68**. Pp: 97-104. DOI: 10.1016/j.archoralbio.2016.04.001

Chandler S. F., and Dodds J. H. (1983). The effect of phosphate, nitrogen and sucrose on the production of phenolics and solasodine in callus cultures of *Solanum laciniatum*. *Plant Cell Reports*, **2**(4). Pp: 205-208. DOI: 10.1007/BF00270105

Charoensiddhi S., Lorbeer A. J., Lahnstein J., Bulone V., Franco C. M. M., and Zhang W. (2016). Enzyme-assisted extraction of carbohydrates from the brown alga *Ecklonia*

radiata : Effect of enzyme type, pH and buffer on sugar yield and molecular weight profiles. *Process Biochemistry*, **51**(10). Pp: 1503-1510. DOI: 10.1016/j.procbio.2016.07.014

Charrad R., Berraies A., Hamdi B., Ammar J., Hamzaoui K., and Hamzaoui A. (2016). Anti-inflammatory activity of IL-37 in asthmatic children: Correlation with inflammatory cytokines TNF-alpha, IL-beta, IL-6 and IL-17A. *Immunobiology*, **221**(2). Pp: 182-7. DOI: 10.1016/j.imbio.2015.09.009

Chen X., Yu G., Fan S., Bian M., Ma H., Lu J., and Jin L. (2014). Sargassum fusiforme polysaccharide activates nuclear factor kappa-B (NF-kappaB) and induces cytokine production via Toll-like receptors. *Carbohydr Polym*, **105**. Pp: 113-20. DOI: 10.1016/j.carbpol.2014.01.056

Choi Y. K., Ye B. R., Kim E. A., Kim J., Kim M. S., Lee W. W., Ahn G. N., Kang N., Jung W. K., and Heo S. J. (2018). Bis (3-bromo-4,5-dihydroxybenzyl) ether, a novel bromophenol from the marine red alga *Polysiphonia morrowii* that suppresses LPS-induced inflammatory response by inhibiting ROS-mediated ERK signaling pathway in RAW 264.7 macrophages. *Biomed Pharmacother*, **103**. Pp: 1170-1177. DOI: 10.1016/j.biopha.2018.04.121

de Araújo I. W. F., Vanderlei E. d. S. O., Rodrigues J. A. G., Coura C. O., Quinderé A. L. G., Fontes B. P., de Queiroz I. N. L., Jorge R. J. B., Bezerra M. M., and e Silva A. A. R. (2011). Effects of a sulfated polysaccharide isolated from the red seaweed *Solieria filiformis* on models of nociception and inflammation. *Carbohydrate polymers*, **86**(3). Pp: 1207-1215. DOI: <https://doi.org/10.1016/j.carbpol.2011.06.016>

de Oliveira R. G., de Campos Castilho G. R., da Cunha A. L., Miyajima F., and de Oliveira Martins D. T. (2017). *Dilodendron bipinnatum* Radlk. inhibits pro-inflammatory mediators through the induction of MKP-1 and the down-regulation of MAPKp38/JNK/NF-kappaB pathways and COX-2 in LPS-activated RAW 264.7 cells. *J Ethnopharmacol*, **202**. Pp: 127-137. DOI: 10.1016/j.jep.2017.02.026

DuBois M., Gilles K. A., Hamilton J. K., Rebers P. A., and Smith F. (1956). Colorimetric Method for Determination of Sugars and Related Substances. *Analytical Chemistry*, **28**(3). Pp: 350-356. DOI: 10.1021/ac60111a017

Ferreira J., Ramos A. A., Almeida T., Azqueta A., and Rocha E. (2018). Drug resistance in glioblastoma and cytotoxicity of seaweed compounds, alone and in combination with anticancer drugs: A mini review. *Phytomedicine*, **48**. Pp: 84-93. DOI: 10.1016/j.phymed.2018.04.062

Grivennikov S. I., Greten F. R., and Karin M. (2010). Immunity, inflammation, and cancer. *Cell*, **140**(6). Pp: 883-99. DOI: 10.1016/j.cell.2010.01.025

Ham Y.-M., Ko Y.-J., Song S.-M., Kim J., Kim K.-N., Yun J.-H., Cho J.-H., Ahn G., and Yoon W.-J. (2015). Anti-inflammatory effect of litsenolide B2 isolated from *Litsea japonica* fruit via suppressing NF- κ B and MAPK pathways in LPS-induced RAW264.7 cells. *Journal of Functional Foods*, **13**. Pp: 80-88. DOI: 10.1016/j.jff.2014.12.031

Hatada E. N., Krappmann D., and Scheidereit C. (2000). NF- κ B and the innate immune response. *Current Opinion in Immunology*, **12**(1). Pp: 52-58. DOI: 10.1016/s0952-7915(99)00050-3

Heffernan N., Smyth T., FitzGerald R. J., Vila-Soler A., Mendiola J., Ibáñez E., and Brunton N. (2016). Comparison of extraction methods for selected carotenoids from macroalgae and the assessment of their seasonal/spatial variation. *Innovative Food Science & Emerging Technologies*, **37**. Pp: 221-228. DOI: <https://doi.org/10.1016/j.ifset.2016.06.004>

Herath K. H. I. N. M., Lee J. H., Cho J., Kim A., Shin S. M., Kim B., Jeon Y. J., and Jee Y. (2017). Immunostimulatory Effect of Pepsin Enzymatic Extract from *Porphyra yezoensis* on Murine Splenocytes. *Journal of the Science of Food and Agriculture*. Pp. DOI:

- Islam M. N., Ishita I. J., Jin S. E., Choi R. J., Lee C. M., Kim Y. S., Jung H. A., and Choi J. S. (2013). Anti-inflammatory activity of edible brown alga *Saccharina japonica* and its constituents pheophorbide a and pheophytin a in LPS-stimulated RAW 264.7 macrophage cells. *Food Chem Toxicol*, **55**. Pp: 541-8. DOI: 10.1016/j.fct.2013.01.054
- Kats A., Norgard M., Wondimu Z., Koro C., Concha Quezada H., Andersson G., and Yucel-Lindberg T. (2016). Aminothiazoles inhibit RANKL- and LPS-mediated osteoclastogenesis and PGE2 production in RAW 264.7 cells. *J Cell Mol Med*, **20**(6). Pp: 1128-38. DOI: 10.1111/jcmm.12814
- Kim E.-A., Kim S.-Y., Ye B.-R., Kim J., Ko S.-C., Lee W. W., Kim K.-N., Choi I.-W., Jung W.-K., and Heo S.-J. (2018). Anti-inflammatory effect of Apo-9'-fucoxanthinone via inhibition of MAPKs and NF-kB signaling pathway in LPS-stimulated RAW 264.7 macrophages and zebrafish model. *International immunopharmacology*, **59**. Pp: 339-346.
- Kim Y. K., Na K. S., Myint A. M., and Leonard B. E. (2016). The role of pro-inflammatory cytokines in neuroinflammation, neurogenesis and the neuroendocrine system in major depression. *Prog Neuropsychopharmacol Biol Psychiatry*, **64**. Pp: 277-84. DOI: 10.1016/j.pnpbp.2015.06.008
- Lee M. S., Kwon M. S., Choi J. W., Shin T., No H. K., Choi J. S., Byun D. S., Kim J. I., and Kim H. R. (2012). Anti-inflammatory activities of an ethanol extract of *Ecklonia stolonifera* in lipopolysaccharide-stimulated RAW 264.7 murine macrophage cells. *J Agric Food Chem*, **60**(36). Pp: 9120-9. DOI: 10.1021/jf3022018
- Lee P.-P., Lin Y.-H., Chen M.-C., and Cheng W. (2017). Dietary administration of sodium alginate ameliorated stress and promoted immune resistance of grouper *Epinephelus coioides* under cold stress. *Fish & Shellfish Immunology*, **65**. Pp: 127-135. DOI: <https://doi.org/10.1016/j.fsi.2017.04.007>

Leiro J., Álvarez E., García D., and Orallo F. (2002). Resveratrol modulates rat macrophage functions. *International Immunopharmacology*, **2**(6). Pp: 767-774. DOI: [http://dx.doi.org/10.1016/S1567-5769\(02\)00014-0](http://dx.doi.org/10.1016/S1567-5769(02)00014-0)

Lin H.-T. V., Lu W.-J., Tsai G.-J., Chou C.-T., Hsiao H.-I., and Hwang P.-A. (2016). Enhanced anti-inflammatory activity of brown seaweed *Laminaria japonica* by fermentation using *Bacillus subtilis*. *Process Biochemistry*, **51**(12). Pp: 1945-1953. DOI: [10.1016/j.procbio.2016.08.024](https://doi.org/10.1016/j.procbio.2016.08.024)

Livak K. J., and Schmittgen T. D. (2001). Analysis of relative gene expression data using real-time quantitative PCR and the 2- $\Delta\Delta$ CT method. *Methods*, **25**(4). Pp: 402-408. DOI: [10.1006/meth.2001.1262](https://doi.org/10.1006/meth.2001.1262)

Meng Q., Zhuang Y., Ying Z., Agrawal R., Yang X., and Gomez-Pinilla F. (2017). Traumatic Brain Injury Induces Genome-Wide Transcriptomic, Methylopic, and Network Perturbations in Brain and Blood Predicting Neurological Disorders. *EBioMedicine*, **16**. Pp: 184-194. DOI: [10.1016/j.ebiom.2017.01.046](https://doi.org/10.1016/j.ebiom.2017.01.046)

Murase M., Kawasaki T., Hakozaiki R., Sueyoshi T., Putri D. D. P., Kitai Y., Sato S., Ikawa M., and Kawai T. (2018). Intravesicular Acidification Regulates Lipopolysaccharide Inflammation and Tolerance through TLR4 Trafficking. *The Journal of Immunology*. Pp: [ji1701390](https://doi.org/10.1093/ijl/abz013).

Pacher P., Beckman J. S., and Liaudet L. (2007). Nitric oxide and peroxynitrite in health and disease. *Physiol Rev*, **87**(1). Pp: 315-424. DOI: [10.1152/physrev.00029.2006](https://doi.org/10.1152/physrev.00029.2006)

Pádua D., Rocha E., Gargiulo D., and Ramos A. A. (2015). Bioactive compounds from brown seaweeds: Phloroglucinol, fucoxanthin and fucoidan as promising therapeutic agents against breast cancer. *Phytochemistry Letters*, **14**. Pp: 91-98. DOI: [10.1016/j.phytol.2015.09.007](https://doi.org/10.1016/j.phytol.2015.09.007)

Pangestuti R., and Siahaan E. A. (2018). *Seaweed-Derived Carotenoids*, in *Bioactive Seaweeds for Food Applications*. Elsevier. p. 95-107

Petriccione M., Mastrobuoni F., Zampella L., and Scortichini M. (2015). Reference gene selection for normalization of RT-qPCR gene expression data from *Actinidia deliciosa* leaves infected with *Pseudomonas syringae* pv. *actinidiae*. *Sci Rep*, **5**. Pp: 16961. DOI: 10.1038/srep16961

Ptaschinski C., and Lukacs N. W.(2018). *Chapter 2 - Acute and Chronic Inflammation Induces Disease Pathogenesis*, in *Molecular Pathology (Second Edition)*, W.B. Coleman and G.J. Tsongalis, Editors. Academic Press. p. 25-43

Rahelivao M. P., Gruner M., Andriamanantoanina H., Bauer I., and Knolker H. J. (2015). Brown Algae (Phaeophyceae) from the Coast of Madagascar: preliminary Bioactivity Studies and Isolation of Natural Products. *Nat Prod Bioprospect*, **5**(5). Pp: 223-35. DOI: 10.1007/s13659-015-0068-0

Sanjeewa K. A., and Jeon Y.-J. (2018). Edible brown seaweeds: a review. *Journal of Food Bioactives*, **2**. Pp: 37–50-37–50.

Sanjeewa K. K. A., Fernando I. P. S., Kim E. A., Ahn G., Jee Y., and Jeon Y. J. (2017). Anti-inflammatory activity of a sulfated polysaccharide isolated from an enzymatic digest of brown seaweed *Sargassum horneri* in RAW 264.7 cells. *Nutr Res Pract*, **11**(1). Pp: 3-10. DOI: 10.4162/nrp.2017.11.1.3

Sanjeewa K. K. A., Fernando I. P. S., Samarakoon K. W., Lakmal H. H. C., Kim E.-A., Kwon O. N., Dilshara M. G., Lee J.-B., and Jeon Y.-J. (2016). Anti-inflammatory and anti-cancer activities of sterol rich fraction of cultured marine microalga *Nannochloropsis oculata*. *Algae*, **31**(3). Pp: 277-287. DOI: 10.4490/algae.2016.31.6.29

Sanjeewa K. K. A., Lee J. S., Kim W. S., and Jeon Y. J. (2017). The potential of brown-algae polysaccharides for the development of anticancer agents: An update on anticancer effects reported for fucoidan and laminaran. *Carbohydr Polym*, **177**. Pp: 451-459. DOI: 10.1016/j.carbpol.2017.09.005

Sathya R., Kanaga N., Sankar P., and Jeeva S. (2017). Antioxidant properties of phlorotannins from brown seaweed *Cystoseira trinodis* (Forsskål) C. Agardh. *Arabian Journal of Chemistry*, **10**. Pp: S2608-S2614.

Song S.-M., Ham Y.-M., Ko Y.-J., Ko E.-Y., Oh D.-J., Kim C.-S., Kim D., Kim K.-N., and Yoon W.-J. (2016). Anti-inflammatory activities of the products of supercritical fluid extraction from *Litsea japonica* fruit in RAW 264.7 cells. *Journal of Functional Foods*, **22**. Pp: 44-51. DOI: 10.1016/j.jff.2016.01.008

Sun Z., Dai Z., Zhang W., Fan S., Liu H., Liu R., and Zhao T.(2018). *12 - Antiobesity, Antidiabetic, Antioxidative, and Antihyperlipidemic Activities of Bioactive Seaweed Substances*, in *Bioactive Seaweeds for Food Applications*, Y. Qin, Editor. Academic Press. p. 239-253

Tierney M. S., Smyth T. J., Rai D. K., Soler-Vila A., Croft A. K., and Brunton N. (2013). Enrichment of polyphenol contents and antioxidant activities of Irish brown macroalgae using food-friendly techniques based on polarity and molecular size. *Food chemistry*, **139**(1-4). Pp: 753-761. DOI: <https://doi.org/10.1016/j.foodchem.2013.01.019>

Wijesinghe W. A., and Jeon Y. J. (2012). Enzyme-assistant extraction (EAE) of bioactive components: a useful approach for recovery of industrially important metabolites from seaweeds: a review. *Fitoterapia*, **83**(1). Pp: 6-12. DOI: 10.1016/j.fitote.2011.10.016

Wu G.-J., Shiu S.-M., Hsieh M.-C., and Tsai G.-J. (2016). Anti-inflammatory activity of a sulfated polysaccharide from the brown alga *Sargassum cristaefolium*. *Food Hydrocolloids*, **53**. Pp: 16-23. DOI: 10.1016/j.foodhyd.2015.01.019

Part- 2

**3-Hydroxy-5,6-epoxy- β -ionone isolated from *Sargassum horneri*
protect MH-S mouse lung cells against fine dust induced inflammation
and oxidative stress**

Abstract

Background

Air pollution is a process that mixing of pollutants into the atmosphere, which are potentially harm to humans, and cause negative impacts to the surrounding environment (biotic and abiotic). The negative health effects associated with air pollution, have been reported from both indoor and outdoor environments. Due to the high exposure risk even at the low concentrations of fine dust, which become a major health threat to human society. Specifically, dust storms originated in China and Mongolian desert areas bring large amount of fine dust to Korean atmosphere. Therefore, preventive measures require to reduce health impacts associated with dust to maintain health population. According to the recent statistics one major outcome of fine dust exposure is inflammation and oxidative damage in lungs. Other than the avoiding direct exposure to fine dust, use of functional foods to avoid inflammation and oxidative stress might be a possible long term approach to reduce fine dust related health complications.

Methodology

Lung macrophages (CMT-93) were treated with 3-Hydroxy-5,6-epoxy- β -ionone (HEBI) a pure compound isolated from *Sargassum horneri* (Brown edible seaweed) and after 1 hr stimulated with fine dust (31.3 $\mu\text{g/ml}$). Then, inflammatory and antioxidant parameters were evaluated using western blots, ELISA, RT-qPCR, and MTT assays.

Results

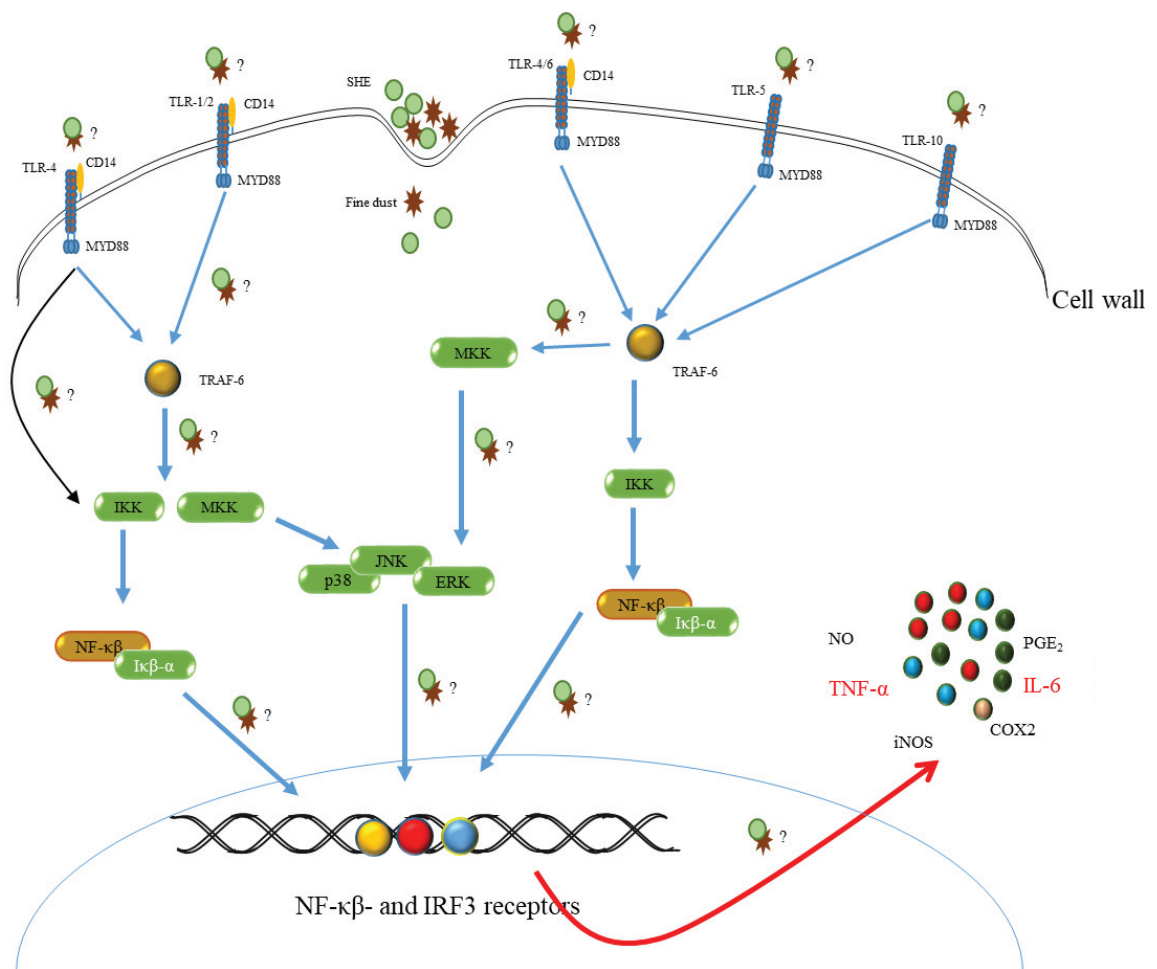
According to the results, at the concentrations between 31.3 - 125 $\mu\text{g/ml}$ significantly reduced the fine dust induced NO, PGE₂, and pro-inflammatory cytokine production, via blocking downstream signal transduction of toll like receptor 2, 3, 4, and 7 in activated

CMT-93 cells. In addition, HEBI treatment also induce the anti-oxidant protein expression levels of FD exposed CMT-93 via P38/Nrf2/Keap1 mediated antioxidant pathway.

Conclusions

The active compound; HEBI isolated from *S. horneri* has the potential to develop as a functional food or as an active ingredient in cosmeceuticals due to its profound effects against fine dust induce inflammation, and oxidative stress in CMT-93 macrophages.

Graphical abstract



Graphical abstract: Protective effect of HEBI against fine dust induced inflammation

2.1. Introduction

Air pollution is a process that mixing of pollutants into the atmosphere, which are potentially harmed to humans, and cause negative impacts to the surrounding environment (biotic and abiotic). The negative health effects associated with air pollution, have been reported from both indoor and outdoor environments. Due to the high exposure risk even at the low concentrations of fine dust, which become a major health threat to human society (Perini et al. 2017). According to Shah et al. (2013), two million deaths to be reported in each year as a direct consequence of air pollution through damage to the respiratory system and lungs (Shah et al. 2013). Fine dust has become a major threat of air pollutions and causing negative health effects on human skin and respiratory system in the East-Asia region (China, Korea, and Japan). Specifically, the extensive arid or semiarid highlands of northern China and Mongolia (Gobi Desert, Hunshdak Sandy Lands, Loess Plateau, and Taklimakan desert) are considering as the major sources of dust in Asia region (Lee et al. 2015). However, coal-burning power plants, rapid developments in industrialization, numerous petroleum vehicles, and large-scale mining operations have contributed to increase the fine dust concentration in the urban areas located in East-Asia region (Fernando et al. 2017). Continuous exposure to air pollution such as fine dust can induce oxidative stress, inflammation, and poses a serious risk to human health (Lee et al. 2015).

Alveolar macrophages stay in the lower respiratory tract and usually phagocyte fine dust particles reach to the lower respiratory tract. However, depending on the size and particle composition, fine dust exposed macrophages may produce inflammatory responses (Pozzi et al. 2003). According to the previous studies, fine dust act as inflammatory stimuli on macrophages. Recently, Zhao et al. (2016) and Bekki et al. (2016) reported that the exposure of macrophages to fine dust induce inflammatory

responses in macrophages via altering multiple cell signaling pathways. The endotoxins presented in fine dust particles found to induce the toll-like receptor 4 mediated inflammation, and reactive oxygen species induce pro-inflammatory cytokine production in macrophages. The continuous/uncontrolled inflammatory activities leading to develop chronic inflammatory responses such as cancer and immunomodulatory diseases (Dalgleish and O'Byrne 2006; Oh et al. 2017). In addition, dust particles inside the lungs phagocyte by macrophages and then were removed by lysosome activation. As a result, the macrophages population decreased and that further reduced the immunity in our body (Su et al. 2017).

Sargassum horneri is a nutrient rich edible brown seaweed, which abundantly grows in the subtidal zone as an annual species along the coasts of Korea, China, and Japan. With the optimum growth conditions, the thallus of *S. horneri* reach around 7 m length and a fresh weight of 3 kg. *S. horneri* also rich in essential vitamins, amino acids, and polysaccharides. In addition, which has been considering as an ingredient in traditional medicine for thousands of years in East-Asia region (Sanjeeva et al. 2017). However, anti-inflammatory effects of *S. horneri* against fine dust yet to be report. Thus, in the present study author attempted to evaluate anti-inflammatory mechanisms associated with 3-Hydroxy-5,6-epoxy- β -ionone isolated from *S. horneri* against fine dust exposed-mouse lung macrophages.

2.2. Materials and methods

2.2.1. Chemicals and reagents

Fine dust (collected from filters located in a central ventilating system installed in a building in Beijing city centre) was purchased from the national institute for environmental studies, Ibaraki, Japan (certified reference material no. 28). MH-S, a murine alveolar macrophage cell line (ATCC[®] CRL-2019[™]) was purchased from American type culture collection, Manassas, Virginia, USA. Roswell Park Memorial Institute medium (RPMI), fetal bovine serum (FBS), and penicillin-streptomycin (10,000 U/ml) purchased from Life Technologies Corporation, Grand Island, NY, USA. Prostaglandin E2 (PGE₂) Parameter[™] assay kit was purchased from R&D Systems Inc. ELISA Kits for Interleukin-1 beta (IL-1 β), IL-6, and tumour necrosis factor alpha (TNF- α) were purchased from BD Biosciences, San Joes, CA, USA. SP-60025, SB-202190, PD-98059, Thiazolyl blue tetrazolium bromide (MTT), Tri-Reagent[™], bacterial lipopolysaccharides (LPS), 2',7'-dichlorodihydrofluorescein diacetate (DCFDA), and dimethyl sulfoxide (DMSO) purchased from Sigma-Aldrich Co (St. Louis, MO, USA). NE-PER[®] nuclear and cytoplasmic extraction kit was purchased from Thermo scientific, Rockford, USA. Superoxide dismutase (SOD) activity was determined using a colorimetric commercial SOD activity assay kit purchased from Abcam, Cambridge, MA, USA. CD14 mouse ELISA kit was purchased from OriGene, Rockville, MD, USA. All other chemicals and reagents used in these experiments were of analytical grade.

2.2.2. Purification and isolation of HEBI from *S. horneri*

First *S. horneri* was extracted with 80% methanol in room temperature and then fractionated into hexane, chloroform, and ethyl acetate. Then the chloroform fraction was further purified using HPCPC. The identification and confirmation of structure was

similar to the method describes in the part 1. The structure of 3-Hydroxy-5,6-epoxy- β -ionone (HEBI) illustrated in figure 2-1. The isolated compound has several names in national center for biotechnology information support center (NCBI) data base and also known as 3-Buten-2-one, 4-(4-hydroxy-2,2,6-trimethyl-7-oxabicyclo[4.1.0]hept-1-yl)-. In addition, PubChem CID of the HEBI is 5371267. Additional details of the compounds are available in the following link.

<https://pubchem.ncbi.nlm.nih.gov/compound/5371267#section=Top>

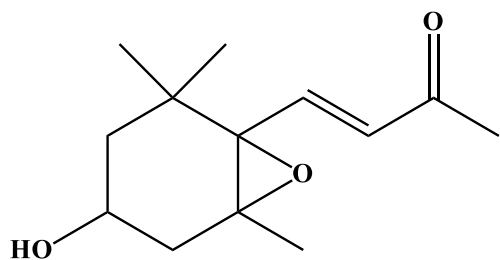


Figure 2-1. The molecular structure of 3-Hydroxy-5,6-epoxy-β-ionone isolated from *Sargassum horneri*. (MW: 224.2), PubChem CID: 5371267, Abbreviation : HEBI

2.2.3. Estimation of fine dust particle size by scanning electron microscopy

The fine dust sample was mounted on double-sided carbon tape and sputter-coated with platinum in a Q150R rotary-pumped sputter coater (Quorum Technologies, Lewes, UK). The surface morphology of fine dust particles was observed using a JSM-6700F field-emission scanning electron microscope (JEOL, Tokyo, Japan) operated at 10,000 V.

2.2.4. Cell culture

MH-S macrophages were cultured in RPMI supplemented with 10% heat inactivated FBS and 1% penicillin-streptomycin (100 Units/ml). The cells were incubated with 5% CO₂ at 37 °C (Sanyo, Moriguchi, Japan). Cells were sub-cultured within 3 day's intervals.

2.2.5. Determination of cell viability

The cytotoxic effect of HEBI, fine dust, or their combinations on MH-S cells were evaluated using a colorimetric MTT assay. The assay was performed similar to the method described by Mosmann in 1983. MH-S cells (1×10^5 cells/ml) seeded in a 24-well plates and incubated for 24 h. Then, the cells were treated with HEBI (15.6, 31.3, 62.5 µg/ml), fine dust (15.6, 31.3, 62.5, 125 µg/ml) or their combinations for 24 h. Then, MTT reagent (200 µg per well) was added to each well. After 1 h of incubation, the formazan crystals were dissolved in DMSO, and absorbance was measured at 540 nm. The optical density at 540 nm in untreated MH-S cells was considered to represent 100% viable cells.

$$\text{Cell viability (\%)} = \frac{(OD_{control} - OD_{sample})}{OD_{control}} \times 100$$

2.2.6. Evaluation of cell death rates by analysis of lactate dehydrogenase (LDH)

levels

Release of LDH in culture supernatants was measured using the CytoTox 96 Non-radioactive cytotoxicity Assay (Promega, Madison, WI, USA). The LDH release from the cells were quantified using the manufactures instructions. Plates were read at an optical density at 490 nm using an ELISA plate reader.

2.2.7. Determination of NO inhibition effect

NO production was evaluated using a method described by Leiro et al. (2002) with slight modifications (Leiro et al. 2002). Briefly, 450 µl of cell suspensions (1×10^5 cells/ml) were incubated on 24-well plates for 24 h. Then treated with 25 µl of HEBI (15.6 - 62.5 µg/ml) to each well and incubated for 1 h and treated with 25 µl of fine dust (62.5 mg/ml) for 24 h. Then 75 µl cell suspensions were mixed with equal volume of Griess reagent. After 10 min incubation, the absorbance was read with an ELISA reader at 540 nm.

$$NO \text{ inhibition (\%)} = \frac{(OD_{control} - OD_{sample})}{(OD_{control} - OD_{fine \text{ dust group}})} \times 100$$

2.2.8. Determination of PGE₂ and pro-inflammatory cytokine production

The levels of PGE₂ and pro-inflammatory cytokines in the culture supernatants were evaluated using commercial ELISA assay kits. Briefly, 450 µl of MH-S cell suspensions (1×10^5 cells/ml) were incubated on 24 well plates for 24 h. Then MH-S cells exposed to 25 µl of HEBI (15.6 - 62.5 µg/ml) and incubated for 1 h. Then MH-S cells with or without HEBI stimulated with 25 µl of fine dust (31.3 mg/ml) for 24 h. The cell culture

supernatants were collected and analysed for PGE₂, IL-1 β , IL-6, and TNF- α using the ELIZA kits according to the vendor's instructions.

2.2.9. Western blot assay

MH-S cells (1×10^5 cells/ml) were seeded in 6-well plates and incubated for 24 h. Then cells exposed to 25 μ l of HEBI (15.6 - 62.5 μ g/ml) and incubated for 1 h. Then MH-S cells stimulated with 25 μ l of fine dust (31.3 mg/ml) for 30 min or 24 h after the treatment of HEBI for 1 h. Protein extraction performed using NE-PER[®] nuclear and cytoplasmic extraction kit with the manufactures instructions. The western blots were carried out according to the previously optimized method as described in (Sanjeeva et al. 2017) for rabbit polyclonal iNOS, COX2, HO-1, MyD-88, Keap1, C23, Nrf2, NF- κ b p50, NF- κ b p65, Pp50, Pp65, P38, Pp 38, P42/44, PP42/44, nucleolin, and β -actin (Cell Signalling Technology, Beverly, USA) antibodies. The expression levels of each protein was normalized by analysing the level of β -actin protein expression levels by using ImageJ program.

2.2.10. Level of ROS in fine-dust exposed MH-S cells

Reactive oxygen species generation in MH-S cells were measured by using a method described by Thakor et al. (2017) with slight modifications. Briefly, 1×10^5 cells were seeded in 6 well plate and incubated for 24 h. Then the cells treated with HEBI and after 1 h stimulated with fine dust. The treated plates were further incubated for 24 h. Then cells were washed with serum free media for twice and then supplemented with serum free media containing 50 μ M 2',7' DCFDA at 37 $^{\circ}$ C for 30 min.

$$ROS (\%) = \frac{(OD_{control} - OD_{sample})}{OD_{control}} \times 100$$

2.2.11. Analysis of SOD Activities

The cultured macrophage cells lysis with 1M Tris/HCl, pH 7.4 containing 0.5% Triton X-100, 5mM β - mercaptoethanol, and 0.1 mg/ml phenylmethylsulfonyl fluoride solution. Then, cell lysates were centrifuged at 14,000 x g for 5 min at 4 °C. The supernatant collected and transferred to a clean e-tube. The amount of proteins in supernatants were quantified and normalized using same lysis solution. The SOD levels in extractants were quantified using colorimetric SOD quantification kit according to the vendor's instructions.

2.2.12. Effect of HEBI on MAPK pathway related proteins

The amount of NO in the culture medium was determined using Griess reagent as previously described. MH-S cells were seeded onto a 24-well plate at a density of 1×10^5 cells/ml and then cultured at 37 °C in 5% CO₂ for 24 h. Later, the cells washed with FBS free medium and suspended in DMEM without FBS. Then pre-treated with vehicle, CE extracts at various concentrations (62.5, 125, 250, and 500 μ g/ml), PD 98059 (ERK inhibitor; 20 μ M), SP600125 (JNK inhibitor; 20 μ M), or SB 203580 (p38 inhibitor; 20 μ M). Following incubation for 1 h at 37 °C, the cells were stimulated with fine dust (31.3 μ g/ml) for 24 h. The supernatant of each well (100 μ l) were transferred onto a 96-well plate and then added equal volume of Griess reagent. The absorbance was measured at 540 nm using a microplate reader.

2.2.13. Total RNA extraction and cDNA synthesis

Total RNA from MH-S cells were extracted using Tri-Reagent™ (Sigma-Aldrich, St. Louis, MO, USA) according to the manufactures instructions. Absorbance was measured at 260 nm and 280 nm using a μ Drop Plate (Thermo Scientific) to determine the concentration and purity of the extracted RNA. Then, RNA samples were diluted (1 μ g/ μ l) and first strand cDNA was synthesized using prime Script™ first-strand cDNA synthesis kit (TaKaRa BIO INC, Japan) according to the manufactures instructions. Finale products (diluted cDNA) were stored at -80 °C until use.

2.2.14. Quantitative real-time PCR (qPCR) analysis

Expression levels of pro-inflammatory cytokines were analyzed using SYBR Green quantitative real-time PCR (qPCR) technique with the Thermal Cycler Dice-Real Time System (TaKaRa, Japan). GAPDH was used as an internal reference gene in amplification. The primers used in this study indicated in Table 2-1 and 2-2 (Bioneer, Seoul, Korea). Reactions were carried out in a 10 μ l volume containing 3 μ l diluted cDNA, 0.4 μ l forward and 0.4 μ l reverse gene specific primers (10 pM), 1.2 μ l PCR grade water, and 5 μ l of 2 \times TaKaRa ExTaq™ SYBR premix. The reaction was performed using the following thermal profile: one cycle at 95 °C for 10 s, followed by 40 cycles at 95 °C for 5 s, 55 °C for 10 s, and 72 °C for 20 s, and a final single cycle at 95 °C for 15 s, 55 °C for 30 s, and 95 °C for 15 s. The relative expression levels were analyzed according to the method [$(2^{-\Delta\Delta CT})$ method] describe by Livak and Schmittgen (2001) (Livak and Schmittgen 2001). The base line was automatically set by Dice™ Real Time System software (version 2.00) to keep reliability. The data are presented as the mean \pm standard error (SE) of the relative mRNA expression from three consecutive

experiments. The two-tailed unpaired Students t-test was used to determine statistical significance (* = $p < 0.05$ and ** = $p < 0.01$).

Table 2-1. Sequence of the primers used to evaluate inflammation related RNA expression levels

Gene	Primer	Sequence (5' → 3')
GAPDH	Sense	AAGGGTCATCATCTCTGCCC
	Antisense	GTGATGGCATGGACTGTGGT
iNOS	Sense	ATGTCCGAAGCAAACATCAC
	Antisense	TAATGTCCAGGAAGTAGGTG
COX2	Sense	CAGCAAATCCTTGCTGTTCC
	Antisense	TGGGCAAAGAATGCAAACATC
IL-1 β	Sense	CAGGATGAGGACATGAGCACC
	Antisense	CTCTGCAGACTCAAACCTCCAC
IL-6	Sense	GTACTCCAGAAGACCAGAGG
	Antisense	TGCTGGTGACAACCACGGCC
TNF- α	Sense	TTGACCTCAGCGCTGAGTTG
	Antisense	CCTGTAGCCCACGTCGTAGC

Table 2-2. Primer sequences of mouse TLRs used for the Real-time RT-qPCR

Gene	Primer	Sequence (5' → 3')
TLR1	Sense	TCAAGTGTGCAGCTGATTGC
	Antisense	TAGTGCTGACGGACACATCC
TLR2	Sense	CAGCTGGAGAACTCTGACCC
	Antisense	CAAAGAGCCTGAAGTGGGAG
TLR3	Sense	CCTCCAACCTGTCTACCAGTTCC
	Antisense	GCCTGGCTAAGTTATTGTGC
TLR4	Sense	CAACATCATCCAGGAAGGC
	Antisense	GAAGGCGATAACAATTCCACC
TLR5	Sense	AGCATTCTCATCGTGGTGG
	Antisense	AATGGTTGCTATGGTTCGC
TLR6	Sense	TGGATGTCTCACACAATCGG
	Antisense	GCAGCTTAGATGCAAGTGAGC
TLR7	Sense	TTCCTTCCGTAGGCTGAACC
	Antisense	GTAAGCTGGATGGCAGATCC
TLR8	Sense	TCTACTTGGCCTTGCAGAGG
	Antisense	ATGGCAGAGTCGTGACTTCC
TLR9	Sense	CAAGAACCTGGTGTCACTGC
	Antisense	TGCGATTGTCTGACAAGTCC

2.2.15. Statistical analysis

All experiments were repeated at least three times to confirm reproducibility. All results were expressed as the mean \pm standard error (SE). The data analyzed by analysis of variance using the Statistical Package for the Social Sciences (SPSS) v 20.0 statistical analysis package. The mean values of each experiment were compared using one-way analysis of variance. Duncan's multiple range test (DMRT) was used to determine mean separation. $P < 0.05$ (*) and < 0.01 (**) was considered statistically significant.

2.3. Results and discussion

2.3.1-Anti-inflammatory properties of HEBI against fine dust induced inflammation in MH-S cells

2.3.1.1. Composition of fine dust

With the recent studies, it is clear that the exposure to air pollutions, like fine dust induce oxidative stress, inflammation, and adverse health effects to human beings (Pardo et al. 2018). As a result of industrial development and natural phenomenon, the level of fine dust in the Korean atmospheres found to increase during the last few decades (Kim 2018). With the increased fine dust concentration, health complications associated with respiratory system also found to increase in Korea, China, and Japan (Pardo et al. 2018). Inflammation associated complications in respiratory system caused by fine dust is one of the major topic discussed during the last few years. Recently, He et al. (2016) attempted to evaluate the allergic inflammatory responses in murine lungs after exposed them into fine dust collected from urban areas and sand storms. In this study, the authors claimed, fine dust particles (PM 2.5) collected from urban areas induced the inflammatory responses in macrophages (He et al. 2016). Electron microscopic image of fine dust particles (fig. 2-2.) shows that the particle sizes are not distributed equally and which contained range of particle sizes. Looking at the particle size distribution, some particles had around 9.6 μm diameter. However, large portion of fine dust particles had less than 2.5 μm diameter (more than 60%). Additionally, fine dust particles had irregular shapes and distributed randomly in electron microscope image.

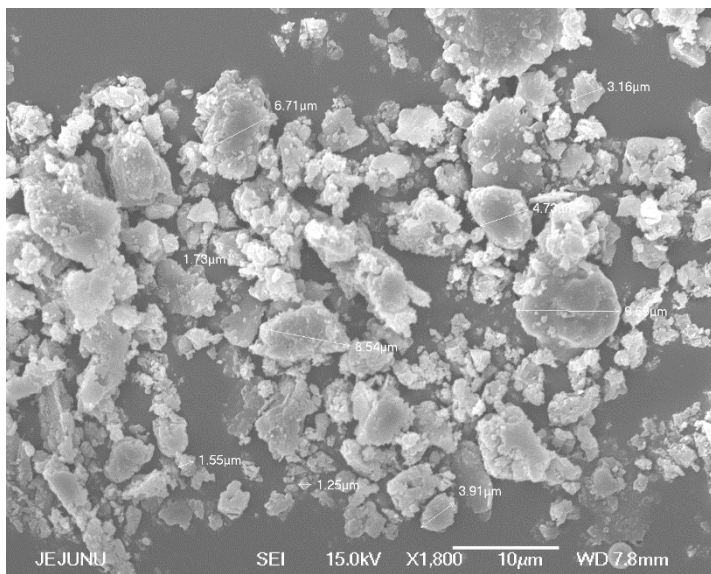


Figure 2-2. Scanning electron microscope image of fine dust particles purchased from the national institute for environmental studies, Ibaraki, Japan (certified reference material no. 28). Scale bar represent 10 μm lengthy.

2.3.1.2. cell viability and NO production in fine dust exposed MH-S cells

Before evaluate the bioactive properties of HEBI, author attempted to evaluate toxicity and NO stimulatory effect in fine dust exposed MH-S cells. According to the results, concentrations higher than the 62.5 $\mu\text{g/ml}$ were dramatically reduced the viability of MH-S cells compared to the un-treated control (fig. 2-3a). In parallel to the cell viability results, the NO secretion increased with fine dust concentrations up to 31.3 $\mu\text{g/ml}$ and then declined (fig. 2-3b). The reduction of NO levels in concentrations higher than the 31.3 $\mu\text{g/ml}$ might be associated with reduced cell viability. Previously, a number of studies reported the exposure of macrophages to fine dust cause to induce chronic inflammatory responses and activate apoptotic cell death. Airborne particulate matter (PM), 2.5 is considering as the most vulnerable size for induce adverse health effects (Bekki et al. 2016). With the electron microscope analysis, large portion of fine dust sample contained less than 2.5 μm diameter PM. Specifically, particles smaller than 2.5 μm can easily go through the throat and nose to reach the alveolus (Bekki et al. 2016). Therefore, fine dust cause to induce adverse health consequences to respiratory system. With these observations, and previous evidences, the author decided to use 31.3 $\mu\text{g/ml}$ concentration of fine dust for further studies.

2.3.1.3. Cyto-toxic effect of HEBI on MH-S cells

The colorimetric MTT assay was performed to select optimal concentrations for the further study. According to the results, the concentrations between 15.6 - 62.5 $\mu\text{g/ml}$ not significantly affected to the viability of MH-S cells (fig. 2-4a). However, the concentrations higher than the 125 $\mu\text{g/ml}$ significantly reduced the MH-S cell viability. Therefore, the concentrations below 125 $\mu\text{g/ml}$ used for the consequent studies.

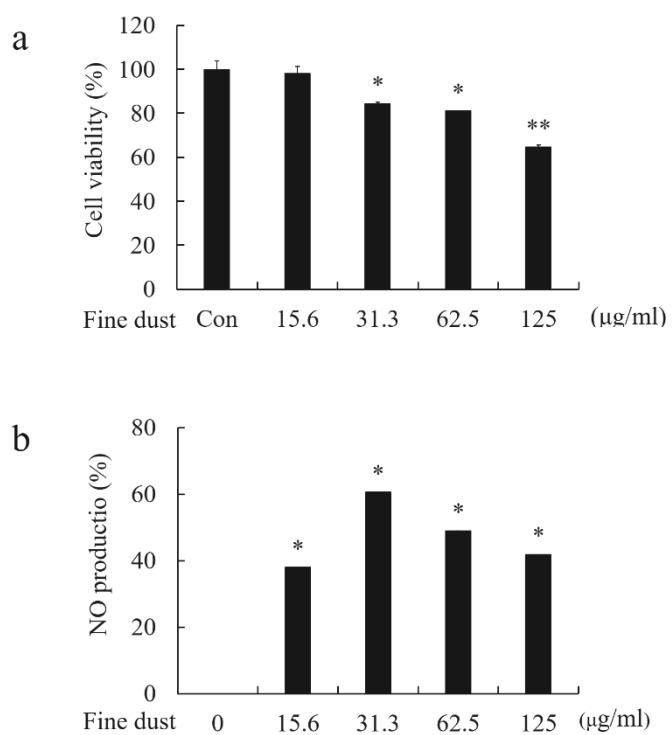


Figure 2-3. Cytotoxicity (a) and NO production levels (b) in fine dust-exposed MH-S cells. Results represent the pooled mean \pm SE of three independent experiments, performed in triplicate. * $p < 0.05$, ** $p < 0.01$, face to the respective control.

2.3.1.4. Protective effect of HEBI against fine dust-induced cell death and NO production in MH-S cells

In the present study, author attempted to evaluate NO inhibition levels and cytoprotective effects of fine dust exposed macrophages with presence of HEBI. Previously, Kim et al. (2018) reported HEBI isolated from *Sargassum muticum* has the potential to reduce LPS-induced inflammatory responses in RAW 264.7 macrophages and zebrafish models via blocking MAPKs and NF- κ B signalling pathways. Other than that, Huang et al. (2003) reported, continuous fine dust exposure link with the pathogenesis of adverse health effects. Furthermore, the authors reported, fine dust exposed individuals were diagnosed with pulmonary neutrophilic inflammation and increased blood fibrinogen (Huang et al. 2003). Similar to these observations, the exposers of MH-S cells to fine dust reduced the cell viability (fig. 2-4b and 2-4c) as well as induce NO production (fig. 2-4d) from MH-S cells. However, pre-treatment of HEBI reduced the cell death rates and NO production levels in fine dust-exposed macrophages in a dose-dependent manner.

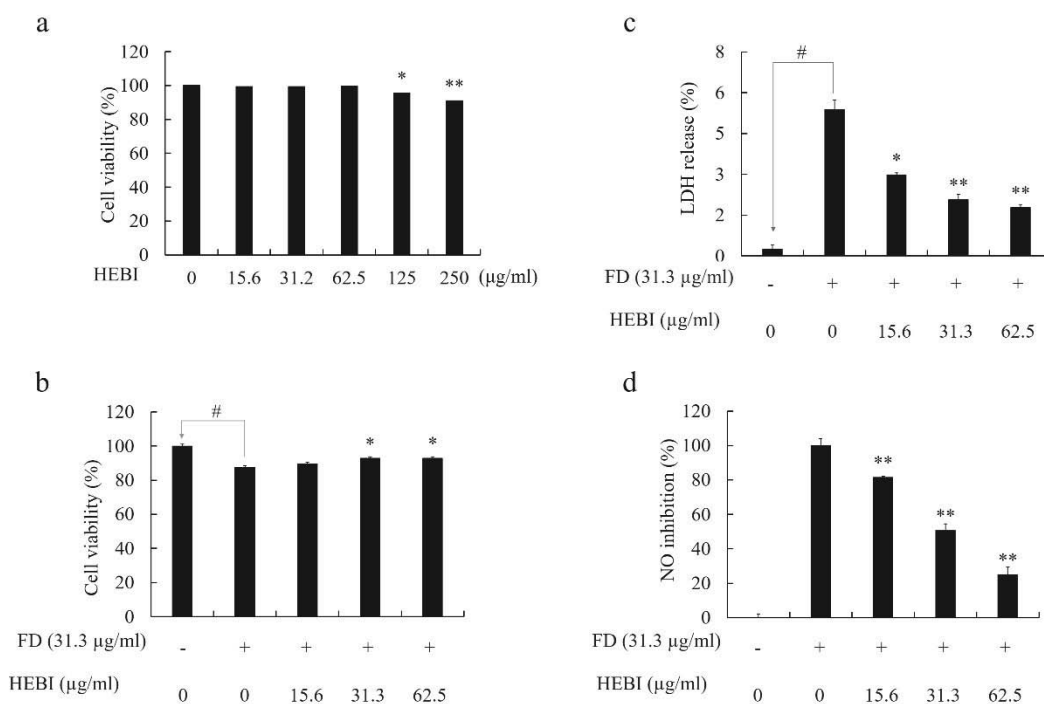


Figure 2-4. Viability of MH-S cells exposed to 3-Hydroxy-5,6-epoxy- β -ionone (HEBI) and fine dust (FD). Cells were exposed to HEBI with or without FD (31.3 $\mu\text{g/ml}$) at the doses of 15.6 - 62.5 $\mu\text{g/ml}$. After 24 h, cell viability was measured by the MTT (a, b) and LDH assays (c). Secreted NO in the culture media was quantified using Griess assay (d). Statistical significance was tested using a Student's t-test. HEBI group vs FD group * $p < 0.05$, ** $p < 0.01$; FD vs control group (positive control) # $p < 0.01$.

2.3.1.5. Effects of HEBI on fine dust induced PGE₂ and pro-inflammatory cytokine secretion (ELISA)

Previously, it has been reported that exposure of macrophages to fine dust resulted in up-regulated production of pro-inflammatory cytokines and PGE₂ (Tsai et al. 2017). Moreover, it is well-known fact that the up-regulated production of PGE₂ and pro-inflammatory cytokines increased the cancer risk and arisen of other chronic inflammatory diseases (Echizen et al. 2016). Therefore, in the present study author attempted to evaluate the protective effects of HEBI against fine dust induced MH-S cells by evaluating production levels of PGE₂ (fig. 2-5a) and pro-inflammatory cytokines. ELISA assays used to evaluate the pro-inflammatory cytokines levels (IL-1 β ; fig. 2-5b, IL-6; fig. 2-5c, and TNF- α ; fig. 2-5d) in fine dust exposed culture supernatants collected from MH-S cells. Similar to previous results, the exposure of macrophages to fine dust increased the secretion of PGE₂, IL-1 β , IL-6, and TNF- α from macrophages. However, the pre-incubation of HEBI dose-dependently decreased the elevated cytokine secretion from macrophages.

2.3.1.6. Effects of HEBI on FD-induced iNOS and COX2 protein production

The production of NO and PGE₂ mainly depend on the expression levels of iNOS and COX2 proteins, respectively. The production of NO in the cellular environment depends on the conversion of l-arginine to l-citrulline by the enzyme nitric oxide synthase (NOS). There are three known isoforms of NOS, namely neuronal NO synthase (nNOS/NOS1), inducible NO synthase (iNOS/NOS2) and endothelial NO synthase (eNOS/NOS3). In general, the activation of nNOS and eNOS caused to produce nano-molar concentrations of NO for short time periods (seconds or minutes). However, the activation of iNOS caused to generates higher amounts of NO, in the micro-molar range and for relatively

long time period (from hours to days) (Vannini et al. 2015). Besides the iNOS; COX2 is the product of an "immediate-early" gene that is rapidly inducible and tightly regulated (Crofford 1997). Moreover, COX2 is the inducible form of cyclo-oxygenase and play an important role in inflammation by stimulating conversion of arachidonic acid to prostaglandins. In normal situations, COX2 not present in the cells and expression is avoided. However, during the inflammation process cells produce a large amount of COX2 to facilitate inflammatory responses (Crofford 1997; Sutcliffe and Pontari 2016). Thus, author compared the cytosolic expression levels of iNOS and COX2 in fine dust-stimulated MH-S cells and HEBI co-treated cells. According to the results, exposure of fine dust triggers the production of iNOS and COX2 from MH-S cells (fig. 2-6a). However, pre-treatment of HEBI decreased the elevated COX2 (fig. 2-6b) and iNOS (fig. 2-6c) from fine dust exposed macrophages.

Upon the activation of toll like receptors, TLR/MyD88 complex dislocate, resulting down-stream activation of the transcription factors related to NF- κ B and MAPKs which are the primary contributors to pro-inflammatory gene expression (Mitchell et al. 2018). Therefore, author attempted to evaluate the MyD88 expression levels in the fine dust exposed MH-S cells (fig. 2-6a). According to the image analysis results, fine dust significantly increased the cytosolic MyD88 levels compared to the untreated control. However, the pre-treatment of HEBI prior to the fine dust exposure reduced the elevated levels of MyD88 in fine dust exposed cells (fig. 2-6d).

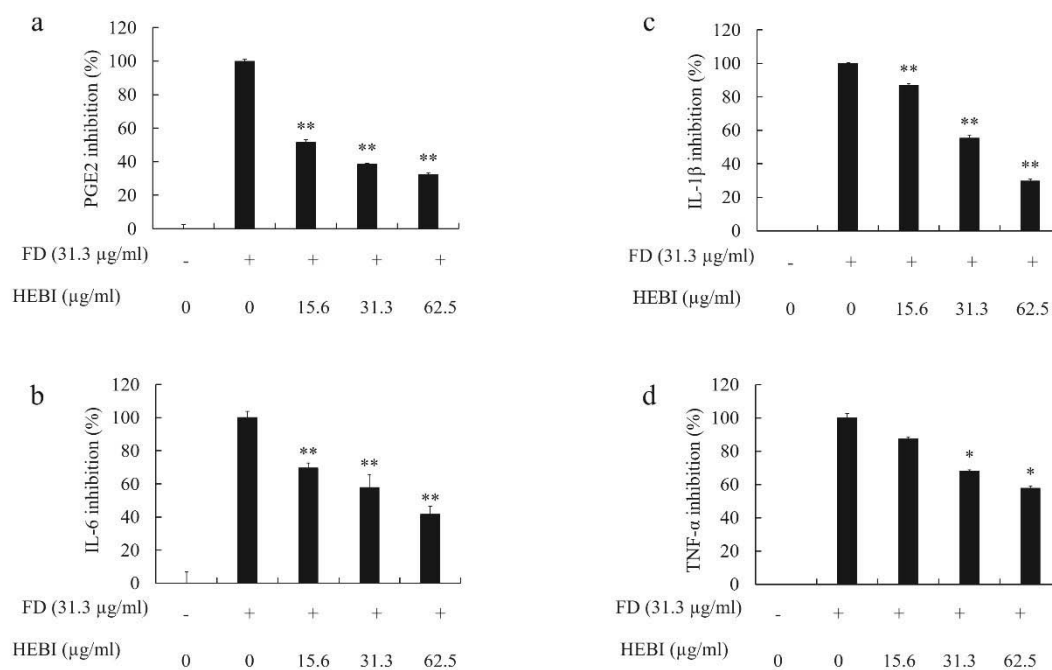


Figure 2-5. Effects of HEBI on production of PGE₂ and pro-inflammatory cytokines in fine dust (FD)-activated MH-S cells. Percentage of PGE₂ (a), IL-6 (b), IL-1β (c), and TNF-α (d) in cell cultures. Results represent the pooled mean ± SE of three independent experiments, performed in triplicate. **p* < 0.05, ***p* < 0.01, face to the respective control (ANOVA, Duncan's multiple range test).

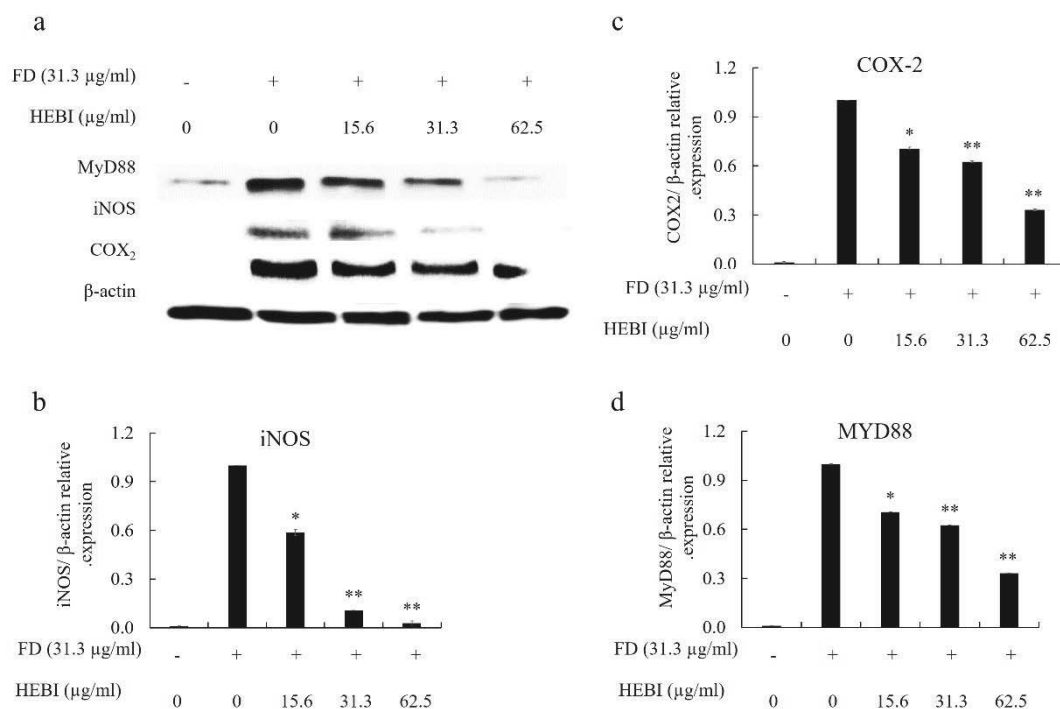


Figure 2-6. Effects of HEBI on the fine dust (FD)-induced expression of MyD-88, iNOS, and COX2 in MH-S macrophages (a). Lysates were prepared from cells that were not treated or pre-treated with HEBI (15.6 - 62.5 μg/ml) for 1 h and then stimulated FD (31.3 μg/ml) for 24 h. Density ratios of COX2 (b), iNOS (c), and MyD88 (d) were measured using densitometry. The values shown are the means ± SD of three independent experiments. * $p < 0.05$, ** $p < 0.01$.

2.3.1.7. Suppressive effect of HEBI in fine dust induced NF- κ B phosphorylation and translocation to the nucleus in MH-S macrophages

The transcription factor NF- κ B has been considering as a key mediator in inflammation. The activation of NF- κ B depends on the range of factors such as LPS, viral infection, inflammatory cytokines (TNF or IL-1), UV irradiation, T cell and B cell activation, and by other non-physiological and physiological factors (Baldwin 1996). The activation and translocation of NF- κ B strictly control by the inhibitor protein called I κ B. Phosphorylation and sub-sequent degradation of I κ B allows the activation and translocation of NF- κ B to nucleus (Tak and Firestein 2001). In the cytoplasm three forms of I κ B indemnified and called them as I κ B- α , I κ B- β , and I κ B- ϵ . The first protein I κ B- α is associated with transient NF- κ B activation. Out of 3 I κ B subunits, only I κ B- α binds to the p50 heterodimer and p50-p65 homodimer. In the nucleus, NF- κ B dimers bind to its target DNA elements and then triggers the transcription of genes responsible for inflammation (Baeuerle and Baltimore 1996; Baldwin 1996; Tak and Firestein 2001). The translocation and activation of NF- κ B proteins are graphically illustrated in the figure 2-7a. Thus, first evaluated the phosphorylation levels of cytosolic I κ B- α , p50, and p65 using western blot analysis. According to the western blot analysis, fine dust increased the phosphorylation of I κ B- α from fine dust exposed cells compared to the untreated control (fig 2-7b). However, the elevated phosphorylation levels were dose-dependently decreased with the treatment of HEBI. These results suggesting the isolated compound has an inhibitory effect on phosphorylation of I κ B- α . As second step author attempted to evaluate the NF- κ B related cytosolic p50 and p65 phosphorylation levels using western blot analysis. Similar to the I κ B- α phosphorylation both p50 and p65 phosphorylation increased with fine dust exposure and dose-dependently decreased with HEBI treatment (fig. 2-8a). In addition to our study, Kim et al. (2014) reported an

ethanolic extract collected from *S. horneri* had suppressive effect on phosphorylation of p65 in LPS-stimulated macrophages. Similar to Kim et al. (2014) observations, HEBI inhibited fine dust induced p65 phosphorylation than the p50 phosphorylation in activated macrophages (fig. 2-8a).

In addition, author also attempted to the evaluate NF- κ B activation levels in the nucleus. In response to fine dust, levels of p50 and p65 increased dramatically in MH-S cells (fig 2-8b). However, the co-treatment of HEBI down-regulated the elevated p50 and p65 protein expression in the nucleus.

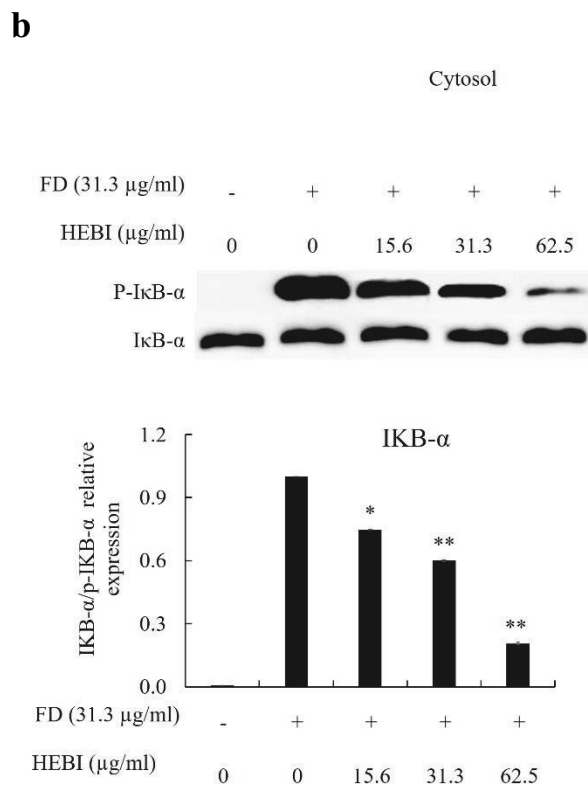
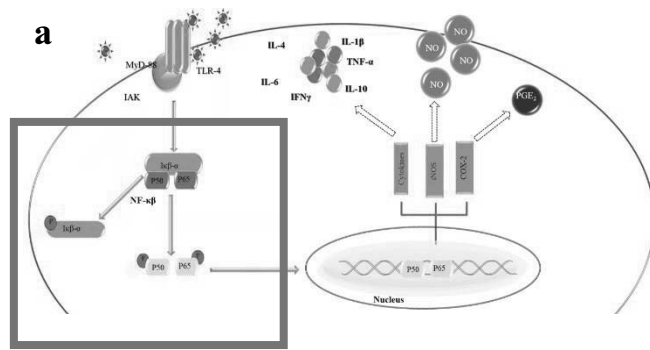


Figure 2-7. The graphical illustration of activation and translocation of NF-κB from cytosol to nucleus (a). The inhibitory effects of HEBI on fine dust (FD)-stimulated NFκB related (IκB-α, and p-IκB-α) protein expression (b). The gel shown is a representative of the results from three separate experiments. * $p < 0.05$, ** $p < 0.01$, face to the respective control (ANOVA, Duncan's multiple range test).

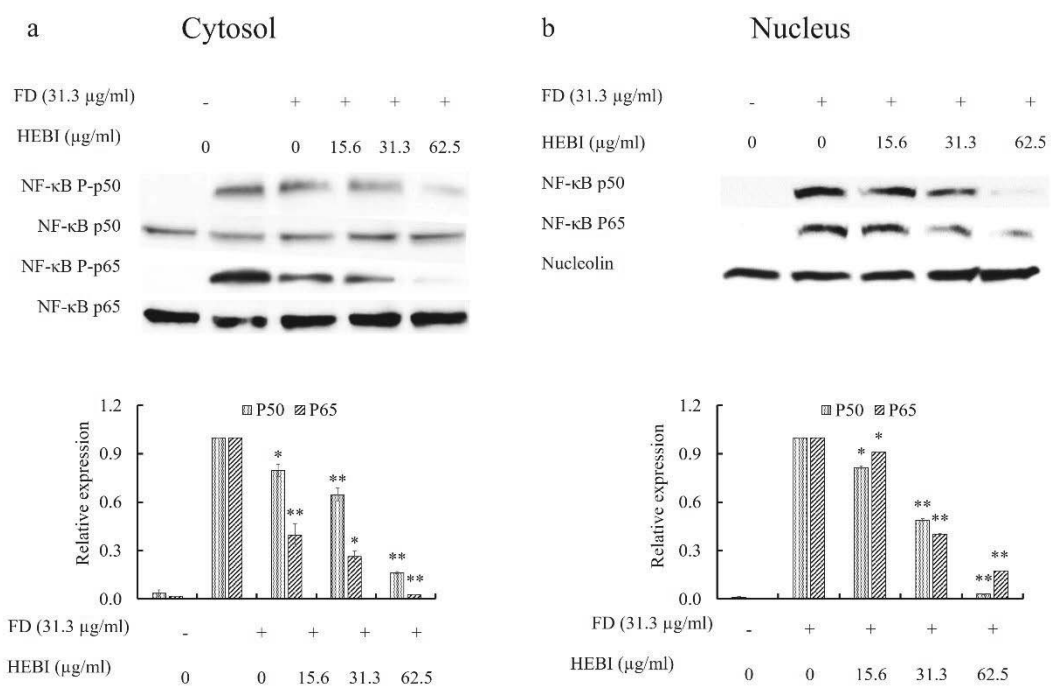


Figure 2-8. The effects of HEBI on NF-κB expression in fine dust (FD)-exposed MH-S cells. Western blotting was performed to analyze the protein phosphorylation of NF-κB p50 and p65 in the cytosol (a) and the nucleus (b). The values presented are the mean ± SD of three independent experiments. * $p < 0.05$, ** $p < 0.01$, face to the respective control (ANOVA, Duncan's multiple range test).

2.3.1.8. HEBI inhibits MAPK protein expression in fine dust exposed MH-S cells

Mitogen-activated protein kinases (MAPK) are an evolutionarily preserved family of enzymes which are capable to form a highly integrated network required to achieve specialized cell functions such as apoptosis, cell differentiation, and cell proliferation (Hommes et al. 2003). ERK1/2, JNK, and p38 are three known MAPK's involved in the inflammatory gene regulation. To the date, it has been reported that the MAPK kinase (MKK)1 and MKK-2 are involved in the activation of ERK1/2; MKK3, MKK4, and MKK6 are involved in the p38 MAPK activation; and MKK4 and MKK7 are involved in the activation of JNK (Kaminska 2005).

Inflammatory stimuli such as bacteria, fungi, and dust activate macrophages through the receptors located in cell membrane. The activation of receptors triggers intracellular signalling cascades like MAPK pathways and the which directly and indirectly responsible for activation of the NF- κ B related signal transduction. The activation of MAPK pathway up-regulate the production of pro-inflammatory cytokines such as TNF- α , IL-6, IL-8, IL-1 β , collagenase-1, and collagenase-3 (Kyriakis and Avruch 2001). Specifically, TNF- α is a potent activator of NF- κ B signal transduction pathway and MAPK's are potent inducers of TNF- α . This positive feedback is key to chronic inflammatory complications including cancer, rheumatoid arthritis, and inflammatory bowel disease (Arango Duque and Descoteaux 2014). Therefore, the compounds capable to inhibit or down-regulate MAPK related protein might have a potential to developed as anti-inflammatory drugs. In the present study, author attempted to evaluate phosphorylation levels of MAPK's in fine dust exposed MH-S cells and HEBI co-treated MH-S cells together with fine dust. According to the results, phosphorylated forms of JNK, ERK1/2, and P38 increased in fine dust-exposed MH-S cells. According to the results, co-treatment of HEBI decreased the phosphorylation

levels of JNK and ERK1/2 in a dose-dependent manner (fig 2-9). However, the phosphorylation level of P38 increased in a dose-dependent manner after co-treatment of HEBI. The up-regulated expression of P38 linked with the anti-oxidant pathways in macrophages and could be considering as an important effect of HEBI. The effects of up-regulated P38 phosphorylation in related to the antioxidant mechanisms are later discuss in details.

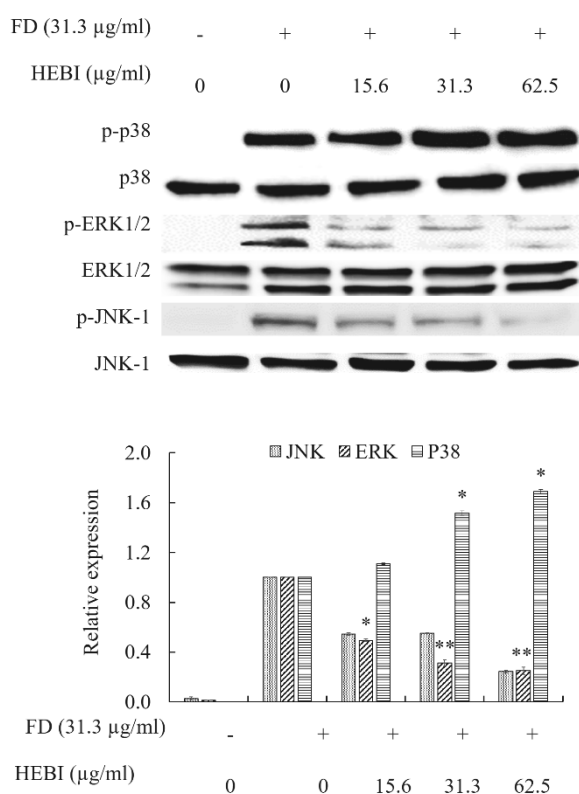


Figure 2-9. Effect of HEBI MAPKs in fine dust (FD)-stimulated MH-S macrophages. Data represent the mean \pm SEM of three independent experiments (N = 3). One of the similar results from three separate experiments is represented, and the relative ratio (%) is also shown, where the p-p38, p-JNK and p-ERK signals were normalized to the p38, JNK and ERK signals. * $p < 0.05$, ** $p < 0.01$, face to the respective control (ANOVA, Duncan's multiple range test).

2.3.1.9. Effect of HEBI against fine dust induced inflammatory gene expression in MH-S cells

The inflammation related genes including IL-1 β , IL-6, TNF- α , iNOS, and COX2 were examined using RT-qPCR in order to identify the gene expression levels and protective effect of HEBI against fine dust induced inflammation in MH-S cells. In response to fine dust the mRNA levels of iNOS and COX2 were significantly increased in MH-S cells (fig. 2-10a/b). However, the co-treatment of HEBI down-regulated the elevated levels of iNOS and COX2 in fine dust exposed MH-S cells. Previously, it has been reported that, the exposure of cells to fine dust, has the potential to induce transcription of inflammation related genes such as iNOS, COX2, TNF- α , IL-1 β , and IL-6 (Seok et al. 2018). Specifically, the levels of TNF- α (~ 35 folds) and IL-6 (~ 8 folds) mRNA levels were up-regulated after exposed to the fine dust (fig. 2-10 c-e). According to the previous observations, the up-regulated expression of TNF- α trigger the NF- κ B inflammatory pathway via activating TLR/MyD88 dependent inflammatory pathway (Arango Duque and Descoteaux 2014). Therefore, the up regulated expression of TNF- α might worsen the inflammatory responses in macrophages via over activating NF- κ B signal cascade. Therefore, as next study author attempted to evaluate mRNA expression levels of TLRs using RT-qPCR.

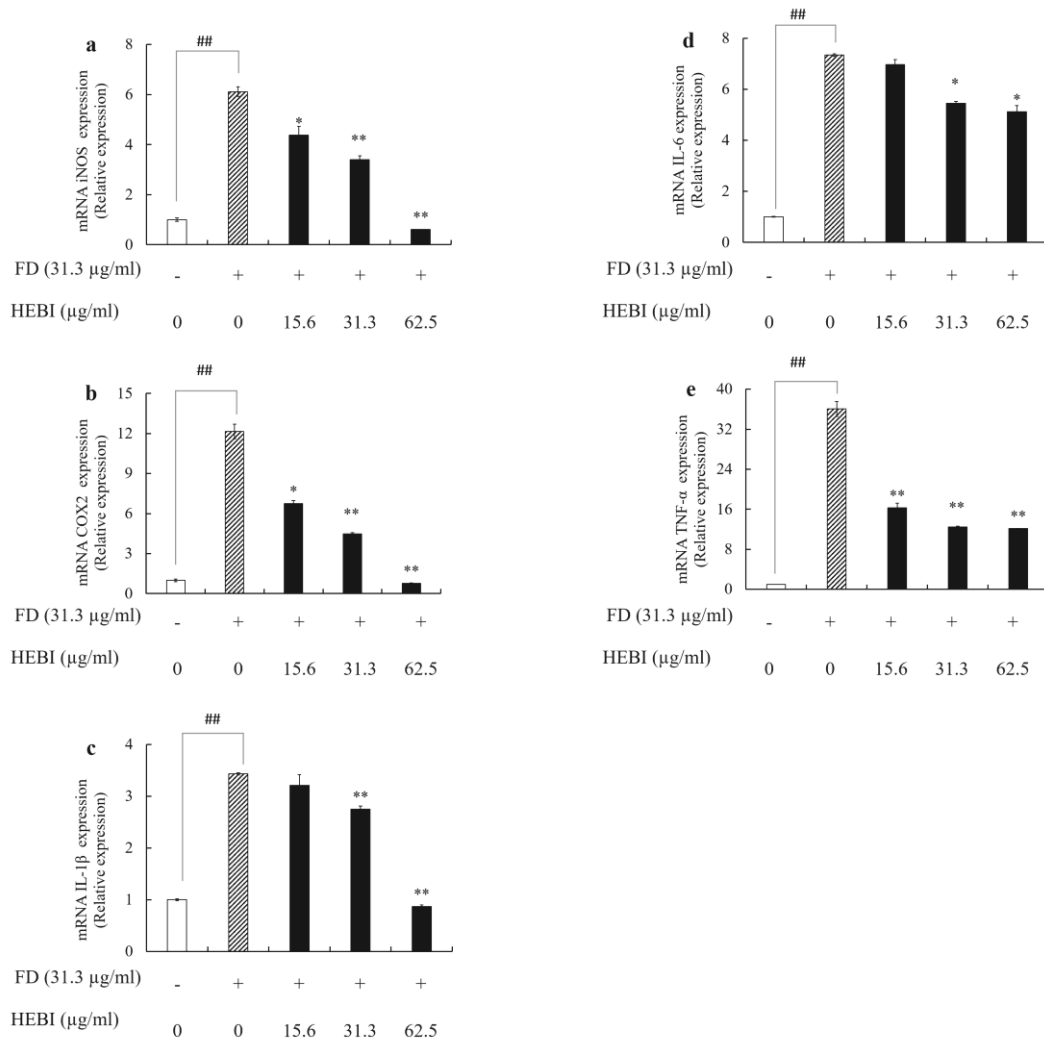


Figure 2-10. Inhibition of fine dust induced iNOS (a), COX2 (b), IL-1 β (c), IL-6 (d), and TNF- α (e) mRNA expression by HEBI in MH-S macrophages. The results were analyzed by the Delta-Ct method and expression of target genes was normalized to GAPDH expression. Control was obtained in the absence of fine dust and HEBI. The values shown are the means \pm SEs of three independent experiments; * p < 0.05, ** p < 0.01 vs. the fine dust treated group or # p < 0.05, ### p < 0.01 vs. the un-stimulated group.

2.3.1.10 inhibitory effect of HEBI against fine dust induced TLR activations (RT-qPCR).

The principle role of toll-like receptors (TLRs), is reorganization of specific molecular patterns identical to microbial components. Activation of TLR control the distinct patterns of gene expressions linked with the protective mechanisms. It has been identified, TLRs are involved in activation of innate immunity and the development of antigen-specific acquired immunity (Akira and Takeda 2004). In the present study, author evaluated the gene expression levels of TLRs (1-9) using RT-qPCR to identify the effect of fine dust on TLRs activation. According to the results, only TLR 2, 3, and 4 response to fine dust and others were not sufficinty expressed under the tested conditions. Therefore,author conclude that only TLR 2, 3, 4, and 7 involved in the fine dust induced inflammation in MH-S cells (fig 2-11). In addition, treatment of HEBI, dose-dependelty reduced the expression levels TLR 2 (fig. 2-11 b), 3(fig. 2-11 c), and 4 (fig. 2-11 d).

According to Akira and Takeda (2004), the activation of TLR 2, 3, and 4 triggers the production of inflammatory cytokines as wells as which are involved in MyD88-dependent NF- κ B pathway activation. Threfore, the upregulated inflammatory responces observed in MH-S cells after the fine dust exposure should related to the TLR/MY88 pathway mediated NF- κ B and MAPK protein expressions.

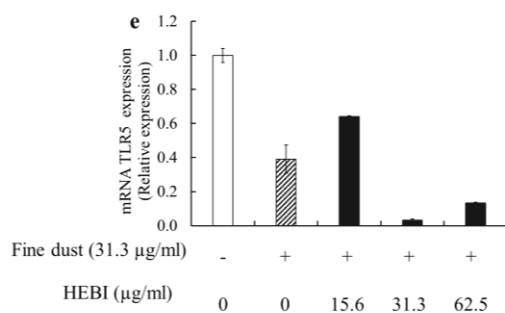
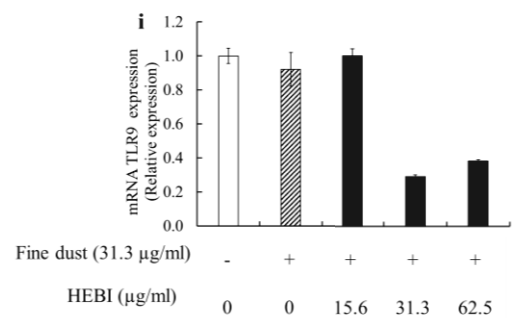
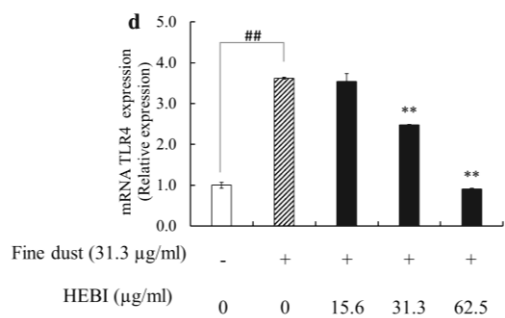
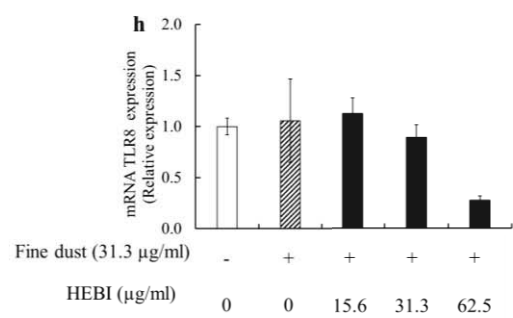
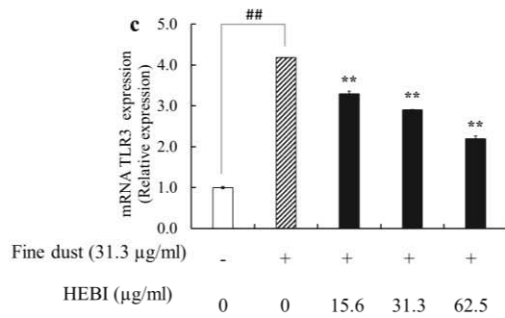
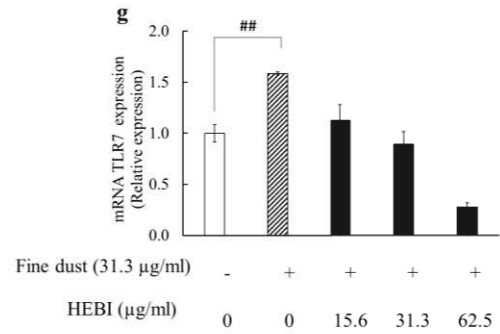
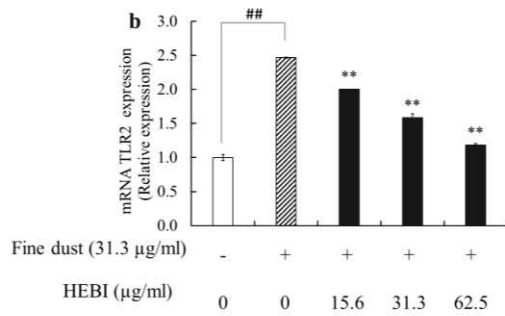
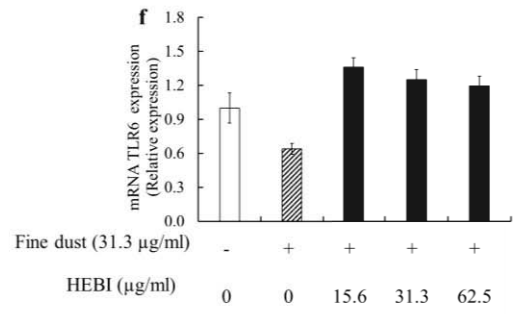
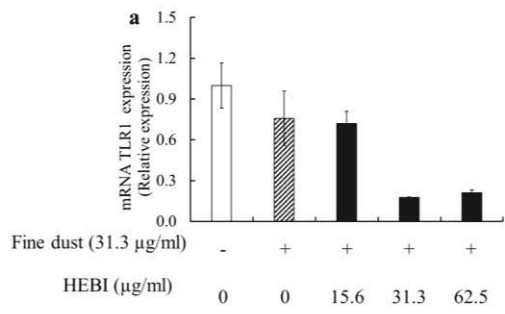


Figure 2-11. Effect of HEBI against mRNA expression of fine dust (FD)-induced toll like receptors (TLR) (1-9; a-h) in MH-S macrophages. After FD exposure for 6 h, total RNA was extracted from MH-S macrophages and RT-qPCR was performed for the TLRs genes using TaqMan reagents. The results were analyzed by the Delta-Ct method and expression of target genes was normalized to GAPDH expression. Control was obtained in the absence of FD and HEBI. The values shown are the means \pm SEs of three independent experiments; * p < 0.05, ** p < 0.01 vs. the FD treated group or # p < 0.05, ## p < 0.01 vs. the un-stimulated group.

2.3.2-Anti-oxidant properties of HEBI against FD-induced inflammation in MH-S cells

Oxidative stress is a major cause of apoptosis and involves the formation of reactive oxygen species (ROS) and reactive nitrogen species (RNS) via activating apoptosis related signal pathways linked to the Ca^{2+} overload, mitochondrial inhibition, and inflammatory responses such as over production of RNS (Yang et al. 2009). Therefore, it is important to avoid oxidative stress built inside the cells to protect them from apoptosis and inflammation related complications.

Antioxidants are a group of substances that react at different stages of free-radical formation and which are able to reduce free-radical concentrations in the cells, organs, and in the body (Perchyonok et al. 2016). Enzymes such as glutathione peroxidase, superoxide dismutase, catalase, and glutathione reductase are well-known endogenous anti-oxidant enzymes synthesized within the cell (Mulgund et al. 2015). The activation of these enzymes monitored by specific signal transduction pathways such as NF-E2-related factor 2 (Nrf2)/ heme oxygenase(HO-1). Nrf2 is a nuclear transcription factor that binds to antioxidant response element and co-ordinately activates a battery of detoxifying/defensive genes. This leads to protection and cell survival (Powell et al. 2012). In general, Nrf2 is attached with Kelch-like ECH-associated protein 1 (Keap-1) and make inactive complex in cytoplasm. However, with the oxidative stress or electrophiles Keap-1 is inactivated by direct modification of reactive cysteine residues. The phosphorylation of Keap-1 breaks the complex between Nrf2 and Keap-1. The breakdown of Nrf2/Keap-1 facilitate the translocation of Nrf2 in to the nucleus and transcription of antioxidant and detoxification related genes. Nrf2 cause to activate number of genes such as xenobiotic disposition (quinone reductases, GSTs, and Mrps,), protection from electrophiles (GSH synthesis, superoxide dismutase; SOD), and general

stress response (HO-1, thioredoxin) (Lehman-McKeeman 2013). Thus, activation of Nrf2 is play an important role to protect cells against oxidative stress. Moreover, previously it has been reported that fine dust has a potential to induce oxidative stress in macrophages (Lei et al. 2005; Meng and Zhang 2006; Nel 2005). Meng and Zhang, (2006) reported that the exposure of fine dust cause to induce oxidative damage to lung heart and liver cells via reducing SOD, GSH levels in fine dust-exposed rat tissues. In addition, Cheng et al, (2005) reported the exposure of fine dust to streptozotocin-diabetic rats cause to elevate expression levels of pro-inflammatory cytokines (IL-6 and TNF- α) and plasma nitric oxide levels (Lei et al. 2005). Thus, in the present section author attempted to evaluate antioxidant properties of HEBI against fine dust induced oxidative stress.

2.3.2.1 HEBI inhibits fine dust induced ROS levels in MH-S cells

Previously, number of studies confirmed the exposure of cells to the fine dust ends up with up regulated production of ROS. Recently, Pardo et al, (2018) reported that the prolonged exposure of fine dust, induced the oxidative stress and inflammation in mouse lung and liver cells. Similarly, author also noted that the exposure of MH-S to fine dust cause to increase ROS levels MH-S cells (fig. 2-12a). According to the DCF-DA assay results, pre-incubation of HEBI, dose-dependently decreased ROS levels in fine dust-stimulated MH-S cells. In addition, pre-incubation of HEBI dose-dependent reduced the fine dust-induced cell death rates observed in MH-S macrophages (fig. 2-12b).

2.3.2.2. Effect of HEBI in fine dust induced SOD and catalase levels in MH-S cells

Superoxide dismutase; SOD is an important endogenous antioxidant, and the first line of defence against free radicals. SOD comprises a family of metalloproteins. Generally,

SOD categorised into four major groups as, manganese-containing SOD (Mn-SOD), copper/zinc-containing SOD (Cu/Zn-SOD), iron-containing SOD (Fe-SOD), and nickel-containing SOD (Ni-SOD). It converts superoxide radicals to H_2O_2 . However, the production H_2O_2 , which mainly produced $HO\cdot$ radicals and lead to lipid peroxidation. However, H_2O_2 produced with the SOD, subsequently converted in to H_2O through the Fenton reaction by cytosolic antioxidant protein; catalase (CAT) (Yenkoyan et al. 2018). Thus, the compound capable to induce production of these antioxidant enzymes might have the potential to protect the host cells against ROS induced damages. As an initial step author attempted to evaluate SOD levels using ELISA assay (fig. 2-12c). Similar to the previous studies, fine dust decreased the SOD levels in MH-S cells compared to the control. The decreased SOD levels might be the possible reason for high level of ROS and cell death rates in fine dust-exposed MH-S (fig 2-12 a/b). However, the co-treatment of HEBI caused to increase SOD levels in fine dust-exposed macrophages.

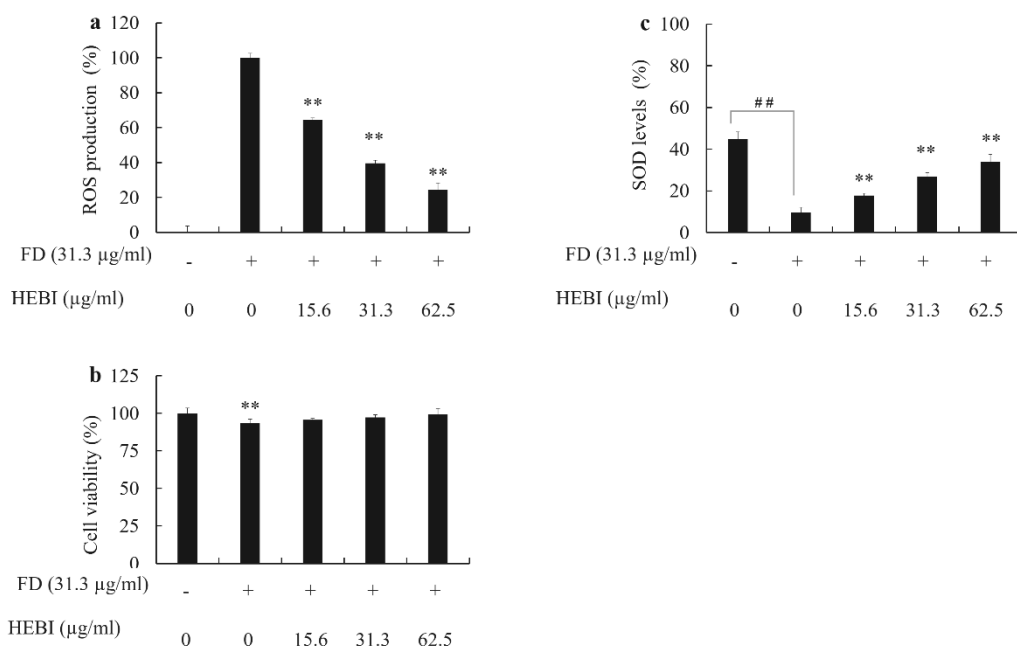


Figure 2-12. Effect of HEBI against fine dust (FD)-induced ROS production (a), cell viability (b), and SOD levels (c) in MH-S cells. The experiments were performed as described in the materials and methods sections. The values shown are the means \pm SEs of three independent experiments; * $p < 0.05$, ** $p < 0.01$ vs. the fine dust treated group or ## $p < 0.01$ vs control.

2.3.2.3. HEBI increased the cytosolic antioxidant protein levels in fine dust exposed

MH-S cells

In most cases, oxidative stress is mainly caused due to the deficiency of antioxidants and/or an excess of reactive oxygen; ROS and nitrogen species; RNS (Gil et al. 2017). In addition to the oxidative damage, intracellular ROS/RNS are triggers the pro-inflammatory cytokine production mechanisms in the cells and act as pro-inflammatory markers; which resulting to worsening the pathological conditions (Stentz et al. 2004). Thus, the compounds with antioxidant and anti-inflammatory properties can be consider as ideal materials to develop functional products. Therefore, in the present study, author evaluated the expression levels of catalase and Cu/Zn-SOD in fine dust stimulated MH-S cells after pre-incubation with HEBI. Catalase and Cu/Zn-SOD are two important antioxidant proteins act against oxidative stress in the cellular environment. The up-regulated expression of those proteins helped to reduce oxidative stress via scavenging ROS produced during the pathological and metabolic events (Liu et al. 2017). Following the fine dust stimulation, evaluation of antioxidant proteins expression levels in MH-S cells using western blots showed that the treatment of HEBI (15.6 - 62.5 $\mu\text{g/ml}$) significantly up-reregulated the Catalase and Cu/Zn-SOD levels in cytosol compared to the only fine dust group (fig. 2-13). The up-regulated expression of this antioxidant proteins effectively reduce the oxidative stress in fine dust induced MH-S cells and ultimately protects cells from apoptosis and chronic inflammation.

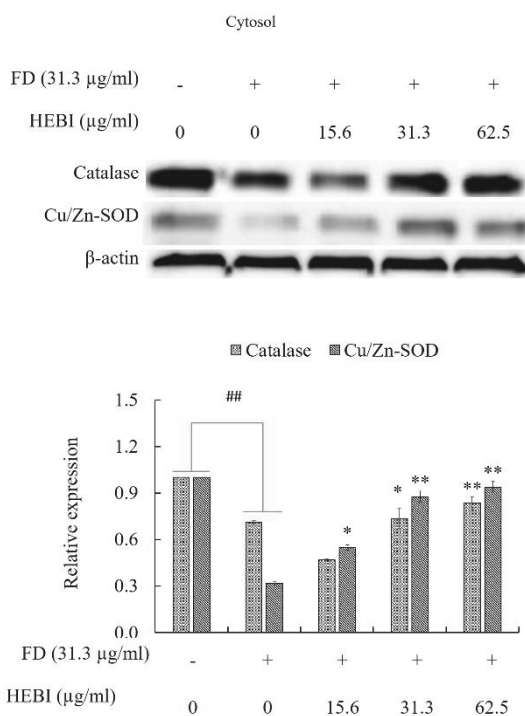


Figure 2-13. HEBI involved in the regulation of antioxidant enzymes function. The relative protein levels of catalase Cu/Zn-SOD in fine dust (FD)-exposed MH-S cells prior to HEBI treatment. Western blot analysis showing the expression of catalase and Cu/Zn-SOD in cells treated as in the figure. Western blotting signal of individual enzyme was normalized by β -actin and FD induced group was defined as 1 of relative expression. $*p < 0.05$, $**p < 0.01$ vs. the FD treated group or $##p < 0.01$ vs control.

2.2.2.4 HEBI induced antioxidant mechanism in fine dust exposed MH-S cells through Nrf2/Keap1 mediated antioxidant pathway.

Nuclear Factor-Like 2 (Nrf2) has been identified as a main transcription factor; translocate into nucleus and mediate antioxidant and anti-apoptotic gene expression under oxidative stress conditions (Niture et al. 2014). Recently, several studies have reported, the activation of Nrf2 and its downstream antioxidants enzymes help to reduce oxidative stress via encoding anti-oxidant related genes and following antioxidant mechanisms (Li and Leung 2017). In normal (non-oxidative stress) conditions, levels of Nrf2 in cytosol are low, and Nrf2 is retained in the cytoplasm together with its cytosolic inhibitor Keap1. The main role of Keap1 is act as an adaptor protein in the cullin 3 (Cul3)-based E3 ligase complex that ubiquitinates Nrf2 resulting in proteasomal degradation. Thus, the level of Nrf2 less when the cells contains large amount of Keap1 in cytosol. In response to oxidative stress, Nrf2 is stabilized and translocated to the nucleus and binds to the antioxidant response element (ARE) (Kobayashi et al. 2004; Russell and Cotter 2015). Author therefore hypothesized that HEBI regulates fine dust induced oxidative stress in MH-S cells by targeting Nrf2 function. Macrophages were exposed to the fine dust prior to the treatment of HEBI for 1 h and then Nrf2, Keap-1, and HO-1 protein levels in nuclear or cytosolic fraction was measured by Western blotting analysis. Upon treatment of HEBI, the cytosolic Keap-1 dose-dependently decreased (fig. 2-14) and the translocation of Nrf2 to the nucleus notable increased (fig. 2-15). Moreover, at the same time the levels of HO-1 in nucleus and cytosol increased dose-dependently with the treatment of HEBI. Thus, our results strongly suggest that HEBI facilitates Nrf2 nuclear translocation and triggers the antioxidant mechanisms in fine dust exposed cells. Specifically, up-regulated expression of HO-1, Cu/Zn-SOD, and Catalase important to reduced oxidative damage caused by the fine dust.

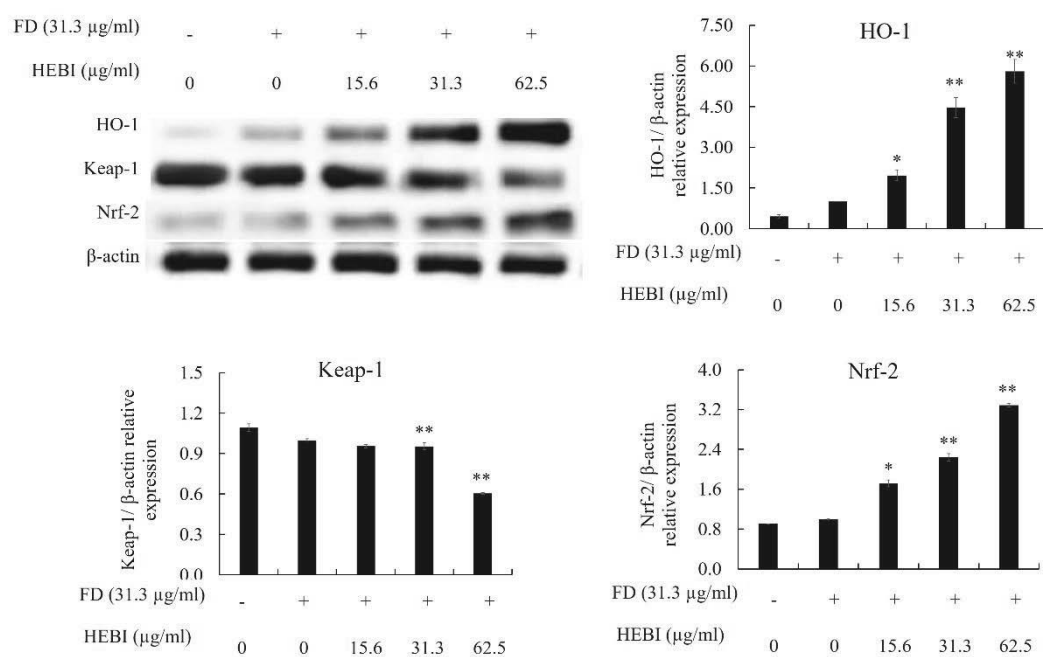


Figure 2-14. Effect of HEBI against fine dust (FD)-induced cytosolic HO-1, Nrf-2, and Keap-1 expressions. β -actin was used as internal control. Quantitative data was analyzed using ImageJ software (1.43V). Results are expressed as the mean \pm SD of three separate experiments. * $p < 0.05$ and ** $p < 0.01$.

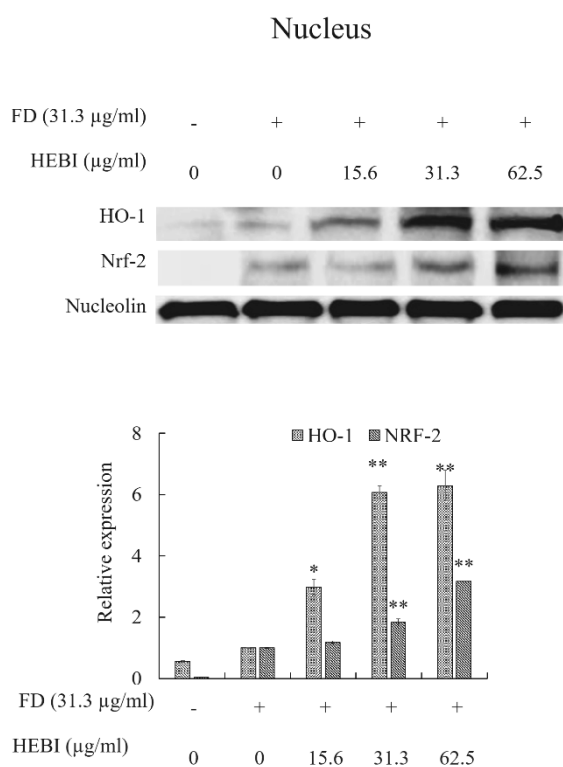
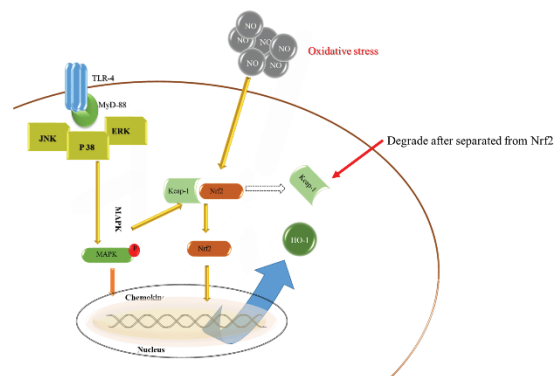
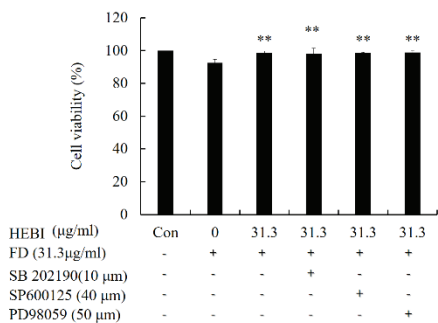
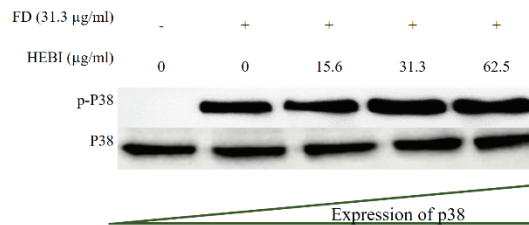
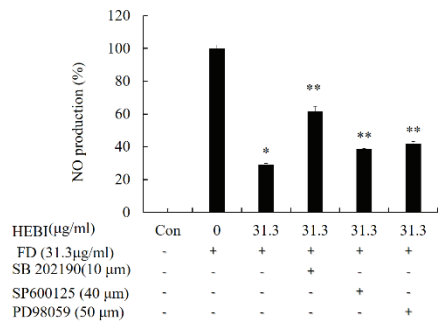


Figure 2-15. Protective effect of HEBI against fine dust (FD)-induced HO-1 and Nrf2 suppression. The expression levels of proteins were measured by western blot (a) and relevant quantitative data (d). Nucleolin was used as internal control. Quantitative data was analyzed using ImageJ software (1.43V). Results are expressed as the mean \pm SD of three separate experiments. * $p < 0.05$ and ** $p < 0.01$.

2.2.2.5. Fine dust induced NO production and Effect of MAPK inhibitors

p38, ERK, and JNK are well-characterized sub families of MAPK, which only prevail in multicellular organisms. The up-regulated phosphorylation of MAPKs triggers the breakdown of Nrf2/Keap1 complex and induce the translocation of Nrf2 to the nucleus (Johnson and Lapadat 2002). Therefore, author attempted to evaluate antioxidant effect of HEBI using specific MAPK inhibitors. Three MAPK inhibitors namely SB 202190 (p38 inhibitor) SP 600125 (JNK inhibitor), and PD98059 (ERK inhibitor) used to evaluate the effect of HEBI against oxidative stress induced fine dust exposed MH-S on MAPK signal transduction pathway. Number of studies, used these inhibitors to demonstrate the role of MAPKs in antioxidant mechanisms (Peluso et al. 2017; Schwartz et al. 2018). Figure 2-16 shows the stimulation of MH-S cells by fine dust and co-treatment of HEBI 31.3 $\mu\text{g/ml}$.

According to the results, fine dust-exposed macrophages showed elevated levels of NO in the culture supernatants. In addition to the SB 202190, the p38 inhibitor, up-regulated the NO production significantly with a minimal effect on cell viability. Even though slight up-regulation of NO observed with the SP600125; JNK inhibitor and PD98059; ERK1/2 treatments, they did not exhibit a strong effect compared to fine dust and HEBI co-treatment. In addition to the NO inhibition effect author compared the Phosphorylation levels of p38 using western blot analysis to confirm the results. Taken together, our results suggesting that, HEBI has the potential to induce antioxidant mechanisms through the p38 MAPK mediated down-stream signal transduction in fine dust exposed MH-S cells.



SB 202190 = P 38 inhibitor; SP 600125 = JNK inhibitor; PD98059 = ERK inhibitor

Figure 2-16. The antioxidant effect of HEBI against the fine dust (FD)-induced oxidative damage in MH-S cells. (a) Cell viability and (b) NO inhibitory effect in the presence of specific MAPKs inhibitors. The cells were treated with indicated concentrations of HEBI (31.3 $\mu\text{g ml}^{-1}$) for 24 h in the presence or absence of each selective inhibitor. SB 202190 (p38 inhibitor) SP 600125 (JNK inhibitor), and PD98059 (ERK inhibitor). (c) Effects of HEBI on FD-induced NFR2/Keap-1 pathway related p38 expression in MH-S cells. P38 and p-P38 levels were determined using western blotting. Quantitative data was analyzed using ImageJ software. Results are expressed as the mean \pm SD of three separate experiments. * $p < 0.05$ and ** $p < 0.01$.

2.4. Conclusions

In the present study, author attempted to evaluate anti-inflammatory and antioxidant properties of a pure compound isolated from *S. horneri* using fine dust exposed MH-S macrophages. According to the results, exposure of fine dust to MH-S cells cause to induce oxidative stress and inflammation in macrophages. The real time qPCR data confirmed that the exposure of fine dust cause to activation of TLR 2,3, 4, and 7 in MH-S cells. The activation of those TLR is a one main reason to activate inducible genes such as iNOS and COX2 through NF- κ B and MAPKs. According to the mRNA expression data, TNF- α levels were up-regulated in the fine dust exposed cells. TNF- α is a known stimulator of NF- κ B pathway and end product of MAPKs. This phenomenon should be a one reason for activation of NF- κ B pathway in fine dust exposed MH-S cells.

In addition, fine dust also reduced the expression levels of antioxidant proteins and genes in macrophages in exposed cells. However, the treatment of HEBI, inhibited the fine dust induced inflammation and oxidative stress via blocking TLR/MyD88 mediated inflammatory pathways and up-regulated the brake down of Keap1/Nrf2 to accelerate the production of antioxidant genes. Therefore, HEBI has the potential to develop as a functional materials to avoid oxidative stress and chronic inflammation in human body. Therefore, the development of functional material from HEBI will be a useful approach to reduce fine dust induced complications in humans.

2.5. References

- Akira S., and Takeda K. (2004). Toll-like receptor signalling. *Nat Rev Immunol*, **4**(7). Pp: 499-511. DOI: 10.1038/nri1391
- Arango Duque G., and Descoteaux A. (2014). Macrophage cytokines: involvement in immunity and infectious diseases. *Front Immunol*, **5**. Pp: 491. DOI: 10.3389/fimmu.2014.00491
- Baeuerle P. A., and Baltimore D. (1996). NF- κ B: Ten Years After. *Cell*, **87**(1). Pp: 13-20. DOI: 10.1016/s0092-8674(00)81318-5
- Baldwin A. S., Jr. (1996). The NF-kappa B and I kappa B proteins: new discoveries and insights. *Annu Rev Immunol*, **14**(1). Pp: 649-83. DOI: 10.1146/annurev.immunol.14.1.649
- Bekki K., Ito T., Yoshida Y., He C., Arashidani K., He M., Sun G., Zeng Y., Sone H., Kunugita N., and Ichinose T. (2016). PM2.5 collected in China causes inflammatory and oxidative stress responses in macrophages through the multiple pathways. *Environ Toxicol Pharmacol*, **45**. Pp: 362-9. DOI: 10.1016/j.etap.2016.06.022
- Crofford L. J. (1997). COX-1 and COX-2 tissue expression: implications and predictions. *J Rheumatol Suppl*, **49**. Pp: 15-9. DOI: <https://europepmc.org/abstract/med/9249646>
- Dalgleish A. G., and O'Byrne K.(2006). *Inflammation and Cancer*, in *The Link Between Inflammation and Cancer: Wounds that do not heal*, A.G. Dalgleish and B. Haefner, Editors. Springer US: Boston, MA. p. 1-38
- Echizen K., Hirose O., Maeda Y., and Oshima M. (2016). Inflammation in gastric cancer: Interplay of the COX-2/prostaglandin E2 and Toll-like receptor/MyD88 pathways. *Cancer Sci*, **107**(4). Pp: 391-7. DOI: 10.1111/cas.12901

Fernando I. P. S., Kim H.-S., Sanjeeva K. K. A., Oh J.-Y., Jeon Y.-J., and Lee W. W. (2017). Inhibition of inflammatory responses elicited by urban fine dust particles in keratinocytes and macrophages by diphlorethohydroxycarmalol isolated from a brown alga *Ishige okamurae*. *Algae*, **32**(3). Pp: 261-273. DOI: 10.4490/algae.2017.32.8.14

Gil D., Rodriguez J., Ward B., Vertegel A., Ivanov V., and Reukov V. (2017). Antioxidant Activity of SOD and Catalase Conjugated with Nanocrystalline Ceria. *Bioengineering (Basel)*, **4**(1). Pp: 18. DOI: 10.3390/bioengineering4010018

He M., Ichinose T., Kobayashi M., Arashidani K., Yoshida S., Nishikawa M., Takano H., Sun G., and Shibamoto T. (2016). Differences in allergic inflammatory responses between urban PM_{2.5} and fine particle derived from desert-dust in murine lungs. *Toxicol Appl Pharmacol*, **297**. Pp: 41-55. DOI: 10.1016/j.taap.2016.02.017

Hommes D. W., Peppelenbosch M. P., and van Deventer S. J. (2003). Mitogen activated protein (MAP) kinase signal transduction pathways and novel anti-inflammatory targets. *Gut*, **52**(1). Pp: 144-51. DOI: 10.1136/gut.52.1.144

Huang Y. C., Ghio A. J., Stonehuerner J., McGee J., Carter J. D., Grambow S. C., and Devlin R. B. (2003). The role of soluble components in ambient fine particles-induced changes in human lungs and blood. *Inhal Toxicol*, **15**(4). Pp: 327-42. DOI: 10.1080/08958370304460

Johnson G. L., and Lapadat R. (2002). Mitogen-activated protein kinase pathways mediated by ERK, JNK, and p38 protein kinases. *Science*, **298**(5600). Pp: 1911-2. DOI: 10.1126/science.1072682

Kaminska B. (2005). MAPK signalling pathways as molecular targets for anti-inflammatory therapy--from molecular mechanisms to therapeutic benefits. *Biochim Biophys Acta*, **1754**(1-2). Pp: 253-62. DOI: 10.1016/j.bbapap.2005.08.017

Kim P. W. (2018). Operating an environmentally sustainable city using fine dust level big data measured at individual elementary schools. *Sustainable Cities and Society*, **37**. Pp: 1-6. DOI: 10.1016/j.scs.2017.10.019

Kobayashi A., Kang M. I., Okawa H., Ohtsuji M., Zenke Y., Chiba T., Igarashi K., and Yamamoto M. (2004). Oxidative stress sensor Keap1 functions as an adaptor for Cul3-based E3 ligase to regulate proteasomal degradation of Nrf2. *Mol Cell Biol*, **24**(16). Pp: 7130-9. DOI: 10.1128/MCB.24.16.7130-7139.2004

Kyriakis J. M., and Avruch J. (2001). Mammalian mitogen-activated protein kinase signal transduction pathways activated by stress and inflammation. *Physiol Rev*, **81**(2). Pp: 807-69. DOI: 10.1152/physrev.2001.81.2.807

Lee Y. G., Ho C.-H., Kim J.-H., and Kim J. (2015). Quiescence of Asian dust events in South Korea and Japan during 2012 spring: Dust outbreaks and transports. *Atmospheric Environment*, **114**. Pp: 92-101. DOI: 10.1016/j.atmosenv.2015.05.035

Lehman-McKeeman L. D.(2013). *Chapter 1 - Biochemical and Molecular Basis of Toxicity*, in *Haschek and Rousseaux's Handbook of Toxicologic Pathology (Third Edition)*, W.M. Haschek, C.G. Rousseaux, and M.A. Wallig, Editors. Academic Press: Boston. p. 15-38

Lei Y. C., Hwang J. S., Chan C. C., Lee C. T., and Cheng T. J. (2005). Enhanced oxidative stress and endothelial dysfunction in streptozotocin-diabetic rats exposed to fine particles. *Environ Res*, **99**(3). Pp: 335-43. DOI: 10.1016/j.envres.2005.03.011

Leiro J., Alvarez E., Garcia D., and Orallo F. (2002). Resveratrol modulates rat macrophage functions. *Int Immunopharmacol*, **2**(6). Pp: 767-74. DOI: [http://dx.doi.org/10.1016/S1567-5769\(02\)00014-0](http://dx.doi.org/10.1016/S1567-5769(02)00014-0)

Li L., and Leung P. S.(2017). *Chapter 13 - Pancreatic Cancer, Pancreatitis, and Oxidative Stress*, in *Gastrointestinal Tissue*, J. Gracia-Sancho and J. Salvadó, Editors. Academic Press. p. 173-186

Liu K., Wang X., Sha K., Zhang F., Xiong F., Wang X., Chen J., Li J., Churilov L. P., Chen S., Wang Y., and Huang N. (2017). Nuclear protein HMGN2 attenuates pyocyanin-induced oxidative stress via Nrf2 signaling and inhibits *Pseudomonas aeruginosa* internalization in A549 cells. *Free Radic Biol Med*, **108**. Pp: 404-417. DOI: 10.1016/j.freeradbiomed.2017.04.007

Livak K. J., and Schmittgen T. D. (2001). Analysis of relative gene expression data using real-time quantitative PCR and the $2^{-\Delta\Delta CT}$ method. *Methods*, **25**(4). Pp: 402-408. DOI: 10.1006/meth.2001.1262

Meng Z., and Zhang Q. (2006). Oxidative damage of dust storm fine particles instillation on lungs, hearts and livers of rats. *Environ Toxicol Pharmacol*, **22**(3). Pp: 277-82. DOI: 10.1016/j.etap.2006.04.005

Mitchell J., Kim S. J., Seelmann A., Veit B., Shepard B., Im E., and Rhee S. H. (2018). Src family kinase tyrosine phosphorylates Toll-like receptor 4 to dissociate MyD88 and Mal/Tirap, suppressing LPS-induced inflammatory responses. *Biochem Pharmacol*, **147**. Pp: 119-127. DOI: 10.1016/j.bcp.2017.11.015

Mosmann T. (1983). Rapid colorimetric assay for cellular growth and survival: Application to proliferation and cytotoxic assay. *J. Immunol. Meth.*, **65**. Pp: 55-63. DOI: 10.1016/0022-1759(83)90133-8

Mulgund A., Doshi S., and Agarwal A. (2015). *Chapter 25 - The Role of Oxidative Stress in Endometriosis*, in *Handbook of Fertility*, R.R. Watson, Editor. Academic Press: San Diego. p. 273-281

Nel A. (2005). Atmosphere. Air pollution-related illness: effects of particles. *Science*, **308**(5723). Pp: 804-6. DOI: 10.1126/science.1108752

Niture S. K., Khatri R., and Jaiswal A. K. (2014). Regulation of Nrf2-an update. *Free Radic Biol Med*, **66**. Pp: 36-44. DOI: 10.1016/j.freeradbiomed.2013.02.008

Oh G.-W., Ko S.-C., Lee D. H., Heo S.-J., and Jung W.-K. (2017). Biological activities and biomedical potential of sea cucumber (*Stichopus japonicus*): a review. *Fisheries and Aquatic Sciences*, **20**(1). Pp: 28. DOI: 10.1186/s41240-017-0071-y

Pardo M., Xu F., Qiu X., Zhu T., and Rudich Y. (2018). Seasonal variations in fine particle composition from Beijing prompt oxidative stress response in mouse lung and liver. *Sci Total Environ*, **626**. Pp: 147-155. DOI: 10.1016/j.scitotenv.2018.01.017

Peluso I., Yarla N. S., Ambra R., Pastore G., and Perry G. (2017). MAPK signalling pathway in cancers: Olive products as cancer preventive and therapeutic agents. *Semin Cancer Biol*. Pp. DOI: 10.1016/j.semcancer.2017.09.002

Perchyonok T., Reher V., and Grobler S.(2016). *Chapter 9 - Bioactive-functionalized interpenetrating network hydrogel (BIOF-IPN)*, in *Engineering of Nanobiomaterials*, A.M. Grumezescu, Editor. William Andrew Publishing. p. 287-306

Perini K., Ottel  M., Giulini S., Magliocco A., and Roccotiello E. (2017). Quantification of fine dust deposition on different plant species in a vertical greening system. *Ecological Engineering*, **100**. Pp: 268-276. DOI: 10.1016/j.ecoleng.2016.12.032

Powell S. R., Herrmann J., Lerman A., Patterson C., and Wang X.(2012). *Chapter 9 - The Ubiquitin-Proteasome System and Cardiovascular Disease*, in *Progress in Molecular Biology and Translational Science*, T. Grune, Editor. Academic Press. p. 295-346

Pozzi R., De Berardis B., Paoletti L., and Guastadisegni C. (2003). Inflammatory mediators induced by coarse (PM2.5-10) and fine (PM2.5) urban air particles in RAW 264.7 cells. *Toxicology*, **183**(1-3). Pp: 243-54. DOI: [https://doi.org/10.1016/S0300-483X\(02\)00545-0](https://doi.org/10.1016/S0300-483X(02)00545-0)

Russell E. G., and Cotter T. G.(2015). *Chapter Six - New Insight into the Role of Reactive Oxygen Species (ROS) in Cellular Signal-Transduction Processes*, in *International Review of Cell and Molecular Biology*, K.W. Jeon, Editor. Academic Press. p. 221-254

Sanjeeva K. K. A., Fernando I. P. S., Kim E. A., Ahn G., Jee Y., and Jeon Y. J. (2017). Anti-inflammatory activity of a sulfated polysaccharide isolated from an enzymatic digest of brown seaweed *Sargassum horneri* in RAW 264.7 cells. *Nutr Res Pract*, **11**(1). Pp: 3-10. DOI: 10.4162/nrp.2017.11.1.3

Schwartz M., Bockmann S., Borchert P., and Hinz B. (2018). SB202190 inhibits endothelial cell apoptosis via induction of autophagy and heme oxygenase-1. *Oncotarget*, **9**(33). Pp: 23149-23163. DOI: 10.18632/oncotarget.25234

Seok J. K., Lee J. W., Kim Y. M., and Boo Y. C. (2018). Punicalagin and (-)-Epigallocatechin-3-Gallate Rescue Cell Viability and Attenuate Inflammatory Responses of Human Epidermal Keratinocytes Exposed to Airborne Particulate Matter PM10. *Skin Pharmacol Physiol*, **31**(3). Pp: 134-143. DOI: 10.1159/000487400

Shah A. S., Langrish J. P., Nair H., McAllister D. A., Hunter A. L., Donaldson K., Newby D. E., and Mills N. L. (2013). Global association of air pollution and heart failure: a systematic review and meta-analysis. *Lancet*, **382**(9897). Pp: 1039-48. DOI: 10.1016/S0140-6736(13)60898-3

Stentz F. B., Umpierrez G. E., Cuervo R., and Kitabchi A. E. (2004). Proinflammatory cytokines, markers of cardiovascular risks, oxidative stress, and lipid peroxidation in patients with hyperglycemic crises. *Diabetes*, **53**(8). Pp: 2079-86.

Su R., Jin X., Zhang W., Li Z., Liu X., and Ren J. (2017). Particulate matter exposure induces the autophagy of macrophages via oxidative stress-mediated PI3K/AKT/mTOR pathway. *Chemosphere*, **167**. Pp: 444-453. DOI: 10.1016/j.chemosphere.2016.10.024

Sutcliffe S., and Pontari M. A.(2016). *Chapter 2 - Inflammation and Infection in the Etiology of Prostate Cancer*, in *Prostate Cancer (Second Edition)*, J.H. Mydlo and C.J. Godec, Editors. Academic Press: San Diego. p. 13-20

Tak P. P., and Firestein G. S. (2001). NF-kappaB: a key role in inflammatory diseases. *J Clin Invest*, **107**(1). Pp: 7-11. DOI: 10.1172/JCI11830

Tsai M. H., Hsu L. F., Lee C. W., Chiang Y. C., Lee M. H., How J. M., Wu C. M., Huang C. L., and Lee I. T. (2017). Resveratrol inhibits urban particulate matter-induced COX-2/PGE2 release in human fibroblast-like synoviocytes via the inhibition of activation of NADPH oxidase/ROS/NF-kappaB. *Int J Biochem Cell Biol*, **88**. Pp: 113-123. DOI: 10.1016/j.biocel.2017.05.015

Vannini F., Kashfi K., and Nath N. (2015). The dual role of iNOS in cancer. *Redox Biol*, **6**. Pp: 334-43. DOI: 10.1016/j.redox.2015.08.009

Yang C., Zhang X., Fan H., and Liu Y. (2009). Curcumin upregulates transcription factor Nrf2, HO-1 expression and protects rat brains against focal ischemia. *Brain Res*, **1282**. Pp: 133-41. DOI: 10.1016/j.brainres.2009.05.009

Yenkoyan K., Harutyunyan H., and Harutyunyan A. (2018). A certain role of SOD/CAT imbalance in pathogenesis of autism spectrum disorders. *Free Radic Biol Med*, **123**. Pp: 85-95. DOI: 10.1016/j.freeradbiomed.2018.05.070

Zhao Q., Chen H., Yang T., Rui W., Liu F., Zhang F., Zhao Y., and Ding W. (2016). Direct effects of airborne PM2.5 exposure on macrophage polarizations. *Biochim Biophys Acta*, **1860**(12). Pp: 2835-43. DOI: 10.1016/j.bbagen.2016.03.033

Part- 3

Anti-inflammatory and antioxidant mechanisms of 3-Hydroxy-5,6-epoxy- β -ionone isolated from *Sargassum horneri* on fine dust-exposed CMT-93 mouse epithelial cells (digestive tract)

Abstract

Background

The health complication of fine dust exposed lungs have been well established. However, effect of fine dust in digestive system not yet study in details. Fine dust in the air (particulate matter; PM 2.5) can also move to digestive tract through the swelling and directly by air and through the foods. Therefore, fine dust might cause inflammation and oxidative stress in epithelial cells located in digestive system and could be link to the pathogenesis of chronic inflammatory diseases and cancer. Therefore, in the present study author attempted to evaluate effect of fine dust after exposed to CMT-93; epithelial cells in digestive tract using inflammatory and oxidative stress related bio-markers.

Methodology

CMT-93 cells exposed to fine dust for 24 h after treatment of 3-Hydroxy-5,6-epoxy- β -ionone; (HEBI) a pure compound isolated from *Sargassum horneri* for 1 h. Then the inflammatory and oxidative stress related proteins and genes were evaluated using western blots, RT-qPCR, and ELISA assays.

Results

The exposure of fine dust caused to up-regulate the expression of toll like receptors and MyD88 protein expression in CMT-93 cells. Which cause to induce inflammatory responses in CMT-93 cells via activation of NF- κ B and MAPKs. Moreover, fine dust also suppressed the antioxidant related gene and protein expression in CMT-93 cells. However, HEBI treatment inhibited inflammatory responses in fine dust exposed CMT-93 cells via blocking the TLR/MyD88 mediated NF- κ B and MAPKs expression. In addition, HEBI also up-regulated the Keap1/Nrf2 mediated antioxidant pathway

activities. In addition, anti-inflammatory cytokines such as IL-4 expression were dose-dependently increased with the HEBI treatment.

Conclusions

In the present study, author demonstrated protective effect of HEBI against fine dust induced inflammation and oxidative stress in digestive tract epithelial cells. Therefore, incorporation of HEBI as active ingredient in functional food might be a useful approach to reduce fine dust induced inflammation and oxidative stress in digestive tract.

3.1. Introduction

The mucosal surface of the gastrointestinal tract is one ideal place for pathogen invasions. However, the immune cells associated with the digestive tract hypo-responsive to food antigens and bacterial strains. Due to this strong protection given by immune cells, the pathogen invasions are limited through the digestive track (Karin et al. 2006). Intestinal epithelial cells (CMT-93) is a protective cell type acting as a primary physical barrier against immune-stimulators including commensal and pathogenic micro-organisms in the gastrointestinal tract (Zaph et al. 2007). Nevertheless, studies have reported, immune protective mechanisms of CMT-93 cause to triggers the chronic inflammatory responses (Kim et al. 2010). Specifically, Kim et al. (2010) demonstrated how parasites regulate and suppress their host immune responses to maintain their parasitism for a prolonged period using CMT-93 cells. Moreover, Kim et al. (2010) reported the stimulation of CMT-93 cells through immune stimulant cause the activation of NF- κ B and MAPK proteins and lead to development of inflammatory responses.

It is a well-established fact that the continuous exposure of internal organs to air pollutions such as fine dust cause to induce oxidative stress, inflammation, and poses a serious risk to human health (Lee et al. 2015). Fine dust identified as a major health threat to human society, because of the high exposure risk even at the low concentrations (Perini et al. 2017). According to the recent statistics, 2 million deaths are occurring globally in each year as a direct consequence of air pollution through damage to the respiratory system and lungs (Shah et al. 2013). Other than the respiratory system related complications, functions of digestive system also altered from the fine dust particles (Lomer et al. 2002). Specially, Lomer et al. (2002) reported the ultrafine particles of the diet case to change mucosal immune response and association between Crohn's disease. Crohn's disease is a condition characterised by transmural inflammation of the

gastrointestinal tract. In corporation of functional foods to regular diet might be a faceable approach to avoid inflammation induced by fine dust in the digestive tract. However, there are limited research attention to elucidate connections between fine dust and inflammation in the digestive system.

Sargassum horneri (Sargassaceae, Fucales, Phaeophyta) is an edible brown seaweed, abundant worldwide in shallow sea-water eco-systems. *S. horneri* play an important role in coastal waters and provides habitats for other marine organisms such as fish and shellfish (Kubo et al. 2017). Other than the ecological importance of this seaweed, which also popular as a nutrient rich edible seaweed specifically in the East-Asian countries. Usually Korean people consume this seaweed as a soup after boiled with meat and other land vegetables (Sanjeewa and Jeon 2018). In Japan, *S. horneri* is known as “akamoku” and is harvested at the maturation stage as a sea vegetable in regions along the Sea of Japan (Terasaki et al. 2017). Taken together, in the present study, author attempted to evaluate anti-inflammatory effects of a 3-Hydroxy-5,6-epoxy- β -ionone (fig 3.1) an active compound isolated from brown seaweed *S. horneri* against fine dust induced inflammation and oxidative stress in CMT-93.

SHF2-2
DMSO

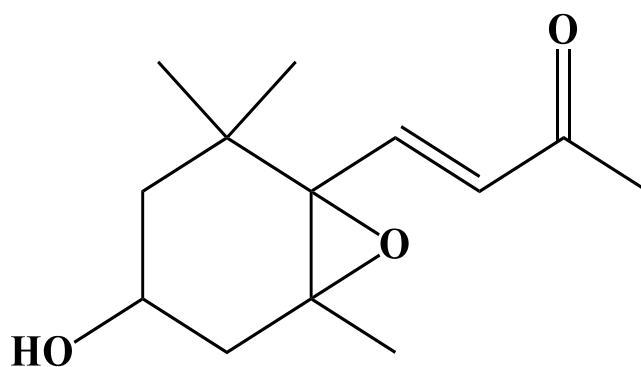


Figure 3-1. 3-Hydroxy-5,6-epoxy-β-ionone isolated from *Sargassum horneri*. PubChem

CID: 5371267, Abbreviation : HEBI

3.2. Materials and methods

3.2.1. Chemicals and reagents

CRM certified fine dust reference material (CRM No. 28 Urban Aerosols) was purchased from the Center for Environmental Measurement and Analysis, National Institute for Environmental studies, Ibaraki, Japan. Dulbecco's modified Eagle's medium (DMEM), penicillin-streptomycin, and fetal bovine serum (FBS) were purchased from Gibco BRL (Burlington, ON, Canada). 3-(4, 5- dimethyl sulfoxide (DMSO), Tri-Reagent™, and Dimethylthiazol-2-yl)-2, 5-diphenyltetrazolium bromide (MTT) were purchased from Sigma-Aldrich (St. Louis, MO, USA). NE-PER® nuclear and cytoplasmic extraction kit was purchased from Thermo scientific, Rockford, USA. Enzyme-linked immunosorbent assay (ELISA) kits for TNF- α , IL-1 β , IL-6, and PGE₂ were purchased from R&D Systems Inc. (Minneapolis, MN, USA). All other chemicals and reagents used in these experiments were of analytical grade.

3.2.2. Estimation of fine dust particle size by scanning electron microscopy

The fine dust sample was mounted on double-sided carbon tape and sputter-coated with platinum in a Q150R rotary-pumped sputter coater (Quorum Technologies, Lewes, UK). The surface morphology of fine dust particles was observed by a JSM-6700F field-emission scanning electron microscope (JEOL, Tokyo, Japan) operated at 10.00 kV.

3.2.3. Culture conditions of CMT-93 cell line

CMT-93 mouse intestinal epithelial cells were purchased from the American Type Culture Collection (ATCC) (Manassas, VA, USA). The cells were maintained in DMEM supplemented with 10% heat-inactivated FBS, and 1% penicillin-streptomycin (100 units/ml of penicillin, and 100 μ g/ml of streptomycin). The cells were cultured at 37 °C

in a humidified atmosphere containing 5% CO₂. For the all the studies cells were plated in at 1 × 10⁵ cells/well and incubated for the given time periods.

3.2.4. Cell viability assay (MTT) and measurement of nitrite by Griess reaction

CMT-93 (1 × 10⁵ cells/ml) cells were seeded in a 24-well plate and incubated for 24 h. Then, the cells were treated with HEBI and stimulated using fine dust for 24 h. Then the cells incubated with 50 µl of MTT (250 µg/ml). After 4 h of incubation, purple color formason crystals were dissolved in DMSO, and cell viability was assessed using plate reader (BioTek Instruments, Inc., Winooski, USA) at 540 nm.

$$\text{Cell viability (\%)} = \frac{(OD_{control} - OD_{sample})}{OD_{control}} \times 100$$

To determine the NO inhibitory effect of HEBI in fine dust-stimulated CMT-93 cells, author performed Griess assay with the previously described method (Leiro et al. 2002). Briefly, CMT-93 cells were seeded in 24-well plates and incubated for 24 h. Then, the cells were treated with HEBI for 1 h and stimulated with fine dust (500 µg/ml) for 24 h. Finally, 50 µl of culture medium mixed with 50 µl of Griess reagent and incubated in room temperature for 10 min. The absorbance was measured at 540 nm using an ELISA plate reader. The results expressed as mean percentages of the NO production versus the NO production of only fine dust-exposed cells.

$$\text{NO inhibition (\%)} = \frac{(OD_{control} - OD_{sample})}{(OD_{control} - OD_{fine\ dust\ group})} \times 100$$

3.2.5. Determination of PGE₂ and pro-inflammatory cytokine secretion levels

CMT-93 cells (1×10^5 cells/ml) were treated with the indicated concentrations of HEBI, and 1 h later cells stimulated with fine dust (250 μ g/ml). After 24 h of incubation, the PGE₂, TNF- α , IFN- γ , IL-6, and IL-1 β concentration in the supernatant was quantified by using a competitive enzyme immunoassay kit, according to the vender's instruction.

3.2.6. Total RNA extraction and cDNA synthesis

Total cellular RNA from CMT-93 cells extracted using Tri-Reagent™ (Sigma-Aldrich, St. Louis, MO, USA). Absorbance was measured at 260 nm and 280 nm using a μ Drop Plate (Thermo Scientific) to determine the concentration and purity of the extracted RNA. Then, RNA samples were diluted (1 μ g/ μ l) and first strand cDNA was synthesized using prime Script™ first-strand cDNA synthesis kit (TaKaRa BIO INC, Japan) according to the manufactures instructions. Finale products were stored at -80 °C until use.

3.2.7. Quantitative real-time PCR (qPCR) analysis

Expression levels of inflammation related genes were analyzed using SYBR Green quantitative real-time PCR (qPCR) technique. GAPDH was used as an internal reference gene in amplification. The primers used in this study purchased from Bioneer, Seoul, Korea. The RT-qPCR was carried out in 10 μ l volume containing 3 μ l of the synthesized cDNA sample, 0.4 μ M primer pairs, 1.2 μ l PCR grade H₂O, and 5 μ l SYBR green PCR master mix in thermal cycler dice-real time system (TaKaRa, Japan). The following protocol was used 95 °C for 10 s followed by 40 cycles at 95 °C for 5 s, 55 °C for 10 s, and 72 °C for 20 s, and a final single cycle at 95 °C for 15 s, 55 °C for 30 s, and 95 °C for 15 s. Relative expression levels of the target genes were calculated based on $2^{-\Delta\Delta Ct}$ describe by Livak and Schmittgen (2001) (Livak and Schmittgen 2001). The base line

was automatically set by Dice™ Real Time System software (version 2.00) to keep reliability. The sequence of primers used in this study were shown in table 3-1 and 3-2. The data are presented as the mean ± standard error (SE) of the relative mRNA expression from three consecutive experiments. The two-tailed unpaired Students t-test was used to determine statistical significance (* = $p < 0.05$ and ** = $p < 0.01$).

3.2.8. Western blot analysis

CMT-93 cells (1×10^5 cells/well) were pre-treated with HEBI for 1 h and stimulated with fine dust (250 µg/ml) for 24 h. Cells were then harvested and cytosolic and nucleus proteins were extracted from CMT-93 cells using commercial protein extraction kit. Protein level of cell lysates were quantified using Bradford's method with BSA standard. Western blot studies were performed using previously optimised protocol (Sanjeeva et al. 2017). Briefly, equal amounts of cell lysates were separated by 12% sodium dodecyl sulphate polyacrylamide gel electrophoresis (SDS-PAGE) and electro-transferred to a nitrocellulose membrane. Then the membranes were blocked by 5% non-fat dry milk for 1 h. Then the nitrocellulose membranes were incubated with the specific primary antibodies, at 4 °C for 12 h. Then the unbind primary antibodies were removed from membranes using TBST and then incubated with peroxidase-conjugated secondary antibody at room temperature for 1 h. Protein expression levels were visualized with the super signal west pico chemiluminescent substrate (Thermo, MA, USA). Densitometry analysis of specific bands were done using ImageJ software version 1.49 (national institute of health, USA). The basal levels of each protein were normalized by analysing the level of β-actin or nucleolin.

Table 3-1. Sequence of the primers used to evaluate RNA expression levels

Gene	Primer	Sequence 5' → 3'
GAPDH	Sense	AAGGGTCATCATCTCTGCCC
	Antisense	GTGATGGCATGGACTGTGGT
iNOS	Sense	ATGTCCGAAGCAAACATCAC
	Antisense	TAATGTCCAGGAAGTAGGTG
COX2	Sense	CAGCAAATCCTTGCTGTTCC
	Antisense	TGGGCAAAGAATGCAAACATC
TNF- α	Sense	TTGACCTCAGCGCTGAGTTG
	Antisense	CCTGTAGCCCACGTCGTAGC
IFN- γ	Sense	CAATGAACGCTACACACTG
	Antisense	CTTGCTGTTGCTGAAGAAGG
IL-1 β	Sense	CAGGATGAGGACATGAGCACC
	Antisense	CTCTGCAGACTCAAACCTCCAC
IL-6	Sense	GTACTCCAGAAGACCAGAGG
	Antisense	TGCTGGTGACAACCACGGCC
IL-4	Sense	ATCCTGCTCTTCTTTCTCGAATGT
	Antisense	GCCGATGATCTCTCTCAAGTGATT
IL-6	Sense	GTACTCCAGAAGACCAGAGG
	Antisense	TGCTGGTGACAACCACGGCC
HO-1	Sense	TGAAGGAGGCCACCAAGGAGG
	Antisense	AGAGGTCACCAGGTAGCGGG
Nrf2	Sense	TGGACGGGACTATTGAAGGC
	Antisense	GCCGCCTTTTCAGTAGTAGG

Table 3-2. Primer sequences of mouse TLRs for Real-time RT-PCR

Gene	Primer	Sequence (5' → 3')
TLR1	Sense	TCAAGTGTGCAGCTGATTGC
	Antisense	TAGTGCTGACGGACACATCC
TLR2	Sense	CAGCTGGAGAACTCTGACCC
	Antisense	CAAAGAGCCTGAAGTGGGAG
TLR3	Sense	CCTCCAACGTCTACCAGTTCC
	Antisense	GCCTGGCTAAGTTATTGTGC
TLR4	Sense	CAACATCATCCAGGAAGGC
	Antisense	GAAGGCGATAACAATTCCACC
TLR5	Sense	AGCATTCTCATCGTGGTGG
	Antisense	AATGGTTGCTATGGTTCGC
TLR6	Sense	TGGATGTCTCACACAATCGG
	Antisense	GCAGCTTAGATGCAAGTGAGC
TLR7	Sense	TTCTTCCGTAGGCTGAACC
	Antisense	GTAAGCTGGATGGCAGATCC
TLR8	Sense	TCTACTTGGCCTTGCAGAGG
	Antisense	ATGGCAGAGTCGTGACTTCC
TLR9	Sense	CAAGAACCTGGTGTCACTGC
	Antisense	TGCGATTGTCTGACAAGTCC

3.2.9. Statistical analysis

All the data were expressed as the mean \pm standard of three determinations. The collected data were analyzed by analysis of variance using the SPSS V.20 statistical analysis package. The mean values of each experiment were compared using one-way analysis of variance. Duncan's multiple range test (DMRT) was used to determine mean separation. A p -value < 0.05 and 0.01 were considered to be statistically significant.

3.3. Results and discussion

3.3.1. Composition of fine dust and size distribution

A number of studies confirmed the airborne particulate matter (PM) adversely affecting to normal functions of cardiovascular and respiratory systems (Khaniabadi et al. 2017). Specifically, with the increased industrial activities and natural phenomenon, the level of fine dust in the Korean peninsula increase dramatically during the last few decades (Kim 2018). According to the previous studies, PM in the fine dust lower than the 2.5 μm cause to induce the activation of macrophages (He et al. 2016). In the present study, author visualized fine dust particles using electron microscope (fig. 3-2a). According to the image analysis results, dust particle sizes are not distributed equally and observed range of particle sizes (fig. 3-2b). Specifically, small amount of fine dust contained PM higher than 10 μm diameter and the large number of particles had less than 2.0 μm diameter (40%). Additionally, fine dust particles had irregular shapes and distributed randomly in electron microscope image. The compositions of elements and mass fraction of polycyclic aromatic hydrocarbons in NIES CRM No. 28 Urban Aerosols are shown in table 3-3 and 3-4, respectively. This information's were obtained from the seller's web site. (<https://www.nies.go.jp/labo/crm-e/aerosol.html> - Date visit; 2018-September 18). According to the heavy metal analysis fine dust contained considerable amounts of metal types including Sr, Cd, Ba, Pb, and U. In addition, tested fine dust sample contained considerable amount of Ba (874 ± 65 mg/kg) and Pb (403 ± 32 mg/kg) residues.

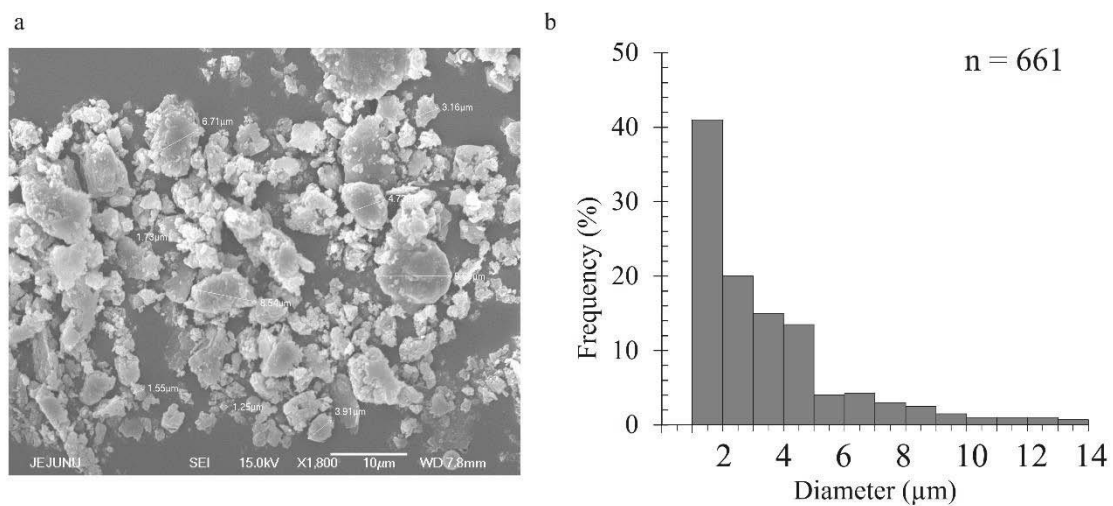


Figure 3-2. Scanning electron microscope image (a) and particle size distribution of fine dust particles (b) purchased from the national institute for environmental studies, Ibaraki, Japan (certified reference material no. 28). Scale bar represent 10 μm lengthly. Source - <https://www.nies.go.jp/labo/crm-e/aerosol.html>

Table 3-3. Certified values of NIES CRM No. 28 Urban Aerosols

Element	Unit	Mass fraction		Analytical method
Na	%	0.796	± 0.065	AAS, ICP-AES, INAA, XRF
Mg	%	1.4	± 0.06	ICP-AES, ICP-MS, XRF
Al	%	5.04	± 0.1	ICP-AES, ICP-MS, INAA, XRF
K	%	1.37	± 0.06	AAS, ICP-AES, XRF
Ca	%	6.69	± 0.24	ICP-AES, ICP-MS, INAA, XRF
Ti	%	0.292	± 0.033	ICP-AES, ICP-MS, INAA, PIXE, XRF
Fe	%	2.92	± 0.17	ICP-AES, ICP-MS, INAA, XRF
Zn	%	0.114	± 0.01	ICP-AES, ICP-MS, INAA, PIXE, XRF
V	mg/kg	73.2	± 7	ICP-AES, ICP-MS, INAA
Mn	mg/kg	686	± 42	ICP-AES, ICP-MS, INAA, PIXE, XRF
Ni	mg/kg	63.8	± 3.4	AAS, ICP-AES, ICP-MS
Cu	mg/kg	104	± 12	ICP-AES, ICP-MS, PIXE, XRF
As	mg/kg	90.2	± 10.7	HG-AAS, HG-ICP-AES, ICP-AES, ICP-MS, INAA, XRF
Sr	mg/kg	469	± 16	ICP-AES, ICP-MS, XRF
Cd	mg/kg	5.6	± 0.43	ICP-AES, ICP-MS
Ba	mg/kg	874	± 65	ICP-AES, ICP-MS, INAA
Pb	mg/kg	403	± 32	ICP-AES, ICP-MS, XRF
U	mg/kg	4.33	± 0.26	ICP-MS, INAA

AAS: atomic absorption spectroscopy; HG-AAS: hydride generation - atomic absorption spectroscopy; HG-ICP-AES: hydride generation-inductively coupled plasma-atomic emission spectrometry; ICP-AES: inductively coupled plasma-atomic emission spectrometry; ICP-MS: inductively coupled plasma-mass spectrometry; INAA: instrumental neutron activation analysis; PIXE: proton induced X-ray emission spectrometry; XRF: X-ray fluorescence spectroscopy. Source - <https://www.nies.go.jp/labo/crm-e/aerosol.html>

Table 3-4. Mass fraction of PAHs in NIES CRM No. 28 Urban Aerosols

Component name	Unit	Mass fraction	Analytical Method
Fluoranthene	mg/kg	7	GC-MS, HPLC-FLU
Pyrene	mg/kg	4	GC-MS, HPLC-FLU
Benz (a) anthracene	mg/kg	2	GC-MS, HPLC-FLU, HR-GC-MS
Benzo (b) fluoranthene	mg/kg	11	GC-MS, HPLC-FLU, HR-GC-MS
Benzo (k) fluoranthene	mg/kg	2	GC-MS, HPLC-FLU, HR-GC-MS
Benzo (a) pyrene	mg/kg	0.9	GC-MS, HPLC-FLU, HR-GC-MS
Benzo (ghi) perylene	mg/kg	2	GC-MS, HPLC-FLU, HR-GC-MS
Indeno (1,2,3-cd) pyrene	mg/kg	3	GC-MS, HPLC-FLU, HR-GC-MS

GC-MS: gas chromatography-mass spectrometry

HPLC-FLU: high performance liquid chromatography-fluorescence detection

HR-GC-MS: high resolution gas chromatography-mass spectrometry

Source - <https://www.nies.go.jp/labo/crm-e/aerosol.html>

3.3.2. cell viability and NO production in fine dust exposed MH-S cells

In this study, author mainly focused on inflammatory effects caused by outdoor air particles and also suggested a green chemical extract (HEBI) as a treatment. After 24 h of fine dust exposure, cell viability and level of NO production from CMT-93 cells were measured using MTT assay and Griess assay. According to the results, viability of CMT-93 cells was decreased with the increasing concentrations of fine dust (fig 3.3a). In addition, fine dust exposure also increased NO production levels in CMT-93 cells (fig 3.3b). According to the cytotoxicity and NO production, 250 µg/ml concentration of fine dust used to stimulate CMT-93 cells in the consequence studies.

After selecting optimal fine dust concentrations for CMT-93 cell stimulation; the cyto-protective effect (fig. 3c) and NO inhibitory effect (fig. 3d) of HEBI in fine dust exposed CMT-93 cells were evaluated. The results revealed that the pre-incubation of HEBI has an inhibitory effect on fine dust induced NO production and cytotoxicity. Therefore, author decided to use 250 µg/ml fine dust to stimulate CMT-93 cells and 31.3-125 µg/ml HEBI treatments to evaluate protective mechanisms of HEBI against fine dust caused damages.

3.3.3 HEBI inhibits fine dust-induced PGE₂ and pro-inflammatory cytokine production from CMT-93 cells (ELISA)

PGE₂, is a product of the cyclooxygenase (COX) pathway, is synthesized by many cells, such as endothelial cells, epithelial cells, macrophages, monocytes, osteoblasts, and fibroblasts (Bou-Gharios and de Crombrughe 2008; Stenson 2007). Recently, a number of studies reported the up-regulated production of PGE₂ link to the pathogenesis of cancers and apoptosis (Parker et al. 2015). Therefore, in the present study, author

attempted to evaluate PGE₂ production levels in the fine dust exposed CMT-93 cells. ELISA results confirmed the exposure of CMT-93 cells to fine dust cause to produce PGE₂ from exposed cells. However, HEBI treatment significantly, reduced the levels of PGE₂ produced in fine dust exposed CMT-93 cells. In addition to PGE₂, the levels of pro-inflammatory cytokines (positive mediators of inflammation) in the culture mediums were quantified using ELISA. Pro-inflammatory cytokines (IL-1, IL-6, IFN- γ , IL-18, and TNF- α) play central role in inflammatory diseases of infectious origins as well as non-infectious origins (Srinivasan et al. 2017). Furthermore, a number of studies reported, the up-regulated pro-inflammatory cytokines linked to pathogenesis of chronic inflammatory disease conditions such as Alzheimer's disease, fibrosis, ductopenia, cholestasis, and malignant transformation (Pinto et al. 2018). Therefore, regulation of pro-inflammatory cytokines considering as important factor to keep healthy cellular environment. Thus, author evaluated the pro-inflammatory cytokine levels in the culture supernatants using ELISA. In response to fine dust, the levels of pro-inflammatory cytokines in the culture mediums were increased compared to the control group. However, the treatment of HEBI reduced the pro-inflammatory cytokine levels in the culture supernatants induced by fine dust. This results suggesting the, treatment of HEBI has a potential to reduce inflammation induced by fine dust accumulated in digestive tract.

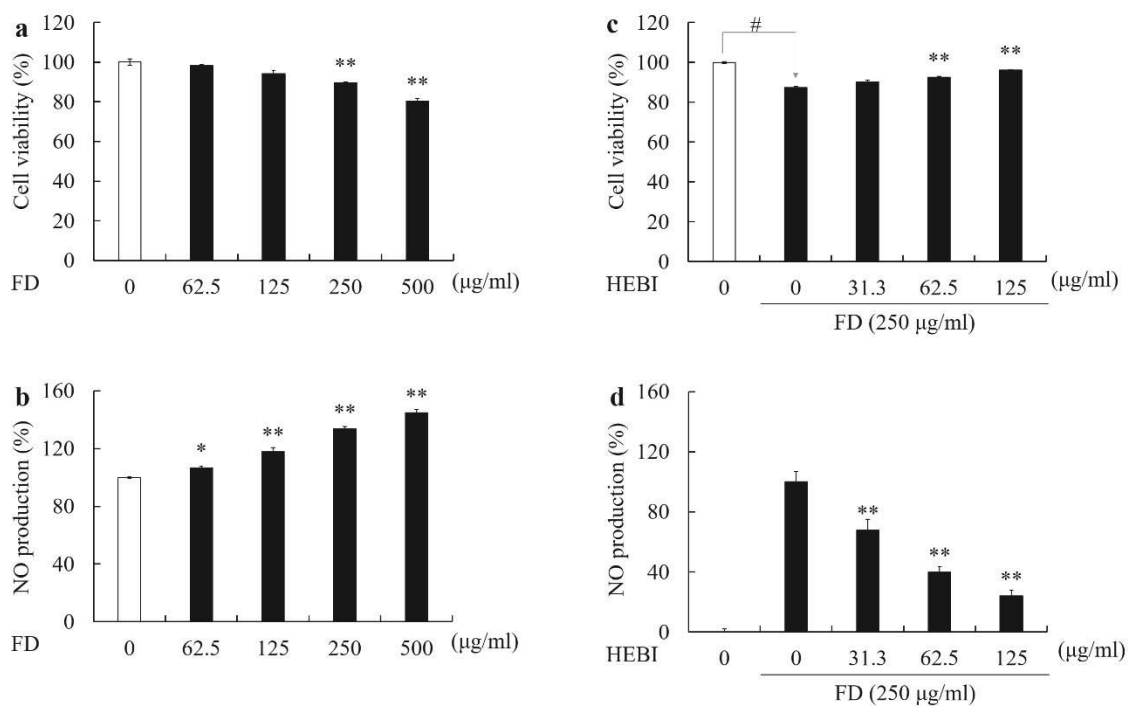


Figure 3-3. Cytotoxicity (a) and NO production levels (b) in fine dust(FD)-exposed CMT-93 cells. CMT-93 cells exposed to the FD (62.5 -500 µg/ml) for 24. Then MTT and Griess assays were used to evaluate cell viability and NO production, respectively. Protective effect of HEBI against FD exposed MH-S cells. Cells were exposed to HEBI with or without FD (250 µg/ml) at the doses of 31.3 - 125 µg/ml. After 24 h cell viability was measured by the MTT (c) and NO secreted in the culture media was quantified using Griess assay (d). Statistical significance was tested using a Student's t-test. HEBI group vs FD group * $p < 0.05$, ** $p < 0.01$

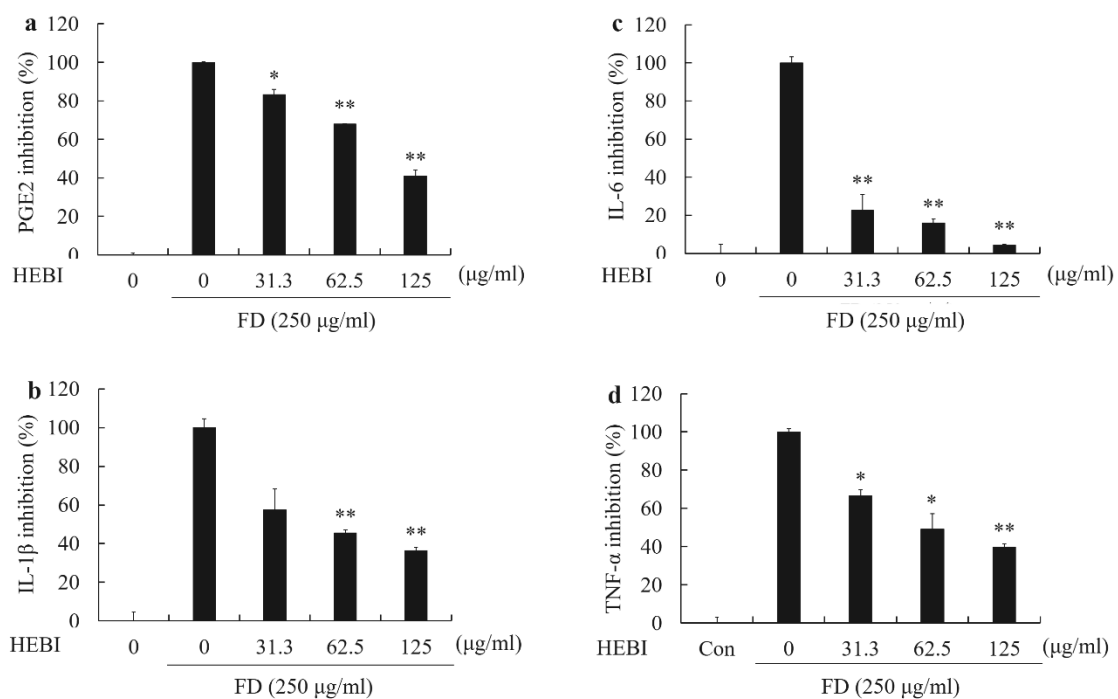


Figure 3-4. Effects of HEBI isolated from *Sargassum horneri* against fine dust (FD)-induced PGE₂ and pro-inflammatory cytokines secretion in CMT-93 cells. Percentage of PGE₂ (a), IL-6 (b), IL-1β (c), and TNF-α (d) in cell cultures. Results represent the pooled mean ± SE of three independent experiments, performed in triplicate. * $p < 0.05$, ** $p < 0.01$, face to the respective control (ANOVA, Duncan's multiple range test).

3.3.4 HEBI inhibits fine dust-induced inflammatory cytokine related gene production from CMT-93 cells (ELISA)

mRNA expression levels of pro-inflammatory and anti-inflammatory cytokines were evaluated using the RT-qPCR to determine the inflammation related gene expression levels in fine dust exposed CMT-93 cells. Similar to the ELISA results, gene expression levels of pro-inflammatory cytokines including IL-1 β (fig. 3.5a), IL-6 (fig. 3.5b), TNF- α (fig. 3.5c), and IFN- γ (fig. 3.5d) were decreased with the HEBI treatment (fig. 3.5). In contrast to the pro-inflammatory cytokines, the activation of anti-inflammatory cytokines also important to suppress the activation of macrophages. According to the previous studies, activation of anti-inflammatory cytokines such as IL-4, IL-10, and IL-13 are reduced the production levels of pro-inflammatory cytokine from macrophages (Szczepanik et al. 2001). Specifically, Szczepanik et al. (2001) demonstrated the link between up-regulated IL-4 production and the IL-6 expression. In that study, the authors, reported the up-regulated expression of IL-4 capable to reduce IL-6 expression in macrophages. Similarly, the down-regulated IL-4 gene (fig. 3.5e) expression in fine dust exposed cells were up-regulated by HEBI in activated CMT-93 cells.

This results suggesting that, HEBI has a potential to up-regulate the production of anti-inflammatory cytokines from fin dust exposed CMT-93 cells. This phenomenon could be one reason for reduction of pro-inflammatory cytokine production from fine dust exposed CMT-93 cells.

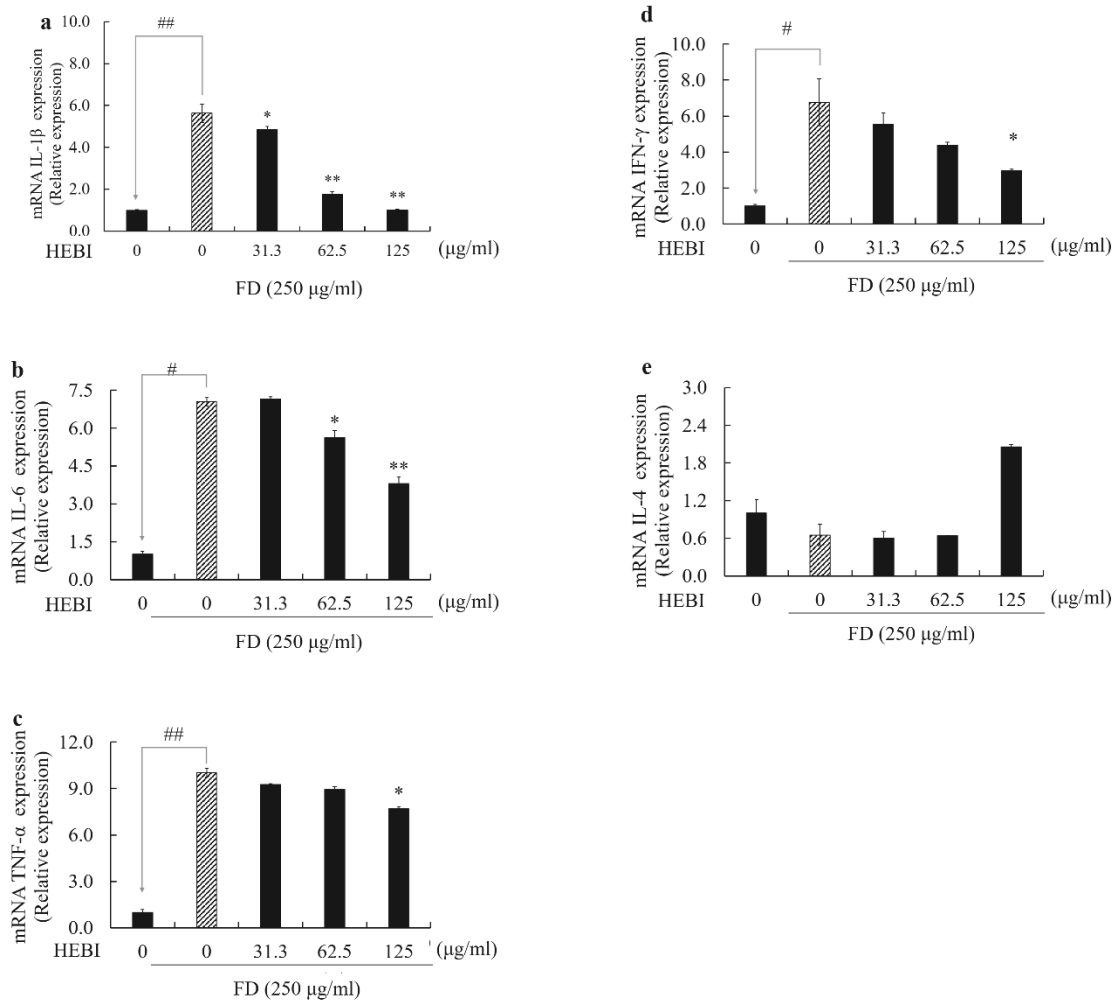


Figure 3-5. Effect of HEBI against fine dust (FD)-induced IL-1 β (a), IL-6 (b), and TNF- α (c), IFN- γ (d), and IL-4 (e) mRNA expression in CMT-93 cells. Cells exposed to FD for 6 h and total RNA was extracted from CMT-93 cells. RT-qPCR was performed using TaqMan reagents. The results were analyzed by the Delta-Ct method and expression of target genes was normalized to GAPDH expression. Control was obtained in the absence of FD and HEBI. The values shown are the means \pm SEs of three independent experiments; * p < 0.05, ** p < 0.01 vs. the FD treated group.

3.3.5 Inhibitory effect of HEBI against iNOS and COX2 production from fine dust stimulated CMT-93 cells

iNOS and COX2 are well known inflammatory mediators involved in many inflammatory diseases. COX2 is a mediator in pain, inflammatory conditions, and some catabolic reactions in inflamed tissues (Liou et al. 2014; Onodera et al. 2015). Previously, a number of studies reported, fine dust can induce inflammatory responses in exposed cells through the up-regulated production of iNOS and COX2 proteins. Gawda et al. (2018) recently found that the exposure of fine dust particles primes macrophages to hyper-inflammatory responses (Gawda et al. 2018). Therefore, in the present study, author attempted to evaluate levels of iNOS and COX2 expression in the fine dust exposed CMT-93 cells. The protein expression levels and gene expression levels were evaluated using the western blots and RT-qPCR.

Inhibition of iNOS and COX2 is an important target of anti-inflammation related therapeutics. Specifically, research studies focused with anti-inflammatory effects of seaweeds bioactivities strongly suggest the active compounds in seaweeds are strong inhibitors of iNOS and COX2 (Fernando et al. 2016). Similar to the previous studies, both western blots and RT-qPCR data (fig 3.6) confirmed that HEBI has an inhibitory effect on fine dust induced iNOS and COX2 production from CMT-93 cells.

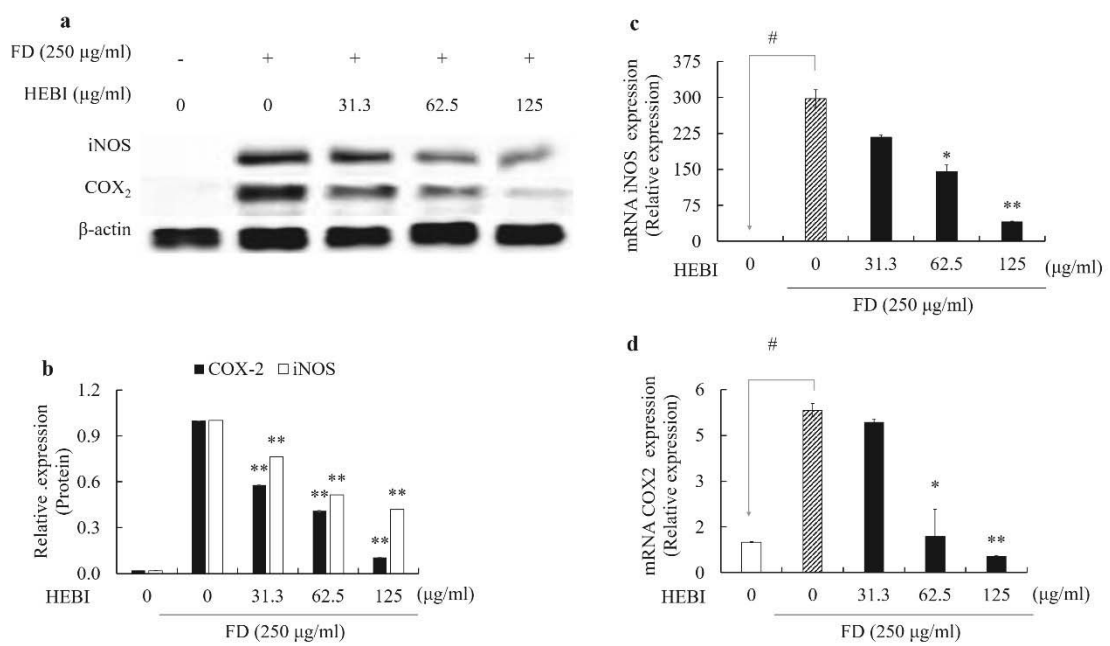


Figure 3-6. Effect of HEBI against fine dust (FD)-induced iNOS and COX2 expression in CMT-93 cells. The protein expression levels (a, b) and mRNA expression levels (c, d) of iNOS and COX2. Western blots and RT-qPCR used evaluate proteins and gene expression levels, respectively. Control was obtained in the absence of FD and HEBI. The values shown are the means \pm SEs of three independent experiments; * p < 0.05, ** p < 0.01 vs. the FD treated group; # p < 0.05, ## p < 0.01 vs. the un-stimulated group.

3.3.6 inhibitory effect of HEBI against fine dust induced TLR activations in CMT-93 cells (RT-qPCR).

Organisms rely on the innate immune system to recognize pathogen-associated molecular patterns. Pathogen-associated molecular patterns are conserved molecular constructs on pathogens. This recognition of pathogens is accomplished by pattern recognition receptors on cells. Different types of pattern recognition receptors lead to the activation of different intracellular molecular pathways such as TLRs. TLRs are highly conserved among animals, from *D. melanogaster* (common fruit fly) to humans. TLRs are group of glycoproteins with extracellular or luminal ligand binding domains with leucine-rich repeat motifs and a cytoplasmic signaling Toll/interleukin-1 receptor homology domain. Upon pathogen-associated molecular patterns recognition, TLRs undergo receptor oligomerization to initiate intracellular signal transduction. Cells such as macrophages, dendritic cells, B lymphocytes, and glia express TLRs on their cell surface or intracellularly within endosomal compartments. Up to now, 11 TLRs are described in humans and 12 in mice (Lin et al. 2012; Zielinski and Krueger 2012). TLRs are classified by what they recognize and are summarized in table 3-6. In the present study, author evaluated activation levels of 9 TLRs in fine dust stimulated CMT-93 cells and suppressive properties of HEBI against fine dust induced TLRs activation. According to the results, fine dust up-regulated the expression of TLR-2, TLR-3, TLR-4, TLR-7, TLR-8, and TLR-9 (fig 3.7). This results suggesting, fine dust contains not only heavy metals, but also microbial contaminates. However, the activation of TLRs activates their down-stream signal proteins associated with the inflammation including NF- κ B and MAPKs (fig. 3-8) through myeloid differentiation factor (MyD88) activation. Therefore, as next study author evaluated the down-stream protein expression levels related to the NF- κ B and MAPKs using western blots.

Table 3-5. Toll like receptors and their stimulators

Receptor	Stimulator	Source
TLR-1	Triacyl lipopeptides	Bacteria
	Lipoproteins	Multiple pathogens
	Peptidoglycan (PGN), porins	Bacteria
TLR-2	Zymosan, beta-Glycan	Fungi
	GPI-mucin	Protozoa
	Envelope glycoproteins	Viruses
TLR-3	Double-stranded RNA	Viruses
	Poly (I:C)	Synthetic analog of ds-RNA
TLR-4	LPS	Bacteria
	Glycoinositolphospholipids	Protozoa
TLR-4	Envelope glycoproteins	Viruses
	Flagellin	Bacteria
TLR-5	Flagellin	Bacteria
TLR-6	Diacyl lipopeptides and lipoteichoic acid (LTA)	Bacteria
TLR-7	Single-stranded RNA	Viruses
TLR-8	Single-stranded RNA	Viruses
TLR-9	Unmethylated CpG DNA	Bacteria, protozoa, and viruses
TLR-10	Unknown	Unknown

Sources: (R&DSystems 2018) and (Zielinski and Krueger 2012)

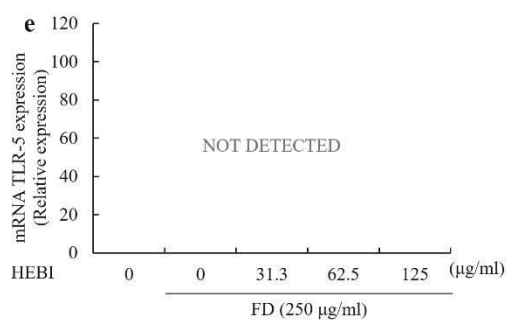
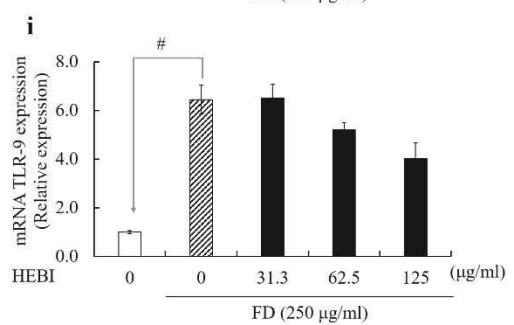
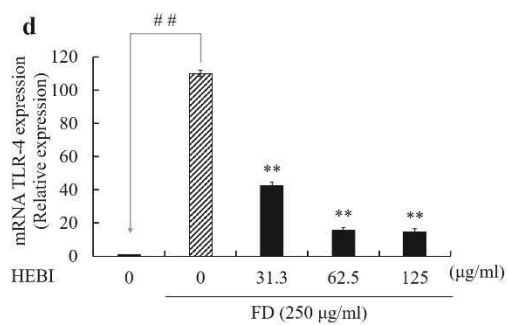
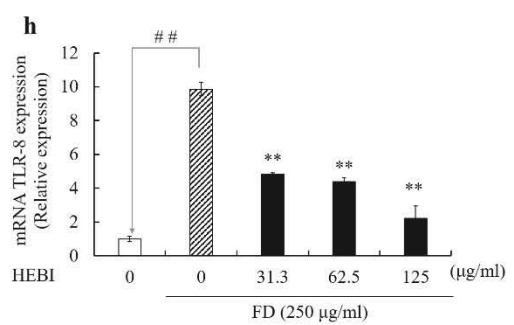
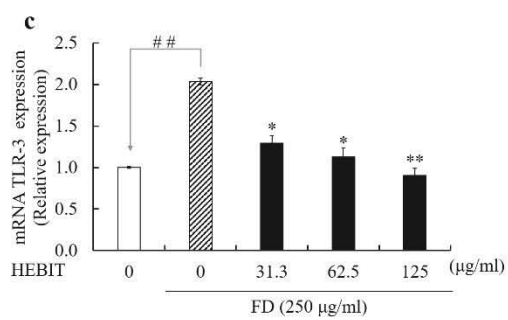
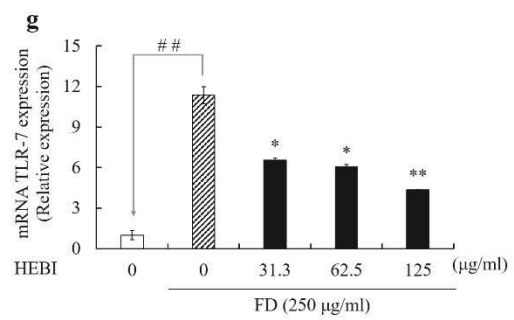
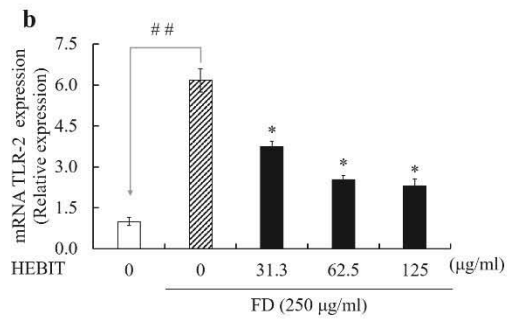
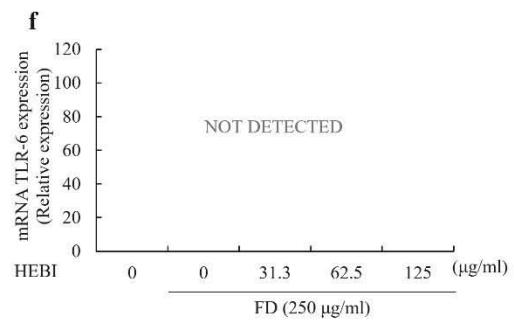
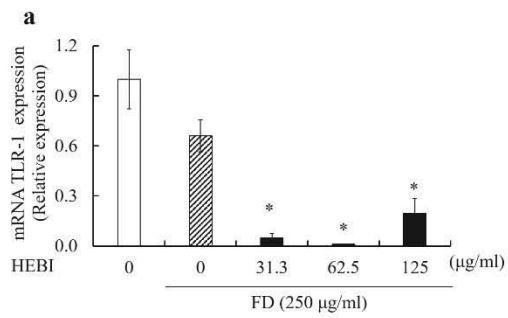


Figure 3-7. Effect of HEBI against mRNA expression of fine dust (FD)-induced toll like receptors (TLR) (1-9; a-h) in CMT-93 cells. After FD exposure for 6 h, total RNA was extracted from CMT-93 cells and RT-qPCR was performed for the TLR genes using TaqMan reagents. The results were analyzed by the Delta-Ct method and expression of target genes was normalized to GAPDH expression. Control was obtained in the absence of FD and HEBI. The values shown are the means \pm SEs of three independent experiments; * $p < 0.05$, ** $p < 0.01$ vs. the FD treated group; # $p < 0.05$, ## $p < 0.01$ vs. the un-stimulated group.

Toll-Like Receptor Signaling Pathways

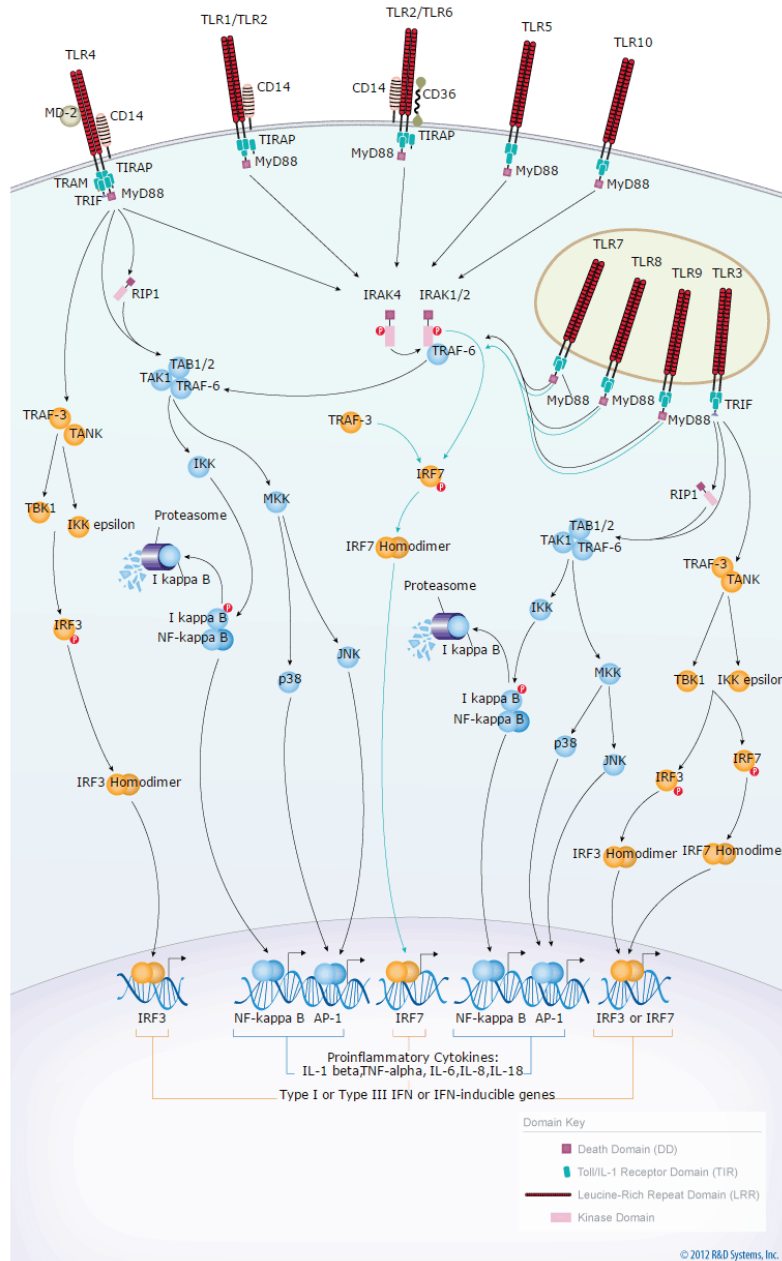


Figure 3-8. Graphical illustration of toll like receptor expression and their down-stream signal transduction mechanisms. Source: <https://resources.rndsystems.com/images/Pathways/full-pathway-image/toll-like-receptor-signaling-pathways-rnd-systems.png>

3.3.7. Effect of HEBI against MyD88 protein expression in fine dust exposed CMT-93 cells

MyD88 is involved in transmitting a variety of activation signals through different receptors. Activation of TLRs through the pattern recognition receptors induces downstream signaling via two individual signal transduction pathways; MyD88 dependent and toll-interleukin 1 receptor (TIR) domain-containing adapter inducing interferon- β (TRIF)-dependent pathway for the induction of pro-inflammatory cytokines and IFN-stimulated genes. Generally, MyD88 is used by number of TLRs (TLR-2, TLR-5, TLR-7, TLR-8, and TLR-9) to activate their down-stream signal cascades. TRIF is used by TLR-3. In addition, MyD88 and TRIF-dependent pathways associate with the TLR-4 (Ahmed et al. 2013; Takeda and Akira 2005). Accumulating scientific evidence suggests the consequence of TLRs and their ligands in pathological conditions specifically in autoimmune complications and inflammation (Kim et al. 2018). Thus, inhibition of MyD88 provides strong support to inhibit signal transduction from TLRs to NF- κ B and MAPKs. Therefore, author attempted to evaluate the activation levels of MyD88 in fine dust induced CMT-93 cells with or without HEBI treatment (fig. 3.9). With the exposure of fine dust, levels of MyD88 proteins increased compared to the control. However, the treatment of HEBI significantly down-regulated the fine dust induced MyD88 production from CMT-93 cells. Specifically, 62.5 and 125 μ g/ml concentrations of HEBI reduced the levels MyD88 expressions than the un-treated control.

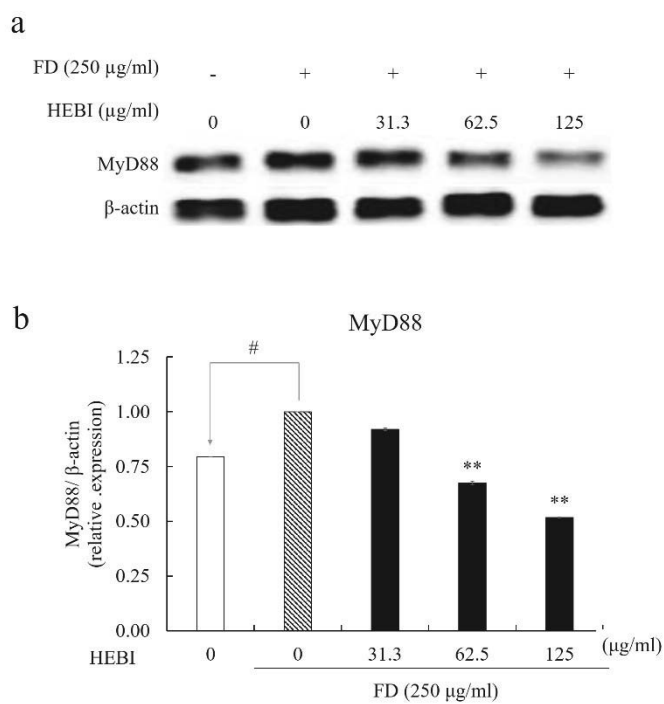


Figure 3-9. Effects of HEBI on the fine dust (FD)-induced expression of MyD88 in CMT-93 cells (a). Density ratios of MyD88 versus β -actin (b) were measured using densitometry. The values shown are the means \pm SEs of three independent experiments. * $p < 0.05$, ** $p < 0.01$ vs. the fine dust treated group and # $p < 0.05$ vs. the un-stimulated group.

3.3.8. Effect of HEBI against fine dust induced NF- κ B protein expression in CMT-93 cells

NF- κ B is an evolutionarily conserved transcription factor which provides a means to achieve inducible, regulated, and specific immune responses to host. The NF- κ B transcription factor was identified three decades ago by David Baltimore and Ranjan Sen; and has since emerged as the master regulator of inflammation and immune homeostasis (Hayden and Ghosh 2008; Zhang et al. 2017). A number of anti-inflammatory and pro-inflammatory factors are depending on the phosphorylation levels of NF- κ B transcription factor. Specifically, studies have evidenced the NF- κ B play critical role in inflammatory diseases like rheumatoid arthritis, inflammatory bowel disease, cancer, and atherosclerosis (Mitchell and Carmody 2018; Zhang et al. 2017).

The inhibitor of NF- κ B (I κ B) family proteins basically controls the activation and translocation of NF- κ B. Under the normal conditions, NF- κ B dimers are sequestered in the cytoplasm in an inactive state by members of the I κ B family of proteins (I κ B α , I κ B β , and I κ B ϵ). In general, I κ B α binds to NF- κ B dimers in the cytoplasm, and block the nuclear localization signals of NF- κ B transcription factors. However, transmittance of inflammatory signals through TLRs to cytoplasm, the I κ B phosphorylated by the I κ B kinase (IKK) complex which triggers lysine48 (K48)- linked polyubiquitination of I κ B α leading to proteasomal degradation of I κ B. Breakdown of I κ B α , P50, and P65 freeing the NF- κ B dimers which facilitate the translocation of P50, and P65 into the nucleus where they can bind to specific sites in DNA to regulate gene transcription (Mitchell and Carmody 2018; Tam et al. 2000). Taken together, as next study author evaluated the I κ B α , P50, and P65 phosphorylation levels of CMT-93 cells following fine dust stimulation using western blot analysis. Upon the exposure of fine dust CMT-93 cells had significant amounts of pI κ B α , pP50, and pP65 in the cytosol (fig 3.10). However, the treatment of

HEBI inhibited the I κ B- α phosphorylation as well as the phosphorylation of p50 and p65. This results, confirms the fine dust can induce the activation of NF- κ B via I κ B α degradation as well as HEBI act against fine dust induced NF- κ B activation through blocking I κ B α degradation.

In addition to the cytosolic NF- κ B phosphorylation it is also important to translocate them in to the nucleus. The translocation of NF- κ B proteins required to activate transcription of target genes related to inflammatory responses (Capece et al. 2018). Therefore, as next study authors evaluated the p50 and p65 levels in the fine dust exposed CMT-93 nucleus protein extracts (fig. 3.11). Similar to the cytosolic NF- κ B expressions, the levels of p50 and p65 levels in the nucleus extracts were decreased upon the HEBI treatment.

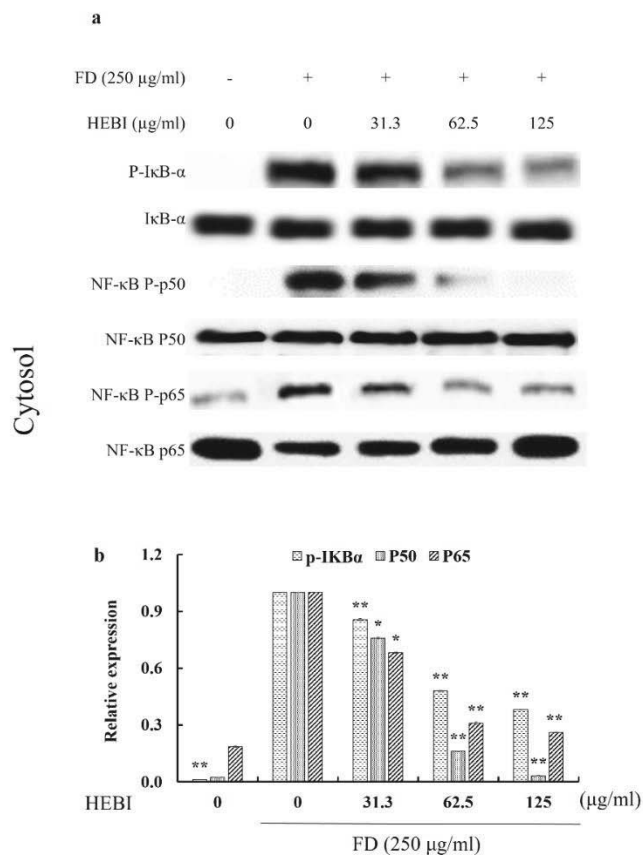


Figure 3-10. Effects of HEBI on the fine dust (FD)-induced expression of cytosolic NF- κ B activation in CMT-93 cells (a). Density ratios of each protein was measured using densitometry (b). The values shown are the means \pm SD of three independent experiments. * $p < 0.05$, ** $p < 0.01$.

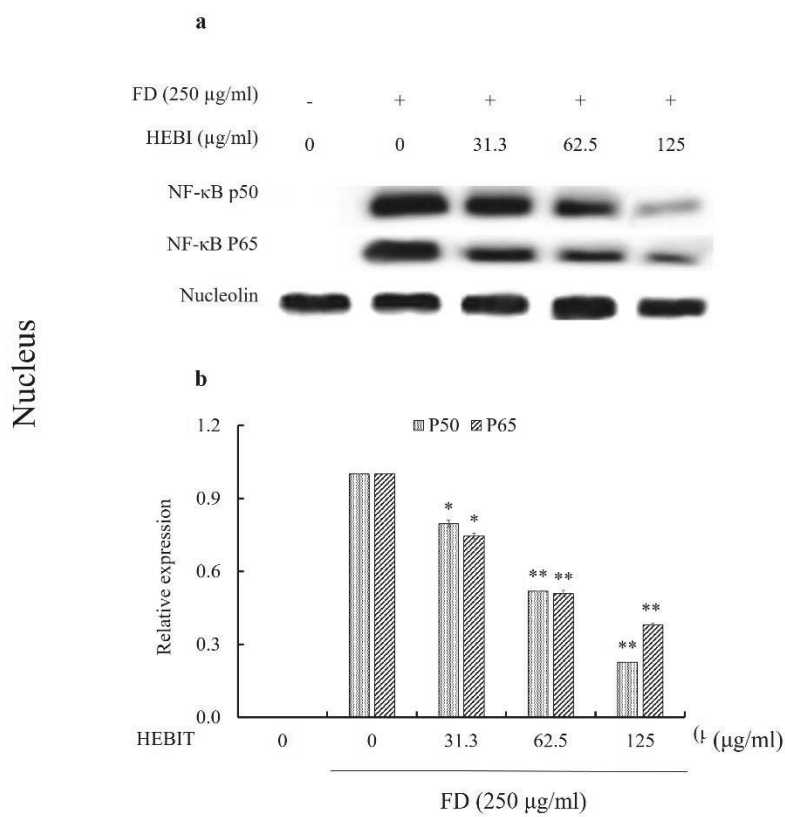


Figure 3-11. HEBI inhibits fine dust (FD)-induced NF-κB translocation to the nucleus. Density ratios of each protein was measured using densitometry (b). The values shown are the means ± SD of three independent experiments. * $p < 0.05$, ** $p < 0.01$.

3.3.9. Effect of HEBI against fine dust induced MAPK expression in CMT-93 cells

Cell signaling is a well-balanced communication to interact with the neighboring cells and extracellular environment. Cells usually contains glycoproteins or glycolipid receptors on the plasma membrane through which cells react to changes in their cellular environment. When a complementary ligand (signaling molecule) binds to the receptor, it initiates a chain of events within the cell. This process can define as signal transduction, ultimately resulting into a response (Kumar et al. 2018). Down-stream activation of TLRs also transmit signals through the kinase cascades. A number of kinases involved into inflammation related signal transduction and are well documented, among them mitogen activated protein kinases (MAPKs) play important role during inflammatory responses (Chistyakov et al. 2018). The MAPKS such as c-jun n-terminal kinases (JNK), p38, and extracellular signal-regulated kinases 1/2 (ERK 1/2) are triggers the activation of transcription factors including protein families of NF- κ B, AP-1, IRF. Activation of aforementioned transcription factors allows them to bind to specific DNA sequences and start the expression of inflammatory genes (Akanda and Park 2017; Chistyakov et al. 2018; Sheng et al. 2011). Taken together, inhibition of MAPKs has important role during the chronic inflammatory responses. Thus, as a next study author evaluated the MAPKs phosphorylation levels in fine dust exposed CMT-93 cells using western blot analysis (fig. 3-12). Fine dust induced phosphorylation of MAPKs family protein ERK 1/2, JNK, and p38 level which was notably attenuated by HEBI pretreatment as related with fine dust. Specifically, the inhibition of JNK comparatively stronger than the ERK1/2 and p38.

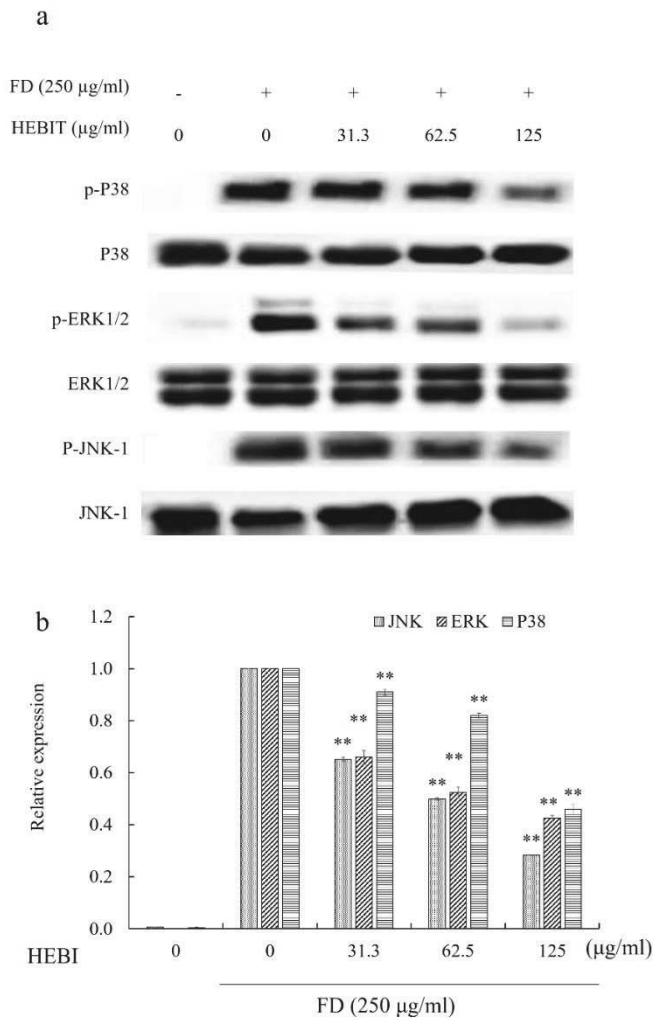


Figure 3-12. Effects of HEBI on the phosphorylation of MAPKs (pERK1/2, pJNK, and pP38) (a). The relative band intensity was measured as compared with total form of each band (b). The values shown are the means \pm SD of three independent experiments. * $p < 0.05$, ** $p < 0.01$.

3.3.10 HEBI up-regulates anti-oxidant proteins expression in fine dust exposed CMT-93 cells

Oxidative stress is induced by many factors such as ionizing radiation, xenobiotics, drugs, and heavy metals. Development of oxidative stress in cellular environments leads to the generation of electrophiles and reactive oxygen species inside the cells. The uncontrolled production of ROS and electrophiles can cause negative effects on cell survival, cell growth and the development (Breimer 1990). Specifically, uncontrolled ROS production in cellular environments can cause diseases such as cardiovascular complications, cancer cell development, chronic inflammatory conditions, and neurodegenerative diseases. Thus, it is clear that cells should constantly labor to control the levels of ROS, to avoid oxidative stress related complications (Kaspar et al. 2009).

Previously, a number of studies reported the exposure of fine dust cause to induce oxidative stress in the fine dust exposed cells. Specifically, the metal groups in fine dust cause to induce ROS production from metal particles exposed cells (Singh et al. 2007; Valko et al. 2005). Other than the metal groups, micro-organisms and other in-organic matters less than 2.5 μM diameter can easily move to the inside organs and can damage to them through oxidative stress (Meng and Zhang 2006). Meng and Zhang 2006 reported, fine dust (collected from china and dust storms) inhaled mouse had significant levels of oxidative damage in lungs, hearts, and livers. Similarly, during this study author also noted the exposure of fine dust to CMT-93 cells cause significant levels of cell viability reduction (fig. 3-3). This cell death might associate with the fine dust induced oxidative stress in the CMT-93 cells. Therefore, author evaluated the ROS and SOD production levels of fine dust exposed CMT-93 cells upon HEBI treatment. Similar to the previously reported studies, fine dust exposed CMT-93 cells had considerable amounts of ROS and low level of SOD compared to the control group (fig. 3-13). However, the treatment of

HEBI decreased the ROS levels observed in the only fine dust treated group (fig. 3-13a). Other than that HEBI also up-regulated the SOD levels in culture supernatants compared to the control and fine dust exposed groups (fig. 3-13b). Specifically, the fine dust exposed group had low levels of SOD in the culture supernatants even low than the control group. This might be associated with the cytotoxicity of fine dust in CMT-93 cells. However, as mentioned before, the treatment of HEBI, before fine dust induction significantly restored the reduced SOD levels in fine dust exposed group.

In addition to the antioxidant enzymes, the levels of antioxidant proteins in fine dust stimulated CMT-93 cells were evaluated using western blots (fig. 3-13c). Catalase and Cu/Zn-SOD expression levels in the cytosol measured as those proteins helped to reduce oxidative stress in cytosol via scavenging ROS produced during the pathological and metabolic events (Liu et al. 2017). According to the results, the treatment of HEBI prior to the fine dust stimulation increased the Catalase and Cu/Zn-SOD levels in cytosol suppressed by the fine dust (fig. 3-13d). The up-regulated expression of this antioxidant proteins useful to reduce the oxidative stress in fine dust exposed CMT-93 cells and ultimately protects cells from apoptosis and chronic inflammation.

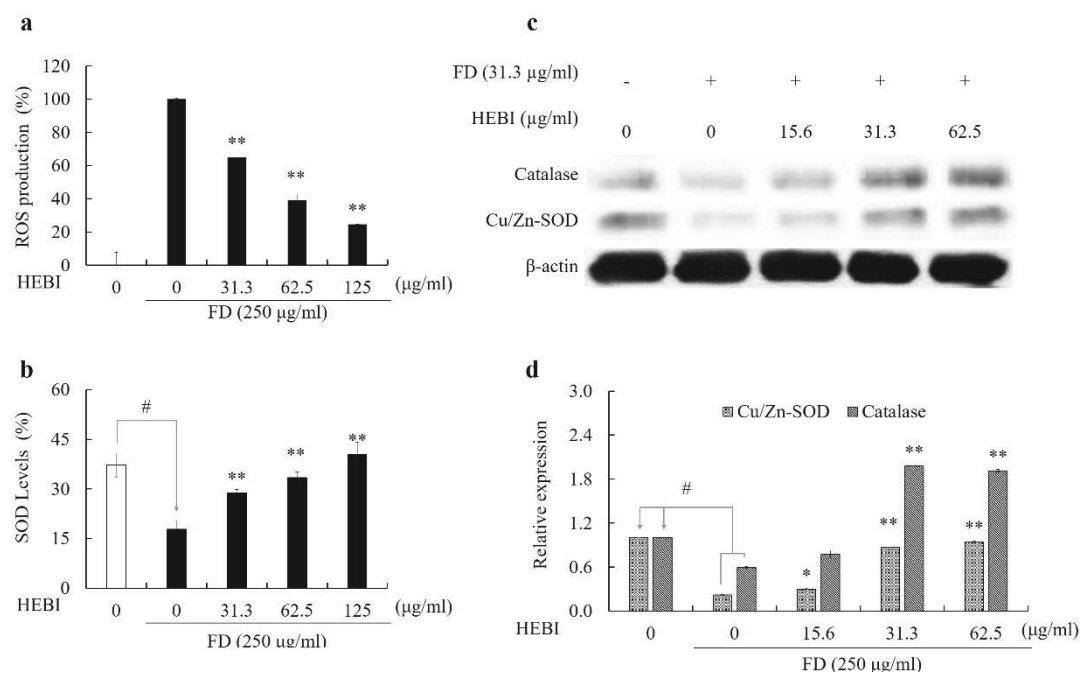


Figure 3-13. Effect of HEBI against fine dust (FD)-induced ROS production (a), and SOD suppression (b) in CMT-93 cells. The relative protein levels of catalase and Cu/Zn-SOD in FD induced CMT-93 cells with or without HEBI (c). The values shown are the means \pm SEs of three independent experiments; * p < 0.05, ** p < 0.01 vs. the FD treated group; # p < 0.05, ## p < 0.01 vs. the un-stimulated group.

3.3.11 HEBI upregulates anti-oxidant gene expressions in fine dust exposed CMT-93 cells

To scavenge ROS from cells, requires activation of inter-cellular anti-oxidant mechanisms. Inside the cytosol, there are group of cellular sensors, which are activate under the oxidative stress conditions. Among those Nrf2:INrf2 (Kelch-like ECH-associating protein 1; Keap1) is a well-characterized cellular sensor which activate upon chemical-induced and radiation-induced oxidative stress conditions (Gong et al. 2018).

A cytosolic inhibitor Keap1, of Nrf2 existing as a dimer, retains Nrf2 in the cytoplasm. The Keap1 work as an adapter for the cullin 3/ring box 1 (Cul3/Rbx1) E3 ubiquitin ligase complex. Cul3 serves as a scaffold protein that forms the E3 ligase complex with Rbx1 and recruits a cognate E2 enzyme. Keap1, via its N-terminal BTB/POZ domain, binds to Cul3 and, via its C-terminal Kelch domain, binds to the substrate Nrf2 (Kobayashi and Yamamoto 2006). This binding degrades and ubiquitination of Nrf2 through the 26S proteasome (Nguyen et al. 2003). Under normal cellular conditions, the cytosolic Keap1/Cul3/Rbx1 complex is regularly degrade Nrf2. During the oxidative stress conditions Nrf2 dissociates from Keap1, stabilizes, and then move into the nucleus, leading to activation of antioxidant gene expression from the nucleus (Copples et al. 2008). Therefore, author attempted to compare the Keap1, Nrf2 levels in cytosol as well as Nrf2 levels in the nucleus to evaluate possible mechanisms associated with the antioxidant mechanisms of HEBI in fine dust exposed CMT-93 cells. In addition, using RT-qPCR gene expression levels of Nrf2 and HO-1 evaluated to confirm the western blot results.

According to the results, treatment of HEBI cause to up-regulate HO-1 levels in cytosol (fig. 3.14a). Moreover, HEBI also decreased the cytosolic Keap1 and Nrf2 levels compared to the control group. This results suggesting, the treatment of HEBI has a

potential to trigger breakdown of cytosolic Nrf2/Keap1 complex. The reduction of cytosolic Keap1 is a strong evidence for mobilization of Nrf2 to the nucleus. According to the previous studies, dislocation of Nrf2/Keap1 complex induce by several protein kinases, including p38, JNK, and ERK (Yu et al. 1999). However, the treatment of HEBI, cause to inhibit the phosphorylation of MAPKs (fig. 3-12). Therefore, the breakdown of Nrf2/Keap1 complex observed with HEBI treatment might following a different signal transduction pathway. Other than the MAPKs, the activation of Nrf2 also mediated by phosphoinositol-3-kinase (PI3K), and protein kinase C (PKC) (Kang et al. 2002). According to Kang et al. (2002), under oxidative stress Nrf2 translocation mediated by the PI3K signal transduction pathway facilitate the breakdown of Keap1/Nrf2 complex through rearrangement of actin microfilaments. According to them, in response to oxidative stress and de-polymerization of actin causes a complex of Nrf2 bound with actin to translocate into nucleus. However, further studies require to explore exact mechanism response to Nrf2 translocation after treatment of HEBI in CMT-93.

Levels of Nrf2 and HO-1 in the nucleus also evaluated using western blots (fig. 3-15a). According the results, the levels of both tested proteins were dose-dependently increased in response to HEBI treatment in fine dust exposed CMT-93 cells (fig 3-15b). Other than the protein expression, the gene expression levels of Nrf2 and HO-1 confirmed using RT-qPCR. According to the results, the gene expression level of both HO-1 (fig. 3-15c) and Nrf2 (fig. 3-15d) dose-dependently increased with HEBI treatment. These results suggesting that HEBI act as a dual agent in fine dust stressed CMT-93 cells as anti-inflammatory compound as well as anti-oxidant compound.

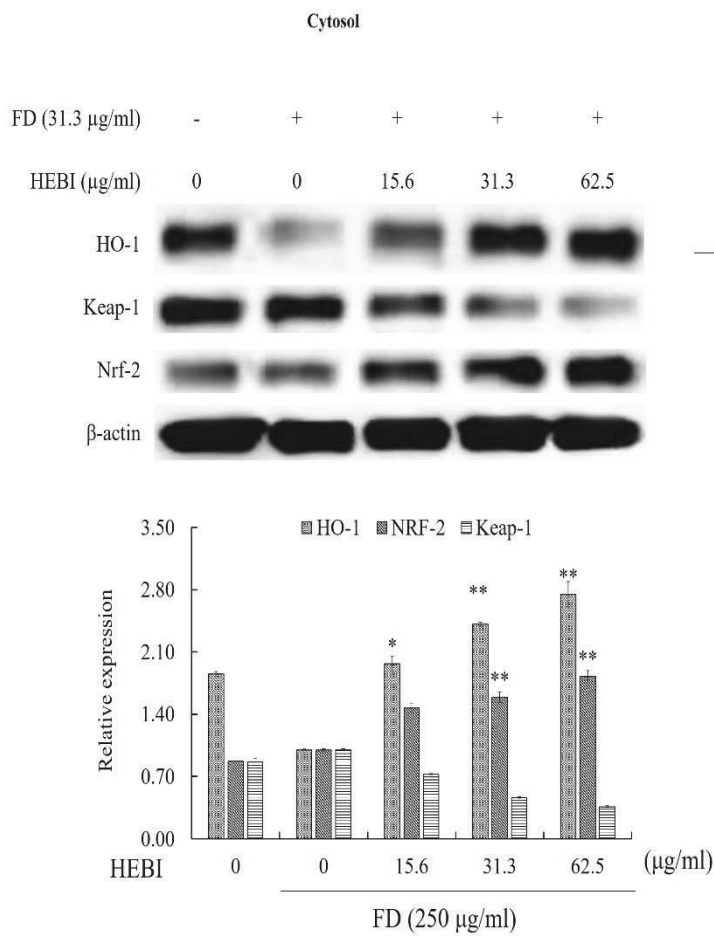


Figure 3- 14. Effect of HEBI against fine dust (FD)-induced cytosolic HO-1, Nrf-2, and Keap-1 expressions in CMT-93 cells. β - actin was used as internal control. Quantitative data was analyzed using ImageJ software (1.43V). Results are expressed as the mean \pm SD of three separate experiments. * $p < 0.05$ and ** $p < 0.01$.

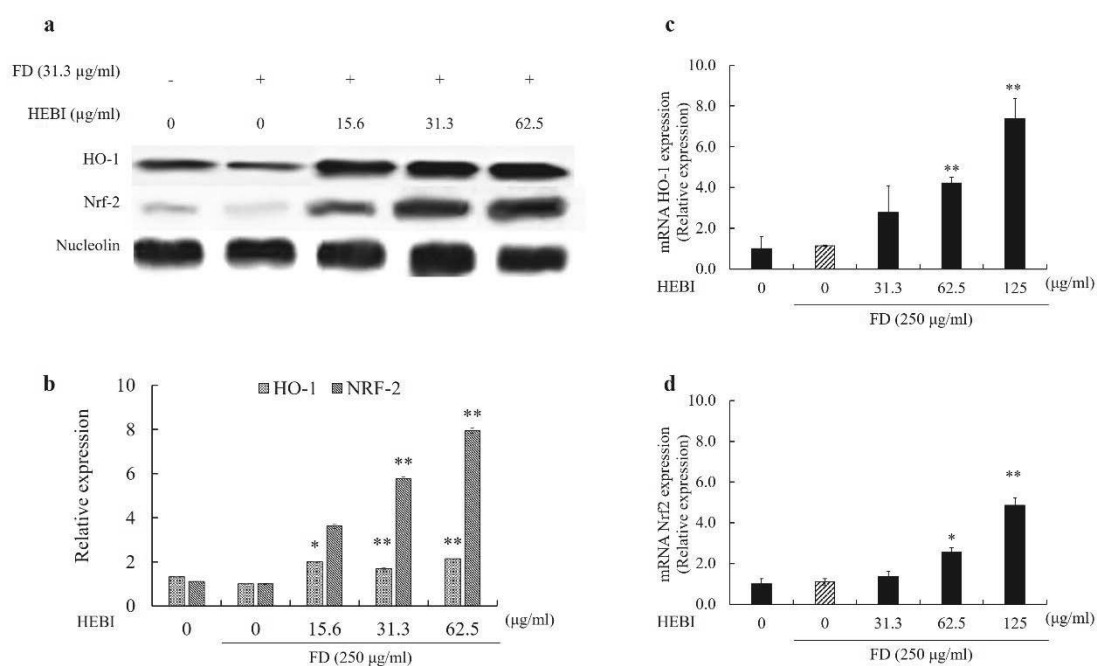


Figure 3- 15. Effect of HEBI against fine dust (FD)-induced HO-1 and Nrf2 protein (a, b) and mRNA expression (c,d). Western blots and RT-qPCR used evaluate proteins and gene expression levels, respectively. Control was obtained in the absence of FD and HEBI. The values shown are the means \pm SEs of three independent experiments; * $p < 0.05$, ** $p < 0.01$ vs. the FD treated group; # $p < 0.05$, ## $p < 0.01$ vs. the un-stimulated group.

3.4. Conclusions

Fine dust is a one of the major risk factor in the airway inflammatory diseases. However, there is a possibility to move fine dust through the digestive tract and accumulate. According to the heavy metal analysis results fine dust contains a large amount of Pb and As. Besides the heavy metals, fine dust composed with micro-organism particles. Therefore, effect of fine-dust in digestive system cannot easily neglect. Taken together in the present study, author attempted to evaluate the effect of fine dust in digestive system using CMT-93 cells as a model cell. According to the results, fine dust-induced the inflammation in CMT-93 cells via activating TLR/MyD88 dependent and independent signal cascades. At the 250 $\mu\text{g/ml}$, fine dust suppresses the production of antioxidant enzymes (HO-1, SOD, and catalase) and anti-inflammatory cytokines (IL-4). In addition, fine dust-induced the gene expression levels of TLR 2, 3, 4, 7, 8, and 9. The activation of aforementioned TLRs are capable to activate NF- κ B and MAPKs through its downstream signal transduction mechanisms.

However, the treatment of HEBI to fine-dust exposed CMT-93 cells reduced the inflammatory responses and oxidative stress induced by fine dust. Specifically, HEBI inhibit the MyD88 protein as well as NF- κ B and MAPKs. In addition, HEBI also reduced the pro-inflammatory cytokines up-regulated by fine dust. Taken together, HEBI has the potential to developed as a functional food that can effectively reduce inflammation and oxidative stress in digestive tract caused by fine dust.

3.5 References

- Ahmed S., Maratha A., Butt A. Q., Shevlin E., and Miggin S. M. (2013). TRIF-mediated TLR3 and TLR4 signaling is negatively regulated by ADAM15. *J Immunol*, **190**(5). Pp: 2217-28. DOI: 10.4049/jimmunol.1201630
- Akanda M. R., and Park B. Y. (2017). Involvement of MAPK/NF-kappaB signal transduction pathways: *Camellia japonica* mitigates inflammation and gastric ulcer. *Biomed Pharmacother*, **95**. Pp: 1139-1146. DOI: 10.1016/j.biopha.2017.09.031
- Bou-Gharios G., and de Crombrughe B.(2008). *Chapter 15 - Type I Collagen Structure, Synthesis, and Regulation*, in *Principles of Bone Biology (Third Edition)*, J.P. Bilezikian, L.G. Raisz, and T.J. Martin, Editors. Academic Press: San Diego. p. 285-318
- Breimer L. H. (1990). Molecular mechanisms of oxygen radical carcinogenesis and mutagenesis: the role of DNA base damage. *Mol Carcinog*, **3**(4). Pp: 188-97. DOI: doi:10.1002/mc.2940030405
- Capece D., Verzella D., Tessitore A., Alesse E., Capalbo C., and Zazzeroni F. (2018). Cancer secretome and inflammation: The bright and the dark sides of NF-kappaB. *Semin Cell Dev Biol*, **78**. Pp: 51-61. DOI: 10.1016/j.semcdb.2017.08.004
- Chistyakov D. V., Astakhova A. A., and Sergeeva M. G. (2018). Resolution of inflammation and mood disorders. *Exp Mol Pathol*, **105**(2). Pp: 190-201. DOI: 10.1016/j.yexmp.2018.08.002
- Copple I. M., Goldring C. E., Kitteringham N. R., and Park B. K. (2008). The Nrf2-Keap1 defence pathway: role in protection against drug-induced toxicity. *Toxicology*, **246**(1). Pp: 24-33. DOI: 10.1016/j.tox.2007.10.029
- Fernando I. P. S., Nah J. W., and Jeon Y. J. (2016). Potential anti-inflammatory natural products from marine algae. *Environ Toxicol Pharmacol*, **48**. Pp: 22-30. DOI: 10.1016/j.etap.2016.09.023

Gawda A., Majka G., Nowak B., Srottek M., Walczewska M., and Marcinkiewicz J. (2018). Air particulate matter SRM 1648a primes macrophages to hyperinflammatory response after LPS stimulation. *Inflamm Res*, **67**(9). Pp: 765-776. DOI: 10.1007/s00011-018-1165-4

Gong W., Chen Z., Zou Y., Zhang L., Huang J., Liu P., and Huang H. (2018). CKIP-1 affects the polyubiquitination of Nrf2 and Keap1 via mediating Smurf1 to resist HG-induced renal fibrosis in GMCs and diabetic mice kidneys. *Free Radic Biol Med*, **115**. Pp: 338-350. DOI: 10.1016/j.freeradbiomed.2017.12.013

Hayden M. S., and Ghosh S. (2008). Shared principles in NF-kappaB signaling. *Cell*, **132**(3). Pp: 344-62. DOI: 10.1016/j.cell.2008.01.020

He M., Ichinose T., Kobayashi M., Arashidani K., Yoshida S., Nishikawa M., Takano H., Sun G., and Shibamoto T. (2016). Differences in allergic inflammatory responses between urban PM2.5 and fine particle derived from desert-dust in murine lungs. *Toxicol Appl Pharmacol*, **297**. Pp: 41-55. DOI: 10.1016/j.taap.2016.02.017

Kang K. W., Lee S. J., Park J. W., and Kim S. G. (2002). Phosphatidylinositol 3-kinase regulates nuclear translocation of NF-E2-related factor 2 through actin rearrangement in response to oxidative stress. *Molecular pharmacology*, **62**(5). Pp: 1001-1010. DOI: <https://doi.org/10.1124/mol.62.5.1001>

Karin M., Lawrence T., and Nizet V. (2006). Innate immunity gone awry: linking microbial infections to chronic inflammation and cancer. *Cell*, **124**(4). Pp: 823-35. DOI: 10.1016/j.cell.2006.02.016

Kaspar J. W., Niture S. K., and Jaiswal A. K. (2009). Nrf2:INrf2 (Keap1) signaling in oxidative stress. *Free Radic Biol Med*, **47**(9). Pp: 1304-9. DOI: 10.1016/j.freeradbiomed.2009.07.035

Khaniabadi Y. O., Daryanoosh S. M., Amrane A., Polosa R., Hopke P. K., Goudarzi G., Mohammadi M. J., Sicard P., and Armin H. (2017). Impact of Middle Eastern Dust

storms on human health. *Atmospheric Pollution Research*, **8**(4). Pp: 606-613. DOI: 10.1016/j.apr.2016.11.005

Kim A. Y., Shim H. J., Kim S. Y., Heo S., and Youn H. S. (2018). Differential regulation of MyD88- and TRIF-dependent signaling pathways of Toll-like receptors by cardamonin. *Int Immunopharmacol*, **64**. Pp: 1-9. DOI: 10.1016/j.intimp.2018.08.018

Kim J. Y., Cho M. K., Choi S. H., Lee K. H., Ahn S. C., Kim D. H., and Yu H. S. (2010). Inhibition of dextran sulfate sodium (DSS)-induced intestinal inflammation via enhanced IL-10 and TGF-beta production by galectin-9 homologues isolated from intestinal parasites. *Mol Biochem Parasitol*, **174**(1). Pp: 53-61. DOI: 10.1016/j.molbiopara.2010.06.014

Kim P. W. (2018). Operating an environmentally sustainable city using fine dust level big data measured at individual elementary schools. *Sustainable Cities and Society*, **37**. Pp: 1-6. DOI: 10.1016/j.scs.2017.10.019

Kobayashi M., and Yamamoto M., *Nrf2-Keap1 regulation of cellular defense mechanisms against electrophiles and reactive oxygen species*, in *Advances in Enzyme Regulation*. 2006. p. 113-140.

Kubo N., Douke A., Nishigaki T., and Tsuji G. (2017). Development and characterization of simple sequence repeat markers for genetic analyses of *Sargassum horneri* (Sargassaceae, Phaeophyta) populations in Kyoto, Japan. *Journal of Applied Phycology*, **29**(3). Pp: 1729-1733. DOI: 10.1007/s10811-016-1041-y

Kumar R., Khandelwal N., Thachamvally R., Tripathi B. N., Barua S., Kashyap S. K., Maherchandani S., and Kumar N. (2018). Role of MAPK/MNK1 signaling in virus replication. *Virus Res*, **253**. Pp: 48-61. DOI: 10.1016/j.virusres.2018.05.028

Lee Y. G., Ho C.-H., Kim J.-H., and Kim J. (2015). Quiescence of Asian dust events in South Korea and Japan during 2012 spring: Dust outbreaks and transports. *Atmospheric Environment*, **114**. Pp: 92-101. DOI: 10.1016/j.atmosenv.2015.05.035

Leiro J., Álvarez E., García D., and Orallo F. (2002). Resveratrol modulates rat macrophage functions. *International Immunopharmacology*, **2**(6). Pp: 767-774. DOI: [http://dx.doi.org/10.1016/S1567-5769\(02\)00014-0](http://dx.doi.org/10.1016/S1567-5769(02)00014-0)

Lin Y. T., Verma A., and Hodgkinson C. P. (2012). Toll-like receptors and human disease: lessons from single nucleotide polymorphisms. *Curr Genomics*, **13**(8). Pp: 633-45. DOI: [10.2174/138920212803759712](https://doi.org/10.2174/138920212803759712)

Liou C. J., Len W. B., Wu S. J., Lin C. F., Wu X. L., and Huang W. C. (2014). Casticin inhibits COX-2 and iNOS expression via suppression of NF-kappaB and MAPK signaling in lipopolysaccharide-stimulated mouse macrophages. *J Ethnopharmacol*, **158 Pt A**. Pp: 310-6. DOI: [10.1016/j.jep.2014.10.046](https://doi.org/10.1016/j.jep.2014.10.046)

Liu K., Wang X., Sha K., Zhang F., Xiong F., Wang X., Chen J., Li J., Churilov L. P., Chen S., Wang Y., and Huang N. (2017). Nuclear protein HMGN2 attenuates pyocyanin-induced oxidative stress via Nrf2 signaling and inhibits *Pseudomonas aeruginosa* internalization in A549 cells. *Free Radic Biol Med*, **108**. Pp: 404-417. DOI: [10.1016/j.freeradbiomed.2017.04.007](https://doi.org/10.1016/j.freeradbiomed.2017.04.007)

Livak K. J., and Schmittgen T. D. (2001). Analysis of relative gene expression data using real-time quantitative PCR and the $2^{-\Delta\Delta CT}$ method. *Methods*, **25**(4). Pp: 402-408. DOI: [10.1006/meth.2001.1262](https://doi.org/10.1006/meth.2001.1262)

Lomer M. C. E., Thompson R. P. H., and Powell J. J. (2002). Fine and ultrafine particles of the diet: influence on the mucosal immune response and association with Crohn's disease. *Proceedings of the Nutrition Society*, **61**(01). Pp: 123-130. DOI: [10.1079/pns2001134](https://doi.org/10.1079/pns2001134)

Meng Z., and Zhang Q. (2006). Oxidative damage of dust storm fine particles instillation on lungs, hearts and livers of rats. *Environ Toxicol Pharmacol*, **22**(3). Pp: 277-82. DOI: [10.1016/j.etap.2006.04.005](https://doi.org/10.1016/j.etap.2006.04.005)

Mitchell J. P., and Carmody R. J.(2018). *Chapter Two - NF- κ B and the Transcriptional Control of Inflammation*, in *International Review of Cell and Molecular Biology*, F. Loos, Editor. Academic Press. p. 41-84

Nguyen T., Sherratt P. J., Huang H. C., Yang C. S., and Pickett C. B. (2003). Increased protein stability as a mechanism that enhances Nrf2-mediated transcriptional activation of the antioxidant response element. Degradation of Nrf2 by the 26 S proteasome. *J Biol Chem*, **278**(7). Pp: 4536-41. DOI: 10.1074/jbc.M207293200

Onodera Y., Teramura T., Takehara T., Shigi K., and Fukuda K. (2015). Reactive oxygen species induce Cox-2 expression via TAK1 activation in synovial fibroblast cells. *FEBS Open Bio*, **5**. Pp: 492-501. DOI: 10.1016/j.fob.2015.06.001

Parker K. H., Beury D. W., and Ostrand-Rosenberg S.(2015). *Chapter Three - Myeloid-Derived Suppressor Cells: Critical Cells Driving Immune Suppression in the Tumor Microenvironment*, in *Advances in Cancer Research*, X.-Y. Wang and P.B. Fisher, Editors. Academic Press. p. 95-139

Perini K., Ottel  M., Giulini S., Magliocco A., and Roccotiello E. (2017). Quantification of fine dust deposition on different plant species in a vertical greening system. *Ecological Engineering*, **100**. Pp: 268-276. DOI: 10.1016/j.ecoleng.2016.12.032

Pinto C., Giordano D. M., Maroni L., and Marzioni M. (2018). Role of inflammation and proinflammatory cytokines in cholangiocyte pathophysiology. *Biochim Biophys Acta Mol Basis Dis*, **1864**(4 Pt B). Pp: 1270-1278. DOI: 10.1016/j.bbadis.2017.07.024

R&DSystems. Toll-Like Receptors. 2018 [cited 2018 09-28]; Available from: <https://www.rndsystems.com/research-area/toll-like-receptors>.

Sanjeeva K., and Jeon Y.-J. (2018). Edible brown seaweeds: a review. *Journal of Food Bioactives*, **2**. Pp: 37–50-37–50. DOI:

Sanjeeva K. K. A., Fernando I. P., Kim E. A., Ahn G., Jee Y., and Jeon Y. J. (2017). Anti-inflammatory activity of a sulfated polysaccharide isolated from an enzymatic digest of brown seaweed *Sargassum horneri* in RAW 264.7 cells. *Nutr Res Pract*, **11**(1). Pp: 3-10. DOI: 10.4162/nrp.2017.11.1.3

Shah A. S., Langrish J. P., Nair H., McAllister D. A., Hunter A. L., Donaldson K., Newby D. E., and Mills N. L. (2013). Global association of air pollution and heart failure: a systematic review and meta-analysis. *Lancet*, **382**(9897). Pp: 1039-48. DOI: 10.1016/S0140-6736(13)60898-3

Sheng W., Zong Y., Mohammad A., Ajit D., Cui J., Han D., Hamilton J. L., Simonyi A., Sun A. Y., Gu Z., Hong J. S., Weisman G. A., and Sun G. Y. (2011). Pro-inflammatory cytokines and lipopolysaccharide induce changes in cell morphology, and upregulation of ERK1/2, iNOS and sPLA(2)-IIA expression in astrocytes and microglia. *J Neuroinflammation*, **8**(1). Pp: 121. DOI: 10.1186/1742-2094-8-121

Singh S., Shi T., Duffin R., Albrecht C., van Berlo D., Hohr D., Fubini B., Martra G., Fenoglio I., Borm P. J., and Schins R. P. (2007). Endocytosis, oxidative stress and IL-8 expression in human lung epithelial cells upon treatment with fine and ultrafine TiO₂: role of the specific surface area and of surface methylation of the particles. *Toxicol Appl Pharmacol*, **222**(2). Pp: 141-51. DOI: 10.1016/j.taap.2007.05.001

Srinivasan L., Harris M. C., and Kilpatrick L. E. (2017). 128 - *Cytokines and Inflammatory Response in the Fetus and Neonate*, in *Fetal and Neonatal Physiology (Fifth Edition)*, R.A. Polin, et al., Editors. Elsevier. p. 1241-1254.e4

Stenson W. F. (2007). Prostaglandins and epithelial response to injury. *Curr Opin Gastroenterol*, **23**(2). Pp: 107-10. DOI: 10.1097/MOG.0b013e3280143cb6

Szczepanik A. M., Funes S., Petko W., and Ringheim G. E. (2001). IL-4, IL-10 and IL-13 modulate A β (1-42)-induced cytokine and chemokine production in primary murine microglia and a human monocyte cell line. *Journal of Neuroimmunology*, **113**(1). Pp: 49-62. DOI: [https://doi.org/10.1016/S0165-5728\(00\)00404-5](https://doi.org/10.1016/S0165-5728(00)00404-5)

Takeda K., and Akira S. (2005). Toll-like receptors in innate immunity. *Int Immunol*, **17**(1). Pp: 1-14. DOI: 10.1093/intimm/dxh186

Tam W. F., Lee L. H., Davis L., and Sen R. (2000). Cytoplasmic sequestration of rel proteins by Ikappa B alpha requires CRM1-dependent nuclear export. *Molecular and Cellular Biology*, **20**(6). Pp: 2269-2284. DOI: 10.1128/mcb.20.6.2269-2284.2000

Terasaki M., Kawagoe C., Ito A., Kumon H., Narayan B., Hosokawa M., and Miyashita K. (2017). Spatial and seasonal variations in the biofunctional lipid substances (fucoxanthin and fucosterol) of the laboratory-grown edible Japanese seaweed (*Sargassum horneri* Turner) cultured in the open sea. *Saudi Journal of Biological Sciences*, **24**(7). Pp: 1475-1482. DOI: 10.1016/j.sjbs.2016.01.009

Valko M., Morris H., and Cronin M. T. D. (2005). Metals, Toxicity and Oxidative Stress. *Current Medicinal Chemistry*, **12**(10). Pp: 1161-1208. DOI: 10.2174/0929867053764635

Yu R., Lei W., Mandlekar S., Weber M. J., Der C. J., Wu J., and Kong A. N. (1999). Role of a mitogen-activated protein kinase pathway in the induction of phase II detoxifying enzymes by chemicals. *J Biol Chem*, **274**(39). Pp: 27545-52. DOI: 10.1074/jbc.274.39.27545

Zaph C., Troy A. E., Taylor B. C., Berman-Booty L. D., Guild K. J., Du Y., Yost E. A., Gruber A. D., May M. J., Greten F. R., Eckmann L., Karin M., and Artis D. (2007). Epithelial-cell-intrinsic IKK- β expression regulates intestinal immune homeostasis. *Nature*, **446**. Pp: 552. DOI: 10.1038/nature05590
<https://www.nature.com/articles/nature05590#supplementary-information>

Zhang Q., Lenardo M. J., and Baltimore D. (2017). 30 Years of NF-kappaB: A Blossoming of Relevance to Human Pathobiology. *Cell*, **168**(1-2). Pp: 37-57. DOI: 10.1016/j.cell.2016.12.012

Zielinski M. R., and Krueger J. M.(2012). *Chapter 48 - Inflammation and Sleep*, in *Therapy in Sleep Medicine*, T.J. Barkoukis, et al., Editors. W.B. Saunders: Philadelphia. p. 607-616

Part- 4

**3-Hydroxy-5,6-epoxy- β -ionone isolated from *Sargassum horneri*
inhibits fine dust-induced oxidative stress and inflammation in
Zebrafish embryo (*Danio rerio*)**

Abstract

Background

The health complications associated with air pollution (pulmonary diseases, cardiovascular diseases, and cancer), have been reported from indoor as well as outdoor environments. The dust storms originated in the China and Mongolian desert areas passed through the Korean peninsula and reduce the air quality in Korea. The particles less than 2.5 μm easily go through the respiratory system and deposited in the lungs. Therefore, exposure to the low concentrations of fine dust, might be ended up with serious health issue. Therefore, preventive measures require to reduce health impacts associated with dust to maintain health population. According to the recent studies, inflammation and oxidative stress in lungs are two major risk factors of fine dust. In addition to the avoiding direct exposure to fine dust, use of functional foods to avoid inflammation and oxidative stress might be a possible long term approach to reduce fine dust related health complications. However, direct use of *in vitro* results to develop functional materials are limited due the artificial growth conditions of culture cells. Therefore, *in vivo* studies are require to validate *in vitro* results. Thus in the present study zebrafish used as *in vivo* research model to evaluate fine dust induced inflammatory responses and protective effect of 3-Hydroxy-5,6-epoxy- β -ionone (HEBI); a pure compound isolated from *Sargassum horneri* brown seaweed.

Methodology

Zebrafish embryos were co-treated with different concentrations of HEBI (31.3 -125 $\mu\text{g/ml}$) for 1 h and then stimulated with 250 $\mu\text{g/ml}$ fine dust. The anti-inflammatory

properties of HEBI in fine dust exposed zebrafish embryos were evaluated using western blot analysis and RT-qPCR.

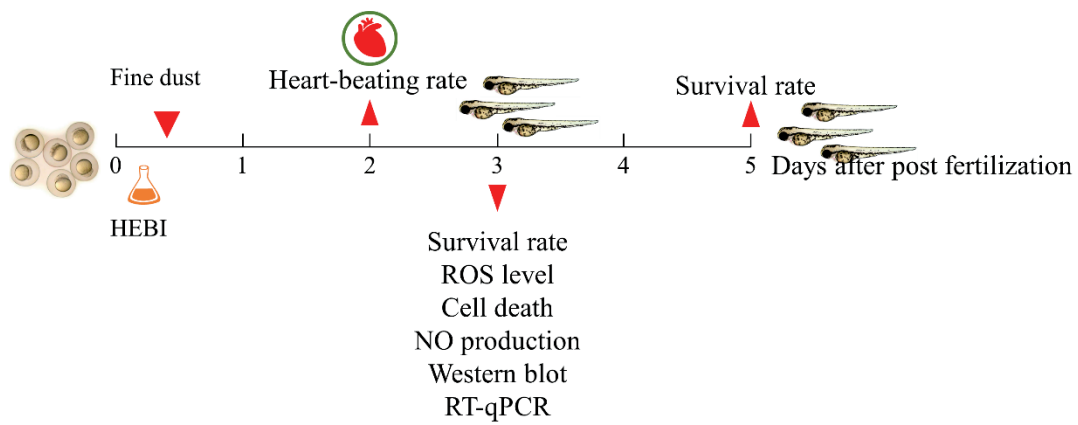
Results

The fine dust exposed zebrafish embryos (250 $\mu\text{g/ml}$) had low survival rates, high level of heart beat rates and up-regulated expression levels of iNOS, COX2, and pro-inflammatory mRNA expression levels. However, the treatment of HEBI (31.3- 125 $\mu\text{g/ml}$) significantly reduced the inflammatory responses in fine dust exposed zebrafish embryos.

Conclusions

According to the results, HEBI is a potential candidate to develop drugs or functional materials to reduce fine dust induced inflammation.

Graphical abstract



Graphical abstract: Inflammatory responses and possible protective mechanisms evaluation of fine dust exposed zebrafish embryo.

4.1 Introduction

Dust storms, are natural phenomenon in some parts of the earth with dry land areas such as deserts and semi-deserts. They are characteristic of great wind velocity, large amounts of dust and sand, and a lead to deteriorate sky visibility (Middleton 2017). In China, the areas affected by dust storms are geographically widespread and involve around 40,000 km². The dust moves with storms contains substantial amounts of metal contaminants such as SiO₂, Al₂O₃, and K₂O (Feng et al. 2002). Other than China; Korea and Japan also suffered from fine dust particles moved with heavy wind storms originated in Kazakhstan, Mongolia, and China (Vellingiri et al. 2015). Interest towards the dust storms has been gradually increase due to negative impacts on global environment as well as their negative impact on the human health (Middleton 2017). Park et al. (2003), studied the levels of crustal species and anthropogenic species in the Korean air during the dust storms events. According to the authors, levels of crustal species (Al, Ca, Fe, Ti, and Zn), as well as anthropogenic species (Pb) increased during the tested periods. In addition, author found the levels of nitrate and non-sea salt (nss)-sulfate) increased when dust storm occurs (Park 2003). Exposure to respirable air particles, defined to contain particles with an aerodynamic diameter less than 10 microns, poses a considerable threat to healthy life. According to the previous epidemiological studies, long term exposure of fine dust particles have shown statistically significant associations between increased mortality, malfunctions of lungs and other respiratory symptoms (Pozzi et al. 2003).

In general, particles between 2.5 to 10 µm are usually filtered by the nose or coughed out of the throat and upper lungs. However, some individuals might effect from fine dust particle in between 2.5 to 10 µm who already suffered from breathing problems or aggravate pre-existing breathing problems (asthma). Fine dust with 2.5 µm diameter or less particles passes easily into the deepest regions of the lungs such as alveoli.

According to the previous studies, fine dust induces pulmonary inflammation, airway hyper-reactivity, impairment of alveolar macrophage, damages in epithelial cells (Meng and Zhang 2006). To avoid the consequence of direct effect as well as side effects associated with fine dust exposure requires immediate attention. Specifically, chronic inflammation is a one known issue associated with fine dust exposure (Hou et al. 2018). Therefore, inhibition of up-regulated inflammatory responses through a functional material might be a good approach to reduce complications associated with long term chronic inflammatory responses.

Sargassum horneri is a sub-tidal brown seaweed species, which belongs to the order Fucales (Genus: Sargassum; Family: Sargassaceae; Order: Fucales; and Class: Phaeophyceae) (Xu et al. 2018). This brown seaweed grows on rocky coasts in the temperate zones and forming underwater forest during the spring and in the summer density of this biomass might get reduced. *S. horneri* is widely distributed along the coasts of the east Asia regions from China to Russia through the Korean Peninsula and Japan except shores of Taiwan and Ryukyu Archipelago (Komatsu et al. 2014). *S. horneri* is a popular as edible seaweed in East Asian countries. Specifically, *S. horneri* use as an ingredient to prepare medicines, side dishes, and soups. Among the popular food recipes “Akamoku” is a popular dish prepare from *S. horneri* in Japan (Terasaki et al. 2017).

Other than the traditional applications, recently a number of studies reported the crude and pure compounds isolated from this brown seaweed has a potential to developed functional materials (Sanjeeva et al. 2017; Terasaki et al. 2017). According to the previous studies, compounds isolated from *S. horneri* found to possess strong antioxidant and anti-inflammatory properties under *in vitro* conditions (Cuong et al. 2015; Fernando et al. 2018; Sanjeeva et al. 2018). However, use of *in vitro* results for the development of functional materials have limited possibility as the culture cells were maintained in

artificial conditions. therefore, to validate *in vitro* results it is compulsory to use *in vivo* research models. Recently, zebrafish (*Danio rerio*) has been recognized as a promising *in vivo* model to use in research areas such as cancer, stem cell research and immunology and infectious diseases research due to its morphological and physiological similarity to the mammals, transparency, easy to handle, and less maintenance cost (Lam et al. 2004; Novoa et al. 2009; Zon and Peterson 2005). Other than that, the optical transparency of zebrafish embryos allows for non-destructive and live imaging of the inflammatory responses developed in embryos (Kim et al. 2018). Due to these specific morphological and physiological features of zebrafish models provide great opportunities to accelerate the process of drug discovery including target identification, disease modelling, lead discovery and toxicology (Lam et al. 2004; Novoa et al. 2009; Zon and Peterson 2005). Taken together, In the present study, author attempted to investigate the effects of fine dust collected from Beijing city center, China, using zebrafish embryo. The objective of this study was to evaluate the effect of fine dust induced inflammation and oxidative stress in zebrafish embryo.

4.2. Materials and methods

4.2.1. Sample collection and purification

First *S. horneri* was extracted with 80% methanol in room temperature and then fractionated into hexane, chloroform, and ethyl acetate. Then the chloroform fraction was further purified using HPCPC. The identification and confirmation of structure was similar to the method describes in the part 1. The structure of 3-Hydroxy-5,6-epoxy- β -ionone (HEBI) illustrated in figure 2-1. The isolated compound has several names in national center for biotechnology information support center (NCBI) data base and also known as 3-Buten-2-one, 4-(4-hydroxy-2,2,6-trimethyl-7-oxabicyclo[4.1.0]hept-1-yl)-. The, PubChem CID of the HEBI is 5371267. Additional details of the HEBI is available in the following link.

(<https://pubchem.ncbi.nlm.nih.gov/compound/5371267#section=Top>)

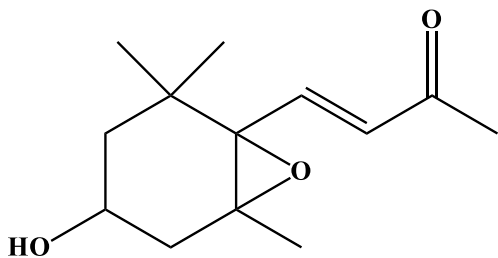


Figure 4-1. The molecular structure of 3-Hydroxy-5,6-epoxy- β -ionone isolated from *Sargassum horneri*. (MW: 224.2), PubChem CID: 5371267, Abbreviation: HEBI
<https://pubchem.ncbi.nlm.nih.gov/compound/5371267#section=Top>

4.2.2. Chemicals and reagents

CRM certified fine dust reference material (CRM No. 28 Urban Aerosols) was purchased from the center for environmental measurement and analysis, national institute for environmental studies, Ibaraki, Japan. NE-PER[®] nuclear and cytoplasmic extraction kit, and DAF-FM Diacetate (4-Amino-5-Methylamino-2',7'-Difluorofluorescein Diacetate) were purchased from Thermo scientific, Rockford, USA. Tri-Reagent[™] for RNA extraction, DCFDA (2',7'-Dichlorofluorescein diacetate), chloroform, isopropanol, ethanol, 2-phenoxy ethanol, and acridine Orange purchased from Sigma-Aldrich Co (St. Louis, MO, USA). SYBR Green prime and prime Script[™] first-strand cDNA synthesis kit were purchased from TaKaRa, Japan. All primers used in this study for RT-qPCR was purchased from Bioneer, Seoul, Korea. Polyvinylidene fluoride membranes (PVDF) were purchased from Millipore, Billerica, MA, USA. Rabbit primary and secondary antibodies were purchased from Cell Signaling, Danvers, MA. PCR grade organic solvents including chloroform, isopropanol, and ethanol were purchased from Sigma Aldrich, USA.

4.2.3. Estimation of fine dust particle size by scanning electron microscopy

A Q150R rotary-pumped sputter coater (Quorum Technologies, Lewes, UK) was used for the fine dust specimen sputter-coating procedure with platinum. Field-emission scanning electron microscope (Model: JSM-6700F) (JEOL, Tokyo, Japan), the surface morphology of Certified reference material (CRM) No. 28 particles was observed. The instrument was operated at 10.00 kV.

4.2.4. In vivo zebrafish experiments

4.2.4.1. Origin and maintenance of parental zebrafish

Adult zebrafish were purchased from a commercial dealer (Seoul aquarium, Seoul, Korea) and were kept in a 3 l acrylic tank with modified environmental conditions as follows; 28.5 °C temperature, 14:10 h light: dark cycle and adult zebrafish were fed twice a day (Tetra GmgH D-49304 Melle, Germany). Embryos were obtained by interbreeding two males and one female. In the morning (8. 30 a.m.), embryos were obtained from natural spawning and collection of the embryos were completed within 30 min (before 9.00 a.m.) in to petri dishes (containing embryo media).

4.2.4.2. Measurement of the toxicity of fine dust and HEBI on zebrafish embryo

Toxicity of HEBI on zebrafish embryos was determined by means of survival rate and the heartbeat rate of the zebrafish embryos (Wijesinghe et al. 2014). Briefly, zebrafish embryos ($n = 15$) at 3 - 4 h post-fertilization (hpf) were randomly transferred to 12-well plates containing 1.8 ml embryo media. Then 100 μ l of different concentration of HEBI, fine dust or their combinations were mixed with the embryo medium. The survival rate of zebrafish embryos of each group determined until 5-day post-fertilization (5dpf).

$$\text{Survival rate (\%)} = \left(\frac{\text{Viable embryos in the tested group}}{\text{Number of embryo used at the beginning}} \right) \times 100$$

4.2.4.3. Measurement of heart-beating rate of zebrafish

The heartbeat rate of both atrium and ventricle of the sample or fine dust-stimulated zebrafish embryo was recorded at 2 dpf for 1 min under the microscope. The results were presented as the percentage of the heart-beating rate per 60 seconds.

$$\text{Heart beating rate (\%)} = \left(\frac{\text{Avg value of each individual in the group}}{\text{Avg value of control group}} \right) \times 100$$

4.2.4.4. The toxicity of HEBI on zebrafish embryo by means of the cell death

Acridine orange staining used to detect cell death rates in HEBI treated zebrafish embryo. At 3 dpf, a zebrafish embryos were transferred to 24 well plate and incubated 30 min with acridine orange solution (7 µg/ml) in the dark room at 28.5 ± 1 °C. After 30 min acridine orange removed from 24 well-plate and washed twice with embryo medium. Then zebrafish larvae were anaesthetized by 2-phenoxy ethanol (1/500 dilution) and observed under the microscope equipped with CoolSNAP-Pro color digital camera (Olympus, Japan). Individual zebrafish larvae fluorescence intensity was quantified using an image J program.

4.2.4.5. Estimation of fine dust induced ROS generation

At the 3 dpf, zebrafish larvae were transferred to 24-well plate, treated with DCF-DA solution (20 µg/mL) and incubated for 1 h in the dark room at 28.5 ± 1 °C. Then the zebrafish larvae were washed twice with fresh embryo media. Finally, zebrafish larvae were anaesthetized by 2-phenoxy ethanol (1/500) and observed under the microscope equipped with CoolSNAP-Pro color digital camera (Olympus, Japan). Individual zebrafish larvae fluorescence intensity was quantified using an image J program.

4.2.4.6. Measurement of in vivo NO production

NO production of fine dust induced zebrafish model was analyzed using a fluorescent probe dye, diaminofluorophore 4-amino-5-methylamino-2',7'-difluorofluorescein

diacetate (DAF-FM DA). At the 3 dpf, zebrafish larvae were transferred to 24-well plates and incubated with DAF-DM-DA solution (5 μ M) for 90 min in the dark room at 28.5 ± 1 °C. After, incubation, the zebrafish larvae were rinsed in fresh embryo medium and anaesthetized by 2-phenoxy ethanol (1/500 dilution sigma) and observed under the microscope equipped with CoolSNAP-Pro color digital camera (Olympus, Japan). Individual zebrafish larvae fluorescence intensity was quantified using an image J program.

4.2.5. Western blot analysis

The embryos, were lysed with commercial protein extraction kit by following vendor's instruction. 20 μ g of proteins were fractionated on 12% SDS-PAGE gels, and transferred to PVDF membranes. Non-specific binding was blocked by incubation of the blots for 3 h at room temperature with 5% non-fat dry milk (Bio-Rad, Hercules, CA) in TBST buffer. Blots were incubated overnight at 4 °C with anti COX2, iNOS, (1:1000). After 3 washes in TBS-T buffer (10 min in each wash and total 30 min), blots were incubated with anti-rabbit HRP-conjugated secondary antibody (1: 3000) for 90 min using orbital shaker at room temperature. Fluorescence images were taken using a FUSION SOLO Vilber Lourmat system (Paris, France). The expression levels of each protein was normalized by analysing the level of β -actin protein expression levels by using ImageJ (V 1.4) program.

4.2.6 RNA extraction, cDNA synthesis and RT- qPCR analysis

Three days after post fertilization, total RNAs of zebrafish embryo were extracted with Tri-Reagent™ for mRNA analysis. Embryos were homogenized with 500 μ l of Tri-Reagent™ incubated for 1 h on ice with continuous shaking. After adding 500 μ l

chloroform gently shake to mix two layers and the suspension was centrifuged at 15,000 *g* for 15 min. Isopropanol precipitation was performed by centrifuging at 4 °C with 12,000 x *g* for 10 min. Resulting RNA pellet was washed in 70% EtOH and dried the RNA pellet at room temperature. First strand cDNA was synthesized using commercial cDNA synthesis kit according to the manufactures instructions. The synthesized cDNA diluted in PCR grade water (20 x) and stored in -80 °C. Working PCR mixture was composed of diluted cDNA (3 µl), forward and reverse primers (0.4 µl), 2x SYBR green master mix (5 µl) and of PCR grade water (1.2 µl) in a total volume of 10 µl. PCR was performed in a thermal cycler dice-real time system (TaKaRa, Japan) with the default thermo-cycle condition. The relative expression levels were analyzed according to the method [$2^{-\Delta\Delta CT}$ method] describe by Livak and Schmittgen (2001) (Livak and Schmittgen 2001). The base line was automatically set by Dice™ real time system software (version 2.00) to keep reliability. The primers used in this study were mentioned in the table 4.1. The data are presented as the mean ± standard error (SE) of the relative mRNA expression from three consecutive experiments. The primers used in this study were shown in Table 4-1. The two-tailed unpaired Students t-test was used to determine statistical significance (* = $p < 0.05$ and ** = $p < 0.01$).

Table 4-1. Sequence of the primers used to evaluate RNA expression levels in zebrafish embryo

Gene	Primer	Sequence 5' → 3'
B-actin	Sense	AGAGCTATGAGCTGCCTGACG
	Antisense	CCGCAAGATTCCATACCCA
iNOS	Sense	CGTGTTTACCATGAGGCTGA
	Antisense	CGCTTCAGGTTCCCTGATCCAA
COX2	Sense	CAAGGGTGCGGGTGTAAT
	Antisense	GAACTCGCTTTGTCTCCA
IL-1 β	Sense	ATGGCAGAAGTACCTAAGCTC
	Antisense	TTAGGAAGACACAAATTGCATGGTGA ACTCAGT
IL-6	Sense	GAGGATACCACTCCCAACAGACC
	Antisense	AAGTGCATCATCGTTGTTTCATACA
TNF- α	Sense	TGACTGAGGAACAAGTGCTTATGAG
	Antisense	GCAGCGCCGAGGTAAATAGTG

4.2.7 Statistical analysis

The data are presented as means \pm standard error (SE). Statistical comparisons of the mean values were performed by analysis of variance (ANOVA), followed by a Duncan's multiple range test using SPSS software. A p -value < 0.05 and 0.01 were considered to be statistically significant.

4.3. Results and discussion

4.3.1. *Composition of fine dust and size distribution analysis of fine dust*

Before begins the studies with fine dust, first author measured the particle size distribution of fine dust particles (fig. 4-1) using electron microscope. According to the seller's information (fig. 4-1a) and image analysis results (fig. 4-1b) majority of particles were distributed in between the 0 - 3 μm diameter (around 50%). In addition to the particle size distribution, metals and other hazards elements levels (Table 4.2) as well as mass fractions levels (Table 4.3) in fine dust mixtures were obtained from the sellers web site (<https://www.nies.go.jp/labo/crm-e/aerosol.html>). According to the metal analysis results, fine dust contained heavy metals including Pb (403 ± 32 mg/kg) Ba (874 ± 65 mg/kg). It has been reported, continuous exposure to heavy metals (Cr, Ni, Pb, Cd, and Cu) containing fine dust increase the risk of respiratory disease conditions such as chronic obstructive pulmonary disease, and asthma (Gautam et al. 2005). Therefore, inhalation of fine dust has a potential to induce inflammation and oxidative stress internal organs. Thus, preventive health measures require to avoid negative health effects associate with fine dust exposure.

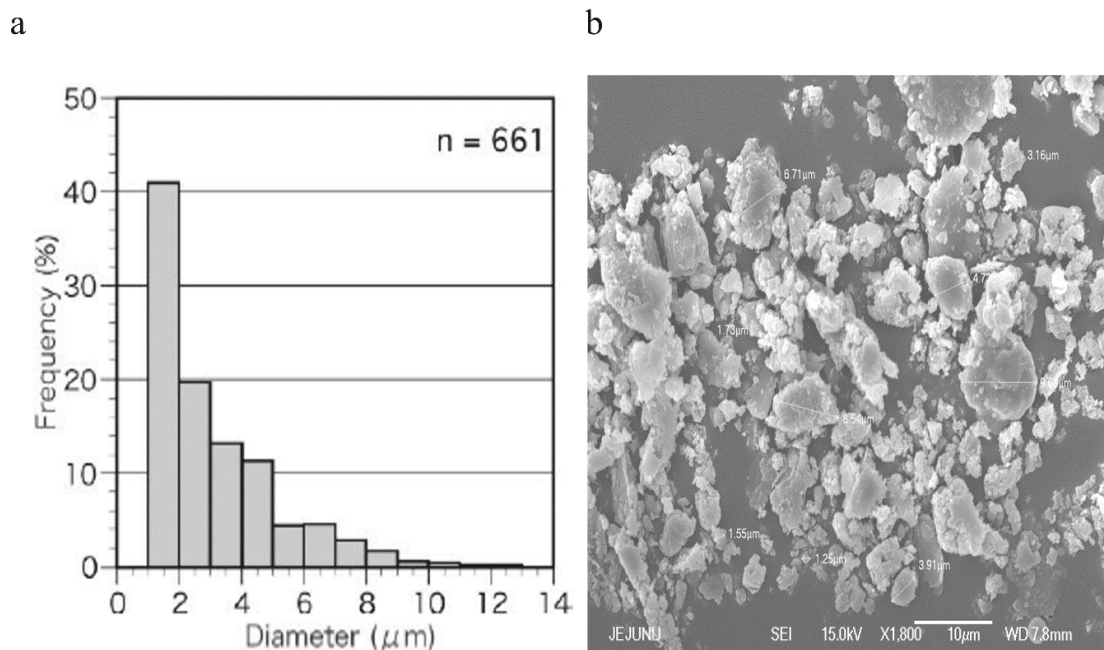


Figure 4-2. Particle size distribution (a) and scanning electron microscope image (b) of fine dust particles. The particle size distribution graph was obtained from the national institute for environmental studies, Ibaraki, Japan (certified reference material no. 28). Scale bar represent 10 μm lengthy.

Source for bar chart - <https://www.nies.go.jp/labo/crm-e/aerosol.html>

Table 4-2. Certified elements values of NIES CRM No. 28 Urban Aerosols

Element	Unit	Mass fraction		Analytical method
Na	%	0.796	± 0.065	AAS, ICP-AES, INAA, XRF
Mg	%	1.4	± 0.06	ICP-AES, ICP-MS, XRF
Al	%	5.04	± 0.1	ICP-AES, ICP-MS, INAA, XRF
K	%	1.37	± 0.06	AAS, ICP-AES, XRF
Ca	%	6.69	± 0.24	ICP-AES, ICP-MS, INAA, XRF
Ti	%	0.292	± 0.033	ICP-AES, ICP-MS, INAA, PIXE, XRF
Fe	%	2.92	± 0.17	ICP-AES, ICP-MS, INAA, XRF
Zn	%	0.114	± 0.01	ICP-AES, ICP-MS, INAA, PIXE, XRF
V	mg/kg	73.2	± 7	ICP-AES, ICP-MS, INAA
Mn	mg/kg	686	± 42	ICP-AES, ICP-MS, INAA, PIXE, XRF
Ni	mg/kg	63.8	± 3.4	AAS, ICP-AES, ICP-MS
Cu	mg/kg	104	± 12	ICP-AES, ICP-MS, PIXE, XRF
As	mg/kg	90.2	± 10.7	HG-AAS, HG-ICP-AES, ICP-AES, ICP-MS, INAA, XRF
Sr	mg/kg	469	± 16	ICP-AES, ICP-MS, XRF
Cd	mg/kg	5.6	± 0.43	ICP-AES, ICP-MS
Ba	mg/kg	874	± 65	ICP-AES, ICP-MS, INAA
Pb	mg/kg	403	± 32	ICP-AES, ICP-MS, XRF
U	mg/kg	4.33	± 0.26	ICP-MS, INAA

AAS: atomic absorption spectroscopy; HG-AAS: hydride generation - atomic absorption spectroscopy; HG-ICP-AES: hydride generation-inductively coupled plasma-atomic emission spectrometry; ICP-AES: inductively coupled plasma-atomic emission spectrometry; ICP-MS: inductively coupled plasma-mass spectrometry; INAA: instrumental neutron activation analysis; PIXE: proton induced X-ray emission spectrometry; XRF: X-ray fluorescence spectroscopy. Source - <https://www.nies.go.jp/lab/crm-e/aerosol.html>

Table 4-3. Mass fraction of PAHs in NIES CRM No. 28 Urban Aerosols

Component name	Unit	Mass fraction	Analytical Method
Fluoranthene	mg/kg	7	GC-MS, HPLC-FLU
Pyrene	mg/kg	4	GC-MS, HPLC-FLU
Benz (a) anthracene	mg/kg	2	GC-MS, HPLC-FLU, HR-GC-MS
Benzo (b) fluoranthene	mg/kg	11	GC-MS, HPLC-FLU, HR-GC-MS
Benzo (k) fluoranthene	mg/kg	2	GC-MS, HPLC-FLU, HR-GC-MS
Benzo (a) pyrene	mg/kg	0.9	GC-MS, HPLC-FLU, HR-GC-MS
Benzo (ghi) perylene	mg/kg	2	GC-MS, HPLC-FLU, HR-GC-MS
Indeno (1,2,3-cd) pyrene	mg/kg	3	GC-MS, HPLC-FLU, HR-GC-MS

GC-MS: gas chromatography-mass spectrometry

HPLC-FLU: high performance liquid chromatography-fluorescence detection

HR-GC-MS: high resolution gas chromatography-mass spectrometry

Source - <https://www.nies.go.jp/labo/crm-e/aerosol.html>

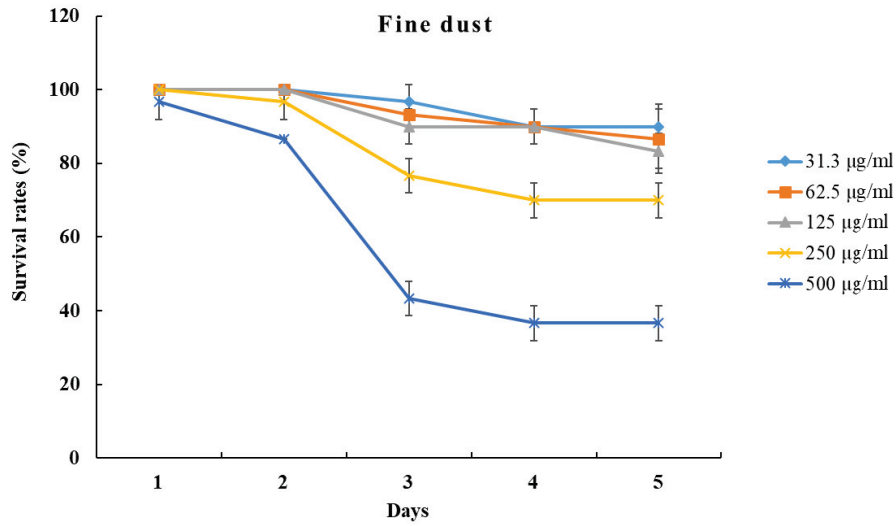
4.3.2. Fine dust induced toxicity rates in zebrafish embryo

Direct use of *in vitro* results to develop functional materials has number of issues due to their physiological and economic relevance under the *in vivo* situations (Choi et al. 2007). The development of *in vivo* models using animals (mouse) or humans also have limitations due to the limited amounts of pure compounds, high cost, laborious routine work, ethical law enforcements for animal models (Choi et al. 2007). Therefore, cheap and easy alternates are an urgent requirement for evaluate or validate *in vitro* results. Among the candidate *in vivo* models zebrafish has been recently identified as an ideal *in vivo* model due to the similar organ systems and gene sequences of zebrafish to humans (Love et al. 2004; Zon and Peterson 2005). Taken together, in the present study author used zebrafish as *in vivo* animal model to validate *in vitro* results obtained from HEBI during the previous studies (part 1, 2, and 3).

First a range of fine dust concentrations were incubated with zebrafish embryos (125-500 $\mu\text{g/ml}$) to determine the optimal concentration to stimulate zebrafish embryo (fig 4.3a). Additionally, embryos were separately incubated with different concentrations of HEBI (15.6 – 500 $\mu\text{g/ml}$) to determine the non-toxic concentrations of HEBI to evaluate its protective effect against fine dust-induced inflammation and oxidative stress. A significant reduction in the survival rate following exposure to 500 $\mu\text{g/ml}$ of fine dust at 3 dpf was observed during the study. However, concentrations less than 250 $\mu\text{g/ml}$ of fine dust did not significantly cause zebrafish embryo death. Additionally, HEBI concentrations between 31.3-125 $\mu\text{g/ml}$ were not expressed any toxic effect on zebrafish embryo (fig. 4.3b). Taken together, fine dust 250 $\mu\text{g/ml}$ and HEBI 31.3 -125 $\mu\text{g/ml}$ used for the consequence studies to stimulate and evaluate the protective effect of HEBI against fine dust stimulation.

As next part of study, the survival rate of embryos after treatment with 250 $\mu\text{g/ml}$ fine dust stimulated and 31.3-125 $\mu\text{g/ml}$ HEBI co-treated were measured (3 dpf). The survival rate of fine dust treated group was significantly decreased ($\sim 73\%$) compared to the control group. However, HEBI treated embryos reduced fine dust-induced death rates in a dose-dependent manner (fig. 4.4a).

a



b

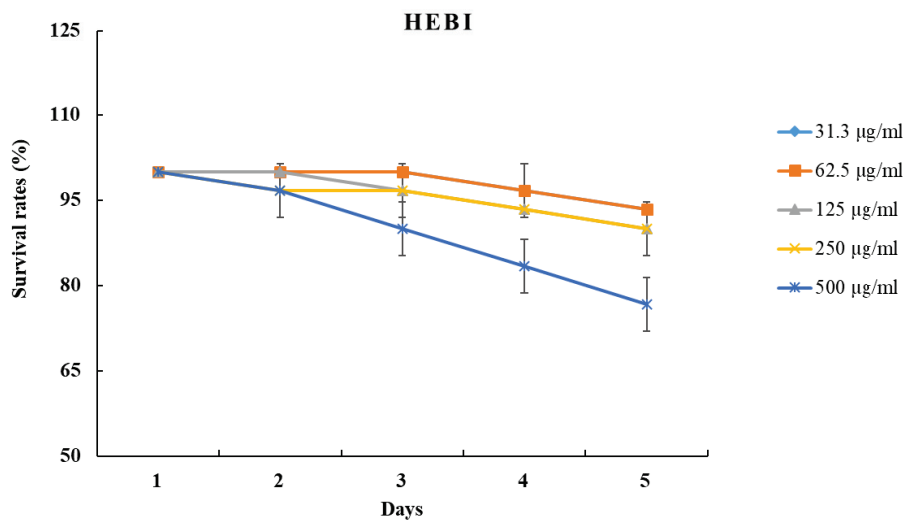


Figure 4-3. Evaluation of fine dust (a) and HEBI (b) induced zebrafish embryo death rates. Experiments were performed in triplicate, and the data are expressed as mean \pm SD, * $p < 0.01$ (n=15)

4.3.3. Effects of HEBI on fine dust-exposed heart-beating rate of zebrafish model

The increased heart beating rates, tail bending, and small head size are used to determine the toxicity and protective effects of compounds used in zebrafish embryo models (Choi et al. 2007). Heart beating rates of zebrafish embryos were recorded to evaluate protective effect of HEBI against fine dust induced toxicity in zebrafish embryo. According to the results, fine dust treated zebrafish embryos had elevated heart beating rates compared to the un-stimulated group (fig. 4-4b). However, the elevated heart beating rates observed in fine dust exposed zebrafish embryos were dose-dependent decreased by HEBI (31.3 - 125 $\mu\text{g/ml}$).

Previously, a number of studies reported the exposure of zebrafish embryo to bacterial lipopolysaccharides (LPS) and AAPH (reactive oxygen species) cause to trigger inflammatory responses from zebrafish embryos such as elevated heart beating rates and NO production. Specifically, Lee et al, (2013) and Kim et al. (2014) reported that the LPS-exposed and AAPH-exposed zebrafish embryos had elevated levels of heart beating rates and cell death rates (Kim et al. 2014; Lee et al. 2013). When consider about composition of fine dust, which is a combination of micro-organisms, heavy metals, and organic matters (known activators of oxidative stress and inflammatory responses). This composition might be the reason to observe high levels of heart beating rates and low survival rates in fine dust exposed zebrafish embryos. Therefore, it is clear that fine dust cause to induce inflammation and mortality in zebrafish embryo as well as HEBI has the potential to protect zebrafish embryo against fine dust induced toxicity.

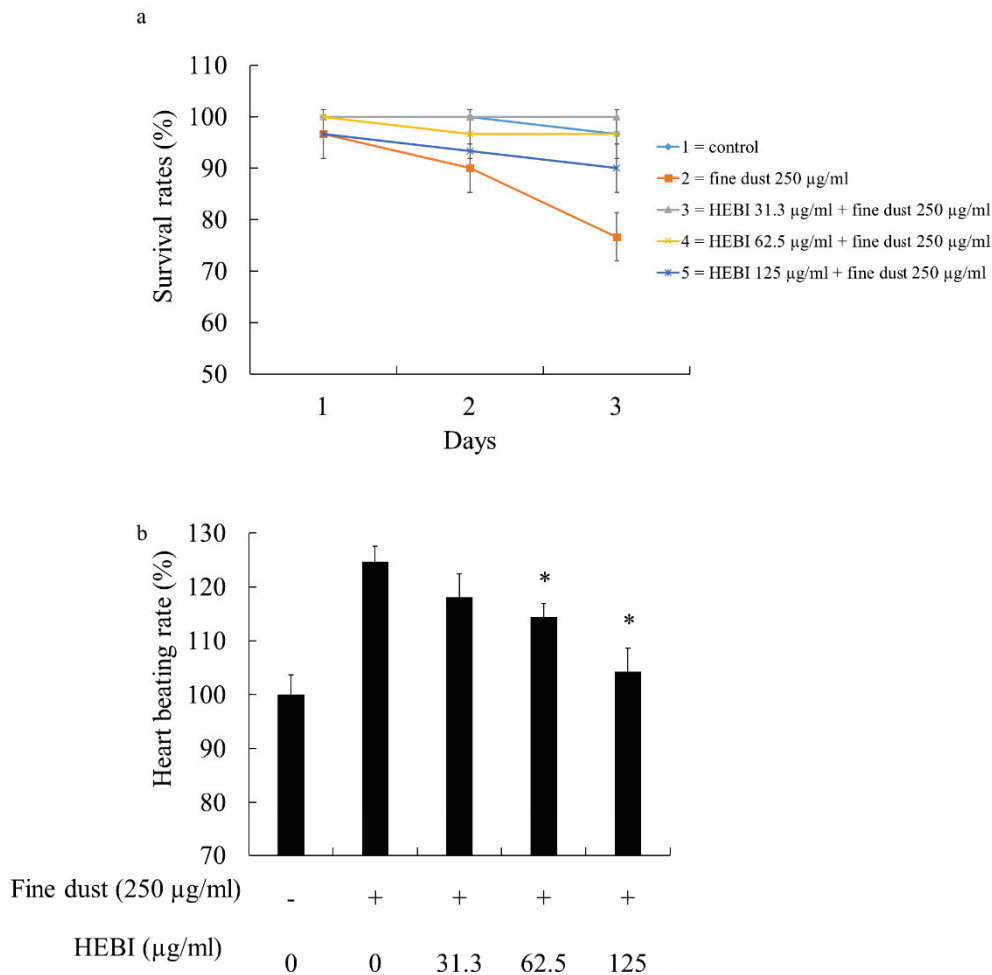


Figure 4-4. Protective effect of HEBI against fine dust induced toxicity (death rates) (a) heart beating rates (b). Experiments were performed in triplicate, and the data are expressed as mean \pm SD, * $p < 0.01$ (n=15)

4.3.4. Protective effect of HEBI against fine dust induced cell deaths in zebrafish embryos

Acridine Orange is a cell-permeant nucleic acid binding dye which emits green fluorescence when attached to dsDNA and red fluorescence when coupled with RNA or ssDNA. This unique features makes acridine orange useful for cell-cycle studies. Acridine orange has also been used as a lysosomal dye (Mozhenok et al. 1997; Russo et al. 2009). Thus, acridine orange can used to determine the necrotic or apoptotic cells (Kim et al. 2014). Therefore, in the present study author attempted to investigate the protective effect of HEBI against fine dust induce cell death in zebrafish embryos. According to the results, acridine orange intensity was significantly high in fine dust exposed embryos (250 µg/ml) (fig. 4-5). However, the pre-incubation of HEBI dose-dependently decreased the acridine orange intensity observed in the fine dust exposed embryos.

4.3.5. protective effect of HEBI on fine dust –induced ROS production in zebrafish embryo

DCF-DA is an oxidant-sensitive fluorescent probe which use to measure levels of ROS in its surrounding environment. DCF-DA react with intercellular ROS and convert in to DCF. In the dark DCF emits fluorescent and it can easily visualize (Handa et al. 2006). Figure 4.6 shows the *in vivo* ROS production in fine dust exposed zebrafish embryos and protective effect of HEBI against ROS generation in fine dust exposed zebrafish embryo. It is a well-establish fact that, the high ROS level induces oxidative stress in biological systems and, which can result in the development of a variety of cell or tissue injuries such as degenerative diseases, including inflammation (Finkel and Holbrook 2000).

The exposure of fine dust to zebrafish embryos cause to up-regulate the production of ROS from zebrafish embryos. However, pre-incubation of HEBI significantly reduced the elevated ROS production observed in zebrafish embryo.

4.3.6. Protective effect of HEBI against fine dust induced NO production in zebrafish embryos

DAF-FM Diacetate is a membrane-permeating reagent that is used to detect and quantify low concentrations of NO. DAF-FM Diacetate is essentially non-fluorescent until it reacts with NO to form a fluorescent benzotriazole. Fluorescent benzotriazole emits fluorescence and the fluorescence can easily detect with any instrument that can detect fluorescein, such as microscopes, flow cytometers, and fluorescent microplate readers (Kojima et al. 1999; Vardi et al. 2006; Xu and Krukoff 2007). Therefore, in the present study DAF-FM DA used to evaluate the protective effect of HEBI against fine dust-induced NO production in zebrafish embryo (fig. 4-7). According to the image analysis, fluorescence intensity in fine dust-exposed zebrafish embryos were significantly increased. However, HEBI dose-dependently decreased the elevated levels of intercellular NO in zebrafish embryo (31.3 -125 µg/ml). Thus, it is clear that HEBI has a potential to reduce intercellular ROS and NO induced by fine dust.

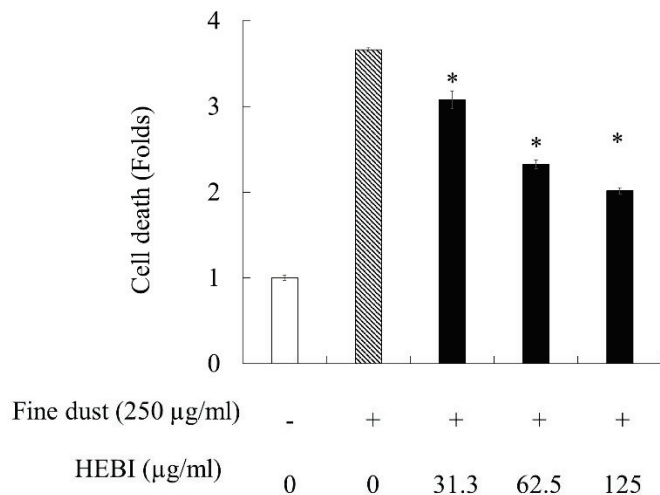
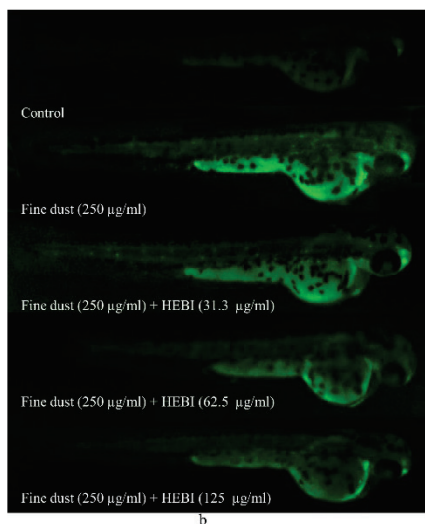


Figure 4-5. HEBI protects zebrafish embryos against fine dust-induced cell death. The cell death levels were measured after acridine orange staining by image analysis and fluorescence microscope. The cell death rates in embryos were quantified using an image J program. Experiments were performed in triplicate, and the data are expressed as mean \pm SD, * $p < 0.01$ (n=15)

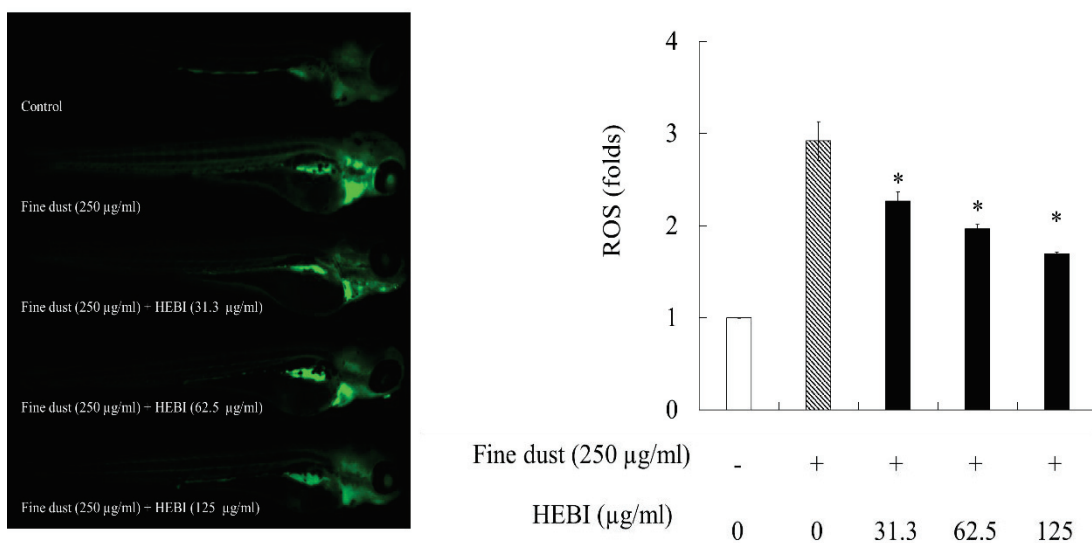


Figure 4-6. Protective effect of HEBI against fine dust-induced ROS generation in zebrafish embryo. ROS levels were measured after DCF-DA staining by image analysis and fluorescence microscope. The cell death rates were quantified using image J program. Experiments were performed in triplicate, and the data are expressed as mean \pm SD, * $p < 0.01$ (n=15)

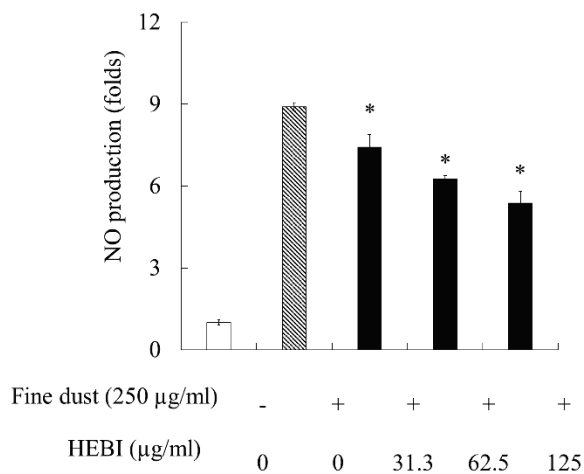
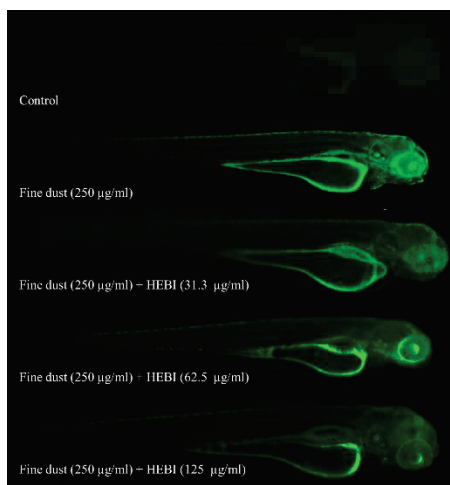


Figure 4-7. HEBI reduced fine dust-induced NO production in zebrafish larvae. The NO levels were measured by image analysis and fluorescence microscope. Individual zebrafish fluorescence intensity was quantified using image J program. Experiments were performed in triplicate, and the data are expressed as mean \pm SD, * $p < 0.01$ (n=15)

4.3.7. HEBI down-regulate fine dust-induced iNOS and COX2 expression in zebrafish embryos

NO production in organs stimulated by number of factors, such as pathogens, damaged cells or irritants (Hwang et al. 2016). The over-production of NO in the cellular environments induces chronic inflammatory responses in the body. Specifically, chronic NO overproduction is also involved in negative cellular physiologic functions, such as induction of DNA damage and genome instability (Aliev et al. 2013; Yang et al. 2013). To evaluate the biological effect of HEBI on the inflammation-end product and its involvement, the mRNA levels and protein levels of iNOS after fine dust challenged zebrafish was tested. According the western bolt analysis (fig. 4.8a and 4.8b) and mRNA data fine dust challenged zebrafish embryos had elevated levels of iNOS protein expression. However, HEBI (31.3 - 125 $\mu\text{g/ml}$) treatment down-regulated the elevated iNOS expression in fine dust challenged zebrafish embryo in a dose-dependent manner.

Prostaglandin-E₂ (PGE₂) is a bioactive lipid that elicits a wide-range of biological responses associated with cancer and inflammatory responses. The up-regulated PGE₂ cause to worsening the disease conditions like inflammatory bowel disease (Nakanishi and Rosenberg 2013). Furthermore, the production of PGE₂ mainly depends on the activation levels of COX2. The cellular PGE₂ is mainly depends on the COX2 expression levels (Kim et al. 2018). Thus, to evaluate the inhibitory effect of HEBI on the COX2 protein and mRNA levels, zebrafish embryos were incubated with the indicated concentrations of HEBI for 1 h and then challenged with fine dust (250 $\mu\text{g/ml}$) for 3 dpf. As shown in figure 4-8d, HEBI down-regulated fine dust-induced COX2 mRNA expressions.

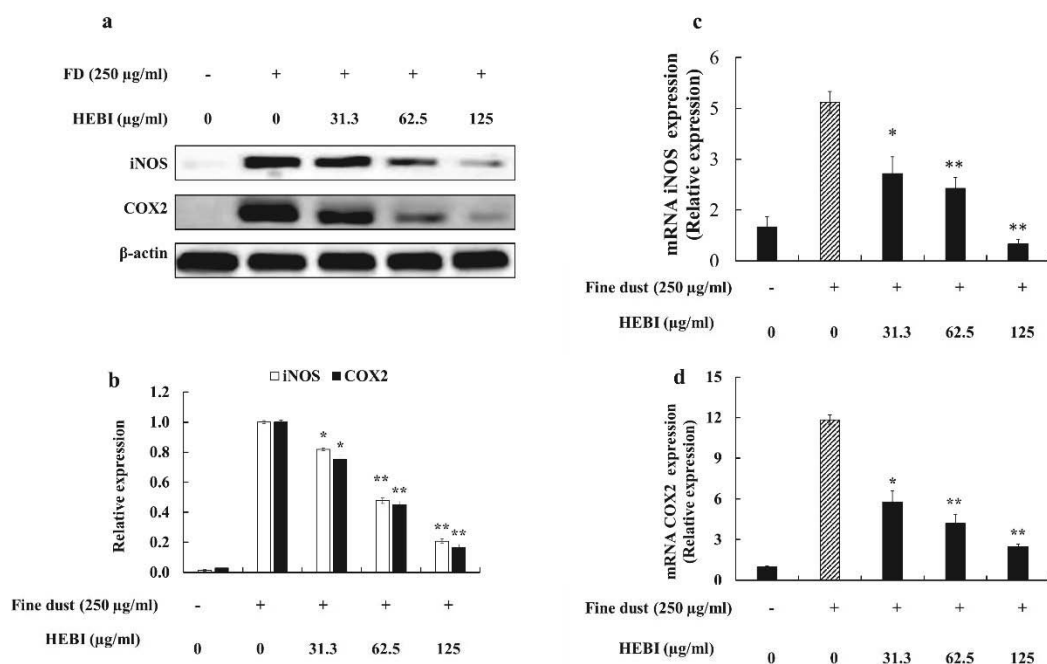


Figure 4-8. Effect of HEBI against fine dust (FD)-induced iNOS and COX2 expression in zebrafish embryos. The mRNA expression levels (a, b) and protein expression levels (c, d) of iNOS and COX2. Western blots and RT-qPCR used evaluate proteins and gene expression levels, respectively. Control was obtained in the absence of FD and HEBI. The values shown are the means \pm SEs of three independent experiments; * $p < 0.05$, ** $p < 0.01$ vs. the FD treated group.

4.3.8 HEBI protects zebrafish embryo against fine dust induced pro-inflammatory cytokine production

Pro-inflammatory cytokines such as interleukin-1 β (IL-1 β), IL-6, and tumour necrosis factor- α (TNF- α) play a vital role in the pathogenesis of inflammatory disease conditions. Specifically, these pro-inflammatory cytokines facilitate the recruitment of leukocytes to the site of inflammation and maintain chronic inflammation (Kim and Moudgil 2017). According to the previous studies, up-regulated pro-inflammatory cytokine production is a one known response to fine dust. Specifically, fine dust is a potent inducer of pro-inflammatory cytokines in the airway cells including epithelial cells and macrophages (Schweitzer et al. 2018). Taken together, in the present study, author attempted to evaluate fine dust induced pro-inflammatory cytokine expression levels in zebrafish embryos and the protective effect of HEBI against fine dust induced pro-inflammatory cytokine production. According to the results, HEBI down-regulated the mRNA expression of fine dust induced pro-inflammatory cytokines IL-1 β (fig. 4-9a), IL-6 (fig. 4-9b), and TNF- α (fig. 4-9c) from zebrafish embryos. Specifically, HEBI at 125 μ g/ml strongly down-regulated all tested pro-inflammatory cytokines observed in fine dust exposed zebrafish embryos. These data indicate that HEBI suppresses fine dust induced iNOS, COX2, and pro-inflammatory cytokine gene expression.

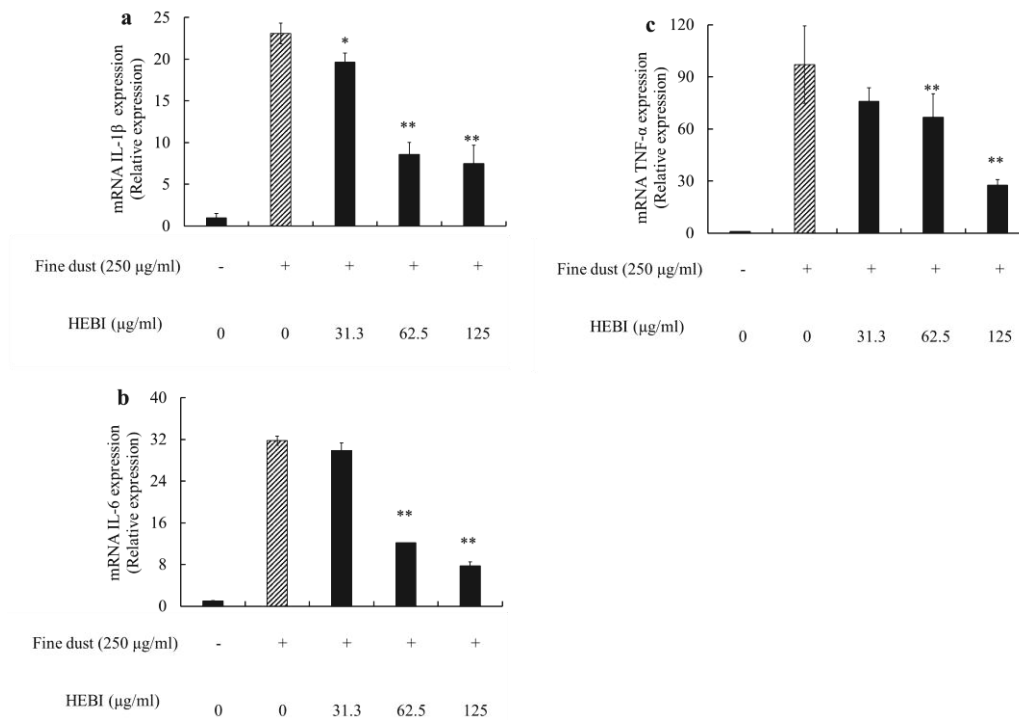


Figure 4-9. Inhibitory effect of HEBI on pro-inflammatory mRNA expression in fine dust exposed zebrafish embryos. Zebrafish embryos were stimulated with fine dust in the presence of HEBI for 3 dpf. The mRNA expression of IL-1 β (a), IL-6 (b), and TNF- α (c), were evaluated through RT-qPCR. The values are expressed as the mean \pm SE. Significant differences from the untreated group were identified at * $p < 0.05$ and ** $p < 0.01$.

4.4. Conclusions

Previously, a number of studies demonstrated the secondary metabolites present in the seaweeds have a potential to reduce elevated inflammatory responses observed in the zebrafish embryos after challenged with different inflammatory stimuli. However, most of the studies were limited to the image analysis results. However, in the present study, author demonstrated the elevated ROS, NO, and cell death rates induced by fine dust reduced by the HEBI via down regulating inflammatory proteins and pro-inflammatory cytokines. According to the western blots and RT-qPCR the expression levels of iNOS, COX2, and other pro-inflammatory cytokines were decreased by HEBI in a dose-dependent manner. The inhibitory effect of HEBI on pro-inflammatory mRNA and protein expression should be the reason for reduction of inflammatory responses and increase of survival rates in fine dust exposed zebrafish embryos. With this solid data it is clear that HEBI has a potential to reduce inflammation induced by fine dust in the human body.

4.5. References

Aliev G., Obrenovich M. E., Tabrez S., Jabir N. R., Reddy V. P., Li Y., Burnstock G., Cacabelos R., and Kamal M. A. (2013). Link between cancer and Alzheimer disease via oxidative stress induced by nitric oxide-dependent mitochondrial DNA overproliferation and deletion. *Oxid Med Cell Longev*, **2013**. Pp: 962984. DOI: 10.1155/2013/962984

Choi T.-Y., Kim J.-H., Ko D. H., Kim C.-H., Hwang J.-S., Ahn S., Kim S. Y., Kim C.-D., Lee J.-H., and Yoon T.-J. (2007). Zebrafish as a new model for phenotype-based screening of melanogenic regulatory compounds. *Pigment Cell Research*, **20**(2). Pp: 120-127. DOI: 10.1111/j.1600-0749.2007.00365.x

Cuong D. X., Boi V. N., Van T. T. T., and Hau L. N. (2015). Effect of storage time on phlorotannin content and antioxidant activity of six *Sargassum* species from Nhatrang Bay, Vietnam. *Journal of Applied Phycology*, **28**(1). Pp: 567-572. DOI: 10.1007/s10811-015-0600-y

Fernando I. P. S., Jayawardena T. U., Sanjeewa K. K. A., Wang L., Jeon Y. J., and Lee W. W. (2018). Anti-inflammatory potential of alginic acid from *Sargassum horneri* against urban aerosol-induced inflammatory responses in keratinocytes and macrophages. *Ecotoxicol Environ Saf*, **160**. Pp: 24-31. DOI: 10.1016/j.ecoenv.2018.05.024

Feng Q., Endo K., and Cheng G. (2002). Dust storms in China: a case study of dust storm variation and dust characteristics. *Bulletin of Engineering Geology and the Environment*, **61**(3). Pp: 253-261. DOI: 10.1007/s10064-001-0145-y

Finkel T., and Holbrook N. J. (2000). Oxidants, oxidative stress and the biology of ageing. *Nature*, **408**(6809). Pp: 239-47. DOI: 10.1038/35041687

Gautam P., Blaha U., and Appel E. (2005). Magnetic susceptibility of dust-loaded leaves as a proxy of traffic-related heavy metal pollution in Kathmandu city, Nepal. *Atmospheric Environment*, **39**(12). Pp: 2201-2211. DOI: 10.1016/j.atmosenv.2005.01.006

Handa O., Kokura S., Adachi S., Takagi T., Naito Y., Tanigawa T., Yoshida N., and Yoshikawa T. (2006). Methylparaben potentiates UV-induced damage of skin keratinocytes. *Toxicology*, **227**(1–2). Pp: 62-72. DOI: <http://dx.doi.org/10.1016/j.tox.2006.07.018>

Hou T., Liao J., Zhang C., Sun C., Li X., and Wang G. (2018). Elevated expression of miR-146, miR-139 and miR-340 involved in regulating Th1/Th2 balance with acute exposure of fine particulate matter in mice. *Int Immunopharmacol*, **54**. Pp: 68-77. DOI: [10.1016/j.intimp.2017.10.003](http://dx.doi.org/10.1016/j.intimp.2017.10.003)

Hwang J. H., Kim K. J., Ryu S. J., and Lee B. Y. (2016). Caffeine prevents LPS-induced inflammatory responses in RAW264.7 cells and zebrafish. *Chem Biol Interact*, **248**. Pp: 1-7. DOI: [10.1016/j.cbi.2016.01.020](http://dx.doi.org/10.1016/j.cbi.2016.01.020)

Kim E.-A., Lee S.-H., Ko C.-i., Cha S.-H., Kang M.-C., Kang S.-M., Ko S.-C., Lee W.-W., Ko J.-Y., Lee J.-H., Kang N., Oh J.-Y., Ahn G., Jee Y. H., and Jeon Y.-J. (2014). Protective effect of fucoidan against AAPH-induced oxidative stress in zebrafish model. *Carbohydrate Polymers*, **102**. Pp: 185-191. DOI: <http://dx.doi.org/10.1016/j.carbpol.2013.11.022>

Kim E. A., Ding Y., Yang H. W., Heo S. J., and Lee S. H. (2018). soft coral *Dendronephthya puetteri* extract ameliorates inflammations by suppressing inflammatory mediators and oxidative stress in lps-stimulated zebrafish. *Int J Mol Sci*, **19**(9). Pp: 2695. DOI: [10.3390/ijms19092695](http://dx.doi.org/10.3390/ijms19092695)

Kim E. A., Kim S. Y., Ye B. R., Kim J., Ko S. C., Lee W. W., Kim K. N., Choi I. W., Jung W. K., and Heo S. J. (2018). Anti-inflammatory effect of Apo-9'-fucoxanthinone via inhibition of MAPKs and NF-kB signaling pathway in LPS-stimulated RAW 264.7 macrophages and zebrafish model. *Int Immunopharmacol*, **59**. Pp: 339-346. DOI: [10.1016/j.intimp.2018.03.034](http://dx.doi.org/10.1016/j.intimp.2018.03.034)

Kim E. Y., and Moudgil K. D. (2017). Immunomodulation of autoimmune arthritis by pro-inflammatory cytokines. *Cytokine*, **98**. Pp: 87-96. DOI: [10.1016/j.cyto.2017.04.012](http://dx.doi.org/10.1016/j.cyto.2017.04.012)

Kim S.-Y., Kim E.-A., Kang M.-C., Lee J.-H., Yang H.-W., Lee J.-S., Lim T. I., and Jeon Y.-J. (2014). Polyphenol-rich fraction from *Ecklonia cava* (a brown alga) processing by-product reduces LPS-induced inflammation in vitro and in vivo in a zebrafish model. *Algae*, **29**(2). Pp: 165.

Kojima H., Urano Y., Kikuchi K., Higuchi T., Hirata Y., and Nagano T. (1999). fluorescent indicators for imaging nitric oxide production. *Angewandte Chemie International Edition*, **38**(21). Pp: 3209-3212. DOI: 10.1002/(SICI)1521-3773(19991102)38:21<3209::AID-ANIE3209>3.0.CO;2-6

Komatsu T., Mizuno S., Natheer A., Kantachumpoo A., Tanaka K., Morimoto A., Hsiao S. T., Rothausler E. A., Shishidou H., Aoki M., and Ajisaka T. (2014). Unusual distribution of floating seaweeds in the East China Sea in the early spring of 2012. *J Appl Phycol*, **26**(2). Pp: 1169-1179. DOI: 10.1007/s10811-013-0152-y

Lam S. H., Chua H. L., Gong Z., Lam T. J., and Sin Y. M. (2004). Development and maturation of the immune system in zebrafish, *Danio rerio*: a gene expression profiling, in situ hybridization and immunological study. *Developmental & Comparative Immunology*, **28**(1). Pp: 9-28. DOI: [http://dx.doi.org/10.1016/S0145-305X\(03\)00103-4](http://dx.doi.org/10.1016/S0145-305X(03)00103-4)

Lee S.-H., Ko C.-I., Jee Y., Jeong Y., Kim M., Kim J.-S., and Jeon Y.-J. (2013). Anti-inflammatory effect of fucoidan extracted from *Ecklonia cava* in zebrafish model. *Carbohydrate Polymers*, **92**(1). Pp: 84-89. DOI: <http://dx.doi.org/10.1016/j.carbpol.2012.09.066>

Livak K. J., and Schmittgen T. D. (2001). Analysis of relative gene expression data using real-time quantitative PCR and the 2^{- $\Delta\Delta$ CT} method. *Methods*, **25**(4). Pp: 402-408. DOI: 10.1006/meth.2001.1262

Love D. R., Pichler F. B., Dodd A., Copp B. R., and Greenwood D. R. (2004). Technology for high-throughput screens: the present and future using zebrafish. *Current*

Opinion in Biotechnology, **15**(6). Pp: 564-571. DOI: <http://dx.doi.org/10.1016/j.copbio.2004.09.004>

Meng Z., and Zhang Q. (2006). Oxidative damage of dust storm fine particles instillation on lungs, hearts and livers of rats. *Environ Toxicol Pharmacol*, **22**(3). Pp: 277-82. DOI: 10.1016/j.etap.2006.04.005

Middleton N. J. (2017). Desert dust hazards: A global review. *Aeolian Research*, **24**. Pp: 53-63. DOI: 10.1016/j.aeolia.2016.12.001

Mozhenok T. P., Beliaeva T. N., Bulychev A. G., Kuznetsova I. M., Leont'eva E. A., and Faddeeva M. D. (1997). The effect of biologically active compounds on lysosome fusion with phagosomes and the F-actin content in mouse peritoneal macrophages and on the status of the lysosomal membranes in mouse hepatocytes. *Tsitologiya*, **39**(7). Pp: 552-9.

Nakanishi M., and Rosenberg D. W. (2013). Multifaceted roles of PGE2 in inflammation and cancer. *Semin Immunopathol*, **35**(2). Pp: 123-37. DOI: 10.1007/s00281-012-0342-8

Novoa B., Bowman T. V., Zon L., and Figueras A. (2009). LPS response and tolerance in the zebrafish (*Danio rerio*). *Fish & Shellfish Immunology*, **26**(2). Pp: 326-331. DOI: <http://dx.doi.org/10.1016/j.fsi.2008.12.004>

Park M. H. (2003). Aerosol composition change due to dust storm: measurements between 1992 and 1999 at Gosan, Korea. *Water, Air, and Soil Pollution: Focus*, **3**(2). Pp: 117-128. DOI: 10.1023/a:1023278104910

Pozzi R., De Berardis B., Paoletti L., and Guastadisegni C. (2003). Inflammatory mediators induced by coarse (PM2.5-10) and fine (PM2.5) urban air particles in RAW 264.7 cells. *Toxicology*, **183**(1-3). Pp: 243-54. DOI: [https://doi.org/10.1016/S0300-483X\(02\)00545-0](https://doi.org/10.1016/S0300-483X(02)00545-0)

Russo I., Oksman A., Vaupel B., and Goldberg D. E. (2009). A calpain unique to alveolates is essential in *Plasmodium falciparum* and its knockdown reveals an involvement in pre-S-phase development. *Proc Natl Acad Sci U S A*, **106**(5). Pp: 1554-9. DOI: 10.1073/pnas.0806926106

Sanjeeva K. K. A., Fernando I. P. S., Kim E. A., Ahn G., Jee Y., and Jeon Y. J. (2017). Anti-inflammatory activity of a sulfated polysaccharide isolated from an enzymatic digest of brown seaweed *Sargassum horneri* in RAW 264.7 cells. *Nutr Res Pract*, **11**(1). Pp: 3-10. DOI: 10.4162/nrp.2017.11.1.3

Sanjeeva K. K. A., Fernando I. P. S., Kim S. Y., Kim H. S., Ahn G., Jee Y., and Jeon Y. J. (2018). In vitro and in vivo anti-inflammatory activities of high molecular weight sulfated polysaccharide; containing fucose separated from *Sargassum horneri*: Short communication. *Int J Biol Macromol*, **107**(Pt A). Pp: 803-807. DOI: 10.1016/j.ijbiomac.2017.09.050

Schweitzer M. D., Calzadilla A. S., Salamo O., Sharifi A., Kumar N., Holt G., Campos M., and Mirsaeidi M. (2018). Lung health in era of climate change and dust storms. *Environ Res*, **163**. Pp: 36-42. DOI: 10.1016/j.envres.2018.02.001

Terasaki M., Kawagoe C., Ito A., Kumon H., Narayan B., Hosokawa M., and Miyashita K. (2017). Spatial and seasonal variations in the biofunctional lipid substances (fucoxanthin and fucosterol) of the laboratory-grown edible Japanese seaweed (*Sargassum horneri* Turner) cultured in the open sea. *Saudi Journal of Biological Sciences*, **24**(7). Pp: 1475-1482. DOI: 10.1016/j.sjbs.2016.01.009

Vardi A., Formiggini F., Casotti R., De Martino A., Ribalet F., Miralto A., and Bowler C. (2006). A stress surveillance system based on calcium and nitric oxide in marine diatoms. *PLoS Biol*, **4**(3). Pp: e60. DOI: 10.1371/journal.pbio.0040060

Vellingiri K., Kim K. H., Ma C. J., Kang C. H., Lee J. H., Kim I. S., and Brown R. J. C. (2015). Ambient particulate matter in a central urban area of Seoul, Korea. *Chemosphere*, **119**. Pp: 812-819. DOI: 10.1016/j.chemosphere.2014.08.049

Wijesinghe W. A. J. P., Kim E.-A., Kang M.-C., Lee W.-W., Lee H.-S., Vairappan C. S., and Jeon Y.-J. (2014). Assessment of anti-inflammatory effect of 5 β -hydroxypalisadin B isolated from red seaweed *Laurencia snackeyi* in zebrafish embryo in vivo model. *Environmental Toxicology and Pharmacology*, **37**(1). Pp: 110-117. DOI: <http://dx.doi.org/10.1016/j.etap.2013.11.006>

Xu M., Sasa S., Otaki T., Hu F.-x., Tokai T., and Komatsu T. (2018). Changes in drag and drag coefficient on small *Sargassum horneri* (Turner) C. Agardh individuals. *Aquatic Botany*, **144**. Pp: 61-64. DOI: 10.1016/j.aquabot.2017.11.002

Xu Y., and Krukoff T. L. (2007). Adrenomedullin stimulates nitric oxide production from primary rat hypothalamic neurons: roles of calcium and phosphatases. *Mol Pharmacol*, **72**(1). Pp: 112-20. DOI: 10.1124/mol.106.033761

Yang Y. C., Chou H. Y., Shen T. L., Chang W. J., Tai P. H., and Li T. K. (2013). Topoisomerase II-mediated DNA cleavage and mutagenesis activated by nitric oxide underlie the inflammation-associated tumorigenesis. *Antioxid Redox Signal*, **18**(10). Pp: 1129-40. DOI: 10.1089/ars.2012.4620

Zon L. I., and Peterson R. T. (2005). In vivo drug discovery in the zebrafish. *Nat Rev Drug Discov*, **4**(1). Pp: 35-44.

Acknowledgements

Though the following dissertation is an individual work, I could never have researched the heights or explored the depths without the support, guidance and efforts lot of people. First and foremost, I would like to express my most sincere gratitude to my supervisor Professor You-Jin Jeon, who has supported me throughout my dissertation with his patience and knowledge whilst allowing me the room to work in my own way. I attribute the level of my PhD degree to his effort and encouragement. Without Professor You-Jin Jeon this thesis, too, would not have been completed or written. I also express my gratitude to Dr. W.A.J.P. Wijesinghe introducing me to my supervisor Professor You-Jin Jeon.

Many thanks to my lab mate Dr. Lee WonWoo and to Professor Youngheun Jee (Department of Veterinary Medicine, Jeju National University) for guiding me to study about fine dust related completions. Those who always encourage me to learn and study about fine dust related completions and helped me to be successful of my research throughout the whole period.

Then, I would like to thank all of my lab members. Specially Mr. Thilina U. Jayawardena who helped me a lot for perform some compulsory research studies to complete this work (western blots and RT-qPCR works). A huge thanks goes to three lab mates Dr. Kim Hyun-Soo, Dr. Kim Seo-young, and Dr. I.P.S Fernando who greatly helped me during last 5 years to accomplished this huge goal in the numerous ways.

Also, I greatly acknowledge my parents, parents-in-law, and to my wife Madushani for their love and support provided me the energy to attain my study. I also can't forget all my foreign friends and other Sri Lankans study in the Jeju National University as well as those who have completed their studies and left the Jeju National University, for the support given me in numerous ways to success my studies in Korea.

At last but not least I would like to thank all those whom I have not mentioned above but helped me during my study period to success my studies in Jeju National University.